

HEAT AND MOISTURE TRANSPORT IN UNSATURATED POROUS MEDIA:
A COUPLED MODEL IN TERMS OF CHEMICAL POTENTIAL

by

Eric R. Sullivan

B.S., Iowa State University, 1998

M.S., University of Colorado at Colorado Springs, 2007

A thesis submitted to the
Faculty of the Graduate School of the
University of Colorado in partial fulfillment
of the requirements for the degree of
Doctor of Philosophy
Applied Mathematics

2013

This thesis for the Doctor of Philosophy degree by

Eric R. Sullivan

has been approved

by

Lynn Schreyer-Bennethum, Advisor

Julien Langou, Chair

Jan Mandel

Richard Naff

Kathleen Smits

Date: April 19, 2013

Sullivan, Eric R. (Ph.D., Applied Mathematics)

Heat and Moisture Transport in Unsaturated Porous Media:
A Coupled Model in Terms of Chemical Potential

Thesis directed by Associate Professor Lynn Schreyer-Bennethum

ABSTRACT

Transport phenomena in porous media are commonplace in our daily lives. Examples and applications include heat and moisture transport in soils, baking and drying of food stuffs, curing of cement, and evaporation of fuels in wild fires. Of particular interest to this study are heat and moisture transport in unsaturated soils. Historically, mathematical models for these processes are derived by coupling classical Darcy's, Fourier's, and Fick's laws with volume averaged conservation of mass and energy and empirically based source and sink terms. Recent experimental and mathematical research has proposed modifications and suggested limitations in these classical equations. The primary goal of this thesis is to derive a thermodynamically consistent system of equations for heat and moisture transport in terms of the chemical potential that addresses some of these limitations. The physical processes of interest are primarily diffusive in nature and, for that reason, we focus on using the macroscale chemical potential to build and simplify the models. The resulting coupled system of nonlinear partial differential equations is solved numerically and validated against the classical equations and against experimental data. It will be shown that under a mixture theoretic framework, the classical Richards' equation for saturation is supplemented with gradients in temperature, relative humidity, and the time rate of change of saturation. Furthermore, it will be shown that restating the water vapor diffusion equation in terms of chemical potential eliminates the necessity for an empirically based fitting parameter.

The form and content of this abstract are approved. I recommend its publication.

Approved: Lynn Schreyer-Bennethum

DEDICATION

To Johnanna

ACKNOWLEDGMENT

There are several people who have either directly or indirectly made this work possible. First and foremost, I would like to extend many thanks to Lynn Schreyer-Bennethum. Without her patience, support, amazing talents as a teacher, mathematical and physical insights, and constant questions I would likely not have been able to get involved so heavily in mathematical modeling. I would like to thank Kate Smits for agreeing to join my committee so late and for sharing her expertise with experimentation. I would also like to thank Jan Mandel, Julien Langou, and Rich Naff for their unending support and patience as my committee members.

There are several people in the UCD community that I would like to thank. To Keith Wojciechowski, who was one of the primary reasons that I started working with Lynn. To Cannanut Chamsri, Tom Carson, and Mark Mueller, my research group comrades, for putting up with my ramblings and never-ending slue of equations during our weekly meetings. To Mark especially, for his thought provoking questions and constant push to tie the math and physics together. To Jeff Larson and Henc Bouwmeester, who have become life-long friends. I appreciated the comic relief, the deep mathematical conversations, the computer help, and the fun that we had. Of course, I cannot forget to thank the many other people who helped me to persevere through graduate school: Jenny Diemunsch, Cathy Erbes, Piezhun Zhu, Brad Lowry, Tim Morris, Samantha Graffeo, and many other.

Finally, I would like to thank my family and friends. Without my *support network* this would have been much tougher. To my parents, Drew and Donna, who have taught me what real hard work really is. To my siblings, Doug, Emily, and Julie, for helping me get to this point in my life. To Emily, especially, who went through grad school along with me. To my friends Fred Hollingworth, Jodie Collins, and Erik Swanson who reminded me that it was equally important to head up into the mountains and go climbing as it was to work. To my *teacher friends* Scott Strain, Ginger Anderson, and Krista Bruckner who have helped to make me a better teacher and better person. Lastly, to Johnanna. I couldn't have done this without you.

TABLE OF CONTENTS

Figures	xi
Tables	xv
<u>Chapter</u>	
1. Introduction	1
1.1 Previous Work	1
1.2 Hybrid Mixture Theory and Thesis Goals	3
1.3 Thesis Outline	5
2. Fick's Law and Microscale Advection Diffusion Models	9
2.1 Comparison of Fick's Laws	9
2.2 Transient Diffusion Models	14
2.3 Conclusion	17
3. Hybrid Mixture Theory	19
3.1 The Averaging Procedure	19
3.1.1 The REV and Averaging	20
3.2 Macroscale Balance Laws	26
3.2.1 Macroscale Mass Balance	27
3.2.2 Macroscale Momentum Balance	30
3.2.3 Macroscale Energy Balance	31
3.3 The Entropy Inequality	32
3.3.1 A Brief Derivation of the Entropy Inequality	33
4. New Independent Variables and Exploitation of the Entropy Inequality . .	36
4.1 A Choice of Independent Variables	37
4.1.1 The Expanded Entropy Inequality	41
4.2 Exploiting the Entropy Inequality	46
4.2.1 Results That Hold For All Time	46
4.2.1.1 Fluid Lagrange Multipliers	47

4.2.1.2	Solid Phase Identities	47
4.2.2	Equilibrium Results	50
4.2.2.1	Fluid Stress Tensor	50
4.2.2.2	Momentum Transfer Between Phases	51
4.2.2.3	Momentum Transfer Between Species	52
4.2.2.4	Partial Heat Flux	53
4.2.3	Near Equilibrium Results	53
4.3	Pressures in Multiphase Porous Media	55
4.4	Chemical Potential in Multiphase Porous Media	59
4.5	Derivations Constitutive Equations	62
4.5.1	Darcy’s Law	63
4.5.2	Darcy’s Law In Terms of Chemical Potential	65
4.5.3	Fick’s Law	68
4.5.4	Fourier’s Law	70
4.6	Conclusion	73
5.	Coupled Heat and Moisture Transport Model	75
5.1	Introduction and Historical Work	75
5.1.1	Richards’ Equation for Fluid Flow	75
5.1.2	Phillip and De Vries’ Diffusion Model	77
5.1.3	De Vries’ Heat Transport Model	78
5.2	Assumptions	79
5.3	Derivation of Heat and Moisture Transport Model	81
5.3.1	Mass Balance Equations	81
5.3.2	Energy Balance Equation	84
5.3.2.1	Energy Transfer in the Total Energy Equation	88
5.3.2.2	Stress in the Total Energy Equation	89
5.3.2.3	Total Energy Balance Equation	91

5.4	Simplifying Assumptions – A Closed System	97
5.4.1	Saturation Equation	103
5.4.1.1	Capillary Pressure and Dynamic Capillary Pressure	104
5.4.2	Gas Phase Diffusion Equation	111
5.4.3	Total Energy Equation	117
5.4.3.1	Dimensional Analysis	121
5.4.4	Constitutive Equations	122
5.5	Conclusion and Summary	126
6.	Existence and Uniqueness Results	130
6.1	Saturation Equation with $\tau \neq 0$	130
6.2	Alt and Luckhaus Existence and Uniqueness Theorems	132
6.2.1	Existence and Uniqueness for Richards' Equation	135
6.2.2	Vapor Diffusion Equation	138
6.2.3	Limits of the Alt and Luckhaus Theorem	142
6.3	Heat Transport Equation	143
6.4	Conclusion	146
7.	Numerical Analysis and Sensitivity Studies	148
7.1	Saturation Equation	150
7.2	Vapor Diffusion Equation	158
7.3	Coupled Saturation and Vapor Diffusion	165
7.4	Coupled Heat and Moisture Transport System	168
7.4.1	Experimental Setup, Material Parameters, and IBCs	168
7.4.2	Numerical Simulations	177
7.5	Conclusion	185
8.	Conclusions and Future Work	189

<u>Appendix</u>	
A. Microscale Nomenclature	195
B. Macroscale Appendix	197
B.1 Nomenclature	197
B.2 Upscaled Definitions	202
B.3 Identities Needed to Obtain Inequality 3.40	205
C. Exploitation of the Entropy Inequality – An Abstract Perspective	206
C.1 Results that Hold For All Time	207
C.2 Equilibrium Results	208
C.3 Near Equilibrium Results	209
C.4 Linearization and Entropy	210
D. Summary of Entropy Inequality Results	212
D.1 Results that Hold For All Time	212
D.2 Equilibrium Results	213
D.3 Near Equilibrium Results	214
D.4 Constitutive Equations	215
E. Dimensional Quantities	216
<u>References</u>	218

FIGURES

Figure		
3.1	Illustration of the definition of the REV via a sequence of porosities corresponding to a sequence of shrinking volumes. (Image similar to Figures 1.3.1 and 1.3.2 in Bear [5])	21
3.2	Cartoon of the microscale, REV, and macroscale in a granular soil. The right-hand plot depicts the mixture of all phases.	22
3.3	Local coordinates in and REV.	22
5.1	Densities as functions of temperature	99
5.2	van Genuchten relative permeability curves. The red curve shows the non-wetting phase, $\kappa_{rnw}(S_e)$, and the blue curves show the wetting phase, $\kappa_{rw}(S_e)$, each for $m = 0.5, 0.67, 0.8$, and 1	104
5.3	Contact angle and effective radius in a capillary tube geometry. θ is the contact angle, r is the effective radius, and κ is the radius of curvature of the interface.	105
5.4	Examples of van Genuchten capillary pressure - saturation curves for various parameters.	108
5.5	Comparison of different diffusion models at constant temperature ($T = 295.15K$). The value for the saturated permeability was chosen to match that of [75] ($\kappa_S = 1.04 \times 10^{-10}m^2$), where they found a fitting parameter $a = 18.2$. The “Present Model” refers to equation (5.68) (with $\nabla T = \mathbf{0}$ and no mass transfer) and the “Enhancement Model” refers to equation (5.3) along with (5.70), (5.72), and (5.73) for the diffusion coefficient, enhancement factor, and tortuosity respectively.	116
5.6	Johansen thermal conductivity model with Côté-Konrad $K_e - S$ relationship (with $\kappa = 15$) plotted in blue, and the weighted sum of the thermal conductivities of the individual phases plotted in red.	120

5.7	Three proposed functional forms of $\tau = \tau(S)$	124
5.8	Level curves of mass transfer rate functions.	126
6.1	The function $b(h) = S(h) - 1$ for $m = 0.8$ and various values of α	136
6.2	Kirchhoff transformation \mathcal{K} for $m = 0.8$ and various values of α	137
7.1	Cartoon of a 1-dimensional packed column experimental apparatus.	148
7.2	Log of Péclet numbers for various values of saturation. The point at $(\alpha = 5.7, m = 0.94)$ indicates the values used in Smits et al. [75]. Warmer colors are associated with higher Péclet number and therefore associated with an advective solution.	152
7.3	Saturation profiles at various times in a drainage experiment with $\alpha = 5.7, n = 17$	154
7.4	Convergence test for drainage experiment depicted in Figure 7.3. N is the number of spatial grid points. In Figure 7.3, $t_1 = 0.025t_c$, $t_2 = 0.050t_c$, $t_3 = 0.075t_c$, and $t_4 = 0.010t_c$	156
7.5	Saturation profiles in a imbibition experiment with $\alpha = 2.5, n = 5$	157
7.6	Convergence test for imbibition experiment depicted in Figure 7.5. In Figure 7.5, $t_1 = 0.025t_c$, $t_2 = 0.050t_c$, $t_3 = 0.075t_c$, and $t_4 = 0.010t_c$	158
7.7	Sample diffusion experiment comparing the enhancement model to the present model. Here, $a = 25$, $m = 0.9$ ($n = 10$), and $\kappa = 10^{-10}$ with Dirichlet boundary conditions and an exponential initial profile.	160
7.8	Comparison of diffusion coefficients for various van Genuchten parameters all taken with $\kappa_s = 1.04 \times 10^{-10}$ and $\varepsilon = 0.334$ to match the experiment in [75].	161
7.9	Comparison of diffusion coefficients for various van Genuchten parameters all taken with $\kappa_s = 4.0822 \times 10^{-11}$ and $\varepsilon = 0.385$ to match the experiment in [67].	162

7.10	The blue and green curves show the left-hand side of equation (7.8) for different saturated permeabilities, and the red lines show level curves for right-hand side for various values of a . The blue and green curves can be used to predict the value of a before experimentation.	165
7.11	Comparison of coupled saturation-diffusion models for various weights of C_φ^l with parameters: $\kappa_s = 1.04 \times 10^{-10}$, $\varepsilon = 0.334$, $H_0 = 10^{-3}$, $\alpha = 4$, and $m = 0.667$	167
7.12	Schematic of the Smits et al. experimental apparatus. Saturation and temperature sensors numbered 1 - 11, temperature sensors 12 - 15, and relative humidity sensors 1 and 2 [75]. The geometric x coordinate is shown on the left. (Image recreated with permission from [75])	169
7.14	Relative humidity and temperature data showing measurement variations in the first few days of the experiment. (Image recreated with permission from [75])	170
7.13	Broken sensor data. Saturation sensor #3 shown in blue and relative humidity sensor #1 shown in red. It is evident from these plots that these sensors are not working properly as they give non-physical readings. (Image recreated with permission from [75])	171
7.15	Relative humidity and temperature data at a window beginning roughly 12.5 days into the experiment. This window is chosen since the sensor noise is qualitatively minimal in this region. (Image recreated with permission from [75])	172
7.16	Approximations to relative humidity and temperature boundary conditions at the surface of the soil.	173
7.17	Approximate initial conditions at the 2000 th data point ($t \approx 13.9$ days). Error bars indicate approximate sensor accuracy.	174
7.18	Illustration of how the gas-phase domain might evolve in time.	175

7.19	Comparison of relative humidity and saturation for the fully coupled saturation-diffusion-temperature model as compared to data from [75]. Boundary conditions are taken from a sinusoidal approximation of boundary data. Thermal conductivities are taken as either weighted sum (5.78) or Côté-Konrad (5.80).	183
7.20	Comparison of relative humidity and saturation for the fully coupled saturation-diffusion-temperature model as compared to data from [75]. Boundary conditions are taken from a smoothed square wave approximation of boundary data. Thermal conductivities are taken as either weighted sum (5.78) or Côté-Konrad (5.80).	184
7.21	Blowup comparison of relative humidity and saturation for the fully coupled saturation-diffusion-temperature model as compared to data from [75]. The inset plots give a closer look at the behavior exhibited by these particular solutions.	185
7.22	Comparison of temperature solutions for the fully coupled saturation-diffusion-temperature model as compared to data from [75]. Boundary conditions are taken from a sinusoidal approximation of boundary data.	186
7.23	Comparison of temperature solutions for the fully coupled saturation-diffusion-temperature model as compared to data from [75]. Boundary conditions are taken from a smoothed square wave approximation of boundary data.	187

TABLES

Table	
2.1	Mass and molar flux forms of Fick's law 10
7.1	Measured and predicted value of the fitting parameter a based on equation (7.8). 165
7.2	Material parameters for experimental setup [75]. 170
7.3	Relative errors measured using equation (7.13) for the classical mathematical model consisting of Richards' equation for saturation, the enhanced diffusion model for vapor diffusion, and the de Vries model for heat transport. These are compared for the two thermal conductivity functions of interest (weighted sum (5.78) and Côté-Konrad (5.80)). 180
7.4	Relative errors measured using equation (7.13) for instances within the parameter space consisting of the thermal conductivity function (weighted sum (5.78) and Côté-Konrad (5.80)), C_φ^l , C_T^l , and τ . These are taken for a (smoothed) square wave approximation to the boundary conditions. (The starred rows indicate failure of the numerical method, and the errors from the classical model are repeated for clarity) 181
7.5	Percent improvement of the present model over the classical model using equation (7.13) as the error metric. 188
E.1	Dimensional quantities 216
E.2	Typical values of hydraulic conductivity (K) for water and air, and associated values for permeability (κ). Note that $K = \kappa\rho g/\mu$ where $\rho^g = 1kg/m^3$, $\rho^l = 1000kg/m^3$, $\mu_l = 10^{-3}Pa \cdot s$, and $\mu_g = 10^{-5}Pa \cdot s$. Modified from Bear pg. 136 [5] 217

1. Introduction

Water flow, water vapor diffusion, and heat transport within variably saturated soils (above the groundwater and below the soil surface) are important physical processes in evaporation studies, contaminant transport, and agriculture. The mathematical models governing these physical processes are typically combinations of classical empirical law (e.g. Darcy’s law) and volume averaged conservation laws. The resulting equations are valid in many situations, but recent experimental and mathematical research has suggested modifications and corrections to these models. The primary goal of this thesis is to build a thermodynamically consistent mathematical model for heat and moisture transport that takes these recent advancements into consideration. To realize this goal Hybrid Mixture Theory (HMT) and the macroscale chemical potential are used as the primary modeling tools.

1.1 Previous Work

In 1856, Henri Darcy published his research on the use of sand filters to clean the water sources for the fountains in Dijon, France. He found that the flux of water across sand filters was directly proportional to the gradient of the pressure head. This simple observation has become known as Darcy’s law and is one of the main modeling tools in hydrology and soil science [30]. Darcy’s law is an example of a historical rule (or *law*) that has perpetuated to the present day. Darcy’s law was originally derived for saturated porous media, but near the turn of the century it was extended for use in unsaturated soils. In 1931, L.A. Richards coupled Darcy’s law with liquid mass balance to derive what is now known as Richards’ equation. This equation relies on the assumption that Darcy’s law is valid for unsaturated media, but it also relies on an empirically-derived relationship between pressure and saturation.

The pressure-saturation relationship is known to be hysteretic in nature (depends on the direction of wetting), and only recently have researchers been able to move toward functional relationships that capture this effect [47]. Correction terms

in Richards' equation have been proposed via HMT that suggest that the rate at which the capillary pressure is changing may play a role in the overall dynamics of the saturation [45, 46]. This proposed, third-order, term in Richards' equation has only recently been studied mathematically and experimentally. One possible physical interpretation of this term is that it accounts for how fast the liquid-gas interfaces are rearranging at the pore scale.

In the 1950s, Philip and deVries published their works on vapor and heat transport in porous media [31, 60]. Their approach accounts for water flow in both the liquid and fluid phases in response to water content and temperature gradients in the soil. In order to account for the observation that Fickian diffusion inadequately describes diffusion in porous media, Philip and deVries implemented an *enhancement* factor, η , to adjust the diffusion coefficient. This factor is fitted to the measured diffusion data for a particular medium. In [24], Cass et al. found that η increases with saturation (with $\eta \approx 1$ for dry soils). Philip and deVries proposed that thermal gradients and the condensation and evaporation through "liquid islands" are the pore-scale mechanisms that cause the observed enhancement. Counter intuitively, the governing equation holds at the macroscale while these mechanisms are inherently pore-scale. The Philip and de Vries model has not been validated in a laboratory setting.

More recent works question the validity of the Philip and deVries model. Shokri et al. [72] suggests that the coupling between the water flow and Fickian diffusion is the key to estimating the vapor flux. They suggest that under this consideration there is no need for the enhancement factor. Webb [79], and more recently Shahareeni et al. [69], showed that enhancement can exist in the absence of thermal gradients. It was initially thought that enhancement couldn't occur in the absence of thermal gradients and was therefore ignored. Based on the observation that enhancement can occur without the need for thermal gradients, it is clear that the Philip and de Vries model needs modification. Cass [24] and Campbell [23] give a functional form of the

enhancement factor that is commonly used (e.g. [67, 75]), but relies on an empirical fitting parameter. In the present work we take the view of Shokri et al. that there is no need for the enhancement fact, and we derive a diffusion equation simply based on liquid and vapor flow. The novelty of the present approach is the use of the chemical potential as the driving force for both types of flow.

For energy transport, the 1958 deVries model [31] is still commonly used (e.g. [67, 75]). Similar to the enhanced diffusion model, deVries built this model so as to account for the flux of the fluid phases. This is sensible as the fluid phases will certainly transport heat. More recently, Bennethum et al. [14] and Kleinfelder [51] used Hybrid Mixture Theory to derive heat transport equations in porous media (Bennethum et al. studies saturated porous media and Kleinfelder studied multiscale unsaturated media). They verified many of the findings by deVries but also proposed several new terms associated with the physical processes of heat transport. In this work we extend the Bennethum et al. and Kleinfelder approaches to unsaturated media.

1.2 Hybrid Mixture Theory and Thesis Goals

To build the models in this work we make extensive use of Hybrid Mixture Theory (HMT). HMT, statistical upscaling, and homogenization have all been used as techniques to re-derive, confirm, and extend Darcy's, Fick's, and Fourier's laws in porous media. For a technical summary of some of these methods see [29]. HMT is a term for the process of using volume averaged pore-scale conservation laws along with the second law of thermodynamics to give thermodynamically consistent constitutive equations in porous media. The technique as applied to porous media was developed by several parties, the most notable being Hassanizadeh and Gray [38, 42] and Cushman et al. [11, 13, 28], but the general principles were developed by Coleman and Noll [26].

In the present work we use HMT to derive new extensions to these laws in the case of unsaturated porous media. These extensions are then used to derive a model for total moisture transport in unsaturated soils. While this sort of modeling has been done in the past, rarely have the three principle physical process (movement of saturation fronts, vapor diffusion, and thermal conduction) been considered from first principles and put on the same theoretical footing (HMT in this case). No known work attempts to couple these three different effects together with one physical measurement: the chemical potential. This is one of the unique features of this work.

In the most general sense, the chemical potential is a measure of the tendency of a substance (thinking particularly of a fluid or species) to diffuse. This diffusion could be of a species within a mixture (e.g. water vapor diffusing through air) or it could be a phase diffusing into another (e.g. water into a Darcy-type sand filter). The fact that most physical processes in porous media are of this type gives an inspiration for the potential usefulness of the chemical potential as a modeling tool. That is, from a broad point of view, it should be possible to restate the physical processes of moving saturation fronts and vapor diffusion more naturally by the chemical potential. This approach has not been thoroughly explored in the past since the chemical potential is not directly measureable and the theoretical footings of upscaling the chemical potential are relatively new. In the saturated case, extensions to Darcy's law have also been developed via HMT, and the results indicate that the macroscale chemical potential is a viable modeling tool for diffusive velocity in saturated porous media [15, 68, 80]. In the present work we give chemical potential forms of Darcy's and Fick's law as well as presenting simplifications to Fourier's law based on the chemical potential. In the case of a pure liquid phase we will show that the chemical potential form of Darcy's law is no different than the more traditional pressure formulation. In the gas phase, on the other hand, we will show that the pairings of chemical potential forms of Fick's and Darcy's laws gives a new form of the diffusion coefficient that

does not need the *enhancement factor* indicated in the work by Phillip and DeVries [60]. The chemical potential will finally be used to derive a novel form of Fourier's law for heat conduction in multiphase media.

Once we have derived new forms of the classical constitutive equations we pair these equations with volume averaged conservation laws to give a coupled system of partial differential equations governing heat and moisture transport. The second law of thermodynamics is used to suggest additional closure conditions for each of the equations. Together, the system consists of a nonlinear pseudo-parabolic equation for saturation, a nonlinear parabolic equation for vapor diffusion, and a nonlinear parabolic-hyperbolic equation for heat transport.

In summary, this work serves several purposes: (1) it is a step toward better understanding the role of the chemical potential in multiphase porous media, (2) it makes strides toward understanding the phenomenon of *enhanced vapor diffusion* in porous media, and (3) finally we propose a novel coupled system of equations for heat and moisture transport.

1.3 Thesis Outline

In Chapter 2 we take a step back from porous media and discuss pore-scale diffusion models. This is done in an attempt to elucidate the assumptions, derivations, and models used in various disciplines as there tends to be confusion about where the myriad of assumptions are valid. In this chapter we give mathematical and physical reasons for the many commonly used assumptions as well as proposing an alternative advection-diffusion model as compared to the popular Bird, Stewart, and Lightfoot model [18].

In Chapter 3 we present the necessary background information in order to understand volume averaging and the exploitation of the entropy inequality. Much of this chapter is paraphrased from previous works, such as [11, 13, 38, 42, 80, 85]. In the beginning of Chapter 4 we use the tools from Chapter 3 to build and exploit a

version of the entropy inequality specific for multiphase media where each phase consists of multiple species. The remainder of Chapter 4 is dedicated to the exploitation of the entropy inequality for a novel choice of independent variables describing these media. Appendix C serves as a companion to this discussion as it gives the abstract formulation and logic of the entropy inequality. Throughout Chapter 4, the goal is to derive new forms of Darcy's, Fick's, and Fourier's laws and to propose extensions to these laws in terms of the macroscale chemical potential. As part of these derivations we arrive at new expressions for the pressure and wetting potentials in unsaturated media. All of these derivations are done in a general sense with as few assumptions as possible. This leaves open the possibilities of future research.

In Chapter 5 we couple the results found from the exploitation of the entropy inequality (Chapter 4) with the volume averaged conservation laws derived in Chapter 3. In Section 5.1, a more in-depth historical perspective of the classical equations used for heat and moisture transport is given to orient the reader to the recent research. Fluid transport equations are presented in Section 5.3.1 along with a discussion of the relationship between mass transfer and chemical potential. Considerable effort is put toward deriving a heat transport equation with the final equation presented in Section 5.3.2.3. In Section 5.4 several simplifying assumptions are presented in order to close the system of equations. In particular, Sections 5.4.1, 5.4.2, and 5.4.3 give simplifications, assumptions, and dimensional analysis for the liquid, gas, and heat equations respectively. In Section 5.4.4 we present the remaining constitutive equations necessary to close the system of equations. Since so many assumptions and simplifications are made throughout the chapter a summary of all of the results is presented in Section 5.5.

In Chapter 6 we examine the proper regularity and assumptions needed for existence and uniqueness of solutions. These results are preliminary and do not constitute a complete existence and uniqueness study for these equations.

In Chapter 7 we perform numerical analysis on the equations derived in Chapter 5. In Sections 7.1, 7.2, and 7.3 we examine numerical solutions and parameter sensitivity for the saturation equation, vapor diffusion equation, and the coupled saturation-vapor diffusion equations respectively. In Section 7.4 we compare numerical solutions to the fully coupled heat and moisture transport model to the experimental data collected in [75].

In Chapters 5 - 7 we work toward building and analyzing the saturation, vapor diffusion, and heat equations. The flow of thought for these chapters is to apply each set of new assumptions or simplifications to each of the three equations before moving to the next set of assumptions. That is, if a set of assumptions are proposed then the subsequent sections will apply those assumptions to the saturation, vapor diffusion, and heat equations in turn. Only then will the next set of assumptions be discussed. This is done so that each set of assumptions are only stated once and since many of the assumptions create interleaving effects between the equations.

Finally, as an aid to the reader there are several appendices. Appendix A contains a nomenclature index for the pore-scale diffusion processes considered in Chapter 2. Appendix B.1 contains a nomenclature index for the macroscale results in the remaining chapters. There is some overlap between the nomenclature for these distinct parts, and effort has been made to not create any excessive notational confusions (even though this work is necessarily notation heavy). Appendix B.2 gives a list (in alphabetical order) of the upscaled definitions of variables defined in chapters 3 and 4. As mentioned previously, Appendix C gives an abstract view of the entropy inequality in an effort to make the exploitation process more clear to the interested reader. Appendix D gives a summary of the results extracted from the entropy inequality in Chapter 4. This is done for ease of reference mostly on the author's part, but it is also done to provide an index of these results for use in future research. Finally, Appendix E gives several tables of dimensional quantities used throughout.

It is suggested that the detail-oriented reader have Appendix A at hand when reading Chapter 2 and Appendix B.1 at hand when reading chapters 3 - 5. There are some minor abuses of notation, but effort was made to bring them to the reader's attention whenever possible and to use notation that didn't confuse the immediate discussion.

2. Fick's Law and Microscale Advection Diffusion Models

This chapter consists of a short technical note related to pore-scale diffusion problems. Vapor diffusion in macroscale porous media is an important phenomenon with many applications (e.g. evaporation from soils, moisture transport through filters, and CO₂ sequestration). In order to better understand macroscale diffusion it behooves the researcher to first understand pore-scale mechanics and models. This chapter attempts to elucidate the models and assumptions used for diffusion at the pore-scale so that when we turn our attention to macroscale diffusion we are firmly grounded. A secondary goal of this chapter is to give a thorough discussion of the diffusion coefficient used in Fick's law. This is necessary since this coefficient is typically wrongly assumed constant for all choices of dependent variables (mass concentration, molar concentration, chemical potential, etc.).

To make matters simpler, we focus our pore-scale discussion on the, so called, Stefan diffusion tube problem. This is a well-studied problem that models the diffusion of a species through an ideal binary gas mixture above a liquid-gas interface [6, 18, 22, 32, 50, 83, 84]. This is an idealization of the juxtaposition of phases in a capillary tube geometry, and a capillary tube geometry is an idealization of geometry of pore-scale porous media. To derive a mathematical model for the time evolution of the evaporating (or condensing) species, one typically couples Fick's first law with the mass balance equation.

In Section 2.1 we discuss the various forms of Fick's law and briefly discuss the relationships between the diffusion coefficients. In Section 2.2 we derive the transient diffusion equations associated with Fick's law and compare with the associated equation of Bird, Stewart, and Lightfoot [18] (henceforth referred to as BSL).

2.1 Comparison of Fick's Laws

For a system consisting of an ideal mixture of water vapor, g_v , and inert air, g_a , Fick's law can be written in terms of molar concentration, mass concentration,

Table 2.1: Mass and molar flux forms of Fick's law

Flux Type	Flux Expression	Fick's Law
mass flux [$ML^{-2}T$]	$\mathbf{J}_\rho^{g_j} = \rho^{g_j} \mathbf{v}^{g_j,g}$	$\mathbf{J}_\rho^{g_j} = -\rho^g D_\rho \nabla C^{g_j}$ (2.1)
molar flux [$(mol)L^{-2}T$]	$\mathbf{J}_c^{g_j} = c^{g_j} \mathbf{v}_c^{g_j,g}$	$\mathbf{J}_c^{g_j} = -c^g D_c \nabla x^{g_j}$ (2.2)
mass flux [$ML^{-2}T$]	$\mathbf{J}_{\mu,\rho}^{g_j} = \rho^{g_j} \mathbf{v}^{g_j,g}$	$\mathbf{J}_{\mu,\rho}^{g_j} = -D_{\mu,\rho} \left(\frac{\rho^{g_j}}{R^{g_j} T} \right) \nabla \mu_\rho^{g_j}$ (2.3)
mole flux [$(mol)L^{-2}T$]	$\mathbf{J}_{\mu,c}^{g_j} = c^{g_j} \mathbf{v}_c^{g_j,g}$	$\mathbf{J}_{\mu,c}^{g_j} = -D_{\mu,c} \left(\frac{c^{g_j}}{RT} \right) \nabla \mu_c^{g_j}$ (2.4)

or the chemical potential. This is potentially confusing since there are inherently different diffusion coefficients for the different forms of Fick's law. The purpose of this subsection is to clarify the relationships between these coefficients. In porous media it is common to use mass flux for Fick's law, but in chemistry (and related fields) it is more common to use molar flux. As such, we will make most of our comparisons between mass and molar flux.

According to BSL [18], the mass and molar forms of Fick's law are given by equations (2.1) and (2.2) (modified from BSL Table 17.8-2). In Table 2.1, $\mathbf{v}^{g_j,g} = \mathbf{v}^{g_j} - \mathbf{v}^g$ is the diffusive velocity relative to a mass weighted velocity, $\mathbf{v}_c^{g_j,g} = \mathbf{v}^{g_j} - \mathbf{v}_c^g$ is the diffusive velocity relative to a mole weighted velocity, ρ^{g_j} is the mass density of species j , $C^{g_j} = \rho^{g_j}/\rho^g$ is the mass concentration of species j in the mixture, $c^{g_j} = mol(g_j)/vol(g)$ is the molar density of species j , and $x^{g_j} = c^{g_j}/c^g$ is the molar concentration of species j in the mixture.

The chemical potential forms of Fick's law can be given in terms of two different types of chemical potential: mass weighted (equation (2.3)) or mole weighted (equation (2.4)). In physical chemistry and thermodynamics [21, 55] the chemical potential is known as the *tendency for a species to diffuse*, and for this reason it is a natural candidate for the statement of Fick's law (an exact thermodynamic definition

will be presented in subsequent chapters). In equations (2.3) and (2.4), $\mu_c^{g_j}$ is the mole weighted chemical potential [$J(\text{mol})^{-1}$] and $\mu_\rho^{g_j}$ is the mass weighted chemical potential [JM^{-1}].

The reader should first note that the two fluxes are measured with respect to different velocities. The mass weighted velocity is $\rho^g \mathbf{v}^g = \sum_{j=v,a} \rho^{g_j} \mathbf{v}^{g_j}$ and the mole weighted velocity is $c^g \mathbf{v}_c^g = \sum_{j=v,a} c^{g_j} \mathbf{v}^{g_j}$ where \mathbf{v}^{g_j} is the velocity of the species relative to a fixed coordinate system. This means that that there cannot be a direct comparison between the two different types of flux without considering them relative to the same frame of reference. Using these definitions of \mathbf{v}^g and \mathbf{v}_c^g we see that the difference between the two bulk velocities, $\mathbf{v}^g - \mathbf{v}_c^g$ is

$$\mathbf{v}^g - \mathbf{v}_c^g = \sum_{j=1}^N \left(\frac{\rho^{g_j} - x^{g_j} \rho^g}{\rho^g} \right) \mathbf{v}^{g_j}. \quad (2.5)$$

In (2.5), the summation over j indicates that this is an accumulation over the N species in the gas mixture. In future work we will be interested in the diffusion of water vapor ($j = v$) and will consider the gas mixture as binary: $j \in \{v, a\}$, where $j = a$ represents the mixture of all species that are not water vapor. Therefore we can write (2.5) as

$$\begin{aligned} \mathbf{v}^g - \mathbf{v}_c^g &= \sum_{j=v,a} \left(\frac{\rho^{g_j} - x^{g_j} \rho^g}{\rho^g} \right) \mathbf{v}^{g_j} \\ &= (x^{g_a} C^{g_v} - x^{g_v} C^{g_a}) \mathbf{v}^{g_v} + (x^{g_v} C^{g_a} - x^{g_a} C^{g_v}) \mathbf{v}^{g_a}. \end{aligned} \quad (2.6)$$

Converting to a mass weighted velocity we see that $\mathbf{v}_c^{g_j,g} = \mathbf{v}^{g_j,g} + (\mathbf{v}^g - \mathbf{v}_c^g)$, and therefore the molar flux is $\mathbf{J}_c^{g_j} = c^{g_j} \mathbf{v}_c^{g_j,g} = c^{g_j} \mathbf{v}^{g_j,g} + c^{g_j} (\mathbf{v}^g - \mathbf{v}_c^g)$. Assuming that $c^{g_j} x^{g_k} C^{g_l} \ll 1$ we see that the difference between the frame of reference is potentially quite small.

Next note that the diffusion coefficients are (initially) assumed to be different for each choice of independent variable as indicated by the subscripts. To compare D_ρ

and D_c we note that $\mathbf{J}_\rho^{g_j} = m^{g_j} \mathbf{J}_c^{g_j}$ and

$$\nabla C^{g_j} = \left(\frac{m^{g_j} m^{g_k}}{(x^{g_j} m^{g_j} + x^{g_k} m^{g_k})^2} \right) \nabla x^{g_j} \quad (2.7)$$

to conclude that

$$\left(\frac{C^{g_k}}{x^{g_k}} \right) D_\rho = D_c, \quad (2.8)$$

where m^{g_j} is the molar mass of species j and the minuscule, k , represents the *other* species. If the molar density form of the diffusion coefficient, D_c , is assumed to be constant (at constant temperature) we conclude that the mass density version of the diffusion coefficient is not constant (and visa versa). The fraction, C^{g_k}/x^{g_k} can be interpreted as the ratio of the molar mass of species k to the molar mass of the mixture. If $j = v$ is the water vapor in an air-water mixture then $k = a$ is the inert air and the scaling factor between the diffusion coefficients is the ratio of molar mass of the air to the molar mass of the mixture. For sufficiently dilute systems (where the amount of water vapor is small) the ratio is approximately 1 and the diffusion coefficients can be considered as approximately equal.

For ideal air-water mixtures, the densities are related through $\rho^g = \rho^{g_v} + \rho^{g_a}$ and the water vapor density is related to the relative humidity through $\rho^{g_v} = \rho_{sat}^{g_v} \varphi$. Here we are taking $\rho_{sat}^{g_v}$ as the saturated vapor density and φ as the relative humidity. At standard temperature and pressure we note that $\rho_{sat}^{g_v} \approx 0.02 \text{ kg/m}^3$ and $\rho^g \approx 1 \text{ kg/m}^3$. This indicates that at standard temperature and pressure we can likely assume that the mixture is always *sufficiently dilute*. Therefore, in the systems under consideration we can assume that the diffusion coefficients are approximately equal.

For the diffusion coefficients associated with the chemical potential forms of Fick's law we first observe that if we multiply and divide the right-hand side of the molar form by the molar mass of species j then

$$\mathbf{J}_{\mu,c}^{g_j} = -D_{\mu,c} \left(\frac{c^{g_j}}{RT} \right) \left(\frac{m^{g_j}}{m^{g_j}} \right) \nabla \mu_c^{g_j} = - \left(\frac{D_{\mu,c}}{m^{g_j}} \right) \left(\frac{\rho^{g_j}}{R^{g_j} T} \right) \nabla \mu^{g_j}. \quad (2.9)$$

Here, $R^{g_j} = R/m^{g_j}$ is the specific gas constant, and we have used $\mu^{g_j} = \mu_c^{g_j}/m^{g_j}$. Again noting that $\mathbf{J}_{\mu,\rho}^{g_j} = m^{g_j} \mathbf{J}_{\mu,c}^{g_j}$ we conclude that $D_{\mu,c} = D_{\mu,\rho}$.

It remains to compare D_ρ to $D_{\mu,\rho}$ and D_c to $D_{\mu,c}$. We focus here on the mass fluxes without loss of generality. If the mass fluxes are equal, then in particular

$$\rho^g D_\rho \nabla C^{g_v} = D_\mu \left(\frac{\rho^{g_v}}{R^{g_v} T} \right) \nabla \mu^{g_v}.$$

Rearranging, it can be seen that

$$D_\rho \nabla C^{g_v} = C^{g_v} D_\mu \nabla \left(\frac{\mu^{g_v}}{R^{g_v} T} \right)$$

(assuming constant temperature). From physical chemistry [55], recall that the chemical potential is related to a reference chemical potential ($\mu_*^{g_v}$) and the ratio of partial pressure, p^{g_v} , to bulk pressure, p^g , via

$$\mu^{g_v} = \mu_*^{g_v} + R^{g_v} T \ln \left(\frac{p^{g_v}}{p^g} \right). \quad (2.10)$$

Therefore,

$$\nabla \left(\frac{\mu^{g_v}}{R^{g_v} T} \right) = \nabla \left(\ln \left(\frac{p^{g_v}}{p^g} \right) \right) = \left(\frac{p^g}{p^{g_v}} \right) \nabla \left(\frac{p^{g_v}}{p^g} \right). \quad (2.11)$$

Using Dalton's law for ideal gases, $p^g = p^{g_v} + p^{g_a}$, and using the specific gas constants we note that the partial pressure of species j can be written as $p^{g_j} = R^{g_j} T \rho^{g_j}$. Therefore,

$$p^g = R^{g_v} T \rho^{g_v} + R^{g_a} T \rho^{g_a}, \quad (2.12)$$

and, after simplifying,

$$\frac{p^{g_v}}{p^g} = \frac{\rho^{g_v}}{\rho^{g_v} + \left(\frac{R^{g_a}}{R^{g_v}} \right) \rho^{g_a}}. \quad (2.13)$$

From the values found in Appendix E we see that $R^{g_a}/R^{g_v} \approx 0.6$ and therefore equation (2.13) is similar, but not equal to, the mass concentration, $C^{g_v} = \rho^{g_v}/(\rho^{g_v} + \rho^{g_a})$. Defining $C^{g_v} = p^{g_v}/p^g$ we see that

$$\frac{D_\rho}{D_\mu} = \left(\frac{C^{g_v}}{C^{g_v}} \right) \frac{\nabla C^{g_v}}{\nabla C^{g_v}}, \quad (2.14)$$

where division is understood component wise (that is, equation (2.14) represents three equations when the gradient is understood in three spatial dimensions). The right-hand side of equation (2.14) is not constant at 1 for all densities, but the variation in the right-hand side depends mostly on the variation in ρ^{g_a} in the gas mixture. Fortunately, the water vapor density is much smaller than the air-species density, and hence ρ^{g_a} is approximately constant. In one spatial dimension, the right-hand side of (2.14) can therefore be approximated by

$$d(x) := \frac{\left(\frac{x}{x+1}\right) \frac{d}{dx} \left(\frac{x}{x+0.6}\right)}{\left(\frac{x}{x+0.6}\right) \frac{d}{dx} \left(\frac{x}{x+1}\right)}$$

(where $x = \rho^{g_v}$ and $\rho^{g_a} \approx 1$). It is easy to show that $0.98 < d(x) < 1$ for $0 \leq x \leq \rho_{sat}^{g_v}$. Furthermore, for *sufficiently dilute* mixtures, $d(x) \approx 1$, and we therefore conclude that $D_\rho \approx D_\mu$.

The conclusion from this subsection is that while the diffusion coefficients for the molar and mass flux forms of Fick's law are not the same, for dilute mixtures they can be approximated as equal.

2.2 Transient Diffusion Models

In porous media there is a phenomenon known as *enhanced vapor diffusion* [60]. This phenomenon states that vapor diffusion in porous media occurs *faster* than as predicted by Fickian diffusion models. This is merely a statement about the observed imbalance between Fickian diffusion and experimental measure. Since the ultimate goal of this work is to develop macroscale advection diffusion models, we seek to understand the pore-scale diffusion models so that in subsequent chapters we can tackle the enhanced diffusion problem.

To build a transient model for molecular diffusion we couple Fick's law with the appropriate form of the mass balance equation. In the previous subsection we showed that the various forms of Fick's law are approximately equal (for sufficiently dilute mixtures), so the results stated here will only be in terms of the mass flux form of Fick's law (equation (2.1)).

The mass balance equation for species j in the gas phase can be written as

$$\frac{\partial \rho^{g_j}}{\partial t} + \nabla \cdot (\rho^{g_j} \mathbf{v}^{g_j}) = \hat{r}^{g_j} \quad (2.15)$$

where \mathbf{v}^{g_j} is the velocity of species j within the gas mixture relative to a fixed frame of reference, and \hat{r}^{g_j} is a mass exchange term accounting for chemical reactions between species [80, 84]. In the present work we assume that no chemical reactions occur, and therefore $\hat{r}^{g_j} = 0$. The combination of the mass balance equation with the mass flux form of Fick's law (for $j = v$) gives a transport equation for the mass of water vapor via advective, $\rho^{g_v} \mathbf{v}^g$, and diffusive, \mathbf{J}^{g_v} , fluxes:

$$\frac{\partial \rho^{g_v}}{\partial t} + \nabla \cdot (\mathbf{J}^{g_v} + \rho^{g_v} \mathbf{v}^g) = 0. \quad (2.16)$$

Substituting the mass flux form of Fick's law¹ (from equation (2.1)) we get

$$\frac{\partial \rho^{g_v}}{\partial t} + \nabla \cdot (\rho^{g_v} \mathbf{v}^g) = D \nabla \cdot (\rho^g \nabla C^{g_v}). \quad (2.17)$$

Notice here that the diffusion coefficient has been factored out of the divergence operator. This is only valid in constant temperature environments. If the gas-phase density were constant in space then we would arrive at the traditional advection diffusion equation (by dividing equation (2.17) by ρ^g or by rewriting the diffusion term as $D \nabla \cdot \nabla \rho^{g_v}$) and would need an expression for the bulk velocity in terms of density (or concentration) to close the equation. Unfortunately, if the density of the water vapor is allowed to vary then the density of the gas varies. Again, for *sufficiently dilute* mixtures the variation in gas-phase density is very small and the nonlinear diffusion on the right-hand side can be approximated by the linear diffusion term $D \nabla \cdot \nabla \rho^{g_v}$. It should be noted here that this latter case is what is typically thought of as ‘‘Fick's law’’ and is what leads to the traditional linear diffusion equation (when the advection term is neglected) [27].

¹The subscripts on the flux and the diffusion coefficient have been dropped since all of the versions presented in Table 2.1 are approximately equal

A different form of equation (2.17), suggested in BSL [18], is derived by considering the mass weighted bulk velocity. In a binary system,

$$\rho^{g_v} \mathbf{v}^{g_v} = \rho^{g_v} \mathbf{v}^{g_v, g} + \rho^{g_v} \mathbf{v}^g = \rho^{g_v} \mathbf{v}^{g_v, g} + \rho^{g_v} (C^{g_v} \mathbf{v}^{g_v} + C^{g_a} \mathbf{v}^{g_a}).$$

Solving for $\rho^{g_v} \mathbf{v}^{g_v}$

$$\rho^{g_v} \mathbf{v}^{g_v} = \left(\frac{\rho^{g_v}}{1 - C^{g_v}} \right) \mathbf{v}^{g_v, g} + \rho^{g_v} \mathbf{v}^{g_a}. \quad (2.18)$$

Using Fick's law for $\rho^{g_v} \mathbf{v}^{g_v, g}$, and eliminating $\rho^{g_v} \mathbf{v}^{g_v}$ in (2.15) with (2.18) gives

$$\frac{\partial \rho^{g_v}}{\partial t} + \nabla \cdot (\rho^{g_v} \mathbf{v}^{g_a}) = \nabla \cdot \left(\frac{D \rho^g}{1 - C^{g_v}} \nabla C^{g_v} \right). \quad (2.19)$$

Whitaker [84] suggested that “one can develop convincing arguments in favor of . . .” neglecting the air-species flux term. Certainly at steady state we can assume (as is done in BSL) that \mathbf{v}^{g_a} is approximately zero at the interface since “there is no net motion of [water vapor] away from the interface” [18], but in the transient case this would constitute a change of frame of reference. This new frame of reference would be such that the inert air molecules are viewed as stationary with the water vapor diffusing through them.

In either equation (2.17) or (2.19) one must find appropriate conditions or equations to either neglect or rewrite the advective term, $\rho^{g_v} \mathbf{v}^g$ or $\rho^{g_v} \mathbf{v}^{g_a}$ respectively. Typically this term is neglected in a pure diffusion problem. As these are two different simplifications of the same equation one must have different reasons for neglecting the advective term. The easiest fix for this issue is to couple with either the bulk gas mass balance equation or the air-species mass balance equation and to use the mass-weighted velocity: $\rho^g \mathbf{v}^g = \sum_{j=1}^N \rho^{g_j} \mathbf{v}^{g_j}$. The point being that one cannot simply neglect the advection term in the transient case of either equation without proper consideration of the implications: a fixed bulk velocity or a changing frame of reference respectively.

A final comment can be made regarding equations (2.17) and (2.19). The bulk density term, ρ^g , on the right-hand side of these equations is often factored out of the divergence operator. This is an error committed by several researchers [18, 22, 50]. The reasoning for assuming that the density is constant (and hence returning to a linear diffusion model in the absence of advection) is that in an ideal gas, $p^g = \rho^g R^g T$. Under constant temperature conditions, and if the pressure is assumed constant, then the density is assumed to be constant. There are two possible mistakes here. (1): If the species densities are allowed to vary then the bulk density must vary. (2): The value of R^g will vary with the changing composition of the mixture (since the molar mass of the mixture changes). The effect of this is that, while the pressure may remain constant, the component parts are not necessarily constant and therefore cannot be factored from the divergence operator.

2.3 Conclusion

In this chapter we have compared various forms of Fick's law for molecular diffusion. We have shown that, while the diffusion coefficients are indeed different, under certain common circumstances the diffusion coefficients can be considered as approximately equal. It is common to take the diffusion coefficient as constant (or only a function of temperature), and in many cases it is safe to assume the same diffusion coefficient may be used in the common forms of Fick's law.

In the transient case there are two natural formulations for (the mass flux form of) Fick's second law. In either case, the natural governing equation is a nonlinear advection diffusion equation that must be closed with the use of another mass balance equation. When considering the advection term, it is the author's opinion that equation (2.17) is the more natural choice. The reason for this is that the bulk velocity, \mathbf{v}^g , is likely more naturally measured as compared to that of the species velocity. This chapter concludes our discussion on pore-scale modeling. We now turn our attention to building macroscale models, but in doing so we keep in mind the diffusion models

at the pore scale and use cues from this scale to help make proper assumptions about the larger scale.

3. Hybrid Mixture Theory

In this chapter we use a combination of classical mixture theory and rational thermodynamics (henceforth called Hybrid Mixture Theory (HMT)) to study novel extensions to Darcy’s law, Fick’s law, and Fourier’s law in variably saturated porous media. This approach was pioneered by Hassanizadeh and Gray in the 70’s and 80’s [38, 42, 43, 44] and later extended by Bennethum, Cushman, Gray, Hassanizadeh, and many others [28, 29, 40, 80] to model multi-phase, multi-component, and multi-scale media. HMT involves volume averaging, or upscaling, pore-scale balance laws to obtain macroscale analogues. The second law of thermodynamics is then used to derive constitutive restrictions on these macroscale balance laws. Constitutive relations are particular to the medium being studied, and hence depend on a judicious choice of independent variables for the energy of each phase in the medium. There are many excellent resources for the curious reader to gain a more thorough understanding of HMT (eg [29, 80]). For that reason we will not derive every identity along the way. Instead partial derivations of the identities necessary to understand the present application of HMT are presented.

To begin this overview we consider the upscaling of pore-scale balance laws (conservation laws) via a mixture theoretic approach. The subsequent sections in this and the next chapter introduce the entropy inequality and it’s exploitation to derive constitutive laws. A judicious choice of independent variables for the energy of each phase in the medium is chosen and is used to derive novel versions of Darcy’s, Fick’s, and Fourier’s laws. These constitutive equations will be used in subsequent chapters to develop models for moisture transport in variably saturated porous media.

3.1 The Averaging Procedure

When considering a porous medium one cannot avoid discussing the various scales involved. This particular work deals with two principal scales: the microscale and

the macroscale. At the microscale the phases are separate and distinguishable. Typical microscale porous media will have pores that measure on the order of microns to millimeters (depending on the type of solid). At the macroscale the phases are indistinguishable and the typical measurements range from millimeters to meters. The macroscale is where most physical measurements are made, and as such, we seek to derive governing equations that hold at this scale. The microscale structure may vary dramatically for different media depending on the type of solid phase and the microscale behavior of the fluid phases. As such, the microscale geometry can have a dramatic influence on flow and phase interaction.

For any given phase at the pore scale the mass, linear momentum, angular momentum, and energy balance laws must hold. The problem is that it is difficult to obtain geometric information everywhere at this scale. For this reason we seek to average (or *upscale*) the microscale balance laws to the macroscale.

There are many methods for mathematically averaging balance laws. Here we choose the simplest method of weighted integration. Before introducing the technical details of the weighted integration we must first introduce the concept of a Representative Elementary Volume and local geometry in a porous medium. This elementary volume will become our basic unit of volume throughout this research. The following discussions closely follow and paraphrase those of Bear [5], Bennethum [13, 12], Hassanizadeh and Gray [38, 42], Weinstein [80], and Wojciechowski [85].

3.1.1 The REV and Averaging

In this work we consider unsaturated porous media. Characteristic to these media is the juxtaposition of liquid, solid, and gas phases within the pore matrix. We make the assumption that a representative elementary volume (REV), in the sense of Bear [5], exists at every point in space. To properly define the REV we first define the porosity.

Consider a sequence of small volumes within a porous medium, $(\delta V)_k$, each with centroid $\mathbf{x} \in \mathbb{R}^3$. For each k , let $(\delta V_{void})_k$ be the volume of the void space within $(\delta V)_k$. The porosity for the k^{th} volume is given as the ratio

$$\phi_k = \frac{(\delta V_{void})_k}{(\delta V)_k}. \quad (3.1)$$

Generate the sequence, $\{\phi_k\}$, by gradually shrinking $(\delta V)_k$ about \mathbf{x} such that $(\delta V)_1 > (\delta V)_2 > (\delta V)_3 > \dots$. As k increases, the porosity will certainly fluctuate due to heterogeneities in the medium. As $(\delta V)_k$ shrinks there will be a certain value, $k = k^*$, such that for $k > k^*$ the fluctuations in porosity become small and are only due to fluctuations in the arrangement of the solid matrix. If $(\delta V)_k$ is reduced well beyond $(\delta V)_{k^*}$ the sequence of volumes will eventually converge to \mathbf{x} . The point, \mathbf{x} only lies within one phase, so the limit of the sequence of porosities will either be 0 or 1 (completely in the void space or completely in the solid). This indicates that there will be some other intermediate volume, $(\delta V)_{k^{**}} < (\delta V)_{k^*}$, where the sequence of porosities begins to fluctuate again as k gets larger. We define the REV, δV , as any particular volume $(\delta V)_{k^{**}} < \delta V < (\delta V)_{k^*}$. Without loss of generality we can simply choose $\delta V \equiv (\delta V)_{k^{**}}$. Figure 3.1 illustrates two typical sequences of porosities, ϕ_k , as the volume is decreased (right to left).

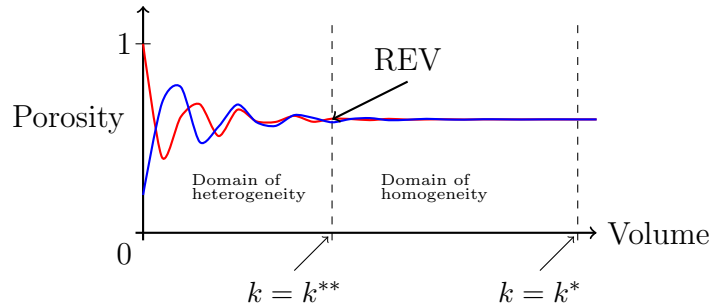


Figure 3.1: Illustration of the definition of the REV via a sequence of porosities corresponding to a sequence of shrinking volumes. (Image similar to Figures 1.3.1 and 1.3.2 in Bear [5])

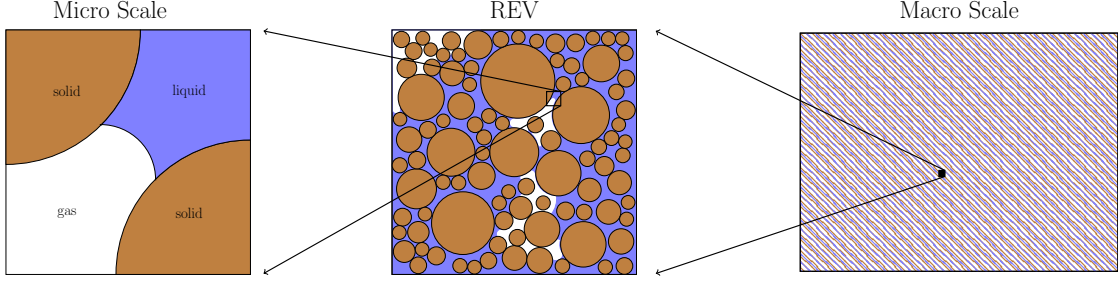


Figure 3.2: Cartoon of the microscale, REV, and macroscale in a granular soil. The right-hand plot depicts the mixture of all phases.

Consider now a coordinate system superimposed on the porous medium. Let \mathbf{x} be the centroid of the REV, and let \mathbf{r} be some other vector inside the REV. Define the vector, $\boldsymbol{\xi}$, as a vector originating from the centroid of the REV such that

$$\mathbf{r} = \mathbf{x} + \boldsymbol{\xi}. \quad (3.2)$$

We can now view $\boldsymbol{\xi}$ as a local coordinate in the REV as in Figure 3.3.

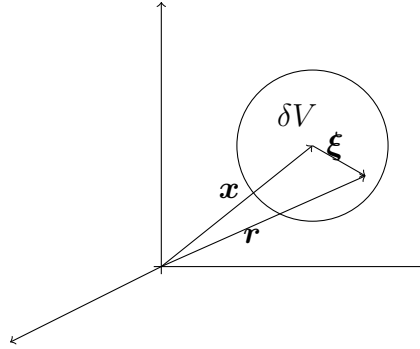


Figure 3.3: Local coordinates in and REV.

Define the *phase indicator function* as

$$\gamma_{\alpha}(\mathbf{r}, t) = \begin{cases} 1, & \mathbf{r} \in \alpha\text{-phase} \\ 0, & \mathbf{r} \notin \alpha\text{-phase} \end{cases}, \quad (3.3)$$

where \mathbf{r} is a position vector as indicated in Figure 3.3. The averaging technique involved multiplying a micro scale quantity (such as density) by γ_{α} and integrate over the REV. This effectively smears out the phases. A consequence of this is that

the averaged value may not accurately represent the actual values being measured at the pore scale. A further mathematical complication arises since the integrations may not make sense in the traditional (Riemannian) sense. Therefore, we must understand all of the following mathematics in the distributional sense (integrals are understood to be Lebesgue, and derivatives are understood to be generalized derivatives). For more specifics on these mathematical tools see standard graduate texts on functional analysis (eg. [58]).

To find the volume of the α phase in the REV we simply integrate γ_α over the REV. Define this volume as $|\delta V_\alpha|$:

$$|\delta V_\alpha| = \int_{\delta V} \gamma_\alpha(\mathbf{r}, t) dv = \int_{\delta V} \gamma_\alpha(\mathbf{x} + \boldsymbol{\xi}, t) dv(\boldsymbol{\xi}). \quad (3.4)$$

The α -phase volume fraction, ε^α , is defined as ¹

$$\varepsilon^\alpha(\mathbf{x}, t) = \frac{|\delta V_\alpha|}{|\delta V|}. \quad (3.5)$$

Since $0 \leq |\delta V_\alpha| \leq |\delta V|$ it is clear that $0 \leq \varepsilon^\alpha \leq 1$. Furthermore, since the REV is made up of all of the phases,

$$\sum_\alpha \varepsilon^\alpha = 1. \quad (3.6)$$

The volume fraction is the first example of a macroscale variable. That is, it is a variable that describes a pore-scale property but is upscaled to the larger, more measurable, scale.

It is useful to note that there are two main types of averaging that will be used: mass averaging and volume averaging [42, 40, 80]. Let ψ^j be the j^{th} constituent of some quantity of interest. To volume average ψ^j we define

$$\langle \psi^j \rangle^\alpha = \frac{1}{|\delta V_\alpha|} \int_{\delta V} \psi^j(\mathbf{r}, t) \gamma_\alpha(\mathbf{r}, t) dv(\boldsymbol{\xi}), \quad (3.7)$$

¹Note: the notation “ ε^α ” for the volume fraction is not necessarily standard. Some authors use “ ϕ^α ”, “ θ^α ”, or “ n^α ”. Furthermore, the superscript notation is sometimes replaced by subscripts. The present notation is chosen to be consistent with the primary references for Hybrid Mixture Theory mentioned in the introduction to this chapter.

and to mass average ψ^j we define

$$\overline{\psi^j}^\alpha = \frac{1}{\langle \rho^j \rangle^\alpha |\delta V_\alpha|} \int_{\delta V} \rho^j(\mathbf{r}, t) \psi^j(\mathbf{r}, t) \gamma_\alpha(\mathbf{r}, t) dv(\boldsymbol{\xi}). \quad (3.8)$$

Implicitly in (3.8) we see that density is volume averaged. That is,

$$\langle \rho^j \rangle^\alpha = \frac{1}{|\delta V_\alpha|} \int_{\delta V} \rho^j(\mathbf{r}, t) \gamma_\alpha(\mathbf{r}, t) dv(\boldsymbol{\xi}). \quad (3.9)$$

(Note: some authors use the mass averaged notation on density even though it is technically volume averaged. Given the definition of a mass averaged quantity there is usually little confusion.)

The basic rules of thumb for deciding whether to volume or mass average were originally proposed by Hassanizadeh and Grey in 1979 [42]. They propose four criteria, listed below, for making this decision. In these criteria it is emphasized that the microscale quantities correspond to small scale pre-averaged quantities, while macroscale quantities are defined via the averaging process.

1. “When an averaging operation involves integration, the integrand multiplied by the infinitesimal element of integration must be an additive quantity. For example, the internal energy density function, E , is not additive, but the total internal energy, $\rho E dv$ is additive and an average defined in terms of this quantity will be physically meaningful.”
2. “The macroscopic quantities should exactly account for the total corresponding microscopic quantity. For example, total macroscopic momentum fluxes through a given boundary must be equal to the total microscopic momentum fluxes through that boundary.”
3. “The primitive concept of a physical quantity, as first introduced into the classical continuum mechanics must be preserved by proper definition of the macroscopic quantity. For instance, heat is a mode of transfer of energy through a

boundary different from work. The definition of macroscopic heat flux must also be a mode of energy transfer different from macroscopic work.”

4. “The averaged value of a microscopic quantity must be the same function that is most widely observed and measured in a field situation or in laboratory practice. For example, velocities measured in the field are usually mass averaged quantities; therefore, the macroscopic velocity should be a mass averaged quantity.” This ensures applicability of the resulting equations.

In the upscaling procedure to follow we wish to apply a weighted integration to a pore-scale balance law (a partial differential equation). This will involve terms such as

$$\int_{\delta V} \frac{\partial \rho^j}{\partial t} \gamma_\alpha dv,$$

and to ensure that we properly define the macroscale variables as either volume or mass averaged quantities, we need a theorem that allows for the interchange of integration and differentiation. This theorem is due to Whitaker and Slattery [74, 81, 82] and a generalization of this theorem is due to Cushman [28].

Theorem 3.1 (Averaging Theorem) *If $\mathbf{w}_{\alpha\beta}$ is the microscopic velocity of the $\alpha\beta$ interface and \mathbf{n}^α is the outward unit normal vector of δV_α indicating that the integrand should be evaluated in the limit as the $\alpha\beta$ interface is approached from the α side, then*

$$\begin{aligned} & \frac{1}{|\delta V|} \int_{\delta V} \frac{\partial f}{\partial t} \gamma_\alpha dv(\boldsymbol{\xi}) \\ &= \frac{\partial}{\partial t} \left[\frac{1}{|\delta V|} \int_{\delta V} f \gamma_\alpha dv(\boldsymbol{\xi}) \right] - \sum_{\beta \neq \alpha} \frac{1}{|\delta V|} \int_{A_{\alpha\beta}} f \mathbf{w}_{\alpha\beta} \cdot \mathbf{n}^\alpha da \end{aligned} \quad (3.10a)$$

$$\begin{aligned} & \frac{1}{|\delta V|} \int_{\delta V} \nabla f \gamma_\alpha dv(\boldsymbol{\xi}) \\ &= \nabla \left[\frac{1}{|\delta V|} \int_{\delta V} f \gamma_\alpha dv(\boldsymbol{\xi}) \right] + \sum_{\beta \neq \alpha} \frac{1}{|\delta V|} \int_{A_{\alpha\beta}} f \mathbf{n}^\alpha da, \end{aligned} \quad (3.10b)$$

where f is the quantity to be averaged.

Keep in mind that f could be a scalar or a vector quantity. In the latter case, the symbol f is replaced with \mathbf{f} and appropriate tensor contractions are inserted.

The averaging procedure is now carried out in the following steps:

1. State the pore-scale balance law for a particular species (or phase).
2. Multiply the equation by γ_α .
3. Average each term over the REV.
4. Apply Theorem 3.1 to arrive at terms representing macroscale quantities.
5. Define physically meaningful macroscopic quantities.

We now turn our attention to averaging pore-scale balance laws in the sense listed above. In the following discussion, \mathbf{v}^j is the microscopic velocity of constituent j , $\mathbf{w}_{\alpha\beta_j}$ is the velocity of the j^{th} constituent in the $\alpha\beta$ interface, and \mathbf{n}^α is the outward unit normal vector of δV_α . A full nomenclature index can be found in Appendix B.1.

3.2 Macroscale Balance Laws

As it is the simplest balance law, let us first consider the mass balance equation for a single constituent:

$$\frac{D\rho^j}{Dt} + \rho^j \nabla \cdot \mathbf{v}^j = \rho^j \hat{r}^j. \quad (3.11)$$

Here, ρ^j is the density of the constituent, \mathbf{v}^j is the velocity of the constituent, and any source of mass from chemical reactions between the constituents is given as \hat{r}^j .

Recall that the material (Lagrangian) derivative is

$$\frac{D^j(\cdot)}{Dt} = \frac{\partial(\cdot)}{\partial t} + \mathbf{v}^j \cdot \nabla(\cdot) \quad (3.12)$$

This derivative contains the usual Eulerian derivative along with an advective term.

Written in terms of the Eulerian time derivative, (3.11) is

$$\frac{\partial \rho^j}{\partial t} + \nabla \cdot (\rho^j \mathbf{v}^j) = \rho^j \hat{r}^j. \quad (3.13)$$

While this is specifically the mass balance equation, it takes the prototypical form of all balance laws: a time derivative plus a flux is equal to any source.

The constituent momentum balance can be written in a similar manner:

$$\frac{\partial(\rho^j \mathbf{v}^j)}{\partial t} + \nabla \cdot (\rho^j \mathbf{v}^j \otimes \mathbf{v}^j - \underline{\underline{\mathbf{t}}}^j) = \rho^j (\mathbf{g} + \hat{\mathbf{i}}^j + \hat{r}^j \mathbf{v}^j). \quad (3.14)$$

Here, $\underline{\underline{\mathbf{t}}}^j$ is the Cauchy stress tensor on species j , and the sources on the right-hand side are gravity, momentum transfer from other constituents, and momentum gained from chemical reactions respectively. These equations describe the change in mass and momentum over time and space within a specific constituent. They are sufficient field equations for modeling systems composed of a single phase gas, liquid, or solid, but equations (3.13) and (3.14) are insufficient for modeling multiphase and multi-constituent systems as a mixture because the interactions between the phases and constituents are not present.

In this work we consider a porous medium consisting of a solid phase and two fluid phases with multiple constituents within each phase. The phases will be denoted as $\alpha = l, g$, and s for liquid, gas, and solid respectively. The constituents will be enumerated $j = 1 : N$ (using MATLAB-style notation to indicate $j = 1, 2, \dots, N$). The following derivations follow similar derivations given by Gray [42], Weinstein [80] and Wojciechowski [85].

3.2.1 Macroscale Mass Balance

To obtain macroscale equations in multiphase and multi-constituent media we multiply a constituent balance equations by the phase indicator function, γ_α , integrate over δV , and divide by $|\delta V|$. Applying the averaging theorem (3.1) to the appropriate terms in equation (3.13) we have

$$\begin{aligned} \frac{1}{|\delta V|} \int_{\delta V} \frac{\partial \rho^j}{\partial t} \gamma_\alpha dv &= \frac{\partial}{\partial t} \left[\frac{|\delta V_\alpha|}{|\delta V| |\delta V_\alpha|} \int_{\delta V} \rho^j \gamma_\alpha dv \right] \\ &\quad - \sum_{\beta \neq \alpha} \frac{1}{|\delta V|} \int_{\delta A_{\alpha\beta}} \rho^j \mathbf{w}_{\alpha\beta_j} \cdot \mathbf{n}^\alpha da \end{aligned}$$

$$= \frac{\partial}{\partial t} \left(\varepsilon^\alpha \overline{\rho^j}^\alpha \right) - \sum_{\beta \neq \alpha} \frac{1}{|\delta V|} \int_{\delta A_{\alpha\beta}} \rho^j \mathbf{w}_{\alpha\beta_j} \cdot \mathbf{n}^\alpha da, \quad (3.15a)$$

$$\begin{aligned} \frac{1}{|\delta V|} \int_{\delta V} \nabla \cdot (\rho^j \mathbf{v}^j) \gamma_\alpha dv &= \nabla \cdot \left[\frac{|\delta V_\alpha|}{|\delta V| |\delta V_\alpha|} \int_{\delta V} \rho^j \mathbf{v}^j \gamma_\alpha dv \right] \\ &+ \sum_{\beta \neq \alpha} \frac{1}{|\delta V|} \int_{\delta A_{\alpha\beta}} \rho^j \mathbf{v}^j \cdot \mathbf{n}^\alpha da \\ &= \nabla \cdot \left(\varepsilon^\alpha \overline{\rho^j}^\alpha \overline{\mathbf{v}^j}^\alpha \right) + \sum_{\beta \neq \alpha} \frac{1}{|\delta V|} \int_{\delta A_{\alpha\beta}} \rho^j \mathbf{v}^j \cdot \mathbf{n}^\alpha da, \text{ and} \end{aligned} \quad (3.15b)$$

$$\frac{|\delta V_\alpha|}{|\delta V| |\delta V_\alpha|} \int_{\delta V} \rho^j \hat{r}^j dv = \varepsilon^\alpha \overline{\rho^j}^\alpha \hat{r}^j. \quad (3.15c)$$

Substituting equations (3.15)(a)-(c) into equation (3.13), recognizing the volume fraction terms, and recognizing the averaged mass and velocity gives the upscaled mass balance equation:

$$\begin{aligned} \frac{\partial \left(\varepsilon^\alpha \overline{\rho^j}^\alpha \right)}{\partial t} + \nabla \cdot \left(\varepsilon^\alpha \overline{\rho^j}^\alpha \overline{\mathbf{v}^j}^\alpha \right) \\ = \sum_{\beta \neq \alpha} \frac{1}{|\delta V|} \int_{\delta A_{\alpha\beta}} \rho^j (\mathbf{w}_{\alpha\beta_j} - \mathbf{v}^j) \cdot \mathbf{n}^\alpha + \varepsilon^\alpha \overline{\rho^j}^\alpha \hat{r}^j. \end{aligned} \quad (3.16)$$

Rewriting equation (3.16) in terms of the material time derivative and defining

$$\rho^{\alpha_j} \equiv \overline{\rho^j}^\alpha, \quad (3.17)$$

$$\mathbf{v}^{\alpha_j} \equiv \overline{\mathbf{v}^j}^\alpha, \quad (3.18)$$

$$\hat{e}_\beta^{\alpha_j} \equiv \frac{\varepsilon^\alpha}{|\delta V_\alpha|} \int_{\delta A_{\alpha\beta}} \rho^j (\mathbf{w}_{\alpha\beta_j} - \mathbf{v}^j) \cdot \mathbf{n}^\alpha da, \text{ and} \quad (3.19)$$

$$\hat{r}^{\alpha_j} \equiv \varepsilon^\alpha \rho^{\alpha_j} \hat{r}^j \quad (3.20)$$

respectively to be the averaged mass over δV_α , the mass averaged velocity, the net rate of mass gained by constituent j in phase α from phase β , and the rate of mass gain due to interaction with other species within phase α , we get

$$\frac{D^{\alpha_j} (\varepsilon^\alpha \rho^{\alpha_j})}{Dt} + \varepsilon^\alpha \rho^{\alpha_j} \nabla \cdot \mathbf{v}^{\alpha_j} = \sum_{\beta \neq \alpha} \hat{e}_\beta^{\alpha_j} + \hat{r}^{\alpha_j}. \quad (3.21)$$

Next we define the corresponding bulk phase variables so that the macroscale equations are consistent with experimentally measured terms as much as possible.

Define:

$$\rho^\alpha \equiv \sum_{j=1}^N \rho^{\alpha_j}, \text{ and} \quad (3.22)$$

$$C^{\alpha_j} \equiv \frac{\rho^{\alpha_j}}{\rho^\alpha} \quad (3.23)$$

respectively to be the mass density of the α phase, and the mass concentration of the j^{th} constituent in the α phase. If equation (3.21) is rewritten as

$$\frac{\partial (\varepsilon^\alpha \rho^\alpha C^{\alpha_j})}{\partial t} + \nabla \cdot (\varepsilon^\alpha \rho^\alpha C^{\alpha_j} \mathbf{v}^{\alpha_j}) = \sum_{\beta \neq \alpha} \hat{e}_\beta^{\alpha_j} + \hat{r}^{\alpha_j}$$

and then summed over $j = 1 : N$ we obtain a mass balance equation for the α phase:

$$\frac{\partial (\varepsilon^\alpha \rho^\alpha)}{\partial t} + \nabla \cdot (\varepsilon^\alpha \rho^\alpha \mathbf{v}^\alpha) = \sum_{\beta \neq \alpha} \hat{e}_\beta^\alpha. \quad (3.24)$$

Here we have used the fact that $\hat{e}_\beta^\alpha = \sum_{j=1}^N \hat{e}_\beta^{\alpha_j}$; the rate of mass transfer to the α phase from the β phase is the sum of the rates of mass transfer to each individual constituent in the α phase from the β phase.

Now use the definition of the material time derivative to write the mass balance equation for the α phase as

$$\frac{D^\alpha (\varepsilon^\alpha \rho^\alpha)}{Dt} + \varepsilon^\alpha \rho^\alpha \nabla \cdot \mathbf{v}^\alpha = \sum_{\beta \neq \alpha} \hat{e}_\beta^\alpha, \quad (3.25)$$

where the following restrictions have been applied:

$$\sum_{j=1}^N \hat{r}^{\alpha_j} = 0, \quad \forall \alpha, \text{ and} \quad (3.26)$$

$$\sum_{\alpha} \sum_{\beta \neq \alpha} \hat{e}_\beta^{\alpha_j} = 0, \quad j = 1 : N. \quad (3.27)$$

Restriction (3.26) states that the rate of net gain of mass within species α from chemical reactions alone must be zero. Equation (3.27) states that the rate of mass gained by phase α from phase β is equal to the rate of mass gained by phase β from phase α .

3.2.2 Macroscale Momentum Balance

We now turn our attention to the momentum balance equation, (3.14). We can apply the same principles to upscale this equation (for full details see [80]). The macroscopic linear momentum balance equation for constituent j in the α phase is

$$\varepsilon^\alpha \rho^{\alpha_j} \frac{D^{\alpha_j} \mathbf{v}^{\alpha_j}}{Dt} - \nabla \cdot (\varepsilon^\alpha \underline{\underline{\mathbf{t}}}^{\alpha_j}) - \varepsilon^\alpha \rho^{\alpha_j} \mathbf{g}^{\alpha_j} = \hat{\mathbf{i}}^{\alpha_j} + \sum_{\beta \neq \alpha} \hat{\mathbf{T}}_\beta^{\alpha_j}, \quad (3.28)$$

and the macroscopic linear momentum balance equation for the α phase is

$$\varepsilon^\alpha \rho^\alpha \frac{D^\alpha \mathbf{v}^\alpha}{Dt} - \nabla \cdot (\varepsilon^\alpha \underline{\underline{\mathbf{t}}}^\alpha) - \varepsilon^\alpha \rho^\alpha \mathbf{g} = \sum_{\beta \neq \alpha} \hat{\mathbf{T}}_\beta^\alpha, \quad (3.29)$$

where $\underline{\underline{\mathbf{t}}}^{\alpha_j}$ and $\underline{\underline{\mathbf{t}}}^\alpha$ are the Cauchy stress tensors for the species and the phase and $\hat{\mathbf{T}}_\beta^{\alpha_j}$ and $\hat{\mathbf{T}}_\beta^\alpha$ are momentum transfer terms. Most specifically, for the momentum transfer terms, the former represents momentum transferred to constituent j in the α phase through mechanical interactions from phase β , and the latter represents the momentum transferred to phase α through mechanical interactions from phase β . Also notable is the $\hat{\mathbf{i}}^{\alpha_j}$ term. This term represents the rate of momentum gain due to mechanical interactions with other species within the same phase.

In the processes of deriving these equations the following restrictions were enforced:

$$\sum_{j=1}^N \left(\hat{\mathbf{i}}^{\alpha_j} + \hat{r}^{\alpha_j} \mathbf{v}^{\alpha_j, \alpha} \right) = 0 \quad \forall \alpha, \text{ and} \quad (3.30)$$

$$\sum_{\alpha} \sum_{\beta \neq \alpha} \left(\hat{\mathbf{T}}_\beta^{\alpha_j} + \mathbf{v}^{\alpha_j} \hat{e}_\beta^{\alpha_j} \right) = 0 \quad j = 1 : N. \quad (3.31)$$

Restriction (3.30) states that linear momentum can only be lost due to interactions with other phases (not within the species), and restriction (3.31) states that the interface can hold no linear momentum. The comma in the superscript of (3.30) indicates a relative term: $\mathbf{v}^{\alpha_j, \alpha} = \mathbf{v}^{\alpha_j} - \mathbf{v}^\alpha$. For a complete list of notation see Appendix B.1.

Lastly, to tie the momentum transfer and stress tensor for the α phase to those of the species we note two identities that were used in the derivation:

$$\underline{\underline{\mathbf{t}}}^\alpha = \sum_{j=1}^N \left(\underline{\underline{\mathbf{t}}}^{\alpha_j} - \rho^{\alpha_j} \mathbf{v}^{\alpha_j, \alpha} \otimes \mathbf{v}^{\alpha_j, \alpha} \right) \quad (3.32)$$

$$\hat{\mathbf{T}}_\beta^\alpha = \sum_{j=1}^N \left(\hat{\mathbf{T}}_\beta^{\alpha_j} + \hat{e}_\beta^{\alpha_j} \mathbf{v}^{\alpha_j, \alpha} \right). \quad (3.33)$$

These identities will be used later and so are presented here for conciseness.

3.2.3 Macroscale Energy Balance

The derivations for the macroscale angular momentum and energy balance laws are more algebraically complicated. The angular momentum equation will not be used in this work since we assume that we're dealing with granular-type media where the angular momentum balance results in the solid phase Cauchy stress tensor being symmetric [15, 42, 80]. The energy balance equation, on the other hand, will allow us to derive a novel form of the heat equation in porous media. For this reason we state the full equation here.

Applying the same routine as in the mass and linear momentum equations we arrive (after significant simplification) at a balance law for the energy in species j :

$$\varepsilon^\alpha \rho^{\alpha_j} \frac{D^{\alpha_j}(e^{\alpha_j})}{Dt} - \nabla \cdot (\varepsilon^\alpha \mathbf{q}^{\alpha_j}) - \varepsilon^\alpha \underline{\underline{\mathbf{t}}}^{\alpha_j} : \nabla \mathbf{v}^{\alpha_j} - \varepsilon^\alpha \rho^{\alpha_j} h^{\alpha_j} = \hat{Q}^{\alpha_j} + \hat{Q}_\beta^{\alpha_j} \quad (3.34)$$

(see [7, 80] for details on the derivation). Here, h^{α_j} is the external supply of energy, e^{α_j} is the energy density, \mathbf{q}^{α_j} is the partial heat flux vector for the j^{th} component of the α phase, \hat{Q}^{α_j} is the rate of energy gain due to interaction with other species within the α phase, and $\hat{Q}_\beta^{\alpha_j}$ is the rate of energy transfer from the β phase to the α phase not due to mass or momentum transfer.

Again, following the derivation of [80], the bulk phase energy equation is

$$\varepsilon^\alpha \rho^\alpha \frac{D^\alpha e^\alpha}{Dt} - \nabla \cdot (\varepsilon^\alpha \mathbf{q}^\alpha) - \varepsilon^\alpha \underline{\underline{\mathbf{t}}}^\alpha : \nabla \mathbf{v}^\alpha - \varepsilon^\alpha \rho^\alpha h^a = \sum_{\beta \neq \alpha} \hat{Q}_\beta^\alpha \quad (3.35)$$

where

To arrive at this form of the energy equation we enforced the following restrictions:

$$\sum_{j=1}^N \left[\hat{Q}^{\alpha_j} + \hat{\mathbf{i}}^{\alpha_j} \mathbf{v}^{\alpha_j, \alpha} + \hat{r}^{\alpha_j} \left(e^{\alpha_j} + \frac{1}{2} (\mathbf{v}^{\alpha_j, \alpha})^2 \right) \right] = 0 \quad \forall \alpha, \text{ and} \quad (3.36a)$$

$$\sum_{\alpha} \sum_{\beta \neq \alpha} \left[\hat{Q}_{\beta}^{\alpha_j} + \hat{\mathbf{T}}_{\beta}^{\alpha_j} \cdot \mathbf{v}^{\alpha_j} + \hat{e}_{\beta}^{\alpha_j} \left(e^{\alpha_j} + \frac{1}{2} (\mathbf{v}^{\alpha_j, \alpha})^2 \right) \right] = 0 \quad j = 1 : N. \quad (3.36b)$$

Restriction (3.36a) states that energy gained or lost due to species interactions within the α phase must be gained or lost due to interactions with other phases. Restriction (3.36b) states that the rate of energy gained or lost by one component in one phase must go to another component or phase. That is, this second restriction states that the interface retains no energy.

A system of equations governed by mass, momentum, and energy balance requires each of the upscaled equations listed. A count of the variables indicates that there are far more variables than equations. It is at this point where we need a method for deriving constitutive equations for these remaining variables. The method chosen for this work uses another macroscale balance law based on the second law of thermodynamics.

3.3 The Entropy Inequality

The development of constitutive laws is central to the modeling process. As we mentioned previously, this has historically been a process of fitting mathematical models to empirical evidence. The construct of Hybrid Mixture Theory (HMT) couples the averaging theorems discussed in the previous section and the second law of thermodynamics to provide us with restriction on the form of the constitutive relations; hence narrowing down the experiments required to those that are thermodynamically admissible. It is then up to the experimentalists to verify and refine these models. Both theoretical and experimental directions of study have their merits, but

putting the constitutive equations on a firm theoretical footing is ultimately preferred whether it is before or after the experiments are run. In this section we give a brief derivation of the upscaled entropy inequality, and we then use this inequality, along with a judicious choice of variables, to derive constitutive equations for unsaturated porous media.

3.3.1 A Brief Derivation of the Entropy Inequality

The second law of thermodynamics states that entropy will never decrease as a system evolves toward equilibrium [4, 21]. The microscale entropy *balance* equation that describes this phenomenon is

$$\rho^j \frac{D^j \eta^j}{Dt} + \nabla \cdot \boldsymbol{\phi}^j - \rho^j b^j = \hat{\eta}^j + \hat{r}^j \mathbf{v}^j + \hat{\Lambda}, \quad (3.37)$$

where η^j is the entropy density of constituent j , $\boldsymbol{\phi}^j$ is the entropy flux, b^j is the external supply of entropy, $\hat{\eta}^j$ is entropy gained from other constituents, and $\hat{\Lambda}$ is the entropy production. Since the second law of thermodynamics must hold we know that $\hat{\Lambda} \geq 0$ for all time.

Applying Theorem 3.1 to equation (3.37) and defining appropriate macroscale definitions of the variables gives the upscaled entropy balance equation:

$$\varepsilon^\alpha \rho^{\alpha_j} \frac{D^{\alpha_j} \eta^{\alpha_j}}{Dt} - \nabla \cdot (\varepsilon^\alpha \boldsymbol{\phi}^{\alpha_j}) - \varepsilon^\alpha \rho^{\alpha_j} b^{\alpha_j} = \sum_{\beta \neq \alpha} \hat{\Phi}_\beta^{\alpha_j} + \hat{\eta}^{\alpha_j} + \hat{\Lambda}^{\alpha_j}, \quad (3.38)$$

where the terms on the right-hand side of equation (3.38) represent transfer of entropy through mechanical interaction, entropy gained due to interactions with other species, and the rate of entropy generation respectively.

Next, assume that the material we are modeling is *simple* in the sense of Coleman and Noll [26]. This means that we assume that the entropy flux and external supply are due to heat fluxes and sources respectively. To remove the dependence on external heat sources we add ($1/T$ times) the upscaled conservation of energy equation (3.34),

$$\varepsilon^\alpha \rho^{\alpha_j} \frac{D^{\alpha_j} e^{\alpha_j}}{Dt} - \nabla \cdot (\varepsilon^\alpha \mathbf{q}^{\alpha_j}) - \varepsilon^\alpha \underline{\mathbf{t}}^{\alpha_j} : \nabla \mathbf{v}^{\alpha_j} - \varepsilon^\alpha \rho^{\alpha_j} h^{\alpha_j} = \hat{Q}^{\alpha_j} + \sum_{\beta \neq \alpha} \hat{Q}_\beta^{\alpha_j}.$$

At this point we perform a Legendre transformation in order to convert internal energy, e^{α_j} , to Helmholtz potential, ψ^{α_j} (see any thermodynamics text, eg [21]):

$$\psi^{\alpha_j} = e^{\alpha_j} - \eta^{\alpha_j} T. \quad (3.39)$$

This is done because internal energy has entropy as a natural independent variable, and entropy is difficult to measure experimentally. It should be noted that the Helmholtz potential is only one choice of thermodynamic potential we could have made. This is done primarily for historical reasons, but the Gibbs potential and possibly the Grand Canonical potential could have also been viable choices. The appeal of the Helmholtz potential is that it naturally has independent variables of temperature and volume (or, in intensive variables, density).

To arrive at a simplified entropy inequality for the total production of entropy (across all constituents and phases) we now solve for $\hat{\Lambda}^{\alpha_j}$ and then sum over $\alpha = l, g, s$ and $j = 1 : N$. This step requires significant algebra so the details of the derivation are omitted for brevity sake. After much simplification, the entropy inequality becomes

$$\begin{aligned} 0 \leq \hat{\Lambda} = & \sum_{\alpha} \left\{ -\frac{\varepsilon^{\alpha} \rho^{\alpha}}{T} \left(\frac{D^{\alpha} \psi^{\alpha}}{Dt} + \eta^{\alpha} \frac{D^s T}{Dt} \right) \right. \\ & + \frac{\varepsilon^{\alpha}}{T} \left(\sum_{j=1}^N \underline{\underline{\mathbf{t}}}^{\alpha_j} \right) : \underline{\underline{\mathbf{d}}}^{\alpha} \\ & + \frac{\varepsilon^{\alpha} \nabla T}{T^2} \cdot \left\{ \mathbf{q}^{\alpha} - \sum_{j=1}^N \left(\underline{\underline{\mathbf{t}}}^{\alpha_j} \cdot \mathbf{v}^{\alpha_j, \alpha} - \rho^{\alpha_j} \mathbf{v}^{\alpha_j, \alpha} \left(\psi^{\alpha_j} + \frac{1}{2} \mathbf{v}^{\alpha_j, \alpha} \cdot \mathbf{v}^{\alpha_j, \alpha} \right) \right) \right\} \\ & - \frac{1}{T} \sum_{j=1}^N \left\{ \left(\sum_{\beta \neq \alpha} \hat{\mathbf{T}}_{\beta}^{\alpha_j} \right) + \hat{\mathbf{i}}^{\alpha_j} + \nabla (\varepsilon^{\alpha} \rho^{\alpha_j} \psi^{\alpha_j}) \right\} \cdot \mathbf{v}^{\alpha_j, \alpha} \\ & + \frac{\varepsilon^{\alpha}}{T} \sum_{j=1}^N \left(\underline{\underline{\mathbf{t}}}^{\alpha_j} - \rho^{\alpha_j} \psi^{\alpha_j} \underline{\underline{\mathbf{I}}} \right) : \nabla \mathbf{v}^{\alpha_j, \alpha} \\ & - \frac{1}{T} \sum_{\beta \neq \alpha} \left\{ \hat{\mathbf{T}}_{\beta}^{\alpha} + \varepsilon^{\alpha} \rho^{\alpha} \eta^{\alpha} \nabla T \right\} \cdot \mathbf{v}^{\alpha, s} \\ & - \frac{1}{2T} \sum_{j=1}^N \left\{ \left(\sum_{\beta \neq \alpha} \hat{\mathbf{e}}_{\beta}^{\alpha_j} \right) + \hat{r}^{\alpha_j} \right\} \mathbf{v}^{\alpha_j, \alpha} \cdot \mathbf{v}^{\alpha_j, \alpha} \end{aligned}$$

$$-\frac{1}{T} \sum_{\beta \neq \alpha} \left\{ \hat{e}_{\beta}^{\alpha} \left(\psi^{\alpha} + \frac{1}{2} \mathbf{v}^{\alpha,s} \cdot \mathbf{v}^{\alpha,s} \right) \right\}, \quad (3.40)$$

where $\hat{\Lambda}$ is the rate of entropy generation.

Several new terms have appeared in (3.40). First, $\underline{\underline{\mathbf{d}}}^{\alpha} = (\nabla \mathbf{v}^{\alpha})_{sym}$ is the rate of deformation tensor (also known as the strain rate). As before, terms with a comma in the superscript are relative terms: $\mathbf{v}^{a,b} = \mathbf{v}^a - \mathbf{v}^b$.

Several identities were needed to derive (3.40). A complete list of these identities has been included in Appendix B.3. The next step is to expand the Helmholtz potential in terms of constitutive independent variables that describe our system. This allows freedom to make choices about which variables control behavior of the system. The choice of these variables is generally non-trivial so in the next section we discuss motivations for the choice of variables.

4. New Independent Variables and Exploitation of the Entropy Inequality

Now that we have an expression for the entropy inequality we must choose a set of independent variables that describes our system of interest. We seek to describe a multiphase system where the solid phase may undergo finite deformation, where the relative saturations of the two fluid phases vary in time and space, and where phase changes between the fluids possibly occurs throughout the porous medium. Hassanizadeh and Gray have modeled similar media in the past [40, 43, 44]. These models include effects from common interfaces, common lines (where three phases meet), and common points (where four phases meet). These models are very thorough and follow the same HMT approach. The down sides to their models, in the author's opinion, are three fold: (1) the complexity of the resulting equations is such that in order to use these equations a host of simplifying assumptions must be made, (2) the thermodynamics of the common points and lines make sense physically but are likely negligible relative to other effects, and (3) constitutive equations must be derived for transfer rates between interfaces, common lines, common points, and phases. This final drawback indicates that a detailed knowledge of the pore-scale physics must be somehow upscaled. Approaches have been taken recently to do just this, but the proposed theories have not yet gained widespread acceptance. Examples of such work include those of Gray et al. [41, 39]

In the present approach we choose not to directly model interfaces and instead strive to eventually write our governing equations in terms of the macroscale chemical potential. The chemical potential is known from physical chemistry and thermodynamics as a *generalized driving force* that is a function of pressure and temperature. It is well known that mass transfer from liquid to gas states is driven by gradients of chemical potential [55], so if we can write constitutive equations (such as Darcy's, Fick's, and Fourier's laws) in terms of this potential we can possibly couple the rele-

vant effects into much simpler governing equations; for example, equations that track changes in chemical potential instead of pressure or concentration. The immediate drawback to the present modeling efforts is that the recent work by Hassanizadeh et al. seems to indicate that saturation and capillary pressure are linked to the amount of interfacial area between phases within the medium [20, 47]. In the present work we will not directly model the fluid-fluid and fluid-solid interfaces. We proceed with the present modeling effort despite the results proposed by Hassanizadeh et al. We will discuss this drawback as we run up against it in future sections and chapters.

4.1 A Choice of Independent Variables

In this section we present a choice of independent variables for the Helmholtz free energy (potential) so as to expand the entropy inequality and to derive the relevant forms of Darcy’s law, Fick’s law, and Fourier’s law. These variables are known as *constitutive* independent variables as they represent a postulation of the variables that control the energy in the system. “Deriving physically meaningful results depends on our ability to relate thermodynamically defined variables to physically interpretable quantities” [80]. To that end, we use our a priori knowledge of thermodynamics to choose some of the variables. For the remainder of this work we restrict our attention to a three-phase system consisting of an elastic solid, a viscous liquid phase, and a gas phase. To begin the modeling process we assume that each of these phases consists of N constituents (also called species or components), and all interfacial effects are neglected. Examples of the constituents include dissolved minerals in the liquid, species evaporated into the gas, or precipitated minerals associated with the solid phase.

The motivation for choosing some of the variables is relatively trivial. For example, to allow for a heat conducting medium, temperature, T , and the gradient of temperature, ∇T , are included in the list of independent variables. The pore space is expected to be variably saturated with the two fluid phases so the volume fractions,

ε^l and ε^g , must be included in the set of variables. The fact that $\sum_{\alpha} \varepsilon^{\alpha} = 1$ precludes us from using all three volume fractions since they are not independent of each other. In future chapters we will further restrict this assumption since for a rigid solid phase the sum of the fluid phase volume fractions is equal to the fixed porosity

$$\varepsilon^l + \varepsilon^g = \varepsilon. \quad (4.1)$$

The reason for not making this assumption initially is that it allows us to develop models for deformable media as well as for media with a rigid solid phase (hence, a more general model may be derived from these assumptions later if necessary).

Recall from thermodynamics that the change in extensive Helmholtz potential, A , with respect to volume is minus the pressure: $\partial A / \partial V = -p$. In terms of intensive variables this means that $\rho^2 \partial \psi / \partial \rho = -p$. To remain consistent with the extensive definition of the Helmholtz potential, the densities must then be included in the set of independent variables. Given the fact that there are N constituents in each phase, this could be done in two different ways: (1) we could include the mass concentrations, C^{α_j} , for $j = 1 : N - 1$ along with the phase density, or (2) we could include all of the constituent densities, ρ^{α_j} for $j = 1 : N$. Bennethum, Murad, and Cushman [15], and also Weinstein [80] took the first of these options when using HMT to derive constitutive relations involving chemical potentials. The trouble with this approach is that the mass concentration of the N^{th} constituent is dependent on the mass concentrations of the previous $N - 1$ constituents (since the concentrations sum to 1). These results indicate that the behavior of the constituents depends on how they are labeled instead of simply being independent. Various techniques were successfully developed in [15] to deal with this complication. To avoid these complications we choose the second option and include the species densities, ρ^{α_j} for $j = 1 : N$. Since each constituent is free to move within each phase, the spatial gradients of the species densities, $\nabla \rho^{l_j}$ and $\nabla \rho^{g_j}$, are also included.

Darcy’s law and Fick’s law are classical empirical expressions for creeping flow and constitutive diffusion. Darcy’s law is a statement about the relative velocity of a fluid phase in a porous medium, and Fick’s law is a statement about the relative diffusive velocity of a species within a phase. Since we seek novel forms of these two laws we include $\mathbf{v}^{\alpha,s}$ and $\mathbf{v}^{\alpha_j,\alpha}$ for $\alpha = l, g, s$ in the list of independent variables. It should be noted that neither of these variables is *objective* in the sense that they are not frame invariant. This poses a problem since any governing equation should not depend on an observer’s frame of reference. In [33], Eringen proposed a modification to Darcy’s law that creates a frame invariant relative velocity. The new terms needed for this new relative velocity are second order and are assumed to be negligible in Darcy flow. A similar argument can be used for Fick’s law.

The reasoning given in the previous few paragraphs leads us to the set of independent variables for ψ^α to include:

$$T, \nabla T, \varepsilon^l, \varepsilon^g, \rho^{lj}, \rho^{gj}, \nabla \rho^{lj}, \nabla \rho^{gj}, \mathbf{v}^{l,s}, \mathbf{v}^{g,s}, \mathbf{v}^{lj,l}, \mathbf{v}^{gj,g}, \text{ and } \mathbf{v}^{sj,s}$$

where $j = 1 : N$. It is apparent, now, that solid-phase terms corresponding to the density and gradient of density are missing. The principle of equipresence, from constitutive theory in continuum mechanics, states that “all constitutive variables are a function of the same set of independent variables” [68]. To give symmetry between the phases we include ρ^s and $\nabla \rho^s$. The Stokes assumption for the Cauchy stress tensor in a viscous fluid states that stress is the sum of the fluid pressure and the strain rate. For this reason we include the strain rate (also known as the rate of deformation tensor) for the fluid phases: $\underline{\underline{\mathbf{d}}^l}$ and $\underline{\underline{\mathbf{d}}^g}$. The theory of equipresence also states that if we include strain rate in the fluid phases then we must include a comparable term in the solid phase.

A natural choice of variables for the solid phase are the solid phase volume fraction, density, and the (averaged) strain. Weinstein [80] pointed out that these three variables are not independent, as explained below, and used a modified set of inde-

pendent variables for the solid phase. The same modified set will be used here, so the following simply states Weinstein’s results with brief derivations.

Let J^s be the Jacobian of the solid phase given by $J^s = \det((\underline{\underline{\mathbf{F}}^s})^T \cdot \underline{\underline{\mathbf{F}}^s})$, where $\underline{\underline{\mathbf{F}}^s}$ is the deformation gradient

$$\underline{\underline{\mathbf{F}}^s} = \frac{\partial x_k^s}{\partial X_K^s}, \quad (4.2)$$

\mathbf{x}^s is the Eulerian coordinate, and \mathbf{X}^s is the Lagrangian coordinate. Using standard identities from Continuum Mechanics, the Jacobian can be rewritten as

$$J^s = \det(2\underline{\underline{\mathbf{E}}^s} + \underline{\underline{\mathbf{I}}}). \quad (4.3)$$

Furthermore, through the conservation of mass, the Jacobian is also a scaling factor for volumetric changes, $J^s = (\varepsilon_0^s \rho_0^s) / (\varepsilon^s \rho^s)$. This clearly shows the dependence of the three variables. To mitigate this issue, Weinstein [80] adopted ideas from solid mechanics and considered a “multiplicative decomposition” of the deformation gradient, $\underline{\underline{\mathbf{F}}^s}$, and the Green’s deformation tensor, $\underline{\underline{\mathbf{C}}^s}$, as

$$\underline{\underline{\mathbf{C}}^s} = (J^s)^{2/3} \overline{\underline{\underline{\mathbf{C}}^s}}, \quad (4.4)$$

$$\underline{\underline{\mathbf{F}}^s} = (J^s)^{1/3} \overline{\underline{\underline{\mathbf{F}}^s}}, \quad (4.5)$$

where $(J^s)^{1/3} \underline{\underline{\mathbf{I}}}$ and $(J^s)^{2/3} \underline{\underline{\mathbf{I}}}$ represent volumetric deformation, and “ $\overline{\underline{\underline{\mathbf{F}}^s}}$ and $\overline{\underline{\underline{\mathbf{C}}^s}}$ are the modified deformation gradient and the modified right Cauchy-Green tensor, respectively.” With this modification to the solid strain, the solid phase variables we consider here are $J^s, \overline{\underline{\underline{\mathbf{C}}^s}}, C^{sk}$ and ∇C^{sk} where $k = 1 : N - 1$. We note here that in order to get physically meaningful results for phase change, we include the same components, so that C^{sj}, C^{lj} , and C^{gj} all refer to the same component. Pairing the mass concentrations and the Jacobian gives a description of the density of the solid phase, and the modified Cauchy-Green tensor is used in place of strain.

The principle of equipresence states that all of the constitutive variables must be a function of the same set of the postulated independent variables. In particular, we

postulate that the Helmholtz potential for each phase is a function of the following set of variables:

$$\{T, \nabla T, \varepsilon^l, \varepsilon^g, \rho^{lj}, \rho^{gj}, \nabla \rho^{lj}, \nabla \rho^{gj}, \mathbf{v}^{\alpha,s}, \underline{\mathbf{d}}^l, \underline{\mathbf{d}}^g, \mathbf{v}^{\alpha_j, \alpha}, J^s, \overline{\mathbf{C}}^s, C^{sk}, \nabla C^{sk}\}, \quad (4.6)$$

where $\alpha = l, g, s$; $j = 1 : N$ and $k = 1 : N - 1$. We postulate that a three phase porous medium with an elastic solid phase and N constituents per phase can be modeled by set (4.6).

4.1.1 The Expanded Entropy Inequality

Consider now that the first line of the entropy inequality, (3.40), contains a material time derivative of the Helmholtz potential for the α phase. Using the identity

$$\frac{D^\alpha(\cdot)}{Dt} = \frac{D^s(\cdot)}{Dt} + \mathbf{v}^{\alpha,s} \cdot \nabla(\cdot), \quad (4.7)$$

and applying the chain rule, the entropy inequality can be expanded to include each of our constitutive independent variables. The central idea to the exploitation of the second law of thermodynamics is that no term in the entropy inequality can take values such that entropy generation is negative. A close examination of the expanded entropy inequality reveals that there are many terms that show up linearly. In these linear terms we notice some that are neither independent nor constitutive. Examples of such coefficients are ∇T , ∇C^{sj} , $\nabla \rho^{lj}$, $\nabla \rho^{gj}$, $\underline{\mathbf{d}}^l$, $\underline{\mathbf{d}}^g$, $\mathbf{v}^{l,s}$, $\mathbf{v}^{g,s}$, $\mathbf{v}^{s_j,s}$, $\mathbf{v}^{l_j,l}$, $\mathbf{v}^{g_j,g}$, \dot{T} , $\dot{\rho}^{\alpha_j}$, and $\nabla \mathbf{v}^{\alpha_j, \alpha}$ (where the dot notation (e.g. \dot{T}) indicates a material time derivative). Loosely speaking, we have no control over these variables and they could take values that violate the second law. For example, take as a thought experiment a process where all of these variables except \dot{T} are zero. From Bennethum [10],

“Since none of the other terms in the entropy inequality are a function of \dot{T} , by varying the value of \dot{T} we can make the left-hand side of the entropy inequality as large positive or as large negative as we want - hence violating the entropy inequality. Since the entropy inequality must hold

for all processes (including those for which T is any value), the entropy inequality can be violated unless the coefficient of \dot{T} is zero.”

In order not to violate the inequality in (4.13), the coefficients of all of these factors must be zero. This implies that terms such as $\sum_{\alpha} (\varepsilon^{\alpha} \rho^{\alpha} \frac{\partial \psi^{\alpha}}{\partial \nabla T})$ are zero and will therefore be left out of the expansion of (3.40) for brevity. The time rates of change of volume fractions are not this type of variable since they are constitutive; that is, we assume a rule for the time rates of change of volume fractions that depends on the specific medium of interest.

With this simplification in mind, (3.40) becomes

$$\begin{aligned}
T\Lambda = & \sum_{\alpha} \varepsilon^{\alpha} \rho^{\alpha} \left(\frac{\partial \psi^{\alpha}}{\partial T} + \eta^{\alpha} \right) \dot{T} - \sum_{\alpha} \left(\varepsilon^{\alpha} \rho^{\alpha} \frac{\partial \psi^{\alpha}}{\partial \varepsilon^l} \right) \dot{\varepsilon}^l - \sum_{\alpha} \left(\varepsilon^{\alpha} \rho^{\alpha} \frac{\partial \psi^{\alpha}}{\partial \varepsilon^g} \right) \dot{\varepsilon}^g \\
& - \sum_{\alpha} \sum_{j=1}^{N-1} \left(\varepsilon^{\alpha} \rho^{\alpha} \frac{\partial \psi^{\alpha}}{\partial C^{s_j}} \right) \dot{C}^{s_j} \\
& - \sum_{\alpha} \sum_{j=1}^N \left(\varepsilon^{\alpha} \rho^{\alpha} \frac{\partial \psi^{\alpha}}{\partial \rho^{l_j}} \right) \dot{\rho}^{l_j} - \sum_{\alpha} \sum_{j=1}^N \left(\varepsilon^{\alpha} \rho^{\alpha} \frac{\partial \psi^{\alpha}}{\partial \rho^{g_j}} \right) \dot{\rho}^{g_j} \\
& - \sum_{\alpha} \left(\varepsilon^{\alpha} \rho^{\alpha} \frac{\partial \psi^{\alpha}}{\partial J^s} \right) \dot{J}^s - \sum_{\alpha} \left(\varepsilon^{\alpha} \rho^{\alpha} \frac{\partial \psi^{\alpha}}{\partial (\underline{\underline{C}}^s)} \right) : \underline{\underline{\dot{C}}}^s \\
& - \left[\varepsilon^l \rho^l \left\{ \left(\frac{\partial \psi^l}{\partial T} + \eta^l \right) \nabla T + \frac{\partial \psi^l}{\partial \varepsilon^l} \nabla \varepsilon^l + \frac{\partial \psi^l}{\partial \varepsilon^g} \nabla \varepsilon^g \right. \right. \\
& \quad \left. \left. + \sum_{j=1}^{N-1} \frac{\partial \psi^l}{\partial C^{s_j}} \nabla C^{s_j} + \sum_{j=1}^N \frac{\partial \psi^l}{\partial \rho^{l_j}} \nabla \rho^{l_j} + \sum_{j=1}^N \frac{\partial \psi^l}{\partial \rho^{g_j}} \nabla \rho^{g_j} \right. \right. \\
& \quad \left. \left. + \frac{\partial \psi^l}{\partial J^s} \nabla J^s + \frac{\partial \psi^l}{\partial \underline{\underline{C}}^s} : \nabla (\underline{\underline{C}}^s) \right\} + \hat{T}_s^l + \hat{T}_g^l \right] \cdot \mathbf{v}^{l,s} \\
& - \left[\varepsilon^g \rho^g \left\{ \left(\frac{\partial \psi^g}{\partial T} + \eta^g \right) \nabla T + \frac{\partial \psi^g}{\partial \varepsilon^l} \nabla \varepsilon^l + \frac{\partial \psi^g}{\partial \varepsilon^g} \nabla \varepsilon^g \right. \right. \\
& \quad \left. \left. + \sum_{j=1}^{N-1} \frac{\partial \psi^g}{\partial C^{s_j}} \nabla C^{s_j} + \sum_{j=1}^N \frac{\partial \psi^g}{\partial \rho^{l_j}} \nabla \rho^{l_j} + \sum_{j=1}^N \frac{\partial \psi^g}{\partial \rho^{g_j}} \nabla \rho^{g_j} \right. \right. \\
& \quad \left. \left. + \frac{\partial \psi^g}{\partial J^s} \nabla J^s + \frac{\partial \psi^g}{\partial \underline{\underline{C}}^s} : \nabla (\underline{\underline{C}}^s) \right\} + \hat{T}_s^g + \hat{T}_l^g \right] \cdot \mathbf{v}^{g,s} \\
& + \sum_{\alpha} \left[\varepsilon^{\alpha} \left(\sum_{j=1}^N \underline{\underline{t}}^{\alpha_j} \right) : \underline{\underline{d}}^{\alpha} \right]
\end{aligned}$$

$$\begin{aligned}
& + \sum_{\alpha} \left[\frac{\varepsilon^{\alpha} \nabla T}{T} \cdot \left\{ \mathbf{q}^{\alpha} - \sum_{j=1}^N \left(\underline{\mathbf{t}}^{\alpha_j} \cdot \mathbf{v}^{\alpha_j, \alpha} - \rho^{\alpha_j} \mathbf{v}^{\alpha_j, \alpha} \left(\psi^{\alpha_j} + \frac{1}{2} (\mathbf{v}^{\alpha_j, \alpha})^2 \right) \right) \right\} \right] \\
& - \sum_{\alpha} \sum_{j=1}^N \left\{ \left(\sum_{\beta \neq \alpha} \hat{\mathbf{T}}_{\beta}^{\alpha_j} \right) + \hat{\mathbf{i}}^{\alpha_j} + \nabla (\varepsilon^{\alpha} \rho^{\alpha_j} \psi^{\alpha_j}) \right\} \cdot \mathbf{v}^{\alpha_j, \alpha} \\
& + \sum_{\alpha} \left\{ \varepsilon^{\alpha} \sum_{j=1}^N \left(\underline{\mathbf{t}}^{\alpha_j} - \rho^{\alpha_j} \psi^{\alpha_j} \underline{\mathbf{I}} \right) : \nabla \mathbf{v}^{\alpha_j, \alpha} \right\} \\
& - \frac{1}{2} \sum_{\alpha} \sum_{j=1}^N \left\{ \left(\sum_{\beta \neq \alpha} \hat{\varepsilon}_{\beta}^{\alpha_j} \right) + \hat{r}^{\alpha_j} \right\} (\mathbf{v}^{\alpha_j, \alpha})^2 \\
& - \sum_{\alpha} \sum_{\beta \neq \alpha} \left\{ \hat{\varepsilon}_{\beta}^{\alpha} \left(\psi^{\alpha} + \frac{1}{2} (\mathbf{v}^{\alpha, s})^2 \right) \right\} \geq 0 \tag{4.8}
\end{aligned}$$

The next step is to enforce two additional relationships using Lagrange multipliers. In doing so, the Lagrange multipliers become unknowns of the system. We will see in subsequent sections that the Lagrange multipliers are associated with partial pressures and chemical potentials of species in the fluid phases. The first relationship considered is the dependence of the diffusive velocities:

$$\sum_{j=1}^N (C^{\alpha_j} \mathbf{v}^{\alpha_j, \alpha}) = \mathbf{0}. \tag{4.9}$$

One can see this since

$$\sum_{j=1}^N C^{\alpha_j} \mathbf{v}^{\alpha_j, \alpha} = \sum_{j=1}^N C^{\alpha_j} \mathbf{v}^{\alpha_j} - \sum_{j=1}^N C^{\alpha_j} \mathbf{v}^{\alpha} = \mathbf{v}^{\alpha} - \mathbf{v}^{\alpha} = \mathbf{0}. \tag{4.10}$$

The implication is that if we know the concentrations and diffusive velocities of the first $N - 1$ constituents, then we would know the concentration and diffusive velocity of the N^{th} constituent. Multiplying by the density, taking the gradient, and using the product rule gives the following relationship:

$$\nabla \left(\sum_{j=1}^N \rho^{\alpha_j} \mathbf{v}^{\alpha_j, \alpha} \right) = \sum_{j=1}^N (\rho^{\alpha_j} \nabla \mathbf{v}^{\alpha_j, \alpha} + \mathbf{v}^{\alpha_j, \alpha} \nabla \rho^{\alpha_j}) = \mathbf{0}. \tag{4.11}$$

Following Bennethum, Murad, and Cushman [15], we enforce this relationship with a Lagrange multiplier so as to account for the N^{th} term dependence.

The second relationship to be enforced with Lagrange multipliers is the mass balance equation for each of the constituents (3.21):

$$\frac{D^{\alpha_j} (\varepsilon^\alpha \rho^{\alpha_j})}{Dt} + \varepsilon^\alpha \rho^{\alpha_j} \nabla \cdot \mathbf{v}^{\alpha_j} = \sum_{\beta \neq \alpha} \hat{e}_\beta^{\alpha_j} + \hat{r}^{\alpha_j}.$$

Let Λ_{old} denote Λ from equation (4.8), and let λ^{α_j} and $\underline{\lambda}^{\alpha_N}$ be the Lagrange multipliers for the mass balance and N^{th} term dependencies, (4.11), respectively.

The entropy inequality is rewritten as follows:

$$\begin{aligned} \Lambda_{new} = & \Lambda_{old} + \sum_{\alpha} \sum_{j=1}^N \frac{\lambda^{\alpha_j}}{T} \left[\frac{D^{\alpha_j} (\varepsilon^\alpha \rho^{\alpha_j})}{Dt} + \varepsilon^\alpha \rho^{\alpha_j} \nabla \cdot \mathbf{v}^{\alpha_j} - \left(\sum_{\beta \neq \alpha} \hat{e}_\beta^{\alpha_j} + \hat{r}^{\alpha_j} \right) \right] \\ & + \sum_{\alpha} \sum_{j=1}^N \frac{\varepsilon^\alpha}{T} \underline{\lambda}^{\alpha_N} : \nabla (\rho^{\alpha_j} \mathbf{v}^{\alpha_j, \alpha}). \end{aligned} \quad (4.12)$$

After a significant amount of algebraic simplification (with no additional physical assumptions), this yields the following form of the entropy inequality:

$$\begin{aligned} T\Lambda = & \sum_{\alpha} \left\{ \varepsilon^\alpha \rho^\alpha \left(\frac{\partial \psi^\alpha}{\partial T} + \eta^\alpha \right) \right\} \dot{T} \\ & - \sum_{\beta=l,g} \left\{ \left[\sum_{\alpha} \left(\varepsilon^\alpha \rho^\alpha \frac{\partial \psi^\alpha}{\partial \varepsilon^\beta} \right) - \sum_{j=1}^N (\lambda^{\beta_j} \rho^{\beta_j}) \right] \dot{\varepsilon}^\beta \right\} \\ & - \sum_{j=1}^{N-1} \left[\left(\sum_{\alpha} \varepsilon^\alpha \rho^\alpha \frac{\partial \psi^\alpha}{\partial C^{s_j}} \right) - \lambda^{s_j} \varepsilon^s \rho^s \right] \dot{C}^{s_j} \\ & - \sum_{\beta=l,g} \left\{ \sum_{j=1}^N \left[\left(\sum_{\alpha} \varepsilon^\alpha \rho^\alpha \frac{\partial \psi^\alpha}{\partial \rho^{\beta_j}} \right) - \lambda^{\beta_j} \varepsilon^\beta \right] \dot{\rho}^{\beta_j} \right\} \\ & - \left[\sum_{\alpha} \left(\varepsilon^\alpha \rho^\alpha \frac{\partial \psi^\alpha}{\partial J^s} \right) - \frac{1}{3} \frac{\varepsilon^s}{J^s} \left(\sum_{j=1}^N tr(\underline{\mathbf{t}}^{s_j}) \right) \right] \dot{J}^s \\ & - \left[\sum_{\alpha} \left(\varepsilon^\alpha \rho^\alpha \frac{\partial \psi^\alpha}{\partial (\underline{\mathbf{C}}^s)} \right) - \frac{\varepsilon^s}{2} \left((\underline{\mathbf{F}}^s)^{-1} \cdot \left(\sum_{j=1}^N \underline{\mathbf{t}}^{s_j} \right) \cdot (\underline{\mathbf{F}}^s)^{-T} \right) \right. \\ & \quad \left. - \frac{\varepsilon^s}{2} \left((\underline{\mathbf{F}}^s)^{-1} \cdot (\underline{\mathbf{F}}^s)^{-T} \right) \left(\sum_{j=1}^N \lambda^{s_j} \rho^{s_j} \right) \right] : \dot{\underline{\mathbf{C}}}^s \\ & - \sum_{\substack{\beta=l,g \\ \gamma \neq \beta}} \left\{ \left[\varepsilon^\beta \rho^\beta \left\{ \left(\frac{\partial \psi^\beta}{\partial T} + \eta^\beta \right) \nabla T + \sum_{j=1}^{N-1} \frac{\partial \psi^\beta}{\partial C^{s_j}} \nabla C^{s_j} \right. \right. \right. \end{aligned}$$

$$\begin{aligned}
& + \left(\frac{\partial \psi^\beta}{\partial \varepsilon^\beta} - \frac{1}{\varepsilon^\beta \rho^\beta} \sum_{j=1}^N \lambda^{\beta_j} \rho^{\beta_j} \right) \nabla \varepsilon^\beta + \frac{\partial \psi^\beta}{\partial \varepsilon^\gamma} \nabla \varepsilon^\gamma \\
& + \sum_{j=1}^N \left(\frac{\partial \psi^\beta}{\partial \rho^{\beta_j}} - \frac{\lambda^{\beta_j}}{\rho^\beta} \right) \nabla \rho^{\beta_j} + \sum_{j=1}^N \frac{\partial \psi^\beta}{\partial \rho^{\gamma_j}} \nabla \rho^{\gamma_j} \\
& + \left. \frac{\partial \psi^\beta}{\partial J^s} \nabla J^s + \frac{\partial \psi^\beta}{\partial \underline{\underline{C}}^s} : \nabla (\underline{\underline{C}}^s) \right\} + \hat{\mathbf{T}}_s^\beta + \hat{\mathbf{T}}_\gamma^\beta \Big] \cdot \mathbf{v}^{\beta,s} \Big\} \\
& + \sum_{\beta=l,g} \left\{ \varepsilon^\beta \sum_{j=1}^N (\underline{\mathbf{t}}^{\beta_j} + \lambda^{\beta_j} \rho^{\beta_j} \underline{\mathbf{I}}) : \underline{\mathbf{d}}^\beta \right\} \\
& + \sum_\alpha \left[\frac{\varepsilon^\alpha \nabla T}{T} \cdot \left\{ \mathbf{q}^\alpha - \sum_{j=1}^N \left(\underline{\mathbf{t}}^{\alpha_j} \cdot \mathbf{v}^{\alpha_j,\alpha} \right. \right. \right. \\
& \qquad \qquad \qquad \left. \left. \left. - \rho^{\alpha_j} \mathbf{v}^{\alpha_j,\alpha} \left(\psi^{\alpha_j} + \frac{1}{2} \mathbf{v}^{\alpha_j,\alpha} \cdot \mathbf{v}^{\alpha_j,\alpha} \right) \right) \right\} \right] \\
& - \sum_\alpha \sum_{j=1}^N \left\{ \left(\sum_{\beta \neq \alpha} \hat{\mathbf{T}}_\beta^{\alpha_j} \right) + \hat{\mathbf{i}}^{\alpha_j} + \nabla (\varepsilon^\alpha \rho^{\alpha_j} \psi^{\alpha_j}) \right. \\
& \qquad \qquad \left. - \lambda^{\alpha_j} \nabla (\varepsilon^\alpha \rho^{\alpha_j}) - \varepsilon^\alpha \underline{\underline{\lambda}}^{\alpha_N} \cdot \nabla \rho^{\alpha_j} \right\} \cdot \mathbf{v}^{\alpha_j,\alpha} \\
& + \sum_\alpha \sum_{j=1}^N \left\{ \varepsilon^\alpha \underline{\mathbf{t}}^{\alpha_j} + \varepsilon^\alpha \rho^{\alpha_j} (\lambda^{\alpha_j} - \psi^{\alpha_j}) \underline{\mathbf{I}} + \varepsilon^\alpha \rho^{\alpha_j} \underline{\underline{\lambda}}^{\alpha_N} \right\} : \nabla \mathbf{v}^{\alpha_j,\alpha} \\
& - \sum_\alpha \sum_{j=1}^N \left\{ \hat{r}^{\alpha_j} \left(\lambda^{\alpha_j} + \frac{1}{2} (\mathbf{v}^{\alpha_j,\alpha})^2 \right) \right\} \\
& - \sum_{j=1}^N \hat{e}_g^{l_j} \left\{ (\lambda^{l_j} + \psi^{l_j}) - (\lambda^{g_j} + \psi^{g_j}) \right. \\
& \qquad \qquad \left. + \frac{1}{2} \left((\mathbf{v}^{l,s})^2 - (\mathbf{v}^{g,s})^2 \right) + \frac{1}{2} \left((\mathbf{v}^{l_j,l})^2 - (\mathbf{v}^{g_j,g})^2 \right) \right\} \\
& - \sum_{j=1}^N \hat{e}_l^{s_j} \left\{ (\lambda^{s_j} + \psi^{s_j}) - (\lambda^{l_j} + \psi^{l_j}) - \frac{1}{2} (\mathbf{v}^{l,s})^2 + \frac{1}{2} \left((\mathbf{v}^{s_j,s})^2 - (\mathbf{v}^{l_j,l})^2 \right) \right\} \\
& - \sum_{j=1}^N \hat{e}_s^{g_j} \left\{ (\lambda^{g_j} + \psi^{g_j}) - (\lambda^{s_j} + \psi^{s_j}) + \frac{1}{2} (\mathbf{v}^{g,s})^2 + \frac{1}{2} \left((\mathbf{v}^{g_j,g})^2 - (\mathbf{v}^{s_j,s})^2 \right) \right\} \geq 0
\end{aligned} \tag{4.13}$$

The exploitation of equation (4.13) will be the source of all of the constitutive relations for the remainder of this work. The next section outlines the details of this exploitation to form constitutive relations specific to multiphase media governed by

our choice of constitutive independent variables, (4.6).

4.2 Exploiting the Entropy Inequality

In this section we exploit the entropy inequality, (4.13), in the sense of Colman and Noll [26]. The basic principle here is that, according to the second law of thermodynamics, entropy is always non-decreasing as time evolves. This fact is used to extract constitutive relationships from the entropy inequality. Not every result from this exploitation is relevant to the current study, so we only present the more notable and useful results in the next subsections. Furthermore, we exploit equation (4.13) with an eye toward deformable, multiphase, media. The assumption of deformable media will be removed in the future, but this leaves open the possibility of returning to these results for future work. For an abstract summary of how the exploitation of the entropy inequality works, along with subtle but important assumptions, see Appendix C.

4.2.1 Results That Hold For All Time

As mentioned in Section 4.1.1, several of the terms that appear linearly in the entropy inequality have factors that are neither independent nor constitutive. We now use this fact to derive relationships that must hold for all time in order to not violate the second law of thermodynamics. To illustrate this point consider the coefficient of \dot{T} . If this coefficient is set to zero we recover with the thermodynamic constraint that temperature and entropy are conjugate variables,

$$\frac{\partial \psi^\alpha}{\partial T} = -\eta^\alpha. \quad (4.14)$$

This is a classical result known from thermodynamics.

4.2.1.1 Fluid Lagrange Multipliers

For the gas and liquid phases, the definitions of the Lagrange multipliers stem from the coefficient of $\dot{\rho}^{\alpha_j}$ and $\nabla \mathbf{v}^{\alpha_j, \alpha}$. Setting the coefficient of $\dot{\rho}^{\alpha_j}$ to zero gives the definition of the Lagrange multiplier for the mass balance equations:

$$\lambda^{\beta_j} = \sum_{\alpha} \frac{\varepsilon^{\alpha} \rho^{\alpha}}{\varepsilon^{\beta}} \frac{\partial \psi^{\alpha}}{\partial \rho^{\beta_j}}. \quad (4.15)$$

Setting the coefficient of $\nabla \mathbf{v}^{\alpha_j, \alpha}$ to zero, summing over $j = 1 : N$, and solving for $\underline{\underline{\lambda}}^{\alpha_N}$ yields an expression for the other Lagrange multiplier:

$$\underline{\underline{\lambda}}^{\alpha_N} = -\frac{1}{\rho^{\alpha}} \sum_{j=1}^N [\underline{\underline{\mathbf{t}}}^{\alpha_j} + (\rho^{\alpha_j} \lambda^{\alpha_j}) \underline{\underline{\mathbf{I}}}] + \psi^{\alpha} \underline{\underline{\mathbf{I}}}. \quad (4.16)$$

4.2.1.2 Solid Phase Identities

Several identities for the solid phase can be derived from the terms associated with the time derivatives of the solid phase Jacobian, \dot{J}^s , and the modified Cauchy-Green, $\underline{\underline{\dot{\mathbf{C}}}}^s$ terms. From the \dot{J}^s term we see that

$$\frac{1}{3} \sum_{j=1}^N \text{tr}(\underline{\underline{\mathbf{t}}}^{s_j}) = \frac{J^s}{\varepsilon^s} \sum_{\alpha} \left(\varepsilon^{\alpha} \rho^{\alpha} \frac{\partial \psi^{\alpha}}{\partial J^s} \right). \quad (4.17)$$

Next, consider the identity

$$\underline{\underline{\mathbf{t}}}^{\alpha} = \sum_{j=1}^N (\underline{\underline{\mathbf{t}}}^{\alpha_j} + \rho^{\alpha_j} \mathbf{v}^{\alpha_j, \alpha} \otimes \mathbf{v}^{\alpha_j, \alpha}) \quad (4.18)$$

resulting from upscaling the momentum balance equation. Taking the trace of (4.18), neglecting the diffusive terms, and substituting this into (4.17) gives a definition for the solid phase pressure:

$$p^s := -\frac{1}{3} \text{tr}(\underline{\underline{\mathbf{t}}}^s) = -\frac{J^s}{\varepsilon^s} \sum_{\alpha} \left(\varepsilon^{\alpha} \rho^{\alpha} \frac{\partial \psi^{\alpha}}{\partial J^s} \right). \quad (4.19)$$

This is a generalization of the solid phase pressure found by Weinstein for saturated porous media in [80].

The coefficient of the $\underline{\underline{\dot{\mathbf{C}}}}^s$ term gives a relationship for the stress in the solid phase. This will give a generalization of the solid phase stress [8, 9] and closely follows the

derivations of Bennethum [9] and Weinstein [80]. Setting the coefficient of the $\underline{\underline{\mathbf{C}}}^s$ term to zero, left multiplying by the modified deformation gradient, $\overline{\underline{\underline{\mathbf{F}}}}^s$, and right multiplying by the transpose of the deformation gradient gives a relationship that defines the Lagrange multiplier for the solid phase, λ^{sj} :

$$\sum_{j=1}^N \underline{\underline{\mathbf{t}}}^{sj} + \sum_{j=1}^N \lambda^{sj} \rho^{sj} \underline{\underline{\mathbf{I}}} = \frac{2}{\varepsilon^s} \overline{\underline{\underline{\mathbf{F}}}}^s \cdot \left[\sum_{\alpha} \left(\varepsilon^{\alpha} \rho^{\alpha} \frac{\partial \psi^{\alpha}}{\partial \underline{\underline{\mathbf{C}}}^s} \right) \right] \cdot (\overline{\underline{\underline{\mathbf{F}}}}^s)^T. \quad (4.20)$$

Using identity (4.18) in the stress term of (4.20), neglecting the diffusive velocities, taking one-third the trace of the result, and using equation (4.19) for the solid-phase pressure yields a relationship for the solid phase Lagrange multiplier:

$$\sum_{j=1}^N \lambda^{sj} \rho^{sj} = p^s + \frac{2}{3\varepsilon^s} \sum_{\alpha} \left(\varepsilon^{\alpha} \rho^{\alpha} \frac{\partial \psi^{\alpha}}{\partial \underline{\underline{\mathbf{C}}}^s} \right) : \overline{\underline{\underline{\mathbf{C}}}}^s. \quad (4.21)$$

Substituting (4.21) back into (4.20) gives the following relation for the solid phase stress:

$$\underline{\underline{\mathbf{t}}}^s = -p^s \underline{\underline{\mathbf{I}}} + \frac{2}{\varepsilon^s} \overline{\underline{\underline{\mathbf{F}}}}^s \cdot \left[\sum_{\alpha} \left(\varepsilon^{\alpha} \rho^{\alpha} \frac{\partial \psi^{\alpha}}{\partial \underline{\underline{\mathbf{C}}}^s} \right) \right] \cdot (\overline{\underline{\underline{\mathbf{F}}}}^s)^T - \frac{2}{3\varepsilon^s} \sum_{\alpha} \left(\varepsilon^{\alpha} \rho^{\alpha} \frac{\partial \psi^{\alpha}}{\partial \underline{\underline{\mathbf{C}}}^s} \right) : \overline{\underline{\underline{\mathbf{C}}}}^s \underline{\underline{\mathbf{I}}}. \quad (4.22)$$

This can be rewritten as

$$\underline{\underline{\mathbf{t}}}^s = -p^s \underline{\underline{\mathbf{I}}} + \underline{\underline{\mathbf{t}}}_e^s + \frac{\varepsilon^l}{\varepsilon^s} \underline{\underline{\mathbf{t}}}_h^l + \frac{\varepsilon^g}{\varepsilon^s} \underline{\underline{\mathbf{t}}}_h^g \quad (4.23)$$

where

$$\underline{\underline{\mathbf{t}}}_e^s = 2 \left(\rho^s \overline{\underline{\underline{\mathbf{F}}}}^s \cdot \frac{\partial \psi^s}{\partial \underline{\underline{\mathbf{C}}}^s} \cdot (\overline{\underline{\underline{\mathbf{F}}}}^s)^T - \frac{1}{3} \rho^s \frac{\partial \psi^s}{\partial \underline{\underline{\mathbf{C}}}^s} : \overline{\underline{\underline{\mathbf{C}}}}^s \underline{\underline{\mathbf{I}}} \right), \quad (4.24a)$$

$$\underline{\underline{\mathbf{t}}}_h^l = 2 \left(\rho^l \overline{\underline{\underline{\mathbf{F}}}}^s \cdot \frac{\partial \psi^l}{\partial \underline{\underline{\mathbf{C}}}^s} \cdot (\overline{\underline{\underline{\mathbf{F}}}}^s)^T - \frac{1}{3} \rho^l \frac{\partial \psi^l}{\partial \underline{\underline{\mathbf{C}}}^s} : \overline{\underline{\underline{\mathbf{C}}}}^s \underline{\underline{\mathbf{I}}} \right), \quad (4.24b)$$

$$\underline{\underline{\mathbf{t}}}_h^g = 2 \left(\rho^g \overline{\underline{\underline{\mathbf{F}}}}^s \cdot \frac{\partial \psi^g}{\partial \underline{\underline{\mathbf{C}}}^s} \cdot (\overline{\underline{\underline{\mathbf{F}}}}^s)^T - \frac{1}{3} \rho^g \frac{\partial \psi^g}{\partial \underline{\underline{\mathbf{C}}}^s} : \overline{\underline{\underline{\mathbf{C}}}}^s \underline{\underline{\mathbf{I}}} \right). \quad (4.24c)$$

The stresses above are termed the effective stress, hydrating stress for the liquid phase, and hydrating stress for the gas phase respectively. Equation (4.22) states

that the stress in the solid phase can be decomposed into the solid pressure and stresses felt due to the presence of the fluid phases. It is here that the modifications of the deformation gradient and Cauchy-Green tensors become clear. If we take the trace of the stress tensor then we see that $(1/3)tr(\underline{\underline{\mathbf{t}}^s}) = -p^s$; which is how the solid phase pressure is measured. Therefore, this thermodynamic definition of p^s is consistent with experimental measure. Furthermore, the effective stress and hydrating stresses are terms associated with the interaction between the solid and the fluids. For saturated porous media, Bennethum [8] states the following:

“The effective stress tensor is the stress of the solid phase due to the strain of the porous matrix, and the hydrating stress tensor is the stress the liquid phase supports due to the strain of the solid matrix (which would be negligible if the liquid and solid phase were not interactive, but which becomes significant for swelling porous materials).”

One final note on the solid phase stress is that the total stress in the porous medium is related to the pressures in all three phases. This can be seen by taking the weighted sum of the stresses in each phase:

$$\underline{\underline{\mathbf{t}}} = \sum_{\alpha} \varepsilon^{\alpha} \underline{\underline{\mathbf{t}}^{\alpha}} = -\varepsilon^s p^s \underline{\underline{\mathbf{I}}} + \varepsilon^s \underline{\underline{\mathbf{t}}^s_e} + \varepsilon^l (\underline{\underline{\mathbf{t}}^l_h} + \underline{\underline{\mathbf{t}}^l}) + \varepsilon^g (\underline{\underline{\mathbf{t}}^g_h} + \underline{\underline{\mathbf{t}}^g}). \quad (4.25)$$

Taking one-third the trace of the total stress, and recalling that the effective and hydrating stresses are trace free, gives

$$\left(\frac{1}{3}\right) tr(\underline{\underline{\mathbf{t}}}) = -\varepsilon^s p^s + \frac{\varepsilon^l}{3} tr(\underline{\underline{\mathbf{t}}^l}) + \frac{\varepsilon^g}{3} tr(\underline{\underline{\mathbf{t}}^g}). \quad (4.26)$$

In order to fully understand the stresses in the fluid phases we must continue our examination of the results coming from the entropy inequality. Equation (4.26) is similar to the Terzaghi stress principle; suggesting that the fluid phases help to support the pore space in the medium.

4.2.2 Equilibrium Results

There are several more relationships that we can extract from the entropy inequality. In particular, we now seek relationships between the Lagrange multipliers and the fluid-phase pressures. We also seek relationships for the momentum and energy exchange terms. At equilibrium the production of entropy is minimized. Since this is a minimum, the gradient of $\hat{\Lambda}$ with respect to the set of independent variables (4.6) is zero. This indicates that the coefficients of the independent variables that appear linearly in the entropy inequality are zero at equilibrium. In the case of a three phase porous medium of this nature, we define equilibrium to be when a subset of the independent variables are zero. In particular, equilibrium is defined when no heat conduction occurs, $\nabla T = \mathbf{0}$, the strain rates in the fluid phases are zero, $\underline{\underline{\mathbf{d}}}^\beta = \underline{\underline{\mathbf{0}}}$, and all relative velocities are zero, $\mathbf{v}^{\alpha_j, \alpha} = \mathbf{0}$ and $\mathbf{v}^{\alpha, s} = \mathbf{0}$. This *definition* of equilibrium is particular to this type of media and is chosen as it gives physically relevant and meaningful results. Another way to look at this is to say that equilibrium is exactly the state when all of these variables are zero.

4.2.2.1 Fluid Stress Tensor

The first notable equilibrium result comes from the coefficient of the rate of deformation tensor, $\underline{\underline{\mathbf{d}}}^\beta$. Setting the coefficient of $\underline{\underline{\mathbf{d}}}^\beta$ to zero, eliminating the sum of the constituent stress tensors using the identity

$$\underline{\underline{\mathbf{t}}}^\beta = \sum_{j=1}^N [\underline{\underline{\mathbf{t}}}^{\beta_j} + \rho^{\beta_j} \mathbf{v}^{\beta_j, \beta} \otimes \mathbf{v}^{\beta_j, \beta}], \quad (4.27)$$

and noting that at equilibrium the diffusive velocity is zero, yields

$$\sum_{j=1}^N \lambda^{\beta_j} \rho^{\beta_j} = -\frac{1}{3} \text{tr} (\underline{\underline{\mathbf{t}}}^\beta) = p^\beta. \quad (4.28)$$

Equation (4.28) links the Lagrange multipliers to the equilibrium pressure of the fluid phases. This is the classical definition of pressure in a fluid: minus one-third the trace of the stress tensor. Using equation (4.15) the pressure in the fluid phases can now

be written as

$$p^\beta = -\frac{1}{3}tr(\underline{\mathbf{t}}^\beta) = \sum_{j=1}^N \sum_{\alpha} \left(\frac{\varepsilon^\alpha \rho^\alpha \rho^{\beta_j}}{\varepsilon^\beta} \frac{\partial \psi^\alpha}{\partial \rho^{\beta_j}} \right). \quad (4.29)$$

With the definition of pressure in equation (4.29) we note that the coefficient of $\dot{\varepsilon}^\beta$ can now be rewritten as

$$p^\beta - \sum_{\alpha} \left(\varepsilon^\alpha \rho^\alpha \frac{\partial \psi^\alpha}{\partial \varepsilon^\beta} \right). \quad (4.30)$$

The second term is the change in energy with respect to volumetric changes, and is therefore interpreted as the relative affinity for one phase to another. That is, this term is related to the wettability of the α and solid phases by the β fluid phase. The time rate of change of volume fluid phase volume fraction is an equation of state (that is not yet known), but rewriting the coefficient as in (4.30) hints at the fact that the equation of state is related to the pressure and the wettability of the phases. Furthermore, pressure, wettability, and surface tension are related to capillary pressure; hence indicating that the equation of state for the time rate of change of volume fraction is related to capillary pressure. It is here that we note the drawback to the present modeling effort. Recall that in the present expansion of the entropy inequality we do not include interfacial effects. If we were to include these effects then a surface tension term would appear here (as shown in Hassanizadeh and Gray [40]) and these terms together would more readily be associated with capillary pressure. More discussion will be dedicated to the exact equation of state for the time rate of change of volume fraction after a discussion on cross coupling pressures in Section 4.3 and capillary pressure in Chapters 5 and 7.

4.2.2.2 Momentum Transfer Between Phases

The next notable equilibrium result we can extract from (4.13) comes from the coefficient of the fluid phase relative velocities, $\mathbf{v}^{\beta,s}$. Setting this coefficient to zero, recalling that $\nabla T = \mathbf{0}$ at equilibrium, using the definition of the fluid phase pressure,

(4.29), the definition of the fluid phase Lagrange multipliers, (4.15), and solving for the momentum transfer terms gives

$$\begin{aligned}
-\left(\hat{\mathbf{T}}_s^\beta + \hat{\mathbf{T}}_\gamma^\beta\right) &= \left(\varepsilon^\beta \rho^\beta \frac{\partial \psi^\beta}{\partial \varepsilon^\beta} - p^\beta\right) \nabla \varepsilon^\beta + \varepsilon^\beta \rho^\beta \frac{\partial \psi^\beta}{\partial \varepsilon^\gamma} \nabla \varepsilon^\gamma + \varepsilon^\beta \rho^\beta \sum_{j=1}^{N-1} \frac{\partial \psi^\beta}{\partial C^{s_j}} \nabla C^{s_j} \\
&\quad - \sum_{j=1}^N \left[\left(\varepsilon^\gamma \rho^\gamma \frac{\partial \psi^\gamma}{\partial \rho^{\beta_j}} + \varepsilon^s \rho^s \frac{\partial \psi^s}{\partial \rho^{\beta_j}} \right) \nabla \rho^{\beta_j} \right] + \varepsilon^\beta \rho^\beta \sum_{j=1}^N \frac{\partial \psi^\beta}{\partial \rho^{\gamma_j}} \nabla \rho^{\gamma_j} \\
&\quad + \varepsilon^\beta \rho^\beta \frac{\partial \psi^\beta}{\partial J^s} \nabla J^s + \varepsilon^\beta \rho^\beta \frac{\partial \psi^\beta}{\partial \underline{\underline{\mathbf{C}}^s}} : \nabla (\underline{\underline{\mathbf{C}}^s}), \tag{4.31}
\end{aligned}$$

where γ is the *other* fluid phase not equal to β . This particular result will be coupled with the conservation of momentum to yield novel forms of Darcy's law in Section 4.5.1.

4.2.2.3 Momentum Transfer Between Species

Another notable equilibrium results comes from the coefficient of the diffusive velocity, $\mathbf{v}^{\alpha_j, \alpha}$. Equation (4.28) indicates that at equilibrium the definition of the Lagrange multiplier, equation (4.16), simplifies to

$$\underline{\underline{\lambda}}^{\alpha N} = \psi^\alpha \underline{\underline{\mathbf{I}}}. \tag{4.32}$$

This implies that, at equilibrium, the stress tensor for constituent j (from the coefficient of $\nabla \mathbf{v}^{\alpha_j, \alpha}$) can be written as

$$\underline{\underline{\mathbf{t}}}^{\alpha_j} = -\varepsilon^\alpha \rho^{\alpha_j} (\lambda^{\alpha_j} - \psi^{\alpha_j}) \underline{\underline{\mathbf{I}}} - \varepsilon^\alpha \rho^{\alpha_j} \psi^{\alpha_j} \underline{\underline{\mathbf{I}}}. \tag{4.33}$$

Consider the diffusive velocity term in the entropy inequality:

$$\begin{aligned}
& - \sum_{\alpha} \sum_{j=1}^N \left\{ \left(\sum_{\beta \neq \alpha} \hat{\mathbf{T}}_{\beta}^{\alpha_j} \right) + \hat{\mathbf{i}}^{\alpha_j} + \nabla (\varepsilon^\alpha \rho^{\alpha_j} \psi^{\alpha_j}) \right. \\
& \quad \left. - \lambda^{\alpha_j} \nabla (\varepsilon^\alpha \rho^{\alpha_j}) - \varepsilon^\alpha \underline{\underline{\lambda}}^{\alpha N} \cdot \nabla \rho^{\alpha_j} \right\} \cdot \mathbf{v}^{\alpha_j, \alpha}.
\end{aligned}$$

Add $-\sum_{\alpha} \sum_{j=1}^N (\rho^{\alpha_j} \underline{\underline{\lambda}}^{\alpha N} \cdot \nabla \varepsilon^\alpha) \cdot \mathbf{v}^{\alpha_j, \alpha} = 0$ and simplify to get

$$- \sum_{\alpha} \sum_{j=1}^N \left\{ \left(\sum_{\beta \neq \alpha} \hat{\mathbf{T}}_{\beta}^{\alpha_j} \right) + \hat{\mathbf{i}}^{\alpha_j} + \nabla (\varepsilon^\alpha \rho^{\alpha_j} \psi^{\alpha_j}) \right\}$$

$$\left. -\lambda^{\alpha_j} \nabla (\varepsilon^\alpha \rho^{\alpha_j}) - \underline{\underline{\lambda}}^{\alpha_N} : \nabla (\varepsilon^\alpha \rho^{\alpha_j}) \right\} \cdot \mathbf{v}^{\alpha_j, \alpha}.$$

At equilibrium the diffusive velocity is assumed to be zero. By the logic used herein for the exploiting the entropy inequality, and given the fact that $\underline{\underline{\lambda}}^{\alpha_N} = \psi^\alpha \underline{\underline{\mathbf{I}}}$ at equilibrium, we observe that for each j ,

$$\sum_{\beta \neq \alpha} \hat{\mathbf{T}}_\beta^{\alpha_j} + \hat{\mathbf{i}}^{\alpha_j} = -\nabla (\varepsilon^\alpha \rho^{\alpha_j} \psi^{\alpha_j}) + \lambda^{\alpha_j} \nabla (\varepsilon^\alpha \rho^{\alpha_j}) + \psi^\alpha \nabla (\varepsilon^\alpha \rho^{\alpha_j}). \quad (4.34)$$

This is an expression for the momentum transfer for species j in the α phase. This result will be coupled with the constituent conservation of momentum equation to derive a form of Fick's law in Section 4.5.3.

4.2.2.4 Partial Heat Flux

To conclude the equilibrium results we examine the ∇T term in the entropy inequality. We have assumed that $\nabla T = \mathbf{0}$ and $\mathbf{v}^{\alpha_j, \alpha} = \mathbf{0}$ at equilibrium, so by the logic used above we see that the coefficient of ∇T must be zero and

$$\sum_\alpha \varepsilon^\alpha \mathbf{q}^\alpha = \mathbf{0} \quad (4.35)$$

at equilibrium. This is the partial heat flux of the entire porous media and will be used in Section 4.5.4 to derive a generalized Fourier's law.

4.2.3 Near Equilibrium Results

The next step in exploiting the entropy inequality is to derive *near equilibrium* results. These results arise by linearizing the equilibrium results about the equilibrium state. The linearization process is simply the first-order terms of the Taylor series, but one must keep in mind that each of the derivatives is a function of all of the constitutive independent variables that are not zero at equilibrium. For example, if $f = f_{eq}$ at equilibrium, then near equilibrium, $f \approx f_{near} = f_{eq} + (\partial f / \partial (\nabla T)) \cdot \nabla T + \dots + (\partial f / \partial \mathbf{v}^{l,s}) \cdot \mathbf{v}^{l,s}$. This full expansion may yield terms that are not readily

physically interpretable. For this reason, considerable efforts must be made to relate the linearization constants to measurable parameters. For a thorough explanation of the linearization process with the entropy inequality see Appendix C.

For the momentum transfer in the fluid phases, the linearization of equation (4.31) can be simply written as

$$\left(\sum_{\alpha \neq \beta} \hat{\mathbf{T}}_{\alpha}^{\beta} \right)_{near} = \left(\sum_{\alpha \neq \beta} \hat{\mathbf{T}}_{\alpha}^{\beta} \right)_{eq} - (\varepsilon^{\beta})^2 \underline{\underline{\mathbf{R}}}^{\beta} \cdot \mathbf{v}^{\beta,s}. \quad (4.36)$$

The linearization constant, $\underline{\underline{\mathbf{R}}}^{\beta}$, is related to the resistivity of a porous medium; the inverse of the hydraulic conductivity. It should be noted that we have only expanded about one of the possible variables: $\mathbf{v}^{\beta,s}$. Strictly speaking this is incorrect and we should expand about all other variables which are zero at equilibrium. A more thorough expansion is

$$\begin{aligned} \left(\sum_{\alpha \neq \beta} \hat{\mathbf{T}}_{\alpha}^{\beta} \right)_{n.eq} &= \left(\sum_{\alpha \neq \beta} \hat{\mathbf{T}}_{\alpha}^{\beta} \right)_{eq} - (\varepsilon^{\beta})^2 \underline{\underline{\mathbf{R}}}^{\beta} \cdot \mathbf{v}^{\beta,s} \\ &\quad + \underline{\underline{\mathbf{H}}}^{\beta} \cdot \nabla T + \underline{\underline{\mathbf{J}}}^{\beta} \cdot \mathbf{v}^{\beta_j, \beta} + \underline{\underline{\underline{\mathbf{L}}}}^{\beta} : \underline{\underline{\mathbf{d}}}^{\beta} + \dots, \end{aligned} \quad (4.37)$$

where $\underline{\underline{\mathbf{H}}}^{\beta}$ and $\underline{\underline{\mathbf{J}}}^{\beta}$ are second-order tensors and $\underline{\underline{\underline{\mathbf{L}}}}^{\beta}$ is a third-order tensor. The ellipses at the end of this equation indicates that there are higher order terms that are not being written explicitly. The left-hand side of (4.37) is the rate of momentum transfer due to mechanical means. It is reasonable to think that this transfer term might be a function of fluid velocity, but the effects due to thermal gradients, diffusive velocity, and velocity gradients are likely small in comparison. To be completely correct we would have to include these terms in the modeling problems to follow. The trouble is that each of the coefficients needs to be associated with a physical parameter. We will see that $\underline{\underline{\mathbf{R}}}^{\beta}$ is physically associated with a material parameter of the porous medium, but it is presently unclear what the physical interpretations are for the other coefficients. Neglecting these terms simply leaves the door open for future modeling research.

Proceeding in a similar manner, the linearized constituent momentum transfer from equation (4.34) is

$$\left(\sum_{\beta \neq \alpha} \hat{\mathbf{T}}_{\beta}^{\alpha_j} + \hat{\mathbf{i}}^{\alpha_j} \right)_{near} = \left(\sum_{\beta \neq \alpha} \hat{\mathbf{T}}_{\beta}^{\alpha_j} + \hat{\mathbf{i}}^{\alpha_j} \right)_{eq} - \varepsilon^{\alpha} \rho^{\alpha_j} \underline{\underline{\mathbf{R}}}^{\alpha_j} \cdot \mathbf{v}^{\alpha_j, \alpha}. \quad (4.38)$$

The linearization constant is related to the inverse of the diffusion tensor. The linearized partial heat flux from equation 4.35 is

$$\left(\sum_{\alpha} \varepsilon^{\alpha} \mathbf{q}^{\alpha} \right) = \underline{\underline{\mathbf{K}}} \cdot \nabla T \quad (4.39)$$

(recalling that the partial heat flux is zero at equilibrium), and the linearization constant is related to the thermal conductivity.

In each of these linearization results, the factors of volume fraction and density are chosen so that the linearization constants better match experimentally measured coefficients. The signs are chosen so that the entropy inequality is not violated.

Several of the relationships resulting from the entropy inequality rely on proper definitions of the partial derivatives of the energy with respect to particular independent variables. The pressure is one such quantity, but there are several others that appear in the preceding results. For this reason, we now turn our attention to the exact definitions of pressure and chemical potential under our choice of independent variables. This will help to simplify and to attach physical meaning to the terms appearing in each of the linearized results. In saturated swelling porous material, Bennethum and Weinstein [16] showed that there are three pressures acting on the system. These results are extended in the next section to media with multiple fluid phases.

4.3 Pressures in Multiphase Porous Media

We will see in this subsection that the three pressures defined in [16] can be extended to broader definitions in multiphase media. These definitions will help to simplify and attach physical meaning to the terms appearing in each of the linearized

results discussed in the previous subsection. We will also define several new *pressures* acting as coupling terms between the phases in multiphase media. It will be shown that we can return to the three pressure relationship of Bennethum and Weinstein if we simplify these results to a single fluid phase.

Recall from the entropy inequality that the equilibrium pressure in multiphase media can be written as an accumulation of cross effects as follows:

$$p^\beta = \sum_{\alpha} \sum_{j=1}^N \left(\frac{\varepsilon^\alpha \rho^\alpha \rho^{\beta_j}}{\varepsilon^\beta} \frac{\partial \psi^\alpha}{\partial \rho^{\beta_j}} \right). \quad (4.40)$$

The partial derivative is taken while holding ε^α , ρ^{α_k} , ε^β , and ρ^{β_m} fixed where $k = 1 : N$ and $m = 1 : N$, $m \neq j$. Define a cross-coupling pressure as

$$p^{\alpha(\beta)} := \sum_{j=1}^N \left(\frac{\varepsilon^\alpha \rho^\alpha \rho^{\beta_j}}{\varepsilon^\beta} \frac{\partial \psi^\alpha}{\partial \rho^{\beta_j}} \Big|_{\varepsilon^\alpha, \rho^{\alpha_k}, \varepsilon^\beta, \rho^{\beta_m}} \right) \quad (4.41)$$

so that the β -phase pressure can be simply written as the sum of these cross-coupling pressures

$$p^\beta = \sum_{\alpha} p^{\alpha(\beta)} \quad \text{for } \beta \in \{l, g\} \quad \text{and} \quad \alpha \in \{l, g, s\}. \quad (4.42)$$

Now we derive an identity that is analogous to the three pressure relationship derived by Bennethum and Weinstein [16]. To that end, consider the Helmholtz potential as a function of two sets of independent variables where there is a one-to-one relationship between the two sets.

$$\psi^\alpha = \psi^\alpha (\varepsilon^\alpha, \varepsilon^\alpha \rho^{\alpha_j}, \varepsilon^\beta, \varepsilon^\beta \rho^{\beta_j}) \quad \text{and} \quad \hat{\psi}^\alpha = \hat{\psi}^\alpha (\varepsilon^\alpha, \rho^{\alpha_j}, \varepsilon^\beta, \rho^{\beta_j}), \quad (4.43)$$

where $\alpha \in \{l, g\}$ and $\beta \neq \alpha, s$. The Helmholtz potential is actually a function of several other variables, but these are suppressed here to make the notation more readable. Since ψ^α and $\hat{\psi}^\alpha$ are functions of an equivalent set of variables, the total differentials must be equal to each other. Setting $d\hat{\psi}^\alpha = d\psi^\alpha$ gives

$$d\hat{\psi}^\alpha = \frac{\partial \psi^\alpha}{\partial \varepsilon^\alpha} \Big|_{\varepsilon^\alpha \rho^{\alpha_k}, \varepsilon^\beta, \varepsilon^\beta \rho^{\beta_k}} d\varepsilon^\alpha + \sum_{j=1}^N \frac{\partial \psi^\alpha}{\partial (\varepsilon^\alpha \rho^{\alpha_j})} \Big|_{\varepsilon^\alpha, \varepsilon^\alpha \rho^{\alpha_m}, \varepsilon^\beta, \varepsilon^\beta \rho^{\beta_k}} d(\varepsilon^\alpha \rho^{\alpha_j})$$

$$+ \frac{\partial \psi^\alpha}{\partial \varepsilon^\beta} \Big|_{\varepsilon^\alpha, \varepsilon^\alpha \rho^{\alpha_k}, \varepsilon^\beta \rho^{\beta_k}} d\varepsilon^\beta + \sum_{j=1}^N \frac{\partial \psi^\alpha}{\partial (\varepsilon^\beta \rho^{\beta_j})} \Big|_{\varepsilon^\alpha, \varepsilon^\alpha \rho^{\alpha_k}, \varepsilon^\beta, \varepsilon^\beta \rho^{\beta_m}} d(\varepsilon^\beta \rho^{\beta_j}) \quad (4.44)$$

where in each case we are taking $m = 1 : N$ such that $m \neq j$, and $k = 1 : N$. Now take the partial derivative with respect to ε^β while holding ε^α , ρ^{α_k} , and ρ^{β_k} fixed. In this case, the $d\varepsilon^\alpha$ and $d(\varepsilon^\alpha \rho^{\alpha_j})$ terms will be zero. This leaves us with:

$$\begin{aligned} \frac{\partial \hat{\psi}^\alpha}{\partial \varepsilon^\beta} \Big|_{\varepsilon^\alpha, \rho^{\alpha_k}, \rho^{\beta_k}} &= \frac{\partial \psi^\alpha}{\partial \varepsilon^\beta} \Big|_{\varepsilon^\alpha \rho^{\alpha_k}, \varepsilon^\beta, \varepsilon^\beta \rho^{\beta_k}} \frac{\partial \varepsilon^\beta}{\partial \varepsilon^\beta} \Big|_{\varepsilon^\alpha, \rho^{\alpha_k}, \rho^{\beta_k}} \\ &+ \sum_{j=1}^N \frac{\partial \psi^\alpha}{\partial (\varepsilon^\beta \rho^{\beta_j})} \Big|_{\varepsilon^\alpha, \varepsilon^\alpha \rho^{\alpha_k}, \varepsilon^\beta, \varepsilon^\beta \rho^{\beta_m}} \frac{\partial (\varepsilon^\beta \rho^{\beta_j})}{\partial \varepsilon^\beta} \Big|_{\varepsilon^\alpha, \rho^{\alpha_k}, \rho^{\beta_k}} \\ &= \frac{\partial \psi^\alpha}{\partial \varepsilon^\beta} \Big|_{\varepsilon^\alpha \rho^{\alpha_k}, \varepsilon^\beta, \varepsilon^\beta \rho^{\beta_k}} + \sum_{j=1}^N \frac{\rho^{\beta_j}}{\varepsilon^\beta} \frac{\partial \psi^\alpha}{\partial \rho^{\beta_j}} \Big|_{\varepsilon^\alpha, \varepsilon^\alpha \rho^{\alpha_k}, \varepsilon^\beta, \varepsilon^\beta \rho^{\beta_m}}. \end{aligned} \quad (4.45)$$

Now multiply by $-\varepsilon^\alpha \rho^\alpha$ to get

$$-\varepsilon^\alpha \rho^\alpha \frac{\partial \hat{\psi}^\alpha}{\partial \varepsilon^\beta} \Big|_{\varepsilon^\alpha, \rho^{\alpha_k}, \rho^{\beta_k}} = -\varepsilon^\alpha \rho^\alpha \frac{\partial \psi^\alpha}{\partial \varepsilon^\beta} \Big|_{\varepsilon^\alpha \rho^{\alpha_k}, \varepsilon^\beta, \varepsilon^\beta \rho^{\beta_k}} - \sum_{j=1}^N \frac{\varepsilon^\alpha \rho^\alpha \rho^{\beta_j}}{\varepsilon^\beta} \frac{\partial \psi^\alpha}{\partial \rho^{\beta_j}} \Big|_{\varepsilon^\alpha, \varepsilon^\alpha \rho^{\alpha_k}, \varepsilon^\beta, \varepsilon^\beta \rho^{\beta_m}}. \quad (4.46)$$

Notice that the third term is $p^{\alpha(\beta)}$ from equation (4.41). Define the following new terms:

$$\bar{p}^{\alpha(\beta)} := -\varepsilon^\alpha \rho^\alpha \frac{\partial \psi^\alpha}{\partial \varepsilon^\beta} \Big|_{\varepsilon^\alpha, \varepsilon^\alpha \rho^{\alpha_k}, \varepsilon^\beta \rho^{\beta_k}} \quad (4.47)$$

$$\pi^{\alpha(\beta)} := \varepsilon^\alpha \rho^\alpha \frac{\partial \psi^\alpha}{\partial \varepsilon^\beta} \Big|_{\varepsilon^\alpha, \rho^{\alpha_k}, \rho^{\beta_k}} \quad (4.48)$$

to get the relationship

$$p^{\alpha(\beta)} = \bar{p}^{\alpha(\beta)} + \pi^{\alpha(\beta)}. \quad (4.49)$$

Note that the new definitions only hold if $\varepsilon^\beta \neq 0$. This can be seen if one returns back to the Lagrange multiplier equation (at the beginning of this section) for the pressure. Furthermore, this relationship holds if we had taken the derivative with respect to ε^α instead of ε^β .

For completeness sake we define \bar{p}^β and π^β so that our definitions are consistent with [16]:

$$\bar{p}^\beta := \sum_{\alpha} \bar{p}^{\alpha(\beta)} \quad (4.50)$$

$$\pi^\beta := \sum_{\alpha} \pi^{\alpha(\beta)}. \quad (4.51)$$

With these definitions we recover the three pressure relationship derived by Benethum and Weinstein

$$p^\beta = \bar{p}^\beta + \pi^\beta. \quad (4.52)$$

The physical meaning of \bar{p}^β is the change in energy with respect to changes in volume while holding mass fixed. In terms of extensive variables this is the same definition as pressure encountered in classical thermodynamics for a single phase. For this reason we call \bar{p}^β the *thermodynamic* pressure. The physical meaning of π^β is the change in energy with respect to changes in saturation while holding the densities fixed. This *pressure* (or swelling potential as it is called in [16]) relates the deviation between the *classical pressure*, p^β , and the thermodynamic pressure. It can be seen as a preferential wetting function that measures the affinity for one phase over another. With these physical considerations in mind we now return to the coefficient of the $\dot{\varepsilon}^\beta$ terms in the entropy inequality. With the present definitions, the coefficient is

$$p^\beta - \pi^\beta.$$

Using (4.52) this is clearly \bar{p}^β . Since the time rate of change of volume fraction is taken as a constitutive variable, the linearization result for this term can now be stated as

$$\bar{p}^\beta \Big|_{n.eq.} = \bar{p}^\beta \Big|_{eq.} + \tau \dot{\varepsilon}^\beta. \quad (4.53)$$

The coefficient τ arose from linearization and is formally defined as

$$\tau = \frac{\partial \bar{p}^\beta}{\partial \dot{\varepsilon}^\beta} \Big|_{eq.}$$

Equation (4.53) does little to make clear the exact meaning of this equation. The exact meaning will become clear in Chapter 5 under the assumption that the fluid-phase volume fractions are not independent.

The definitions of the three *pressures* allow us to attach more physical meaning (and more convenient notation) to the results found when building constitutive equations in the next sections. Before building these equations we define the upscaled chemical potential for a multiphase system, and after this point we will have all of the tools necessary to derive the new constitutive equations.

4.4 Chemical Potential in Multiphase Porous Media

Chemical potential is defined thermodynamically as the change in energy with respect to changes in the number of molecules in the system [4, 21]. This classical definition has the following characteristics [15]: (1) it is a scalar and measures the energy required to insert a particle into the system, (2) its gradient is the driving force for diffusive flow (Fick's law), and (3) it is constant for a single constituent in two phases at equilibrium. In [68], Bennethum proposed a definition for chemical potential in saturated porous media that satisfies all three of these criteria:

$$\mu^{\alpha_j} = \psi^\alpha + \rho^\alpha \left. \frac{\partial \psi^\alpha}{\partial \rho^{\alpha_j}} \right|_{\varepsilon^\alpha, \rho^{\alpha_m}} = \left. \frac{\partial (\rho^\alpha \psi^\alpha)}{\partial \rho^{\alpha_j}} \right|_{\varepsilon^\alpha, \rho^{\alpha_m}} = \left. \frac{\partial (\varepsilon^\alpha \rho^\alpha \psi^\alpha)}{\partial (\varepsilon^\alpha \rho^{\alpha_j})} \right|_{\varepsilon^\alpha, \rho^{\alpha_m}}, \quad (4.54)$$

for $m = 1 : N$ and $m \neq j$. In saturated media, if the changes in energy in the solid phase due to changes in liquid density are assumed to be zero, then the numerator of the right-hand side of (4.54) can be seen as the total energy in a saturated system. Under this assumption, the chemical potential can be rewritten as

$$\mu^{\alpha_j} = \left. \frac{\partial \psi_T}{\partial (\varepsilon^\alpha \rho^{\alpha_j})} \right|_{\varepsilon^\alpha, \rho^{\alpha_m}} \quad (4.55)$$

This indicates that in a saturated porous medium, the chemical potential of the j^{th} constituent in the α -phase is the change in total energy with respect to changes in mass of constituent j . We now extend this definition to multiphase unsaturated systems.

Extending this idea to multiphase and multiconstituent media, we define chemical potential to be the change in total energy with respect to changes in mass in the constituent. In multiphase media we cannot make the assumption that the energy in one phase is not effected by changes in other phases. With this in mind, we recall that the total energy can be given by $\psi_T = \sum_{\alpha} \varepsilon^{\alpha} \rho^{\alpha} \psi^{\alpha}$. Therefore, the present definition of chemical potential is

$$\mu^{\beta j} = \frac{\partial \psi_T}{\partial (\varepsilon^{\beta} \rho^{\beta j})} \Big|_{\varepsilon^{\alpha}, \varepsilon^{\beta}, \rho^{\alpha k}, \rho^{\beta m}} = \sum_{\alpha} \frac{\partial (\varepsilon^{\alpha} \rho^{\alpha} \psi^{\alpha})}{\partial (\varepsilon^{\beta} \rho^{\beta j})} \Big|_{\varepsilon^{\alpha}, \varepsilon^{\beta}, \rho^{\alpha k}, \rho^{\beta m}}, \quad (4.56)$$

where again, $k = 1 : N$ and $m = 1 : N$, $m \neq j$. Notice that if $\partial \psi^{\alpha} / \partial \rho^{\beta j} = 0$ for $\alpha \neq \beta$ then this definition collapses to equation (4.54). Furthermore, recalling the definition of the Lagrange multiplier, $\lambda^{\alpha j}$, from (4.15), equation (4.56) can be rewritten as

$$\mu^{\beta j} = \psi^{\beta} + \sum_{\alpha} \left(\frac{\varepsilon^{\alpha} \rho^{\alpha}}{\varepsilon^{\beta}} \frac{\partial \psi^{\alpha}}{\partial \rho^{\beta j}} \Big|_{\varepsilon^{\alpha}, \varepsilon^{\beta}, \rho^{\alpha k}, \rho^{\beta m}} \right) = \psi^{\beta} + \lambda^{\beta j}. \quad (4.57)$$

Equation (4.57) only holds for $\beta = l$ and $\beta = g$. A definition of the solid phase chemical potential is beyond the scope of this work.

As a result of this definition of chemical potential we observe an immediate effect on the rate of mass transfer terms in the entropy inequality. Using equation (4.57), the last three terms in the entropy inequality, (4.13), can be rewritten as

$$\begin{aligned} & - \sum_{j=1}^N \hat{e}_g^{lj} \left\{ (\lambda^{lj} + \psi^l) - (\lambda^{gj} + \psi^g) \right. \\ & \quad \left. + \frac{1}{2} \left((\mathbf{v}^{l,s})^2 - (\mathbf{v}^{g,s})^2 \right) + \frac{1}{2} \left((\mathbf{v}^{l,l})^2 - (\mathbf{v}^{g,g})^2 \right) \right\} \\ & - \sum_{j=1}^N \hat{e}_l^{sj} \left\{ (\lambda^{sj} + \psi^s) - (\lambda^{lj} + \psi^l) - \frac{1}{2} (\mathbf{v}^{l,s})^2 + \frac{1}{2} \left((\mathbf{v}^{s_j,s})^2 - (\mathbf{v}^{l_j,l})^2 \right) \right\} \\ & - \sum_{j=1}^N \hat{e}_s^{gj} \left\{ (\lambda^{gj} + \psi^g) - (\lambda^{sj} + \psi^s) + \frac{1}{2} (\mathbf{v}^{g,s})^2 + \frac{1}{2} \left((\mathbf{v}^{g_j,g})^2 - (\mathbf{v}^{s_j,s})^2 \right) \right\} \\ & = - \sum_{j=1}^N \hat{e}_g^{lj} \left\{ \mu^{lj} - \mu^{gj} + \frac{1}{2} \left((\mathbf{v}^{l,s})^2 - (\mathbf{v}^{g,s})^2 \right) + \frac{1}{2} \left((\mathbf{v}^{l,l})^2 - (\mathbf{v}^{g,g})^2 \right) \right\} \\ & - \sum_{j=1}^N \hat{e}_l^{sj} \left\{ (\lambda^{sj} + \psi^s) - \mu^{lj} - \frac{1}{2} (\mathbf{v}^{l,s})^2 + \frac{1}{2} \left((\mathbf{v}^{s_j,s})^2 - (\mathbf{v}^{l_j,l})^2 \right) \right\} \end{aligned}$$

$$- \sum_{j=1}^N \hat{e}_s^{g_j} \left\{ \mu^{g_j} - (\lambda^{s_j} + \psi^s) + \frac{1}{2} (\mathbf{v}^{g,s})^2 + \frac{1}{2} ((\mathbf{v}^{g_j,g})^2 - (\mathbf{v}^{s_j,s})^2) \right\}. \quad (4.58)$$

The square of the relative velocities are likely zero since these models are designed with creeping flow in mind. With these simplifications, the mass transfer terms from the entropy inequality are rewritten as

$$- \sum_{j=1}^N \hat{e}_g^{l_j} \{ \mu^{l_j} - \mu^{g_j} \} - \sum_{j=1}^N \hat{e}_l^{s_j} \{ (\lambda^{s_j} + \psi^s) - \mu^{l_j} \} - \sum_{j=1}^N \hat{e}_s^{g_j} \{ \mu^{g_j} - (\lambda^{s_j} + \psi^s) \}. \quad (4.59)$$

At equilibrium we assume that the mass transfer between phases is zero. Take note that this is an assumption about how the constitutive variable behaves at equilibrium and not an assumption about the equilibrium state itself. This fine point is made since in several works this assumption is made as part of the definition of equilibrium (for example, [16]). In the author's opinion this is a subtle mistake. The assumption that $\hat{e}_g^{l_j} = 0$ at equilibrium implies a final equilibrium relationship; the mass transfer between the fluid phases is proportional to the difference in chemical potentials

$$\begin{aligned} \hat{e}_g^{l_j}|_{n.eq} &= \hat{e}_g^{l_j}|_{eq} + [(\rho^{l_j} - \rho^{g_j}) M] (\mu^{l_j} - \mu^{g_j}) \\ &= [(\rho^{l_j} - \rho^{g_j}) M] (\mu^{l_j} - \mu^{g_j}). \end{aligned} \quad (4.60)$$

This helps to verify our choice of upscaled chemical potential by satisfying the third criteria set forth at the beginning of this subsection. Furthermore, this suggests a natural coupling between the liquid and gas phase mass balance equations. The mass transfer coefficient is chosen to have a factor of the difference in densities so as to better match experimental measures [75]. Given that the units of the rate of mass transfer are $[ML^{-3}t^{-1}]$ we see that the units of the linearization constant are

$$[M] = \frac{t}{L^2} = \frac{1}{(L^2/t)}.$$

A further verification that we have properly defined the multiphase chemical potential correctly can be seen through the Gibbs-Duhem relationship from thermodynamics [21]. Simply stated, the Gibbs-Duhem relationship states that the Gibbs potential of the α phase is the weighted sum of the chemical potentials:

$$\Gamma^\alpha = \sum_{j=1}^N C^{\alpha_j} \mu^{\alpha_j}. \quad (4.61)$$

Equation (4.61) specifies the relationship between the Gibbs potential, Γ^α , and the chemical potential. Substituting (4.57) into the right-hand side of (4.61), carrying out the summation, and applying the definition of pressure, (4.28), gives the equation

$$\Gamma^\alpha = \psi^\alpha + \frac{p^\alpha}{\rho^\alpha}, \quad (4.62)$$

which is the standard thermodynamic relationship between the Helmholtz potential and the Gibbs potential. This clearly demonstrates that the definition of multiphase chemical potential used here is consistent with the classical thermodynamic definition.

At this point we turn our attention toward using the relationships derived from the entropy inequality to develop novel expressions for Darcy's, Fick's, and Fourier's laws of flow, diffusion, and heat conduction. For a concise summary of all of the results derived in this chapter, see Appendix D.

4.5 Derivations Constitutive Equations

In this section we derive general forms of Darcy's, Fick's, and Fourier's laws based on the HMT results in the previous sections. These equations will be coupled with mass and energy balance equations to form a macroscale model for heat and moisture transport for unsaturated media. The results derived in this section extend the classical forms of each of these laws. These extensions suggest terms that, in the author's knowledge, are previously unreported. Also, we propose new forms of these laws in terms of the macroscale chemical potential. This suggests that the chemical potential is a generalized driving force for flow, diffusion, and heat transport.

4.5.1 Darcy's Law

In 1856, Henri Darcy proposed his empirical law governing flow through saturated porous media [30]. This was derived through experimentation on sand filters used to purify the water in the fountains of Dijon, France. In its simplest form, Darcy's law states that the averaged fluid flux is proportional to the gradient of hydraulic head (or fluid pressure)

$$\varepsilon^l \mathbf{v}^{l,s} = -k \nabla h. \quad (4.63)$$

Under the construct of Hybrid Mixture Theory, Darcy's law is obtained by coupling the momentum balance equation for a fluid phase, (3.29), with the linearized constitutive equation for the momentum transfer from other phases. This has been illustrated by several authors (some examples include [13, 12, 42, 80]), and depending on the set of independent variables postulated for the Helmholtz potential, the momentum transfer term can suggest different forms of Darcy's law.

In the present case, we recall from equation (4.36) that the linearized momentum transfer terms can be written as

$$\begin{aligned} \left(\hat{\mathbf{T}}_s^\beta + \hat{\mathbf{T}}_\gamma^\beta \right) &= -\varepsilon^\beta \underline{\underline{\mathbf{R}}}^\beta \cdot (\varepsilon^\beta \mathbf{v}^{\beta,s}) - (\pi^{\beta(\beta)} - p^\beta) \nabla \varepsilon^\beta - \pi^{\beta(\gamma)} \nabla \varepsilon^\gamma \\ &\quad - \varepsilon^\beta \rho^\beta \sum_{j=1}^{N-1} \frac{\partial \psi^\beta}{\partial C^{s_j}} \nabla C^{s_j} + \sum_{j=1}^N \left[\left(\varepsilon^\gamma \rho^\gamma \frac{\partial \psi^\gamma}{\partial \rho^{\beta_j}} + \varepsilon^s \rho^s \frac{\partial \psi^s}{\partial \rho^{\beta_j}} \right) \nabla \rho^{\beta_j} \right] \\ &\quad - \varepsilon^\beta \rho^\beta \sum_{j=1}^N \frac{\partial \psi^\beta}{\partial \rho^{\gamma_j}} \nabla \rho^{\gamma_j} - \varepsilon^\beta \rho^\beta \frac{\partial \psi^\beta}{\partial J^s} \nabla J^s - \varepsilon^\beta \rho^\beta \frac{\partial \psi^\beta}{\partial \underline{\underline{\mathbf{C}}}^s} : \nabla (\underline{\underline{\mathbf{C}}}^s), \end{aligned} \quad (4.64)$$

where we recall that $\underline{\underline{\mathbf{R}}}^\alpha$ is related to the resistivity of the medium and arose from the linearization process.

Linearization of the stress-pressure relationship for the fluid phases gives an expression for the stress near equilibrium:

$$\underline{\underline{\mathbf{t}}}^\beta = -p^\beta \underline{\underline{\mathbf{I}}} + \underline{\underline{\boldsymbol{\nu}}}^\beta : \underline{\underline{\mathbf{d}}}^\beta. \quad (4.65)$$

The fourth-order tensor multiplying the rate of deformation tensor can be simplified, in most cases, to correspond to the viscosity of the medium (see any text on continuum mechanics). Ignoring the acceleration terms in the momentum balance equation (3.29), and substituting equation (4.64) for momentum transfer and (4.65) for the stress tensor gives the following generalization of Darcy's law:

$$\begin{aligned}
\varepsilon^\beta \underline{\underline{\mathbf{R}}}^\beta \cdot (\varepsilon^\beta \mathbf{v}^{\beta,s}) &= -\varepsilon^\beta \nabla p^\beta - \pi^{\beta(\beta)} \nabla \varepsilon^\beta - \pi^{\beta(\gamma)} \nabla \varepsilon^\gamma + \varepsilon^\beta \rho^\beta \mathbf{g} \\
&+ \sum_{j=1}^N \left[\left(\varepsilon^\gamma \rho^\gamma \frac{\partial \psi^\gamma}{\partial \rho^{\beta_j}} + \varepsilon^s \rho^s \frac{\partial \psi^s}{\partial \rho^{\beta_j}} \right) \nabla \rho^{\beta_j} \right] - \varepsilon^\beta \rho^\beta \sum_{j=1}^N \frac{\partial \psi^\beta}{\partial \rho^{\gamma_j}} \nabla \rho^{\gamma_j} \\
&- \varepsilon^\beta \rho^\beta \frac{\partial \psi^\beta}{\partial J^s} \nabla J^s - \varepsilon^\beta \rho^\beta \frac{\partial \psi^\beta}{\partial \underline{\underline{\mathbf{C}}}} : \nabla (\underline{\underline{\mathbf{C}}}) + \nabla \cdot \left(\underline{\underline{\mathbf{v}}}^\beta : \underline{\underline{\mathbf{d}}}^\beta \right). \quad (4.66)
\end{aligned}$$

To arrive at this form of Darcy's law we have also assume that $\nabla C^{sj} \approx \mathbf{0}$ since it assumed that concentration gradients in the solid phase do not affect flow. The first term indicates that flow is primarily due to pressure gradients, as expected. The eighth and ninth terms were previously reported by Weinstein in [80]. Note that the *extra* factor of ε^β on the left-hand side of the equation can be moved to the right. If all but the first term on the right-hand side are then ignored we arrive at the classical Darcy's Law

$$\underline{\underline{\mathbf{R}}}^\beta \cdot (\varepsilon^\beta \mathbf{v}^{\beta,s}) = -\nabla p^\beta, \quad (4.67)$$

where $\mathbf{q}^\beta = \varepsilon^\beta \mathbf{v}^{\beta,s}$ is known as the *Darcy Flux*.

The linearization constant, $\underline{\underline{\mathbf{R}}}^\beta$, is related to the resistivity of the porous medium, the inverse of which is assumed to exist, and we define $\underline{\underline{\mathbf{K}}}^\beta = (\underline{\underline{\mathbf{R}}}^\beta)^{-1}$. The tensor $\underline{\underline{\mathbf{K}}}^\beta$ is related to the hydraulic conductivity. To determine the exact meaning of the linearization constant we consider the units of the simplest terms:

$$\mathbf{q}^\beta \approx -\underline{\underline{\mathbf{K}}}^\beta \cdot \nabla p^\beta.$$

The units of the Darcy flux are length per time $[L/t]$, and the units of the pressure are mass per length per time squared $[M/(L \cdot t^2)]$. This indicates that the linearization

constant has units $[(L^3 \cdot t)/M]$, which can be rewritten as $[(L^2)/(M/(L \cdot t))]$. The numerator of this fraction has units of permeability, κ , and the denominator has units of dynamic viscosity, μ_β . This suggests that

$$\underline{\underline{K}}^\beta = \frac{\underline{\underline{\kappa}}}{\mu_\beta}, \quad (4.68)$$

and this relationship is confirmed in equations (11.4) and (11.5) of Pinder et al. [61]. The hydraulic conductivity of a porous medium is defined as

$$\underline{\underline{k}}_c = \frac{\rho^\beta g \underline{\underline{\kappa}}}{\mu_\beta} = \frac{g \underline{\underline{\kappa}}}{\nu_\beta}, \quad (4.69)$$

where ν_β is the kinematic viscosity of the fluid. This indicates that $\underline{\underline{K}}^\beta$ can also be defined as

$$\underline{\underline{K}}^\beta = \frac{\underline{\underline{k}}_c}{\rho^\beta g}. \quad (4.70)$$

It is clear from these relationships that $\underline{\underline{K}}^\beta$ is a function of both the type of fluid and the geometry of the porous medium. This coefficient “describes, in some sense, the ability of the porous medium to transmit fluid” [61]. In saturated porous media, the permeability is typically assumed only to be a function of geometry. Under Hybrid Mixture Theory we must note that the permeability is a function of any variable which is not necessary zero at equilibrium. Typically it is assumed that the permeability of an unsaturated medium is a function of the volume fractions [5, 61]. The tensorial notation may be dropped in isotropic media, but for anisotropic media it is assumed that the permeability may depend on the direction of flow. We will expand upon this idea in later chapters when building a macroscale mass balance model.

4.5.2 Darcy’s Law In Terms of Chemical Potential

Equation (4.66) couples all of the physical processes that we wished to model at the outset; multiphase flow with constituents in each phase and a deformable solid. In order to build reasonable models based on this constitutive equation, functional forms

for the wetting potentials, $\pi^{\beta(\beta)}$ and $\pi^{\beta(\gamma)}$, and the changes in energy with respect to density are needed. The solid-phase terms are likely negligible for non-deformable media, but dealing with the remaining terms represent a significant modeling task. The goal of this subsection is to greatly simplify this model while maintaining the physical interpretation. This is done by switching thermodynamic potentials.

Recall from thermodynamics that the Gibbs potential, Γ^α , can be written in terms of the Helmholtz potential, ψ^α , as

$$\Gamma^\alpha = \psi^\alpha + \frac{p^\alpha}{\rho^\alpha}. \quad (4.71)$$

Taking the gradient of the Gibbs potential, expanding the resulting gradient of Helmholtz potential in terms of the constitutive independent variables, and multiplying by $-\varepsilon^\beta \rho^\beta$ yields the equation:

$$\begin{aligned} & -\pi^{\beta(\beta)} \nabla \varepsilon^\beta - \pi^{\beta(\gamma)} \nabla \varepsilon^\gamma - \varepsilon^\beta \nabla p^\beta \\ &= \sum_{j=1}^N \varepsilon^\beta \rho^\beta \frac{\partial \psi^\beta}{\partial \rho^{\beta_j}} \nabla \rho^{\beta_j} + \sum_{j=1}^N \varepsilon^\beta \rho^\beta \frac{\partial \psi^\beta}{\partial \rho^{\gamma_j}} \nabla \rho^{\gamma_j} \\ & \quad - \varepsilon^\beta \rho^\beta \nabla \Gamma^\beta - \frac{\varepsilon^\beta p^\beta}{\rho^\beta} \nabla \rho^\beta - \varepsilon^\beta \rho^\beta \eta^\beta \nabla T. \end{aligned} \quad (4.72)$$

Matching the common terms between (4.66) and (4.72), and recognizing the resulting chemical potential terms yields

$$\begin{aligned} & \varepsilon^\beta \underline{\underline{\mathbf{R}}} \cdot (\varepsilon^\beta \mathbf{v}^{\beta,s}) \\ &= -\varepsilon^\beta \rho^\beta \nabla \Gamma^\beta - \frac{\varepsilon^\beta p^\beta}{\rho^\beta} \nabla \rho^\beta - \varepsilon^\beta \rho^\beta \eta^\beta \nabla T + \varepsilon^\beta \rho^\beta \mathbf{g} \\ & \quad + \sum_{j=1}^N [\varepsilon^\beta (\mu^{\beta_j} - \psi^\beta) \nabla \rho^{\beta_j}] + \nabla \cdot \left(\underline{\underline{\boldsymbol{\nu}}}^\beta : \underline{\underline{\mathbf{d}}}^\beta \right). \end{aligned} \quad (4.73)$$

Observe that the summation in eq. (4.73) can be simplified to

$$\sum_{j=1}^N [\varepsilon^\beta (\mu^{\beta_j} - \psi^\beta) \nabla \rho^{\beta_j}] = \varepsilon^\beta (\Gamma^\beta - \psi^\beta) \nabla \rho^\beta + \varepsilon^\beta \rho^\beta \sum_{j=1}^N (\mu^{\beta_j} \nabla C^{\beta_j})$$

by expanding the gradient of ρ^{β_j} and using the Gibbs-Duhem equation (4.61). Substituting this back into (4.73) and simplifying yields the chemical potential form of Darcy's law:

$$\begin{aligned} \varepsilon^\beta \underline{\underline{\mathbf{R}}} \cdot (\varepsilon^\beta \mathbf{v}^{\beta,s}) \\ = -\varepsilon^\beta \rho^\beta \sum_{j=1}^N (C^{\beta_j} \nabla \mu^{\beta_j}) - \varepsilon^\beta \rho^\beta \eta^\beta \nabla T + \varepsilon^\beta \rho^\beta \mathbf{g} + \nabla \cdot \left(\underline{\underline{\boldsymbol{\nu}}}^\beta : \underline{\underline{\mathbf{d}}}^\beta \right) \end{aligned} \quad (4.74)$$

Cancelling the factor of ε^β from the left-hand side, rewriting the coefficient of the $\nabla \mu^{\beta_j}$ term, and multiplying by the inverse of $\underline{\underline{\mathbf{R}}}^\beta$ gives

$$\varepsilon^\beta \mathbf{v}^{\beta,s} = -\underline{\underline{\mathbf{K}}}^\beta \cdot \left[\sum_{j=1}^N (\rho^{\beta_j} \nabla \mu^{\beta_j}) + \rho^\beta \eta^\beta \nabla T - \rho^\beta \mathbf{g} - \frac{1}{\varepsilon^\beta} \nabla \cdot \left(\underline{\underline{\boldsymbol{\nu}}}^\beta : \underline{\underline{\mathbf{d}}}^\beta \right) \right]. \quad (4.75)$$

Equation (4.75) states an amazing fact: the flow of phase β is due only to gradients in chemical potential, temperature, gravity, and viscous forces. The viscous forces are often neglected in creeping flow. This gives

$$\varepsilon^\beta \mathbf{v}^{\beta,s} = -\underline{\underline{\mathbf{K}}}^\beta \cdot \left[\sum_{j=1}^N (\rho^{\beta_j} \nabla \mu^{\beta_j}) + \rho^\beta \eta^\beta \nabla T - \rho^\beta \mathbf{g} \right]. \quad (4.76)$$

It should be emphasized that no additional assumptions were made to arrive at this equation. That is, we still assume multiphase flow with a possibly swelling solid phase. All of the actions, interrelations, and cross coupling effects are tied up within the chemical potential term. This further indicates that the chemical potential is a *generalized force* that, in effect, incorporates several driving forces.

A final simplification is to consider a pure fluid phase where only one constituent is present. In this case, Darcy's law is rewritten as

$$\varepsilon^\beta \mathbf{v}^{\beta,s} = -\underline{\underline{\mathbf{K}}}^\beta \cdot [\rho^\beta \nabla \Gamma^\beta + \rho^\beta \eta^\beta \nabla T - \rho^\beta \mathbf{g}] \quad (4.77)$$

where Γ^β is the macroscale Gibbs potential. The entropy coefficient of the gradient of temperature poses a significant modeling issue as the entropy is not readily measurable. The fact stated by equation (4.77) is that the Darcy flux of a pure species

is truly controlled by gradients in temperature and Gibbs potential. This is a generalization of the classical pressure formulation that captures a wider range of physical effects.

4.5.3 Fick's Law

We now turn our attention to diffusion and Fick's law. In 1855, Adolf Fick published the first mathematical treatment of diffusion [36]. The empirically based equation simply states that the diffusive flux of a species through a mixture is proportional to the gradient in concentration of the species. This has since been generalized through thermodynamics and physical chemistry [21, 55] to state that the diffusive flux is proportional to the gradient in chemical potential of the species. In this subsection we apply the Hybrid Mixture Theory construct to derive a version of Fick's law for multiphase porous media. It should be noted here that the classical chemical potential from the thermodynamic definitions of Fick's law for diffusion in a liquid not in a porous medium is the not the *same* chemical potential as that defined for the porous media. In mixture theory we view the porous medium as a mixture of phases (and species), but the classical thermodynamic definition considers one phase with a mixture of species. With this difference in mind, it is not immediately clear that the multiphase version of Fick's law will be the same.

To derive the present version of Fick's law we first consider a linearization of the coefficient of the $\nabla \mathbf{v}^{\alpha_j, \alpha}$ term in the entropy inequality. The gradient of the diffusive velocity, $\nabla \mathbf{v}^{\alpha_j, \alpha}$, is taken to be zero at equilibrium so this coefficient is zero (since entropy generation is minimized at equilibrium). Therefore,

$$\varepsilon^\alpha \underline{\underline{\mathbf{t}}}^{\alpha_j} + \varepsilon^\alpha \rho^{\alpha_j} (\lambda^{\alpha_j} - \psi^{\alpha_j}) \underline{\underline{\mathbf{I}}} + \varepsilon^\alpha \rho^{\alpha_j} \underline{\underline{\boldsymbol{\lambda}}}^{\alpha_N} = \underline{\underline{\mathbf{0}}} \quad \text{for all } j.$$

Using equation (4.32) for the definition of the Lagrange multiplier, $\underline{\underline{\boldsymbol{\lambda}}}^{\alpha_N}$ at equilibrium and linearizing the coefficient of $\nabla \mathbf{v}^{\alpha_j, \alpha}$ about $\nabla \mathbf{v}^{\alpha_j, \alpha}$ gives

$$\varepsilon^\alpha \underline{\underline{\mathbf{t}}}^{\alpha_j} = \varepsilon^\alpha \underline{\underline{\mathbf{S}}}^{\alpha_j} : \nabla \mathbf{v}^{\alpha_j, \alpha} + (-\varepsilon^\alpha \rho^{\alpha_j} \lambda^{\alpha_j} + \varepsilon^\alpha \rho^{\alpha_j} \psi^{\alpha_j} - \varepsilon^\alpha \rho^{\alpha_j} \psi^\alpha) \underline{\underline{\mathbf{I}}}, \quad (4.78)$$

where $\underline{\underline{\mathbf{S}}}^{\alpha_j}$ is a fourth-order tensor that arises from linearization. Now consider the species conservation of momentum equation (3.28). We ignore the inertial terms since diffusion is assumed to be slow (this is discussed in some detail in Chapter 2). Now eliminate the momentum transfer terms using the linearized momentum transfer derived from the entropy inequality, (4.38), use (4.78) for the stress tensor, and using the fact that $\mu^{\alpha_j} = \lambda^{\alpha_j} + \psi^\alpha$ gives a generalized form of Fick's law:

$$\begin{aligned} (\varepsilon^\alpha)^2 \rho^{\alpha_j} \underline{\underline{\mathbf{R}}}^{\alpha_j} \cdot \mathbf{v}^{\alpha_j, \alpha} = \\ - \varepsilon^\alpha \rho^{\alpha_j} \nabla \mu^{\alpha_j} + \nabla \cdot \left(\varepsilon^\alpha \underline{\underline{\mathbf{S}}}^{\alpha_j} : \nabla \mathbf{v}^{\alpha_j, \alpha} \right) + \varepsilon^\alpha \rho^{\alpha_j} \mathbf{g}. \end{aligned} \quad (4.79)$$

The term containing the gradient of diffusive velocity is likely negligible as it is second order. If not, we would have to relate the fourth-order tensor, $\underline{\underline{\mathbf{S}}}^{\alpha_j}$, with some physical process (similar to viscosity for fluid flow). If we neglect this term then Fick's law can be written as

$$\varepsilon^\alpha \rho^{\alpha_j} \underline{\underline{\mathbf{R}}}^{\alpha_j} \cdot \mathbf{v}^{\alpha_j, \alpha} = -\rho^{\alpha_j} \nabla \mu^{\alpha_j} + \rho^{\alpha_j} \mathbf{g}. \quad (4.80)$$

Despite the novel choice of variables for this work, this form of Fick's law is identical to that found by Bennethum and Murad [15] and Weinstein [80].

The linearization coefficient in Fick's law has a similar meaning to that of the resistivity tensor in Darcy's law. In this case, though, we wish to associate the inverse of this tensor with the diffusivity tensor from classical Fick's law. Assuming that the inverse exists we have

$$\varepsilon^\alpha \rho^{\alpha_j} \mathbf{v}^{\alpha_j, \alpha} = -\rho^{\alpha_j} \underline{\underline{\mathbf{D}}}^{\alpha_j} \cdot [\nabla \mu^{\alpha_j} - \mathbf{g}]. \quad (4.81)$$

The units of the left-hand side are $[ML^{-2}t^{-1}]$, and the left-hand side term is commonly known as *flux*. Therefore, the units of $\underline{\underline{\mathbf{D}}}^{\alpha_j}$ is simply time $[t]$. Typically the diffusivity constant in a gas is measured as $[L^2t^{-1}]$, so we correlate $\underline{\underline{\mathbf{D}}}^{\alpha_j}$ to the diffusion coefficient for that phase, $\underline{\underline{\mathbf{D}}}^g$, via the relationship

$$\underline{\underline{\mathbf{D}}}^{\alpha_j} = \left(\frac{1}{R^{\alpha_j} T} \right) \underline{\underline{\mathbf{D}}}^g, \quad (4.82)$$

where R^{g_j} is the specific gas constant for constituent j . The units of $R^{g_j}T$ are $[L^2t^{-2}]$ and the units of $\underline{\underline{D}}^g$ are $[L^2t^{-1}]$, hence making the units of $\underline{\underline{D}}^{g_j}$ $[t]$. This is consistent with the forms of Fick's law from thermodynamics and physical chemistry [21, 55]. Hence, the gas phase form of Fick's law is

$$\varepsilon^g \rho^{g_j} \mathbf{v}^{g_j,g} = - \left(\frac{\rho^{g_j}}{R^{g_j}T} \right) \underline{\underline{D}}^g \cdot [\nabla \mu^{g_j} - \mathbf{g}]. \quad (4.83)$$

To close this subsection we finally recall from our discussion of pore-scale diffusion (see Chapter 2) that the diffusive velocities are related via

$$\sum_{j=1}^N \rho^{\alpha_j} \mathbf{v}^{\alpha_j,\alpha} = \mathbf{0}. \quad (4.84)$$

Multiplying by the volume fraction and recognizing the left-hand side of Fick's law indicates that

$$\sum_{j=1}^N \left\{ \left(\frac{\rho^{\alpha_j}}{R^{g_j}T} \right) \underline{\underline{D}}^\alpha \cdot [\nabla \mu^{\alpha_j} - \mathbf{g}] \right\} = \mathbf{0} \quad (4.85)$$

near equilibrium. Equation (4.85) simply states that the gradients in chemical potential are not independent of each other. This fact will be used in future chapters as part of a moisture transport model.

4.5.4 Fourier's Law

The final result in this chapter is an extension to Fourier's Law for heat conduction. Notice that in the chemical potential form of Darcy's Law, (4.76), there is a term that involves the gradient of temperature. That is, the Darcy flux is partially driven by a gradient in temperature. This means that Darcy flow is naturally driven by gradients in temperature as well as gradients in chemical potential. To properly handle this coupling we can either assume that the gradient of temperature is zero (constant temperature) or consider the energy balance equation and track temperature as well as chemical potential. To move toward a closed system of equations, we

derive a version of Fourier's Law from the entropy inequality so that we have an expression of heat flux in the energy balance equation. At the outset we first recall that in the entropy inequality we've assumed only one temperature for the entire porous medium. This implies that we've assumed that the separate phases are in thermal equilibrium. For this reason, we will develop an analogue to Fourier's Law that holds for the entire (bulk) medium.

Following Bennethum and Cushman's work on heat transport in porous media [14] we observe that if we sum the energy equation (3.35) over α we obtain the bulk energy balance equation

$$\rho \frac{De}{Dt} - \underline{\underline{t}} : \nabla \mathbf{v} - \nabla \cdot \mathbf{q} - \rho h = 0, \quad (4.86)$$

where

$$\rho = \sum_{\alpha} \varepsilon^{\alpha} \rho^{\alpha} \quad (4.87a)$$

$$\rho \mathbf{v} = \sum_{\alpha} \varepsilon^{\alpha} \rho^{\alpha} \mathbf{v}^{\alpha} \quad (4.87b)$$

$$\mathbf{u}^{\alpha} = \mathbf{v}^{\alpha} - \mathbf{v} \quad (4.87c)$$

$$\underline{\underline{t}} = \sum_{\alpha} [\varepsilon^{\alpha} \underline{\underline{t}}^{\alpha} - \varepsilon^{\alpha} \rho^{\alpha} \mathbf{u}^{\alpha} \otimes \mathbf{u}^{\alpha}] \quad (4.87d)$$

$$\rho e = \sum_{\alpha} [\varepsilon^{\alpha} \rho^{\alpha} e^{\alpha} + \varepsilon^{\alpha} \rho^{\alpha} \mathbf{u}^{\alpha} \cdot \mathbf{u}^{\alpha}] \quad (4.87e)$$

$$\mathbf{q} = \sum_{\alpha} \left[\varepsilon^{\alpha} \mathbf{q}^{\alpha} + \underline{\underline{t}}^{\alpha} \cdot \mathbf{u}^{\alpha} - \rho^{\alpha} \mathbf{u}^{\alpha} \left(e^{\alpha} + \frac{1}{2} \mathbf{u}^{\alpha} \cdot \mathbf{u}^{\alpha} \right) \right] \quad (4.87f)$$

$$\rho h = \sum_{\alpha} \varepsilon^{\alpha} \rho^{\alpha} h^{\alpha}. \quad (4.87g)$$

Given identities (a) - (g), the derivation of (4.86) follows after some significant algebra. Define the medium velocity, \mathbf{v} , as the weighted velocity of the medium, and the relative velocity, $\mathbf{u}^{\alpha} = \mathbf{v}^{\alpha} - \mathbf{v}$, is the α -phase velocity relative to the medium. Note that $\mathbf{v}^{\alpha,s} = \mathbf{v}^{\alpha} - \mathbf{v}^s - \mathbf{v} + \mathbf{v} = \mathbf{u}^{\alpha} - \mathbf{u}^s = \mathbf{u}^{\alpha,s}$. In the case where the velocity of the solid phase relative to the medium is zero ($\mathbf{u}^s = \mathbf{0}$) we immediately see that $\mathbf{u}^{\alpha} = \mathbf{v}^{\alpha,s}$. This

assumption along with equation (4.87f) indicates that there is naturally a coupling between the relative velocities, $\mathbf{v}^{\alpha,s}$, and the total heat flux, \mathbf{q} .

Using the near equilibrium result, $\sum_{\alpha} \varepsilon^{\alpha} \mathbf{q}^{\alpha} = \underline{\underline{\mathbf{K}}} \cdot \nabla T$ (equation (4.39)), we can write the total heat flux as

$$\mathbf{q} = \underline{\underline{\mathbf{K}}} \cdot \nabla T + \sum_{\alpha} \left[\underline{\underline{\mathbf{t}}}^{\alpha} \cdot \mathbf{v}^{\alpha,s} - \rho^{\alpha} \mathbf{v}^{\alpha,s} \left(e^{\alpha} + \frac{1}{2} \mathbf{v}^{\alpha,s} \cdot \mathbf{v}^{\alpha,s} \right) \right]. \quad (4.88)$$

If we were to (wrongly) neglect all of the terms in the summation we would arrive at Fourier's Law for heat conduction. The trouble here is that the terms in the summation are not negligible, and therefore the total heat flux in a porous medium must be a function of the gradient of temperature, the relative velocities, the stress in the fluid phases, and the internal energy.

Since $\mathbf{v}^{s,s} = \mathbf{v}^s - \mathbf{v}^s = \mathbf{0}$ the right-hand side of equation (4.88) is only a function of the fluid velocities relative to the solid phase. Neglecting viscous terms we recall that the fluid-phase stress tensors can be rewritten as $\underline{\underline{\mathbf{t}}}^{\alpha} = -p^{\alpha} \underline{\underline{\mathbf{I}}}$. Neglecting the second-order term, $\mathbf{v}^{\alpha,s} \cdot \mathbf{v}^{\alpha,s}$, the total heat flux is now written as

$$\mathbf{q} = \underline{\underline{\mathbf{K}}} \cdot \nabla T - \sum_{\alpha=l,g} [(p^{\alpha} + \rho^{\alpha} e^{\alpha}) \mathbf{v}^{\alpha,s}]. \quad (4.89)$$

At this point we replace the internal energy term with Gibbs energy in hopes of deriving an extended Fourier's Law in terms of the chemical potential. Recall from thermodynamics that the Gibbs potential and internal energy are related through

$$e^{\alpha} = \Gamma^{\alpha} + T\eta^{\alpha} - \frac{p^{\alpha}}{\rho^{\alpha}}. \quad (4.90)$$

Therefore, the total heat flux can be written in terms of the Gibbs potential as

$$\mathbf{q} = \underline{\underline{\mathbf{K}}} \cdot \nabla T - \sum_{\alpha=l,g} [\rho^{\alpha} (\Gamma^{\alpha} + T\eta^{\alpha}) \mathbf{v}^{\alpha,s}]. \quad (4.91)$$

Using the Gibbs-Duhem relationship, (4.61), this can be rewritten in terms of the chemical potential as

$$\mathbf{q} = \underline{\underline{\mathbf{K}}} \cdot \nabla T - \sum_{\alpha=l,g} \left[\left(\sum_{j=1}^N (\rho^{\alpha_j} \mu^{\alpha_j}) + \rho^{\alpha} T \eta^{\alpha} \right) \mathbf{v}^{\alpha,s} \right]. \quad (4.92)$$

The trouble with both (4.91) and (4.92) is that they both rely on measurements of entropy. One way to work around this issue is to assume that the entropy is only a function of temperature, and then to recall that the specific heat is defined as

$$c_p^\alpha = T \frac{\partial \eta^\alpha}{\partial T} = T \frac{d\eta^\alpha}{dT}.$$

Solving this separable ordinary differential equation (under the assumption that the variation of specific heat with temperature negligible) gives

$$\eta^\alpha(T) = c_p \ln \left(\frac{T}{T_0} \right) + \eta_0^\alpha \quad (4.93)$$

where T_0 is a reference temperature, and η_0^α is a reference entropy. While this is only an approximation it does allow us to move forward without direct measurements of entropy.

The *extended* Fourier's Law (4.91) presented here frames the equations presented in [14] in terms of the Gibbs potential. This will allow for easier coupling with the chemical potential forms of Fick's and Darcy's Laws presented in the previous subsections. The caveat is that the equation for total energy balance, (4.86), is not particularly useful since we do not have constitutive relations for the total stress and total energy. For that reason, we will not use equation (4.91) or (4.92) for Fourier's law in the energy equation. Instead we will use the linearized partial heat flux and the constitutive relations for the phase stresses and relative velocities to derive a generalized heat equation.

4.6 Conclusion

In this chapter we have shown that a novel and judicious choice of independent variables for the Helmholtz Free Energy can be used to derive forms of Darcy's, Fick's, and Fourier's Laws for multiphase porous media. These equations are similar to those found in [11, 14, 15, 80]. Each equation can be written with an eye toward the macroscale chemical potential, and in each case the chemical potential form is

more *mathematically appealing* in the sense that there are fewer terms and many of the physical processes are manifested in the chemical potentials. This illustrates the usefulness of the chemical potential as a modeling tool. Furthermore, since the chemical potential appears naturally in each of these equations we have set the stage for a more natural method of coupling the fluid flow, diffusion, and heat transport. In Chapters 5 and 7 we will couple these equations with the upscaled mass, momentum, and energy balance equations to yield a system of equations that will govern total moisture transport and heat flux in unsaturated porous media.

5. Coupled Heat and Moisture Transport Model

To form governing equations for heat and moisture transport in porous media we pair the constitutive equations derived in Chapter 4 with upscaled mass, momentum, and energy balance equations derived in Chapter 3. There are several existing models for each physical process of interest (fluid flow, diffusion, and heat transport) and recent research indicates a need to understand the fully coupled system of equations as it relates to moisture transport, evaporation, heat transport, and other physical phenomena. In this chapter we derive a model for coupled heat and moisture transport using Hybrid Mixture Theory and knowledge of pore-scale effects. To begin this modeling task we first investigate the classical models used within the past century in Section 5.1. In Sections 5.2 and 5.3 we pair our constitutive equations from Chapter 4 with upscaled balance laws from Chapter 3, perform a dimensional analysis, and discuss forms of the linearization coefficients arising from HMT. This is done in an effort to generate a closed system of governing equations. Several simplifying assumptions are made to close the system in Section 5.4. The solution(s) to the closed system will be discussed in Chapter 7.

5.1 Introduction and Historical Work

To give the reader a better understanding of the work from the past century, we present three classical models here with some discussion on their advantages and disadvantages. First we discuss Richards' equation for unsaturated fluid flow in Section 5.1.1, second we discuss Phillip and De Vries enhanced diffusion model in Section 5.1.2, and lastly we discuss De Vries' heat transport model in Section 5.1.3.

5.1.1 Richards' Equation for Fluid Flow

The classical equation for fluid flow in unsaturated media is known as Richards' equation (also called the saturation equation). This equation was first derived in 1931 by L.A. Richards at Cornell University [64]. It takes a postulated form of the mass

balance equation (similar to equation (3.25)) and replaces the flux term with Darcy's law. The gradient of pressure is rewritten in terms of pressure head ($h = p/(\rho g)$), and then a constitutive relation is assumed for the pressure head as a function of saturation (or volume fraction). Another constitutive relation relating the relative permeability of the medium to saturation is assumed. There are several versions of the constitutive relations, but one of the more *popular* in recent research are those of van Genuchten [78, 61]. Another more recently investigated relationship is the Fayer-Simmons model [35, 67, 75], which is an extension of the van Genuchten model to cover the case of very low saturations.

The result of the assumption and substitutions in the mass balance equation is a nonlinear diffusion equation where the primary unknown is the percent saturation of the medium

$$\frac{\partial S}{\partial t} = \nabla \cdot [D(S)\nabla S - K(S)\mathbf{z}], \quad (5.1)$$

where $K(S)$ is the hydraulic conductivity function and $D(S)$ is the product of $K(S)$ and the derivative of capillary pressure with saturation. Recall that saturation is defined as

$$S = \frac{\varepsilon^l}{1 - \varepsilon^s} = \frac{\varepsilon^l}{\varepsilon^g + \varepsilon^l} = \frac{\varepsilon^l}{\varepsilon} = \frac{\text{volume of liquid}}{\text{volume of pore space}} \quad (5.2)$$

and is understood as the volume of liquid per volume of pore space.

This model has been effectively used for several decades, but there are a few disadvantages of note. First of all, this equation does not allow for phase change between the liquid and gas. The original model was proposed for systems with immiscible fluids, where phase changes likely don't occur, but it is also used for unsaturated soils where phase change is possible and air is always available. A second disadvantage is that humidity and temperature gradients are not considered. A third disadvantage is that the pressure head - saturation curve is hysteretic (depends on the history of

flow). The constitutive laws for pressure head don't account for this hysteretic behavior directly. Instead, it is often assumed that fitting parameters change with changing direction of flow. This leads to the final disadvantage: the use of the van Genuchten capillary pressure - saturation relation. This is a widely used relationship, but relies heavily on two fitting parameters. The measurement of these fitting parameters is difficult, and they are typically found by fitting numerical solutions of Richards' equation to experimental data.

Several extensions and modifications to Richards' equation have been made recently, the most notable of which is that of Hassanizadeh et al. [48, 46]. In these papers, they propose a dynamic relationship between capillary pressure and saturation based on Hybrid Mixture Theory with interfaces. They also propose that the hysteretic effect observed in the capillary pressure - saturation curves is due to the (postulated) fact that the capillary pressure, saturation, and interfacial area density, ε^{lg} , form a unique surface. This partially explains hysteretic effects by seeing them as a projection of this surface onto the capillary pressures - saturation plane in the $p_c - S - \varepsilon^{lg}$ space. This model is gaining in popularity, but is far from widespread acceptance. Some of the relevant publications are [47, 48, 49, 45, 46, 57].

In the present chapter we present a modification to the Richards' equation that incorporates the dynamic capillary pressure relationship of Hassanizadeh et al. The major differences between the present derivations and their work are: (1) modeling in terms of chemical potential, (2) allowing for phase transition, and (3) allowing for humidity and temperature gradients. Our present modeling effort will account for all of these effects, and hence, constitutes a generalization of the existing model.

5.1.2 Phillip and De Vries' Diffusion Model

In 1957, Phillip and de Vries published their comprehensive work on diffusion of water vapor in porous media [60]. In their model they postulate an *enhanced* Fick's

law,

$$\mathbf{q}^{g_v} = -\rho^g D \eta \nabla C^{g_v}, \quad (5.3)$$

where \mathbf{q}^{g_v} is the water vapor flux and η is an *enhancement* factor that is a function of the tortuosity, volume fraction of air, and a “mass-flow factor”. The mass-flow factor is then postulated as a function of pore-scale gradients in saturation and temperature. This model has successfully been applied to several diffusion and evaporation problems (e.g. [75]), but the trouble is that the exact form of the enhancement is based on empirical evidence. Furthermore, this model has come under recent scrutiny due to the fact that the proposed factors affecting η are pore-scale effects and are therefore difficult to accurately measure [25, 70, 71, 69, 72, 73, 75, 79]. Many of these works use x-ray tomography to attempt to measure these pore-scale effects directly.

In the work by Cass et al. [24], an empirical form of the enhancement factor was proposed. In this work, a fitting parameter is used in the enhancement factor to arrive at good agreement with experimental data. This model has been used in more recent works (e.g. [67, 75]) in conjunction with a mass balance equation for the water vapor in the gas phase. The resulting model is a nonlinear diffusion equation for concentration of water vapor that deviates from the more classical de Vries model. Aside from the empirical fitting parameter, the mass transfer between phases also relies on a fitting parameter and an empirically-derived functional form.

In the present chapter we build a model for diffusion based on using the chemical potential as a primary unknown and the Hybrid Mixture Theory construct. The enhanced diffusion is not incorporated into these models, and the mass transfer is modeled by the difference in chemical potentials; a more physically natural formulation. A comparison will be made to the model of Cass et al.

5.1.3 De Vries’ Heat Transport Model

In 1958, de Vries published a second paper coupling heat and moisture transport in porous media [31]. In this research, he proposed an extended heat transport

model for porous media that is still used today. Neither his diffusion nor his heat transport model were thermodynamically derived. Instead, he began each derivation with a postulation of the forms of diffusive and heat flux. For the heat transport equation he included terms similar to the classical Fourier's law, but also proposed that heat transport was due to advective transport in the fluid phases. This model is still popularly used today to couple heat and mass transport in unsaturated media [5, 77, 75]. That being said, the effects included in this equations are based solely on de Vries' supposition of the factors affecting heat flow.

In 1999 Bennethum and Cushman published (to the author's knowledge) the first work using Hybrid Mixture Theory to derive an extended de Vries model for heat transport in swelling saturated porous media [14]. In the present chapter we take a similar approach using HMT to derive a thermodynamically consistent model for heat transport in non-swelling unsaturated media. This is done with an eye toward using gradients in temperature as the thermal diffusion process and the chemical potential to describe the secondary processes such as advection.

5.2 Assumptions

In this section we state the baseline assumptions that will be used throughout the remainder of this work. These assumptions are meant to make minimal limitations on the applicability of the resulting models, but at the same time they are meant to keep the mathematics tractable. Possible relaxations to these assumptions (and the source of possible avenues of future research) will be stated as they are encountered.

The simple set of baseline assumptions are as follows:

Assumption #1: The solid phase is rigid, incompressible, and inert.

Assumption #2: The liquid and gas phases are each made up of N constituents.

Assumption #3: No chemical reactions take place in any of the phases.

The first assumption is the most restrictive. Mathematically it corresponds to setting the Lagrangian derivatives of both density and volume fraction for the solid phase to zero. Assuming that the solid is inert simply means that no mass will precipitate onto, or dissolve away from, the solid phase. With these assumptions, the solid phase mass balance equation (from equation (3.25)) becomes

$$\nabla \cdot \mathbf{v}^s = 0. \quad (5.4)$$

If a deformable solid is considered where the solid-phase volume fraction can change, then this assumption would need to be relaxed. One particular relaxation of this assumption is to allow for incompressibility and inertness of the solid phase but relax the rigidity assumption. Under this relaxation, the solid phase mass balance equation becomes

$$\frac{D^s \varepsilon^s}{Dt} - \varepsilon^s \nabla \cdot \mathbf{v}^s = 0. \quad (5.5)$$

A consequence of fixing the solid phase volume is that $\varepsilon^l + \varepsilon^g = 1 - \varepsilon^s := \varepsilon$, where ε is known as the porosity of the porous medium. A further consequence is that the liquid and gas phase volume fractions are no longer independent of each other. Note that we could have made this assumption up front and exploited the entropy inequality with this assumption (this is done in [43, 44] for a different set of independent variables), but proceeding in this order allows us to return to the present entropy inequality results and consider a deformable solid in the future. Since the fluid-phase volume fractions are no longer independent we can replace them by saturation as defined by

$$S = \frac{\varepsilon^l}{\varepsilon^l + \varepsilon^g} = \frac{\varepsilon^l}{\varepsilon}. \quad (5.6)$$

This implies that the volume fractions are related via $\varepsilon^l = \varepsilon S$ and $\varepsilon^g = \varepsilon(1 - S)$.

Assumption #2 is a byproduct of the principle of equipresence and will be relaxed later for simplicity. In the most general sense, this assumption states that every

species that exists in one fluid phase also exists in the other. In reality this is likely not true. For example, if a constituent is present in the liquid phase it is possible that evaporated particles of the constituent are not be present in the gas phase. Another example would be if we were to extend this model to an oil-water system. The two fluids in this case are immiscible and it is unlikely that every species in the water phase is present in the oil phase (and visa versa). We take this into account by setting the appropriate concentrations to zero after the constitutive equations have been derived.

Assumption #3 indicates that the rate of mass exchange due to chemical reactions, \hat{r}^{α_j} , is zero for all phases. The consequence of this is that the rate of mass generation of a constituent in a phase only occurs between two phases. This is true for some porous media, but chemical reactions can occur in some specific cases such as remediation problems. Under this assumption these cases are henceforth eliminated from the discussion.

Other simplifying assumptions exist for many media, but the three presented herein constitute a set that leads to several mathematical simplifications with as few physical restrictions as possible.

5.3 Derivation of Heat and Moisture Transport Model

In the remainder of this chapter we focus on using the results from Chapters 3 and 4, along with the assumptions from Section 5.2, to derive a closed system of equations for heat and mass transport in unsaturated porous media. This will be done with an eye toward using the chemical potential as the driving force for these processes. We will show that under certain additional simplifying assumptions that a closed system can be derived.

5.3.1 Mass Balance Equations

We first build generalized mass balance equations in terms of the chemical potential under assumptions #1 - #3. Recall from Chapter 3 that the mass balance

equation for the j^{th} constituent in the α -phase is (from equation (3.21))

$$\frac{D^{\alpha_j}(\varepsilon^\alpha \rho^{\alpha_j})}{Dt} + \varepsilon^\alpha \rho^{\alpha_j} \nabla \cdot \mathbf{v}^{\alpha_j} = \sum_{\beta \neq \alpha} \hat{e}_\beta^{\alpha_j} + \hat{r}^{\alpha_j}. \quad (5.7)$$

The last term can be dropped under assumption #3 in Section 5.2. Because of the form of the constitutive equation, and to adhere to the principle of frame invariance, it is convenient to rewrite this equation relative to the solid phase. To do so we recall the identities

$$\frac{D^{\alpha_j}(\cdot)}{Dt} = \frac{D^\alpha(\cdot)}{Dt} + \mathbf{v}^{\alpha_j, \alpha} \cdot \nabla(\cdot) \quad (5.8a)$$

$$\frac{D^\alpha(\cdot)}{Dt} = \frac{D^s(\cdot)}{Dt} + \mathbf{v}^{\alpha, s} \cdot \nabla(\cdot) \quad (5.8b)$$

and expand the Lagrangian time derivatives accordingly to get

$$\frac{D^s(\varepsilon^\alpha \rho^{\alpha_j})}{Dt} + \mathbf{v}^{\alpha_j, \alpha} \cdot \nabla(\varepsilon^\alpha \rho^{\alpha_j}) + \mathbf{v}^{\alpha, s} \cdot \nabla(\varepsilon^\alpha \rho^{\alpha_j}) + \varepsilon^\alpha \rho^{\alpha_j} \nabla \cdot \mathbf{v}^{\alpha_j} = \sum_{\beta \neq \alpha} \hat{e}_\beta^{\alpha_j}. \quad (5.9)$$

Taking the definition of the Lagrangian time derivative,

$$\frac{D^s(\cdot)}{Dt} = \frac{\partial(\cdot)}{\partial t} + \mathbf{v}^s \cdot \nabla(\cdot),$$

adding and subtracting $\varepsilon^\alpha \rho^{\alpha_j} \nabla \cdot \mathbf{v}^\alpha$, and subtracting $\varepsilon^\alpha \rho^{\alpha_j} \nabla \cdot \mathbf{v}^s = \mathbf{0}$ gives

$$\frac{\partial(\varepsilon^\alpha \rho^{\alpha_j})}{\partial t} + \nabla \cdot (\varepsilon^\alpha \rho^{\alpha_j} \mathbf{v}^{\alpha_j, \alpha}) + \nabla \cdot (\varepsilon^\alpha \rho^{\alpha_j} \mathbf{v}^{\alpha, s}) = \sum_{\beta \neq \alpha} \hat{e}_\beta^{\alpha_j}. \quad (5.10)$$

Notice the use of Assumption #1 in the last step, and observe that if Assumption #1 is relaxed then the mass balance equation would involve a time derivative of the solid-phase volume fraction (at least).

Equation (5.10) is the general mass balance equation for both of the fluid phases. Notice that we are not replacing the volume fractions with saturation here since we don't know if α is the liquid or gas phase. Substituting Fick's law for the diffusive flux and Darcy's law for the Darcy flux gives the chemical potential form of the full mass balance equation for species j in phase α :

$$\frac{\partial(\varepsilon^\alpha \rho^{\alpha_j})}{\partial t} - \nabla \cdot \{ \rho^{\alpha_j} \underline{\underline{D}}^{\alpha_j} \cdot [\nabla \mu^{\alpha_j} - \mathbf{g}] \}$$

$$\begin{aligned}
& - \nabla \cdot \left\{ \rho^{\alpha_j} \underline{\underline{\mathbf{K}}}^\alpha \cdot \left[\sum_{k=1}^N (\rho^{\alpha_k} \nabla \mu^{\alpha_k}) + \rho^\alpha \eta^\alpha \nabla T - \rho^\alpha \mathbf{g} \right] \right\} \\
& = \sum_{\beta \neq \alpha} \hat{e}_\beta^{\alpha_j}. \tag{5.11}
\end{aligned}$$

It should be noted here that the Eulerian and Lagrangian time derivatives are equal under the assumption that the solid-phase velocity is zero (Assumption #1). Also note that if we sum over all constituents then we arrive at the mass balance equation for the phase (where we have used $\sum_{j=1}^N \rho^{\alpha_j} \mathbf{v}^{\alpha_j, \alpha} = \mathbf{0}$)

$$\frac{\partial (\varepsilon^\alpha \rho^\alpha)}{\partial t} - \nabla \cdot \left\{ \rho^\alpha \underline{\underline{\mathbf{K}}}^\alpha \cdot \left[\sum_{k=1}^N (\rho^{\alpha_k} \nabla \mu^{\alpha_k}) + \rho^\alpha \eta^\alpha \nabla T - \rho^\alpha \mathbf{g} \right] \right\} = \sum_{\beta \neq \alpha} \hat{e}_\beta^\alpha. \tag{5.12}$$

The chemical potential form of the mass balance equation is only one form. We could have used the pressure formulation for Darcy's law and arrived at a pressure - chemical potential form of the mass balance equation.

The rate of mass transfer term on the right-hand side of the mass balance equation can be rewritten in terms of a linearized result from the entropy inequality. Recall from equation (4.60) that the mass transfer term can be written as

$$\hat{e}_\beta^{\alpha_j} = [(\rho^{\alpha_j} - \rho^{\beta_j}) M] (\mu^{\alpha_j} - \mu^{\beta_j}), \tag{5.13}$$

where the coefficient $(\rho^{\alpha_j} - \rho^{\beta_j})$ is chosen to be consistent with equation (9) of [75]. Also recall that since the interface is assumed to contain no mass we must have that the rate of mass gained from the β phase to the j^{th} species in the α phase must be equal to the rate of mass lost from the α phase to the j^{th} species of the β phase:

$$\hat{e}_\beta^{\alpha_j} = -\hat{e}_\alpha^{\beta_j}.$$

If the chemical potential of the liquid phase is larger than the chemical potential of the water vapor then mass will transfer from liquid to gas and $\hat{e}_g^l < 0$. Similarly, if the chemical potential of the liquid phase is smaller than that of the water vapor then mass will transfer from gas to liquid and $\hat{e}_g^l > 0$. Recall from the discussion adjacent to equation (4.60) that the units of M are the reciprocal of flux.

There are clearly more unknowns than equations in the $2N$ fluid equations since we must account for the densities, temperature, volume fractions, and entropies as well as the chemical potentials. Certain sets of simplifying assumptions can be used to reduce the number of unknowns (e.g. incompressibility of a fluid phase). These will be discussed in Section 5.4. Instead of making these assumptions up front we now turn our attention to deriving a generalized energy balance equation to account for the temperature. This will give one more equation but will add no more unknowns to the system of equations.

5.3.2 Energy Balance Equation

As another step toward developing a closed system of equation equations for heat and moisture transport we next examine the energy balance equation. This will give an equation in terms of temperature, chemical potentials, saturation (volume fractions), entropy, and densities; increasing the equation count but not increasing the variable count. Since we assumed at the outset that all of the phases are in thermal equilibrium we will only have one equation for energy balance. This will be derived by considering the sum of each of the phase energy balance equations. Counter-intuitively, we will not use the form of Fourier's Law (equation (4.87f) or (4.92)) derived for the total heat flux since the energy equation derived in that section is more cumbersome to work with than the individual phase energy equations. Instead we will use the partial heat flux for each phase as derived from linearization about equilibrium (4.39).

From equation (3.35), the volume averaged energy balance equation is

$$\varepsilon^\alpha \rho^\alpha \frac{D^\alpha e^\alpha}{Dt} - \varepsilon^\alpha \underline{\underline{\mathbf{t}}}^\alpha : \underline{\underline{\mathbf{d}}}^\alpha - \nabla \cdot (\varepsilon^\alpha \mathbf{q}^\alpha) + \varepsilon^\alpha \rho^\alpha h^\alpha = \sum_{\beta \neq \alpha} \hat{Q}_\beta^\alpha. \quad (5.14)$$

Using the identity $\frac{D^\alpha(\cdot)}{Dt} = \frac{D^s(\cdot)}{Dt} + \mathbf{v}^{\alpha,s} \cdot \nabla(\cdot)$ and using *dot* notation for material time derivatives allows us to rewrite the energy equation as

$$\varepsilon^\alpha \rho^\alpha \dot{e}^\alpha + \varepsilon^\alpha \rho^\alpha \mathbf{v}^{\alpha,s} \cdot \nabla e^\alpha - \varepsilon^\alpha \underline{\underline{\mathbf{t}}}^\alpha : \underline{\underline{\mathbf{d}}}^\alpha - \nabla \cdot (\varepsilon^\alpha \mathbf{q}^\alpha) + \varepsilon^\alpha \rho^\alpha h^\alpha = \sum_{\beta \neq \alpha} \hat{Q}_\beta^\alpha. \quad (5.15)$$

The trouble with (5.15) is that the first and second terms contain the interal energy density, e^α . To tie this equation back to the HMT framework we've used throughout (and to give the equation a more natural set of dependent variables) we perform a Legendre transformation to change the energy term into the Helmholtz potential via the thermodynamic identity $e^\alpha = \psi^\alpha + T\eta^\alpha$. The energy equation is now written as

$$\begin{aligned} \sum_{\beta \neq \alpha} \hat{Q}_\beta^\alpha = & \varepsilon^\alpha \rho^\alpha \frac{D^s \psi^\alpha}{Dt} + \varepsilon^\alpha \rho^\alpha \mathbf{v}^{\alpha,s} \cdot \nabla \psi^\alpha + \varepsilon^\alpha \rho^\alpha T \dot{\eta}^\alpha + \varepsilon^\alpha \rho^\alpha T \mathbf{v}^{\alpha,s} \cdot \nabla \eta^\alpha \\ & + \varepsilon^\alpha \rho^\alpha \eta^\alpha \dot{T} + \varepsilon^\alpha \rho^\alpha \eta^\alpha \mathbf{v}^{\alpha,s} \cdot \nabla T - \varepsilon^\alpha \underline{\mathbf{t}}^\alpha : \underline{\mathbf{d}}^\alpha - \nabla \cdot (\varepsilon^\alpha \mathbf{q}^\alpha) + \varepsilon^\alpha \rho^\alpha h^\alpha. \end{aligned} \quad (5.16)$$

Next we seek to remove the Helmholtz potential and entropy terms from the energy equation. To do this we recall that the Helmholtz potential is a function of all of the variables listed in (4.6). Under the assumptions listed in Section 5.2 we drop the solid phase terms from this list. Furthermore, we know that under these conditions the volume fractions are not independent so we could replace both ε^l and ε^g by saturation, S . This is not done (yet) as the entropy inequality was exploited while assuming that they are independent. The switch can be made at any point later. Therefore, under the present assumptions,

$$\psi^\alpha = \psi^\alpha(\varepsilon^l, \varepsilon^g, \rho^{l_j}, \rho^{g_j}, T) \quad \text{for } j = 1 : N.$$

Entropy, η^α , is assumed to be a function of the same set of variables (since $\eta^\alpha = -\partial\psi^\alpha/\partial T$). Using the chain rule to expand all of the derivatives of ψ^α and η^α in equation (5.16) we arrive at an expanded form of the energy equation:

$$\begin{aligned} \sum_{\beta \neq \alpha} \hat{Q}_\beta^\alpha = & \varepsilon^\alpha \rho^\alpha \left(\frac{\partial \psi^\alpha}{\partial T} + \eta^\alpha + T \frac{\partial \eta^\alpha}{\partial T} \right) \dot{T} \\ & + \varepsilon^\alpha \rho^\alpha \left(\left[\frac{\partial \psi^\alpha}{\partial \varepsilon^l} + T \frac{\partial \eta^\alpha}{\partial \varepsilon^l} \right] \dot{\varepsilon}^l + \left[\frac{\partial \psi^\alpha}{\partial \varepsilon^g} + T \frac{\partial \eta^\alpha}{\partial \varepsilon^g} \right] \dot{\varepsilon}^g \right. \\ & \quad \left. + \sum_{j=1}^N \left[\frac{\partial \psi^\alpha}{\partial \rho^{l_j}} + T \frac{\partial \eta^\alpha}{\partial \rho^{l_j}} \right] \dot{\rho}^{l_j} + \sum_{j=1}^N \left[\frac{\partial \psi^\alpha}{\partial \rho^{g_j}} + T \frac{\partial \eta^\alpha}{\partial \rho^{g_j}} \right] \dot{\rho}^{g_j} \right) \\ & + \varepsilon^\alpha \rho^\alpha \left(\left[\frac{\partial \psi^\alpha}{\partial T} + \eta^\alpha + T \frac{\partial \eta^\alpha}{\partial T} \right] \nabla T \right) \end{aligned}$$

$$\begin{aligned}
& + \left[\frac{\partial \psi^\alpha}{\partial \varepsilon^l} + T \frac{\partial \eta^\alpha}{\partial \varepsilon^l} \right] \nabla \varepsilon^l + \left[\frac{\partial \psi^\alpha}{\partial \varepsilon^g} + T \frac{\partial \eta^\alpha}{\partial \varepsilon^g} \right] \nabla \varepsilon^g \\
& + \sum_{j=1}^N \left[\frac{\partial \psi^\alpha}{\partial \rho^{l_j}} + T \frac{\partial \eta^\alpha}{\partial \rho^{l_j}} \right] \nabla \rho^{l_j} + \sum_{j=1}^N \left[\frac{\partial \psi^\alpha}{\partial \rho^{g_j}} + T \frac{\partial \eta^\alpha}{\partial \rho^{g_j}} \right] \nabla \rho^{g_j} \Big) \cdot \mathbf{v}^{\alpha,s} \\
- \varepsilon^\alpha \underline{\underline{\mathbf{t}}}^\alpha : \underline{\underline{\mathbf{d}}}^\alpha - \nabla \cdot (\varepsilon^\alpha \mathbf{q}^\alpha) + \varepsilon^\alpha \rho^\alpha h^\alpha.
\end{aligned} \tag{5.17}$$

From the entropy inequality we know that the temperature and entropy are conjugate variables. For this reason we can cancel these terms from the \dot{T} and ∇T coefficients.

Equation (5.17) is an expression of energy balance for phase α , but since we are working under the assumption that the phases are in thermal equilibrium we now sum over all of the phases to form one energy balance equation for the entire porous medium. The sum is:

$$\begin{aligned}
\sum_{\alpha} \left\{ \sum_{\beta \neq \alpha} \hat{Q}_{\beta}^{\alpha} \right\} &= \sum_{\alpha} \left\{ \varepsilon^{\alpha} \rho^{\alpha} T \frac{\partial \eta^{\alpha}}{\partial T} \right\} \dot{T} \\
&+ \sum_{\alpha} \left\{ \varepsilon^{\alpha} \rho^{\alpha} \left[\frac{\partial \psi^{\alpha}}{\partial \varepsilon^l} + T \frac{\partial \eta^{\alpha}}{\partial \varepsilon^l} \right] \right\} \dot{\varepsilon}^l + \sum_{\alpha} \left\{ \varepsilon^{\alpha} \rho^{\alpha} \left[\frac{\partial \psi^{\alpha}}{\partial \varepsilon^g} + T \frac{\partial \eta^{\alpha}}{\partial \varepsilon^g} \right] \right\} \dot{\varepsilon}^g \\
&+ \sum_{\alpha} \left\{ \varepsilon^{\alpha} \rho^{\alpha} \sum_{j=1}^N \left[\frac{\partial \psi^{\alpha}}{\partial \rho^{l_j}} + T \frac{\partial \eta^{\alpha}}{\partial \rho^{l_j}} \right] \dot{\rho}^{l_j} \right\} \\
&+ \sum_{\alpha} \left\{ \varepsilon^{\alpha} \rho^{\alpha} \sum_{j=1}^N \left[\frac{\partial \psi^{\alpha}}{\partial \rho^{g_j}} + T \frac{\partial \eta^{\alpha}}{\partial \rho^{g_j}} \right] \dot{\rho}^{g_j} \right\} \\
&+ \sum_{\beta=l,g} \left\{ \varepsilon^{\beta} \rho^{\beta} \left(\left[T \frac{\partial \eta^{\beta}}{\partial T} \right] \nabla T \right. \right. \\
&\quad + \left[\frac{\partial \psi^{\beta}}{\partial \varepsilon^l} + T \frac{\partial \eta^{\beta}}{\partial \varepsilon^l} \right] \nabla \varepsilon^l + \left[\frac{\partial \psi^{\beta}}{\partial \varepsilon^g} + T \frac{\partial \eta^{\beta}}{\partial \varepsilon^g} \right] \nabla \varepsilon^g \\
&\quad + \sum_{j=1}^N \left[\frac{\partial \psi^{\beta}}{\partial \rho^{l_j}} + T \frac{\partial \eta^{\beta}}{\partial \rho^{l_j}} \right] \nabla \rho^{l_j} \\
&\quad \left. \left. + \sum_{j=1}^N \left[\frac{\partial \psi^{\beta}}{\partial \rho^{g_j}} + T \frac{\partial \eta^{\beta}}{\partial \rho^{g_j}} \right] \nabla \rho^{g_j} \right) \cdot \mathbf{v}^{\beta,s} \right\} \\
- \sum_{\alpha} \left\{ \varepsilon^{\alpha} \underline{\underline{\mathbf{t}}}^{\alpha} : \underline{\underline{\mathbf{d}}}^{\alpha} \right\} - \nabla \cdot \left(\sum_{\alpha} \left\{ \varepsilon^{\alpha} \mathbf{q}^{\alpha} \right\} \right) + \sum_{\alpha} \left\{ \varepsilon^{\alpha} \rho^{\alpha} h^{\alpha} \right\}
\end{aligned} \tag{5.19}$$

The \dot{T} term can be rewritten as $\sum_{\alpha} \left\{ \varepsilon^{\alpha} \rho^{\alpha} T \frac{\partial \eta^{\alpha}}{\partial T} \right\} \dot{T} = \rho c_p \dot{T}$, and in doing so we implicitly define the volumetric heat capacity of the entire medium:

$$\rho c_p = \sum_{\alpha} \left\{ \varepsilon^{\alpha} \rho^{\alpha} T \frac{\partial \eta^{\alpha}}{\partial T} \right\}.$$

Next we recall from equation (4.39) that the partial heat flux can be written as $\sum_{\alpha} \left\{ \varepsilon^{\alpha} \mathbf{q}^{\alpha} \right\} = \underline{\mathbf{K}} \cdot \nabla T$ (more will be said about the functional form of $\underline{\mathbf{K}}$ in future sections). The heat source term can be rewritten as $\sum_{\alpha} \left\{ \varepsilon^{\alpha} \rho^{\alpha} h^{\alpha} \right\} = \rho h$, where h is any internal source or sink of heat on the entire medium (i.e. heat sources that are not boundary conditions).

Notice that several of the gradient terms are the same as those in the linearized constitutive equation for the momentum transfer, (4.31) and (4.36). Replacing these terms with the remainder of the momentum balance terms and simplifying gives

$$\begin{aligned} \sum_{\alpha} \left\{ \sum_{\beta \neq \alpha} \hat{Q}_{\beta}^{\alpha} \right\} &= \rho c_p \dot{T} - \nabla \cdot (\underline{\mathbf{K}} \cdot \nabla T) + \rho h - \sum_{\alpha} \left\{ \varepsilon^{\alpha} \underline{\mathbf{t}}^{\alpha} : \underline{\underline{\mathbf{d}}}^{\alpha} \right\} \\ &+ \sum_{\alpha} \left\{ \varepsilon^{\alpha} \rho^{\alpha} \left[\frac{\partial \psi^{\alpha}}{\partial \varepsilon^l} + T \frac{\partial \eta^{\alpha}}{\partial \varepsilon^l} \right] \right\} \dot{\varepsilon}^l + \sum_{\alpha} \left\{ \varepsilon^{\alpha} \rho^{\alpha} \left[\frac{\partial \psi^{\alpha}}{\partial \varepsilon^g} + T \frac{\partial \eta^{\alpha}}{\partial \varepsilon^g} \right] \right\} \dot{\varepsilon}^g \\ &+ \sum_{\alpha} \left\{ \varepsilon^{\alpha} \rho^{\alpha} \sum_{j=1}^N \left[\frac{\partial \psi^{\alpha}}{\partial \rho^{l_j}} + T \frac{\partial \eta^{\alpha}}{\partial \rho^{l_j}} \right] \dot{\rho}^{l_j} \right\} \\ &+ \sum_{\alpha} \left\{ \varepsilon^{\alpha} \rho^{\alpha} \sum_{j=1}^N \left[\frac{\partial \psi^{\alpha}}{\partial \rho^{g_j}} + T \frac{\partial \eta^{\alpha}}{\partial \rho^{g_j}} \right] \dot{\rho}^{g_j} \right\} \\ &+ \sum_{\beta=l,g} \left\{ \left[- \sum_{\gamma \neq \beta} (\hat{\mathbf{T}}_{\gamma}^{\beta}) + p^{\beta} \nabla \varepsilon^{\beta} \right. \right. \\ &\quad \left. \left. + \sum_{j=1}^N \left[\left(\sum_{\alpha} \left(\varepsilon^{\alpha} \rho^{\alpha} \frac{\partial \psi^{\alpha}}{\partial \rho^{\beta_j}} \right) + \varepsilon^{\beta} \rho^{\beta} T \frac{\partial \eta^{\beta}}{\partial \rho^{\beta_j}} \right) \nabla \rho^{\beta_j} \right] \right. \right. \\ &\quad \left. \left. + \varepsilon^{\beta} \rho^{\beta} \left\{ \left[T \frac{\partial \eta^{\beta}}{\partial T} \right] \nabla T + \left[T \frac{\partial \eta^{\beta}}{\partial \varepsilon^l} \right] \nabla \varepsilon^l + \left[T \frac{\partial \eta^{\beta}}{\partial \varepsilon^g} \right] \nabla \varepsilon^g \right. \right. \right. \\ &\quad \left. \left. \left. + \sum_{j=1}^N \left(\left[T \frac{\partial \eta^{\beta}}{\partial \rho^{\gamma_j}} \right] \nabla \rho^{\gamma_j} \right) \right\} \right] \right\} \cdot \mathbf{v}^{\beta,s}. \quad (5.20) \end{aligned}$$

Equation (5.20) expresses the energy balance for the bulk porous medium. Several of the terms can be simplified at this point. Toward this goal, we will

1. derive a relation for the energy transfer terms: $\sum_{\alpha} \sum_{\beta \neq \alpha} \hat{Q}_{\beta}^{\alpha}$
2. rewrite the stress term, $\sum_{\alpha} \varepsilon^{\alpha} \underline{\underline{\mathbf{t}}}^{\alpha} : \underline{\underline{\mathbf{d}}}^{\alpha}$, using constitutive relationships for $\underline{\underline{\mathbf{t}}}^{\alpha}$
3. rewrite the momentum transfer terms, $\hat{\mathbf{T}}_{\gamma}^{\beta}$, using the linearized momentum transfer from the entropy inequality, (4.36)
4. rewrite the advective terms, $\mathbf{v}^{\beta,s}$, using Darcy's law, and
5. relate the changes in entropy, $\frac{\partial \eta^{\alpha}}{\partial(\cdot)}$, to material coefficients.

The first two of these are discussed in the following two subsections. The third and fourth come as a consequence of the first two, and the fifth will be discussed under proper simplifications in future sections.

5.3.2.1 Energy Transfer in the Total Energy Equation

Consider the energy transfer and stress terms: \hat{Q}_{β}^{α} , \hat{Q}^{α_j} , and $\underline{\underline{\mathbf{t}}}^{\alpha}$. From equations (3.36a) and (3.36b) we recall that the restrictions on the interface are

$$\sum_{j=1}^N \left[\hat{Q}^{\alpha_j} + \hat{\mathbf{i}}^{\alpha_j} \cdot \mathbf{v}^{\alpha_j, \alpha} + \hat{r}^{\alpha_j} \left(e^{\alpha_j} + \frac{1}{2} \mathbf{v}^{\alpha_j, \alpha} \cdot \mathbf{v}^{\alpha_j, \alpha} \right) \right] = 0 \quad \forall \alpha, \quad (5.21a)$$

$$\sum_{\alpha} \sum_{\beta \neq \alpha} \left[\hat{Q}_{\beta}^{\alpha_j} + \hat{\mathbf{T}}_{\beta}^{\alpha_j} \cdot \mathbf{v}^{\alpha_j} + \hat{e}_{\beta}^{\alpha_j} \left(e^{\alpha_j} + \frac{1}{2} \mathbf{v}^{\alpha_j} \cdot \mathbf{v}^{\alpha_j} \right) \right] = 0 \quad j = 1 : N. \quad (5.21b)$$

We also note the identity

$$\hat{Q}_{\beta}^{\alpha} = \sum_{j=1}^N \left[\hat{Q}_{\beta}^{\alpha_j} + \hat{\mathbf{T}}_{\beta}^{\alpha_j} \cdot \mathbf{v}^{\alpha_j, \alpha} + \hat{e}_{\beta}^{\alpha_j} \left(e^{\alpha_j, \alpha} + \frac{1}{2} \mathbf{v}^{\alpha_j, \alpha} \cdot \mathbf{v}^{\alpha_j, \alpha} \right) \right] \quad (5.22)$$

(see Appendix A.2 of [80]). With these three identities, the sum of the energy transfer terms can be written as

$$\begin{aligned} \sum_{\alpha} \sum_{\beta \neq \alpha} \hat{Q}_{\beta}^{\alpha} &= \sum_{\alpha} \sum_{\beta \neq \alpha} \sum_{j=1}^N \left[\hat{Q}_{\beta}^{\alpha_j} + \hat{\mathbf{T}}_{\beta}^{\alpha_j} \cdot \mathbf{v}^{\alpha_j, \alpha} + \hat{e}_{\beta}^{\alpha_j} \left(e^{\alpha_j, \alpha} + \frac{1}{2} \mathbf{v}^{\alpha_j, \alpha} \cdot \mathbf{v}^{\alpha_j, \alpha} \right) \right] \\ &= \sum_{j=1}^N \left\{ \sum_{\alpha} \sum_{\beta \neq \alpha} \left[\hat{Q}_{\beta}^{\alpha_j} \right] \right\} \end{aligned}$$

$$\begin{aligned}
& + \sum_{\alpha} \sum_{\beta \neq \alpha} \left[\hat{\mathbf{T}}_{\beta}^{\alpha_j} \cdot \mathbf{v}^{\alpha_j, \alpha} + \hat{e}_{\beta}^{\alpha_j} \left(e^{\alpha_j, \alpha} + \frac{1}{2} \mathbf{v}^{\alpha_j, \alpha} \cdot \mathbf{v}^{\alpha_j, \alpha} \right) \right] \Big\} \\
= & \sum_{j=1}^N \left\{ - \sum_{\alpha} \sum_{\beta \neq \alpha} \left[\hat{\mathbf{T}}_{\beta}^{\alpha_j} \cdot \mathbf{v}^{\alpha_j} + \hat{e}_{\beta}^{\alpha_j} \left(e^{\alpha_j} + \frac{1}{2} \mathbf{v}^{\alpha_j} \cdot \mathbf{v}^{\alpha_j} \right) \right] \right. \\
& \left. + \sum_{\alpha} \sum_{\beta \neq \alpha} \left[\hat{\mathbf{T}}_{\beta}^{\alpha_j} \cdot \mathbf{v}^{\alpha_j, \alpha} + \hat{e}_{\beta}^{\alpha_j} \left(e^{\alpha_j, \alpha} + \frac{1}{2} \mathbf{v}^{\alpha_j, \alpha} \cdot \mathbf{v}^{\alpha_j, \alpha} \right) \right] \right\} \\
= & - \sum_{j=1}^N \left\{ \sum_{\alpha} \sum_{\beta \neq \alpha} \left[\hat{\mathbf{T}}_{\beta}^{\alpha_j} \cdot \mathbf{v}^{\alpha} + \hat{e}_{\beta}^{\alpha_j} e^{\alpha} \right. \right. \\
& \left. \left. - \frac{1}{2} \hat{e}_{\beta}^{\alpha_j} (\mathbf{v}^{\alpha_j, \alpha} \cdot \mathbf{v}^{\alpha_j, \alpha} - \mathbf{v}^{\alpha_j} \cdot \mathbf{v}^{\alpha_j}) \right] \right\}. \quad (5.23)
\end{aligned}$$

Next we examine the momentum transfer term appearing in equation (5.23). Recall from equation (3.33) that

$$\hat{\mathbf{T}}_{\beta}^{\alpha} = \sum_{j=1}^N \left[\hat{\mathbf{T}}_{\beta}^{\alpha_j} + \hat{e}_{\beta}^{\alpha_j} \mathbf{v}^{\alpha_j, \alpha} \right]. \quad (5.24)$$

Rearranging this identity and multiplying by the α -phase velocity we see that

$$\sum_{j=1}^N \hat{\mathbf{T}}_{\beta}^{\alpha_j} \cdot \mathbf{v}^{\alpha} = \hat{\mathbf{T}}_{\beta}^{\alpha} \cdot \mathbf{v}^{\alpha} - \sum_{j=1}^N \left[\hat{e}_{\beta}^{\alpha_j} \mathbf{v}^{\alpha_j, \alpha} \cdot \mathbf{v}^{\alpha} \right]. \quad (5.25)$$

Substituting (5.25) into (5.23), simplifying, and neglecting the second-order terms in velocity we see that

$$\sum_{\alpha} \sum_{\beta \neq \alpha} \left\{ \hat{Q}_{\beta}^{\alpha} \right\} = - \sum_{\beta \neq l} \left\{ \hat{\mathbf{T}}_{\beta}^l \cdot \mathbf{v}^{l, s} \right\} - \sum_{\beta \neq g} \left\{ \hat{\mathbf{T}}_{\beta}^g \cdot \mathbf{v}^{g, s} \right\} - \hat{e}_g^l (e^l - e^g). \quad (5.26)$$

Notice from this simplified version that we have eliminated the energy transfer in favor of the mass and momentum transfer terms after summing over α (and neglecting second-order effects).

5.3.2.2 Stress in the Total Energy Equation

We next derive the proper form of the stress term in equation (5.20). The α -phase stress near equilibrium is given by $\underline{\underline{\mathbf{t}}}^{\alpha} = -p^{\alpha} \underline{\underline{\mathbf{I}}} + \underline{\underline{\boldsymbol{\nu}}}^{\alpha} : \underline{\underline{\mathbf{d}}}^{\alpha}$ from the linearization of the fluid phase stress tensors about equilibrium. For the solid phase

stress tensor, on the other hand, we will not use constitutive relations for $\underline{\underline{\mathbf{t}}}^s$ but keep in mind that it is the sum of effective and hydrating stresses (see equation (4.23)). Therefore,

$$\begin{aligned} \sum_{\alpha} \{ \varepsilon^{\alpha} \underline{\underline{\mathbf{t}}}^{\alpha} : \underline{\underline{\mathbf{d}}}^{\alpha} \} &= \sum_{\alpha=l,g} \left\{ \varepsilon^{\alpha} \left(-p^{\alpha} \underline{\underline{\mathbf{I}}} + \underline{\underline{\mathbf{v}}}^{\alpha} : \underline{\underline{\mathbf{d}}}^{\alpha} \right) : \underline{\underline{\mathbf{d}}}^{\alpha} \right\} + \varepsilon^s \underline{\underline{\mathbf{t}}}^s : \underline{\underline{\mathbf{d}}}^s \\ &= - \sum_{\alpha=l,g} \{ \varepsilon^{\alpha} p^{\alpha} \underline{\underline{\mathbf{I}}} : \underline{\underline{\mathbf{d}}}^{\alpha} \} + \sum_{\alpha=l,g} \left\{ \underline{\underline{\mathbf{v}}}^{\alpha} : \underline{\underline{\mathbf{d}}}^{\alpha} : \underline{\underline{\mathbf{d}}}^{\alpha} \right\} + \varepsilon^s \underline{\underline{\mathbf{t}}}^s : \underline{\underline{\mathbf{d}}}^s. \end{aligned} \quad (5.27)$$

The second term is likely negligible as the viscous terms typically play little role in creeping flow. This means that $\sum_{\alpha} \{ \varepsilon^{\alpha} \underline{\underline{\mathbf{t}}}^{\alpha} : \underline{\underline{\mathbf{d}}}^{\alpha} \}$ can be approximated by

$$\sum_{\alpha} \{ \varepsilon^{\alpha} \underline{\underline{\mathbf{t}}}^{\alpha} : \underline{\underline{\mathbf{d}}}^{\alpha} \} = - \sum_{\alpha=l,g} \{ \varepsilon^{\alpha} p^{\alpha} \underline{\underline{\mathbf{I}}} : \underline{\underline{\mathbf{d}}}^{\alpha} \} + \varepsilon^s \underline{\underline{\mathbf{t}}}^s : \underline{\underline{\mathbf{d}}}^s. \quad (5.28)$$

Using indicial notation we note that for the fluid phases, $\underline{\underline{\mathbf{I}}} : \underline{\underline{\mathbf{d}}}^{\alpha} = \underline{\underline{\mathbf{I}}} : (\nabla \mathbf{v}^{\alpha})_{sym} = \delta_{ij} v_{j,i}^{\alpha} = v_{i,i}^{\alpha} = \nabla \cdot \mathbf{v}^{\alpha}$, and therefore the stress tensor terms can be simplified to

$$\sum_{\alpha} \{ \varepsilon^{\alpha} \underline{\underline{\mathbf{t}}}^{\alpha} : \underline{\underline{\mathbf{d}}}^{\alpha} \} = - \sum_{\alpha=l,g} \{ \varepsilon^{\alpha} p^{\alpha} \nabla \cdot \mathbf{v}^{\alpha} \} + \varepsilon^s \underline{\underline{\mathbf{t}}}^s : \underline{\underline{\mathbf{d}}}^s. \quad (5.29)$$

The solid phase rate-of-deformation tensor is related to the strain rate of the solid phase. Assuming that the strain rate is zero (for a rigid and incompressible solid), we can neglect this term. This implies that the stress tensor term in (5.20) can be approximated by

$$\sum_{\alpha} \{ \varepsilon^{\alpha} \underline{\underline{\mathbf{t}}}^{\alpha} : \underline{\underline{\mathbf{d}}}^{\alpha} \} = - \sum_{\alpha=l,g} \{ \varepsilon^{\alpha} p^{\alpha} \nabla \cdot \mathbf{v}^{\alpha} \}.$$

Using Assumption # 1 from Section 5.2 for the divergence of the solid-phase velocity ($\nabla \cdot \mathbf{v}^s = 0$), we finally conclude that the stress term in (5.20) can be simplified to

$$\sum_{\alpha} \{ \varepsilon^{\alpha} \underline{\underline{\mathbf{t}}}^{\alpha} : \underline{\underline{\mathbf{d}}}^{\alpha} \} = -\varepsilon^l p^l \nabla \cdot \mathbf{v}^{l,s} - \varepsilon^g p^g \nabla \cdot \mathbf{v}^{g,s}. \quad (5.30)$$

Not surprisingly, this states that the stress is related to the fluid pressures.

5.3.2.3 Total Energy Balance Equation

In this subsection we use equations (5.26) and (5.30) to simplify the energy balance equation, (5.20). Substituting these into (5.20) and canceling the momentum transfer terms gives

$$\begin{aligned}
0 = & \rho c_p \dot{T} - \nabla \cdot (\underline{\mathbf{K}} \cdot \nabla T) + \rho h + \varepsilon^l p^l \nabla \cdot \mathbf{v}^{l,s} + \varepsilon^g p^g \nabla \cdot \mathbf{v}^{g,s} + \hat{e}_g^l (e^l - e^g) \\
& + \sum_{\alpha} \left\{ \varepsilon^{\alpha} \rho^{\alpha} \left[\frac{\partial \psi^{\alpha}}{\partial \varepsilon^l} + T \frac{\partial \eta^{\alpha}}{\partial \varepsilon^l} \right] \right\} \dot{\varepsilon}^l + \sum_{\alpha} \left\{ \varepsilon^{\alpha} \rho^{\alpha} \left[\frac{\partial \psi^{\alpha}}{\partial \varepsilon^g} + T \frac{\partial \eta^{\alpha}}{\partial \varepsilon^g} \right] \right\} \dot{\varepsilon}^g \\
& + \sum_{\alpha} \left\{ \varepsilon^{\alpha} \rho^{\alpha} \sum_{j=1}^N \left[\frac{\partial \psi^{\alpha}}{\partial \rho^{l_j}} + T \frac{\partial \eta^{\alpha}}{\partial \rho^{l_j}} \right] \dot{\rho}^{l_j} \right\} \\
& + \sum_{\alpha} \left\{ \varepsilon^{\alpha} \rho^{\alpha} \sum_{j=1}^N \left[\frac{\partial \psi^{\alpha}}{\partial \rho^{g_j}} + T \frac{\partial \eta^{\alpha}}{\partial \rho^{g_j}} \right] \dot{\rho}^{g_j} \right\} \\
& + \sum_{\beta=l,g} \left\{ \left[p^{\beta} \nabla \varepsilon^{\beta} + \sum_{j=1}^N \left[\left(\sum_{\alpha} \left(\varepsilon^{\alpha} \rho^{\alpha} \frac{\partial \psi^{\alpha}}{\partial \rho^{\beta_j}} \right) + \varepsilon^{\beta} \rho^{\beta} T \frac{\partial \eta^{\beta}}{\partial \rho^{\beta_j}} \right) \nabla \rho^{\beta_j} \right] \right. \right. \\
& \quad \left. \left. + \varepsilon^{\beta} \rho^{\beta} \left\{ \left[T \frac{\partial \eta^{\beta}}{\partial T} \right] \nabla T + \left[T \frac{\partial \eta^{\beta}}{\partial \varepsilon^l} \right] \nabla \varepsilon^l + \left[T \frac{\partial \eta^{\beta}}{\partial \varepsilon^g} \right] \nabla \varepsilon^g \right. \right. \right. \\
& \quad \left. \left. \left. + \sum_{j=1}^N \left(\left[T \frac{\partial \eta^{\beta}}{\partial \rho^{\gamma_j}} \right] \nabla \rho^{\gamma_j} \right) \right\} \right] \cdot \mathbf{v}^{\beta,s} \right\}. \tag{5.31}
\end{aligned}$$

Next we discuss the $\varepsilon^{\alpha} p^{\alpha} \nabla \cdot \mathbf{v}^{\alpha,s}$ and $p^{\alpha} \nabla (\varepsilon^{\alpha}) \cdot \mathbf{v}^{\alpha,s}$ terms. Using the product rule it is clear that the sum of these two terms gives $p^{\alpha} \nabla \cdot (\varepsilon^{\alpha} \mathbf{v}^{\alpha,s})$. A choice is made here to remove these terms in lieu of mass transfer terms. To do so, we recall from the mass balance equation that

$$\frac{D^s (\varepsilon^{\alpha} \rho^{\alpha})}{Dt} + \nabla \cdot (\varepsilon^{\alpha} \rho^{\alpha} \mathbf{v}^{\alpha,s}) = \sum_{\beta \neq \alpha} \hat{e}_{\beta}^{\alpha},$$

and solve for $\nabla \cdot (\varepsilon^{\alpha} \mathbf{v}^{\alpha,s})$:

$$\rho^{\alpha} \nabla \cdot (\varepsilon^{\alpha} \mathbf{v}^{\alpha,s}) = -\rho^{\alpha} \dot{\varepsilon}^{\alpha} - \varepsilon^{\alpha} \dot{\rho}^{\alpha} - \varepsilon^{\alpha} \mathbf{v}^{\alpha,s} \cdot \nabla \rho^{\alpha} + \hat{e}_{\beta}^{\alpha}.$$

We have dropped the summation on the mass transfer term since we are assuming that the solid phase is inert and that there are only two fluid phases. Multiplying by $(p^{\alpha}/\rho^{\alpha})$ gives an expression for $p^{\alpha} \nabla \cdot (\varepsilon^{\alpha} \mathbf{v}^{\alpha,s})$:

$$p^{\alpha} \nabla \cdot (\varepsilon^{\alpha} \mathbf{v}^{\alpha,s}) = -p^{\alpha} \dot{\varepsilon}^{\alpha} - \left(\frac{\varepsilon^{\alpha} p^{\alpha}}{\rho^{\alpha}} \right) \dot{\rho}^{\alpha} - \left(\frac{\varepsilon^{\alpha} p^{\alpha}}{\rho^{\alpha}} \right) \mathbf{v}^{\alpha,s} \cdot \nabla \rho^{\alpha} + \left(\frac{p^{\alpha}}{\rho^{\alpha}} \right) \hat{e}_{\beta}^{\alpha}. \tag{5.32}$$

Substituting this into the energy equation gives

$$\begin{aligned}
0 = & \rho c_p \dot{T} - \nabla \cdot (\underline{\mathbf{K}} \cdot \nabla T) + \rho h + \left(\left(\frac{p^l}{\rho^l} + e^l \right) - \left(\frac{p^g}{\rho^g} + e^g \right) \right) \hat{e}_g \\
& + \left\{ -p^l + \sum_{\alpha} \left\{ \varepsilon^{\alpha} \rho^{\alpha} \left[\frac{\partial \psi^{\alpha}}{\partial \varepsilon^l} + T \frac{\partial \eta^{\alpha}}{\partial \varepsilon^l} \right] \right\} \right\} \dot{\varepsilon}^l \\
& + \left\{ -p^g + \sum_{\alpha} \left\{ \varepsilon^{\alpha} \rho^{\alpha} \left[\frac{\partial \psi^{\alpha}}{\partial \varepsilon^g} + T \frac{\partial \eta^{\alpha}}{\partial \varepsilon^g} \right] \right\} \right\} \dot{\varepsilon}^g \\
& + \sum_{j=1}^N \left(\left[- \left(\frac{\varepsilon^l p^l}{\rho^l} \right) + \sum_{\alpha} \left\{ \varepsilon^{\alpha} \rho^{\alpha} \left[\frac{\partial \psi^{\alpha}}{\partial \rho^{l_j}} + T \frac{\partial \eta^{\alpha}}{\partial \rho^{l_j}} \right] \right\} \right] \dot{\rho}^{l_j} \right) \\
& + \sum_{j=1}^N \left(\left[- \left(\frac{\varepsilon^g p^g}{\rho^g} \right) + \sum_{\alpha} \left\{ \varepsilon^{\alpha} \rho^{\alpha} \left[\frac{\partial \psi^{\alpha}}{\partial \rho^{g_j}} + T \frac{\partial \eta^{\alpha}}{\partial \rho^{g_j}} \right] \right\} \right] \dot{\rho}^{g_j} \right) \\
& + \sum_{\beta=l,g} \left\{ \left[\sum_{j=1}^N \left(\left[- \left(\frac{\varepsilon^{\beta} p^{\beta}}{\rho^{\beta}} \right) + \sum_{\alpha} \left\{ \varepsilon^{\alpha} \rho^{\alpha} \left[\frac{\partial \psi^{\alpha}}{\partial \rho^{\beta_j}} + T \frac{\partial \eta^{\alpha}}{\partial \rho^{\beta_j}} \right] \right\} \right] \nabla \rho^{\beta_j} \right) \right. \right. \\
& \quad \left. \left. + \varepsilon^{\beta} \rho^{\beta} \left\{ \left[T \frac{\partial \eta^{\beta}}{\partial T} \right] \nabla T + \left[T \frac{\partial \eta^{\beta}}{\partial \varepsilon^l} \right] \nabla \varepsilon^l + \left[T \frac{\partial \eta^{\beta}}{\partial \varepsilon^g} \right] \nabla \varepsilon^g \right. \right. \right. \\
& \quad \left. \left. \left. + \sum_{j=1}^N \left(\left[T \frac{\partial \eta^{\beta}}{\partial \rho^{\gamma_j}} \right] \nabla \rho^{\gamma_j} \right) \right\} \right] \cdot \mathbf{v}^{\beta,s} \right\}. \tag{5.33}
\end{aligned}$$

There are several more simplifications that can be made. To help with these simplifications recall the following definitions for enthalpy, pressure, wetting potential, chemical potential, and entropy respectively:

$$H^{\alpha} = \frac{p^{\alpha}}{\rho^{\alpha}} + e^{\alpha} \tag{5.34a}$$

$$p^{\beta} = \sum_{\alpha} \sum_{j=1}^N \left(\frac{\varepsilon^{\alpha} \rho^{\alpha} \rho^{\beta_j}}{\varepsilon^{\beta}} \frac{\partial \psi^{\alpha}}{\partial \rho^{\beta_j}} \right) \tag{5.34b}$$

$$\pi^{\beta} = \sum_{\alpha} \left(\varepsilon^{\alpha} \rho^{\alpha} \frac{\partial \psi^{\alpha}}{\partial \varepsilon^{\beta}} \right) \tag{5.34c}$$

$$\mu^{\beta_j} = \psi^{\beta} + \sum_{\alpha} \left(\frac{\varepsilon^{\alpha} \rho^{\alpha}}{\varepsilon^{\beta}} \frac{\partial \psi^{\alpha}}{\partial \rho^{\beta_j}} \right) \tag{5.34d}$$

$$\eta^{\alpha} = - \frac{\partial \psi^{\alpha}}{\partial T}. \tag{5.34e}$$

With these identities in mind we make the following four simplifications:

1. coefficient of the mass transfer term:

$$\left(\left(\frac{p^l}{\rho^l} + e^l \right) - \left(\frac{p^g}{\rho^g} + e^g \right) \right) \hat{e}_g^l = (H^l - H^g) \hat{e}_g^l := L \hat{e}_g^l$$

Recalling that \hat{e}_g^l is the rate of mass transfer between the fluid phases, L is understood as the latent heat of evaporation since this represents the heat lost or gained due to phase exchanged between the fluids. This is consistent with the chemist's definition of latent heat as the change in enthalpy.

2. coefficient of the time rates of change of volume fractions:

$$\begin{aligned} & -p^\beta + \sum_{\alpha} \left\{ \varepsilon^\alpha \rho^\alpha \left[\frac{\partial \psi^\alpha}{\partial \varepsilon^\beta} + T \frac{\partial \eta^\alpha}{\partial \varepsilon^\beta} \right] \right\} \\ & = -p^\beta + \pi^\beta + T \frac{\partial \pi^\beta}{\partial T} \\ & = -\bar{p}^\beta - T \frac{\partial \pi^\beta}{\partial T}, \end{aligned}$$

where we recall that \bar{p}^β is thermodynamic pressure as defined in Chapter 4

$$p^\beta = \bar{p}^\beta + \pi^\beta.$$

At this point we can exchange the time rates of change of volume fractions for time rates of change of saturation. That is, recall $\dot{\varepsilon}^l = \varepsilon \dot{S}$ and $\dot{\varepsilon}^g = -\varepsilon \dot{S}$. The sum of the two associated terms is

$$\begin{aligned} & \left(-\bar{p}^l - T \frac{\partial \pi^l}{\partial T} \right) \varepsilon \dot{S} - \left(-\bar{p}^g - T \frac{\partial \pi^g}{\partial T} \right) \varepsilon \dot{S} \\ & = \left[(\bar{p}^g - \bar{p}^l) + T \left(\frac{\partial \pi^g}{\partial T} - \frac{\partial \pi^l}{\partial T} \right) \right] \varepsilon \dot{S}. \end{aligned}$$

From the near equilibrium results from the entropy inequality we now recall (from equation (4.53)) that

$$\bar{p}^\beta \Big|_{n.eq.} = \bar{p}^\beta \Big|_{eq.} - \tau \dot{\varepsilon}^\beta \tag{5.35}$$

Therefore, the \dot{S} term becomes

$$\left[\left(\bar{p}^g \Big|_{eq.} - \bar{p}^l \Big|_{eq.} \right) + 2\tau\varepsilon\dot{S} + T \frac{\partial}{\partial T} (\pi^g - \pi^l) \right] \varepsilon\dot{S}. \quad (5.36)$$

The first set of parenthesis in (5.36) (approximately) represents the capillary pressure as measured at equilibrium,

$$\left(\bar{p}^g \Big|_{eq.} - \bar{p}^l \Big|_{eq.} \right) = p_c.$$

This will be discussed in more detail in Section 5.4.1.1. The middle term in (5.36) is an effect of the dynamic pressure-saturation relationship (equation (4.53)). The temperature derivative can be interpreted as the effect of temperature on the relative wetting potential. That is, how much does temperature affect the relative affinity for one phase over the other. It is likely that a constitutive equation is needed for this relationship.

3. coefficient of time rates of change of densities:

We wish to rewrite these coefficients in terms of enthalpy and chemical potential since it provides a mathematically simpler expression.

$$\begin{aligned} & \sum_{j=1}^N \left(\left[- \left(\frac{\varepsilon^\beta p^\beta}{\rho^\beta} \right) + \sum_{\alpha} \left\{ \varepsilon^\alpha \rho^\alpha \left[\frac{\partial \psi^\alpha}{\partial \rho^{\beta_j}} + T \frac{\partial \eta^\alpha}{\partial \rho^{\beta_j}} \right] \right\} \right] \dot{\rho}^{\beta_j} \right) \\ &= \sum_{j=1}^N \left(\left[- \left(\frac{\varepsilon^\beta p^\beta}{\rho^\beta} \right) + \varepsilon^\beta (\mu^{\beta_j} - \psi^\beta) - \varepsilon^\beta T \frac{\partial}{\partial T} (\mu^{\beta_j} - \psi^\beta) \right] \dot{\rho}^{\beta_j} \right) \\ &= -\varepsilon^\beta \left[\frac{p^\beta}{\rho^\beta} + \psi^\beta + T\eta^\beta \right] \dot{\rho}^\beta + \varepsilon^\beta \sum_{j=1}^N \left[\left(\mu^{\beta_j} - T \frac{\partial \mu^{\beta_j}}{\partial T} \right) \dot{\rho}^{\beta_j} \right] \\ &= -\varepsilon^\beta H^\beta \dot{\rho}^\beta + \varepsilon^\beta \sum_{j=1}^N \left[\left(\mu^{\beta_j} - T \frac{\partial \mu^{\beta_j}}{\partial T} \right) \dot{\rho}^{\beta_j} \right] \end{aligned}$$

where we recall that H^β is the enthalpy of phase β .

4. coefficient of relative velocity:

For this coefficient we again use the definitions of pressure, chemical potential,

and entropy. We also rely on the Gibbs-Duhem relationship (4.61).

$$\begin{aligned}
& \sum_{j=1}^N \left(\left[- \left(\frac{\varepsilon^\beta p^\beta}{\rho^\beta} \right) + \sum_{\alpha} \left\{ \varepsilon^\alpha \rho^\alpha \left[\frac{\partial \psi^\alpha}{\partial \rho^{\beta_j}} + T \frac{\partial \eta^\beta}{\partial \rho^{\beta_j}} \right] \right\} \right] \nabla \rho^{\beta_j} \right) \\
& \quad + \varepsilon^\beta \rho^\beta \left\{ \left[T \frac{\partial \eta^\beta}{\partial T} \right] \nabla T + \left[T \frac{\partial \eta^\beta}{\partial \varepsilon^l} \right] \nabla \varepsilon^l + \left[T \frac{\partial \eta^\beta}{\partial \varepsilon^g} \right] \nabla \varepsilon^g \right. \\
& \quad \quad \left. + \sum_{j=1}^N \left(\left[T \frac{\partial \eta^\beta}{\partial \rho^{\gamma_j}} \right] \nabla \rho^{\gamma_j} \right) \right\} \\
& = - \left(\frac{\varepsilon^\beta p^\beta}{\rho^\beta} \right) \nabla \rho^\beta + \sum_{j=1}^N [\varepsilon^\beta (\mu^{\beta_j} - \psi^\beta) \nabla \rho^{\beta_j}] + \varepsilon^\beta \rho^\beta c_p^\beta \nabla T \\
& \quad + \varepsilon^\beta \rho^\beta T \frac{\partial}{\partial T} \left\{ \frac{\partial \psi^\beta}{\partial \varepsilon^l} \nabla \varepsilon^l + \frac{\partial \psi^\beta}{\partial \varepsilon^g} \nabla \varepsilon^g \right. \\
& \quad \quad \left. + \sum_{j=1}^N \left(\frac{\partial \psi^\beta}{\partial \rho^{\beta_j}} \nabla \rho^{\beta_j} \right) + \sum_{j=1}^N \left(\frac{\partial \psi^\beta}{\partial \rho^{\gamma_j}} \nabla \rho^{\gamma_j} \right) \right\} \\
& = -\varepsilon^\beta \Gamma^\beta \nabla \rho^\beta + \sum_{j=1}^N [\varepsilon^\beta \mu^{\beta_j} \nabla \rho^{\beta_j}] + \varepsilon^\beta \rho^\beta c_p^\beta \nabla T \\
& \quad + T \frac{\partial}{\partial T} \left\{ - \left(\hat{T}_s^\beta + \hat{T}_\gamma^\beta \right) + p^\beta \nabla \varepsilon^\beta + \sum_{\alpha} \sum_{j=1}^N \left[\varepsilon^\alpha \rho^\alpha \frac{\partial \psi^\alpha}{\partial \rho^{\beta_j}} \nabla \rho^{\beta_j} \right] \right\} \\
& = -\varepsilon^\beta \Gamma^\beta \nabla \rho^\beta + \sum_{j=1}^N [\varepsilon^\beta \mu^{\beta_j} \nabla \rho^{\beta_j}] + \varepsilon^\beta \rho^\beta c_p^\beta \nabla T \\
& \quad + T \frac{\partial}{\partial T} \left\{ (\varepsilon^\beta)^2 \underline{\underline{\mathbf{R}}}^\beta \cdot \mathbf{v}^{\beta,s} + p^\beta \nabla \varepsilon^\beta + \sum_{j=1}^N [\varepsilon^\beta (\mu^{\beta_j} - \psi^\beta) \nabla \rho^{\beta_j}] \right\} \\
& = -\varepsilon^\beta \Gamma^\beta \nabla \rho^\beta + \sum_{j=1}^N [\varepsilon^\beta \mu^{\beta_j} \nabla \rho^{\beta_j}] + \varepsilon^\beta \rho^\beta c_p^\beta \nabla T \\
& \quad + T \frac{\partial}{\partial T} \left\{ (\varepsilon^\beta)^2 \underline{\underline{\mathbf{R}}}^\beta \cdot \mathbf{v}^{\beta,s} + p^\beta \nabla \varepsilon^\beta - \varepsilon^\beta \psi^\beta \nabla \rho^\beta + \sum_{j=1}^N [\varepsilon^\beta \mu^{\beta_j} \nabla \rho^{\beta_j}] \right\} \\
& = -\varepsilon^\beta \Gamma^\beta \nabla \rho^\beta + \sum_{j=1}^N [\varepsilon^\beta \mu^{\beta_j} \nabla \rho^{\beta_j}] + \varepsilon^\beta \rho^\beta c_p^\beta \nabla T \\
& \quad + T \frac{\partial}{\partial T} \left\{ (\varepsilon^\beta)^2 \underline{\underline{\mathbf{R}}}^\beta \cdot \mathbf{v}^{\beta,s} - \varepsilon^\beta \Gamma^\beta \nabla \rho^\beta + \left(\frac{p^\beta}{\rho^\beta} \right) \nabla (\varepsilon^\beta \rho^\beta) + \sum_{j=1}^N [\varepsilon^\beta \mu^{\beta_j} \nabla \rho^{\beta_j}] \right\}
\end{aligned}$$

Since this coefficient is contracted with the relative velocity, $\mathbf{v}^{\beta,s}$, we can likely neglect the relative velocity term in the temperature derivative as it will result

in second-order effects. This simplifies the coefficient of the relative velocity to

$$\begin{aligned}
& -\varepsilon^\beta \Gamma^\beta \nabla \rho^\beta + \sum_{j=1}^N [\varepsilon^\beta \mu^{\beta_j} \nabla \rho^{\beta_j}] + \varepsilon^\beta \rho^\beta c_p^\beta \nabla T \\
& + T \frac{\partial}{\partial T} \left\{ -\varepsilon^\beta \Gamma^\beta \nabla \rho^\beta + \sum_{j=1}^N [\varepsilon^\beta \mu^{\beta_j} \nabla \rho^{\beta_j}] + \left(\frac{p^\beta}{\rho^\beta} \right) \nabla (\varepsilon^\beta \rho^\beta) \right\}. \quad (5.37)
\end{aligned}$$

After these four simplifications and rearrangements, equation (5.33) is now rewritten as

$$\begin{aligned}
0 = & \rho c_p \dot{T} - \nabla \cdot (\underline{\mathbf{K}} \cdot \nabla T) + \rho h + L \hat{e}_g \\
& + \left[\left(\bar{p}^g \Big|_{eq.} - \bar{p}^l \Big|_{eq.} \right) + 2\tau \varepsilon \dot{S} + T \frac{\partial}{\partial T} (\pi^g - \pi^l) \right] \varepsilon \dot{S} \\
& - \varepsilon S H^l \dot{\rho}^l + \varepsilon S \sum_{j=1}^N \left[\left(\mu^{l_j} - T \frac{\partial \mu^{l_j}}{\partial T} \right) \dot{\rho}^{l_j} \right] \\
& - \varepsilon (1 - S) H^g \dot{\rho}^g + \varepsilon (1 - S) \sum_{j=1}^N \left[\left(\mu^{g_j} - T \frac{\partial \mu^{g_j}}{\partial T} \right) \dot{\rho}^{g_j} \right] \\
& + \sum_{\beta=l,g} \left\{ \left[-\varepsilon^\beta \Gamma^\beta \nabla \rho^\beta + \sum_{j=1}^N [\varepsilon^\beta \mu^{\beta_j} \nabla \rho^{\beta_j}] + \varepsilon^\beta \rho^\beta c_p^\beta \nabla T \right. \right. \\
& \quad \left. \left. + T \frac{\partial}{\partial T} \left\{ -\varepsilon^\beta \Gamma^\beta \nabla \rho^\beta + \sum_{j=1}^N [\varepsilon^\beta \mu^{\beta_j} \nabla \rho^{\beta_j}] + \left(\frac{p^\beta}{\rho^\beta} \right) \nabla (\varepsilon^\beta \rho^\beta) \right\} \right] \cdot \mathbf{v}^{\beta,s} \right\}. \quad (5.38)
\end{aligned}$$

Equation (5.38) depends on temperature, wetting potentials, enthalpies, chemical potentials, Gibbs potentials, saturation, densities, pressures, and relative velocities. Since the Gibbs potentials are functions of densities and chemical potentials this does not add more unknowns to the system of equations. The pressures and relative velocities can be paired with forms of Darcy's law, and constitutive equations are needed for the enthalpies and wetting potentials. We now turn our attention to the coupling of the fluid-phase mass balance equations and the present energy equation.

5.4 Simplifying Assumptions – A Closed System

A host of simplifying assumptions can be made on the system consisting of equations (5.11) (for $\alpha = l, g$) and (5.38). These are made to reduce the number of unknowns and equations to a count that is more easily handled by numerical solvers. This is also done to avoid having to model any secondary (possibly second-order) physical processes (examples of which include very slow processes such as those on the order of $(\mathbf{v}^{l,s})^2$ or $(\mathbf{v}^{\alpha_j,\alpha})^2$). These assumptions are in addition to Assumptions #1 - #3 made in Section 5.2.

Assumption #4: Assume that the liquid phase is composed of a pure fluid with no additional species. Strictly speaking this is not realistic since the water in field measurements contains contaminants, dissolved solids, charged ions (such as sodium), and other impurities. The consequence of this assumption is that the diffusive terms within the liquid mass balance equation are zero

$$\mathbf{v}^{lj,l} = \mathbf{v}^{ll} = \mathbf{0}.$$

Assumption #5: The liquid phase is assumed to be incompressible. This assumption is valid under moderate pressures and allows us to remove the liquid phase material time derivative of density from the liquid mass balance equation

$$\frac{D^l \rho^l}{Dt} = 0.$$

In isothermal conditions the density of the liquid phase can be assumed constant in space and time. In the presence of thermal gradients, on the other hand, we presume that the density of the liquid phase is a function only of temperature given by the empirical model

$$\rho^l(T) = 10^3 \left(1 - 7.37 \times 10^{-6} (T - 277.15)^2 + 3.79 \times 10^{-8} (T - 277.15)^3 \right) \quad (5.39)$$

measured in kg/m^3 (and where $[T]=K$). See Figure 5.1(a).

Assumption #6: The gas phase is assumed to be an ideal binary mixture of water vapor and inert *air*. There are most certainly more than two species in most practical gas mixtures, but here we are concerned with with the diffusion, evaporation, and condensation of water vapor within the gas mixture. The other species are assumed to be non-reactive and are therefore all grouped together into the *air* species. We choose the mixture to be ideal so that we can take advantage of the ideal gas law. This is valid since (a) the gas pressures under most experimental considerations are close to atmospheric, (b) under Richards' assumption [61, 64], the bulk gas pressure doesn't vary much under most experimental considerations, and (c) the temperatures under consideration aren't *far* from standard room temperature. The use of an ideal gas mixture will break down under higher pressures, higher temperatures, and possibly under high variations in temperature.

Assumption #7: The gas-phase chemical potentials and densities are only functions of the relative humidity and temperature

$$\mu^{g_j} = \mu^{g_j}(\varphi, T) \quad \rho^{g_j} = \rho^{g_j}(\varphi, T). \quad (5.40)$$

We make this assumption based on the fact that at the pore scale we can easily convert between the chemical potential, the density, and the relative humidity. Furthermore, this allows for us to tie the gas-phase mass balance equation to experimentally measurable quantities such as the relative humidity.

Just as at the pore scale, we define the macroscale relative humidity, φ , via the saturated vapor density, ρ_{sat} , and the density of the water vapor in the mixture:

$$\rho^{g_v} = \rho_{sat}\varphi, \quad (5.41)$$

where $\rho_{sat} = \rho_{sat}(T)$ can be expressed through the empirical equation

$$\rho_{sat} = \frac{\exp(31.37 - 6014.79/T - 7.92 \times 10^{-3}T)}{T} \times 10^{-3}. \quad (5.42)$$

(see Figure 5.1(b)).

The chemical potential of the water vapor is defined through the ideal gas law as

$$\mu^{g_v} = \mu_*^{g_v} + R^{g_v} T \ln(\lambda\varphi) \quad (5.43)$$

where $\lambda = p_{sat}/p_*$ is a function of temperature from (5.42) and p_* is atmospheric pressure.

The reason we are calling this an “assumption” is that, strictly speaking, these relationships hold for the pore-scale chemical potentials and pressures. We are dealing with averaged (upscaled) quantities so we make the assumption that these quantities follow the same functional forms. It is known that the upscaled pressure, density, and chemical potential are not the same as the pore-scale pressure, so in effect we are defining the upscaled relative humidity through these relationships.

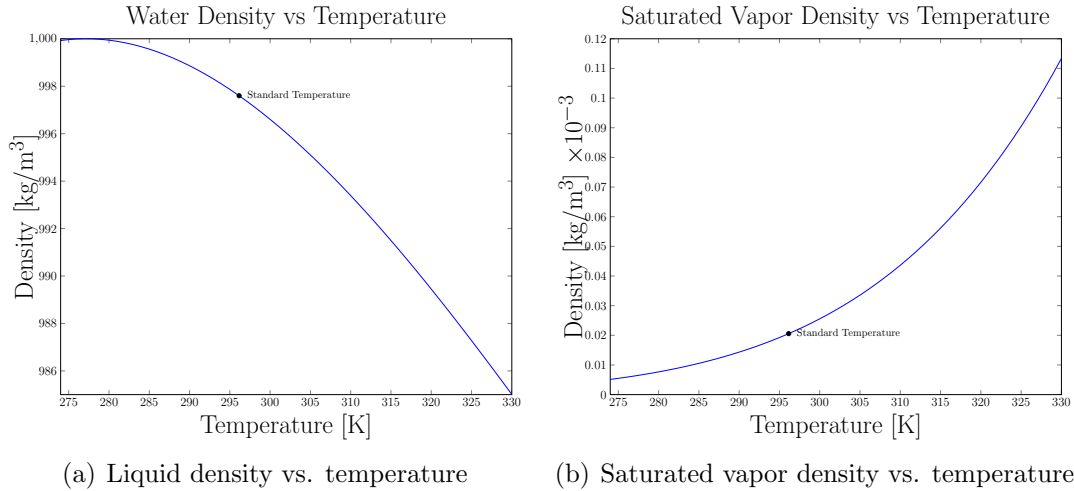


Figure 5.1: Densities as functions of temperature

Under assumptions 4 and 5 on the liquid phase we reflect now on the choice of the form of Darcy’s law for the liquid phase. In the absence of species it may not be

reasonable to use the chemical potential form and instead revert to the pressure form. Recall from equation (4.77) that the Darcy flux for a fluid with one species is driven by gradients in Gibbs potential and temperature. Recall also that the coefficient of the temperature gradient is the macroscale entropy. To side step the necessity of modeling the liquid phase entropy and Gibbs potential directly we use the pressure form of the Darcy flux: equation (4.66). Given one liquid species, a rigid solid phase, two gas species (see assumption #6), and the assumption that the gas densities are functions of temperature and relative humidity (see assumption #7), the Darcy flux for the liquid phase can be written as

$$\begin{aligned}
\varepsilon^l \underline{\mathbf{R}}^l \cdot (\varepsilon^l \mathbf{v}^{l,s}) &= -\varepsilon^l \nabla p^l - \pi^{l(l)} \nabla \varepsilon^l - \pi^{l(g)} \nabla \varepsilon^g + \varepsilon^l \rho^l \mathbf{g} \\
&\quad + \left(\varepsilon^g \rho^g \frac{\partial \psi^g}{\partial \rho^l} + \varepsilon^s \rho^s \frac{\partial \psi^s}{\partial \rho^l} \right) \nabla \rho^l - \varepsilon^l \rho^l \sum_{j=v,a} \left(\frac{\partial \psi^l}{\partial \rho^{g_j}} \nabla \rho^{g_j} \right) \\
&= -\varepsilon^l \nabla p^l - \varepsilon (\pi^{l(l)} - \pi^{l(g)}) \nabla S + \varepsilon^l \rho^l \mathbf{g} \\
&\quad + \left(\varepsilon^g \rho^g \frac{\partial \psi^g}{\partial \rho^l} + \varepsilon^s \rho^s \frac{\partial \psi^s}{\partial \rho^l} \right) \frac{\partial \rho^l}{\partial T} \nabla T \\
&\quad - \varepsilon^l \rho^l \sum_{j=v,a} \left(\frac{\partial \psi^l}{\partial \rho^{g_j}} \left[\frac{\partial \rho^{g_j}}{\partial T} \nabla T + \frac{\partial \rho^{g_j}}{\partial \varphi} \nabla \varphi \right] \right) \\
&= -\varepsilon^l \nabla p^l - \varepsilon (\pi^{l(l)} - \pi^{l(g)}) \nabla S + \varepsilon^l \rho^l \mathbf{g} - \varepsilon^l C_T^l \nabla T - \varepsilon^l C_\varphi^l \nabla \varphi. \quad (5.44)
\end{aligned}$$

The functions C_T^l and C_φ^l are implicitly defined by equations (5.44) and may be functions of any variable(s) from the set of independent variables for the Helmholtz Potential. The coefficient of the saturation gradient can be rewritten as

$$\begin{aligned}
\varepsilon (\pi^{l(l)} - \pi^{l(g)}) &= \varepsilon \varepsilon^l \rho^l \left(\frac{\partial \psi^l}{\partial \varepsilon^l} - \frac{\partial \psi^l}{\partial \varepsilon^g} \right) \\
&= \varepsilon \varepsilon^l \rho^l \left(\frac{\partial \psi^l}{\partial \varepsilon^l} - \frac{\partial \psi^l}{\partial \varepsilon^g} \right) \\
&= 2\varepsilon^l \rho^l \frac{\partial \psi^l}{\partial S} := \varepsilon^l C_S^l. \quad (5.45)
\end{aligned}$$

This coefficient function measures the changes in liquid energy due to changes in saturation while holding density fixed. The notation chosen for these coefficients

is meant to be descriptive; the subscript indicates the associated gradient and the superscript indicates the phase.

Dividing both sides of (5.44) by ε^l gives the simplified pressure, saturation, temperature, and relative humidity formulation of the liquid Darcy flux

$$\underline{\underline{\mathbf{R}}}^l \cdot (\varepsilon^l \mathbf{v}^{l,s}) = -\nabla p^l + \rho^l \mathbf{g} - C_S^l \nabla S - C_T^l \nabla T - C_\varphi^l \nabla \varphi. \quad (5.46)$$

The first two terms on the right-hand side are the classical Darcy terms, and the functions C_S^l , C_T^l , and C_φ^l are, as of yet, unknown. All of these new functions measure cross coupling effects due to the presence of other phases. Thought experiments used to make sense of these new terms will be presented in Section 5.4.1.1 after a deeper discussion of capillary pressure.

Under assumptions #1 - #7, the heat and mass transport system can now be written as:

$$\begin{aligned} \varepsilon \frac{\partial S}{\partial t} - \nabla \cdot \{ \underline{\underline{\mathbf{K}}}^l \cdot [\nabla p^l + C_S^l \nabla S + C_T^l \nabla T + C_\varphi^l \nabla \varphi - \rho^l \mathbf{g}] \} \\ = \left(\frac{M(\rho^l - \rho^{g_v})}{\rho^l} \right) (\mu^l - \mu^{g_v}) \end{aligned} \quad (5.47a)$$

$$\begin{aligned} \varepsilon(1-S) \frac{\partial \rho^{g_v}}{\partial t} - \varepsilon \rho^{g_v} \frac{\partial S}{\partial t} \\ - \nabla \cdot \{ \rho^{g_v} \underline{\underline{\mathbf{D}}}^{g_v} \cdot [\nabla \mu^{g_v} - \mathbf{g}] \} \\ - \nabla \cdot \{ \rho^{g_v} \underline{\underline{\mathbf{K}}}^g \cdot [\rho^{g_v} \nabla \mu^{g_v} + \rho^{g_a} \nabla \mu^{g_a} + \rho^g \eta^g \nabla T - \rho^g \mathbf{g}] \} \\ = -M(\rho^l - \rho^{g_v}) (\mu^l - \mu^{g_v}) \end{aligned} \quad (5.47b)$$

$$\begin{aligned} 0 = \rho c_p \dot{T} - \nabla \cdot (\underline{\underline{\mathbf{K}}} \cdot \nabla T) + \rho h + L \dot{e}_g \\ + \left[\left(\bar{p}^g \Big|_{eq.} - \bar{p}^l \Big|_{eq.} \right) + 2\tau \varepsilon \dot{S} + T \frac{\partial}{\partial T} (\pi^g - \pi^l) \right] \varepsilon \dot{S} \\ - \varepsilon(1-S) H^g \dot{\rho}^g + \varepsilon(1-S) \sum_{j=v,a} \left[\left(\mu^{g_j} - T \frac{\partial \mu^{g_j}}{\partial T} \right) \dot{\rho}^{g_j} \right] \\ + \left[\left(\rho^l c_p^l + e^l \frac{d\rho^l}{dT} \right) \nabla T + \frac{T}{\varepsilon^l} \frac{\partial p^l}{\partial T} \nabla \varepsilon^l \right] \cdot (\varepsilon^l \mathbf{v}^{l,s}) \\ + \left[-\Gamma^g \nabla \rho^g + \sum_{j=v,a} [\mu^{g_j} \nabla \rho^{g_j}] + \rho^g c_p^g \nabla T \right] \end{aligned}$$

$$+T \frac{\partial}{\partial T} \left\{ -\Gamma^g \nabla \rho^g + \sum_{j=v,a} [\mu^{gj} \nabla \rho^{gj}] + \left(\frac{p^g}{\varepsilon^g \rho^g} \right) \nabla (\varepsilon^g \rho^g) \right\} \cdot (\varepsilon^g \mathbf{v}^{g,s}). \quad (5.47c)$$

This system of equations originated from mass, momentum, and energy conservation and was supplemented with constitutive forms of the rates of mass, momentum, and energy transfer. We used the incompressibility of the liquid phase to arrive at the fourth line of the energy equation. In the gas phase, the change in pressure with temperature is given via the ideal gas law:

$$p^g = \left(\frac{\rho^g R}{M^g} \right) T, \quad (5.48)$$

$$\frac{\partial p^g}{\partial T} = \left(\frac{\rho^g R}{M^g} \right) + \left(\frac{TR}{M^g} \right) \frac{\partial \rho^g}{\partial T} \quad (5.49)$$

where M^g is the molar mass of the gas mixture and R is the universal gas constant. In the liquid phase, the change in pressure with temperature is the ratio of isobaric and isothermal compressibilities of liquid water

$$\frac{\partial p^l}{\partial T} = - \left(\frac{1}{V^l} \frac{\partial V^l}{\partial T} \right) / \left(- \frac{1}{V^l} \frac{\partial V^l}{\partial p^l} \right) = \frac{\alpha^l}{\beta^l}.$$

Recall that $\rho^l = \rho^l(T)$, $\rho^{gv} = \rho^{gv}(\varphi, T)$, $\mu^{gj} = \mu^{gj}(\varphi, T)$, $\varepsilon^l = \varepsilon S$, $\varepsilon^g = \varepsilon(1 - S)$, and $\eta^\alpha = \eta^\alpha(T)$. Furthermore, $\varepsilon^\alpha \mathbf{v}^{\alpha,s}$ is the Darcy flux associated with the α -phase (see equation (4.76)) and the latent heat, L , is an empirically based function of temperature. Therefore, assuming that the enthalpy, internal energy, and the linearization coefficients are known functions of these same variables, equations (5.47a) - (5.47c) can be seen as a closed system of equations in saturation (S), relative humidity (φ), and temperature (T). It remains to find relationships for the linearization coefficients, the cross coupling Darcy terms, the gas-phase entropy, the enthalpy, and the chemical potentials. In the next subsections we discuss dimensional analysis, functional forms of the coefficients, and further simplifications for each equation one at a time.

5.4.1 Saturation Equation

In the liquid phase, the linearization constant, $\underline{\underline{K}}^l$, is a function of the ease in which fluid flows through the medium. This is known as the hydraulic conductivity of the medium. The hydraulic conductivity is also known to be a function of the permeability of the medium. In saturated (rigid) media this is considered constant (or at least a tensor), but in unsaturated media they are typically taken as functions of saturation. In the present case, a careful inspection of the units indicate that

$$\underline{\underline{K}}^l = \frac{\underline{\underline{\kappa}}}{\mu_l} = \frac{\underline{\underline{k}}_c}{\rho^l g}, \quad (5.50)$$

where $\underline{\underline{\kappa}}$ is the permeability tensor of the medium, $\underline{\underline{k}}_c$ is the hydraulic conductivity tensor, and μ_l is the dynamic viscosity [5, 61]. Notationally “ μ^α ” (with a superscript) will denote chemical potential, and “ μ_α ” (with a subscript) will denote dynamic viscosity.

The permeability, $\underline{\underline{\kappa}}$, is typically separated into a saturated permeability, $\underline{\underline{\kappa}}_s$, and a relative permeability, $\kappa_{r\alpha}$. The relative permeability is assumed to be a function of saturation and depends on whether α is the wetting or non-wetting phase [61]. There are several functional forms of $\kappa_{r\alpha}$, but one of the more commonly used is that of van Genuchten [78],

$$\kappa_{rl} = \kappa_{rw} = (S_e)^{1/2} \left\{ 1 - \left[1 - (S_e)^{1/m} \right]^m \right\}^2 \quad (5.51a)$$

$$\kappa_{rg} = \kappa_{rnw} = [1 - (S_e)]^{1/3} \left[1 - (S_e)^{1/m} \right]^{2m}, \quad (5.51b)$$

where m is a fitting parameter, and S_e is the effective saturation defined by

$$S_e = \frac{S - S_{min}}{S_{max} - S_{min}} \quad S_e \in [0, 1]. \quad (5.52)$$

Typical values of m are less than 1 where $m = 2/3$ is commonly used as a starting point for fitting numerical models to experimental data. Typical relative permeability curves are shown in Figure 5.2. The reader is to keep in mind that there are several such models in the literature [5, 61]. The van Genuchten model simply constitutes a widely used relative permeability model. Note that there is not a symmetry in

$k_{r_{nw}}$ and k_{r_w} in the sense that $k_{r_{nw}}(S_e) \neq k_{r_w}(1 - S_e)$ as would naively be assumed. This is a manifestation of the fact that unsaturated media *behave* differently during imbibition and drainage. The value of $\underline{\kappa}_s$ is chosen based on the type of medium. If the medium is isotropic then the tensorial notation can be dropped and values from Table E.2 can be used.

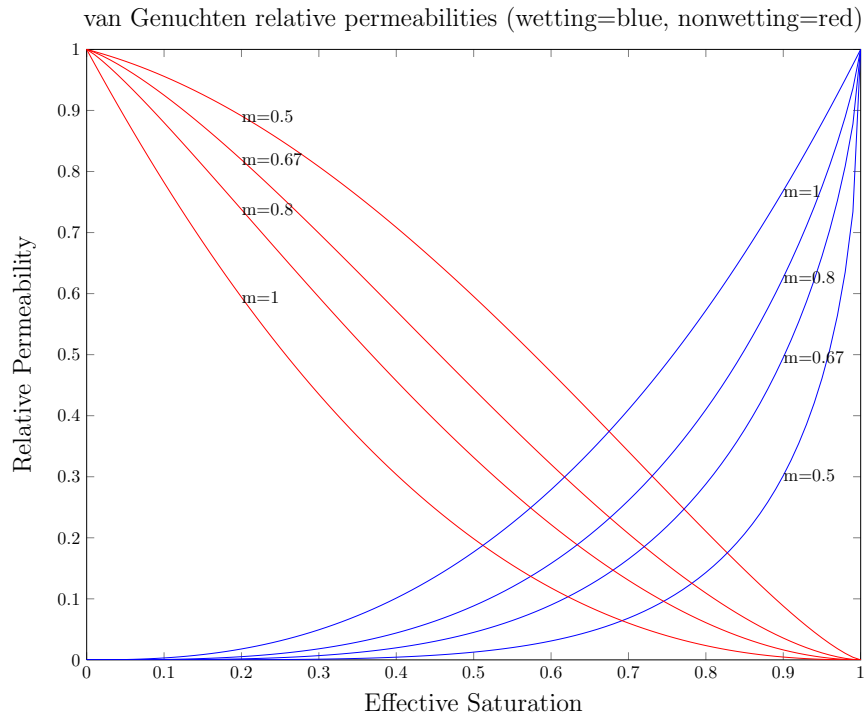


Figure 5.2: van Genuchten relative permeability curves. The red curve shows the non-wetting phase, $\kappa_{r_{nw}}(S_e)$, and the blue curves show the wetting phase, $\kappa_{r_w}(S_e)$, each for $m = 0.5, 0.67, 0.8$, and 1 .

5.4.1.1 Capillary Pressure and Dynamic Capillary Pressure

The capillary pressure, p_c , is typically defined as the difference between the non-wetting (gas) and wetting (liquid) phase pressures when measured in a tube at equilibrium

$$p_c = p_{non-wetting} - p_{wetting}. \quad (5.53)$$

At the microscale, the difference is related to the surface tension of the fluid, the contact angle, and the effective radius through the Young-Laplace equation (see Figure 5.3)

$$p_c = \frac{2\gamma \cos \theta}{r}. \quad (5.54)$$

The question is which *pressure* (thermodynamic, classical, or wetting (see Section

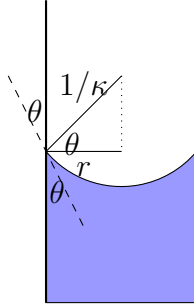


Figure 5.3: Contact angle and effective radius in a capillary tube geometry. θ is the contact angle, r is the effective radius, and κ is the radius of curvature of the interface.

4.3)) represents the non-wetting and wetting pressures in equation (5.53). The capillary pressure is measured with a force transducer in the same manner that the *classical* pressure is measured. For this reason we define the capillary pressure as

$$p_c = p^g - p^l. \quad (5.55)$$

Now that we understand which *pressure* is associated with the capillary pressure we turn to the entropy inequality to derive a constitutive equation for the time rate of change of saturation. In Richards' equation it is standard practice (as mentioned in Section 5.1.1) to take the capillary pressure as a function of saturation. These relations are reasonable for an equilibrium relationships. In the present modeling effort we look toward the entropy inequality to determine an appropriate form of p_c away from equilibrium. In the entropy inequality (equation (4.13)) there are two terms associated with the time rate of change of saturation:

$$-\bar{p}^l \dot{\epsilon}^l \quad \text{and} \quad -\bar{p}^g \dot{\epsilon}^g.$$

Since $\dot{\varepsilon}^g = -\dot{\varepsilon}^l$ these terms can be combined to give $(\bar{p}^g - \bar{p}^l)\dot{\varepsilon}^l$. The time rate of change of volume fraction is a constitutive variable so the associated linearized equation is

$$(\bar{p}^g - \bar{p}^l) \Big|_{n.eq} = (\bar{p}^g - \bar{p}^l) \Big|_{eq} - \tau \dot{\varepsilon}^l, \quad (5.56)$$

where the equilibrium state is not necessarily zero and the minus sign is chosen to be consistent with the entropy inequality. From the three pressures relationship, (4.52), the classical pressure is given as

$$p^\alpha = \bar{p}^\alpha + \pi^\alpha$$

where \bar{p}^α is the *thermodynamic* pressure and π^α is a wetting potential. The difference in thermodynamic pressures is therefore rewritten as

$$\bar{p}_c := \bar{p}^g - \bar{p}^l = (p^g - \pi^g) - (p^l - \pi^l) = p_c - (\pi^g - \pi^l) = p_c - \pi_c$$

and equation (5.56) becomes

$$(p_c - \pi_c) \Big|_{n.eq} = (p_c - \pi_c) \Big|_{eq} - \tau \dot{\varepsilon}^l. \quad (5.57)$$

Rewriting we get

$$p_c \Big|_{n.eq} = p_c \Big|_{eq} + \left(\pi_c \Big|_{n.eq} - \pi_c \Big|_{eq} \right) - \tau \dot{\varepsilon}^l \quad (5.58)$$

We assume that the effect of the solid phase on the capillary pressure is completely captured by the preferential wetting, π_c . Without the solid phase, the normal pressures of the liquid and gas phases are zero (this is the case with a flat interface). With this assumption the thermodynamic pressures are equal across the phases at equilibrium. Therefore, $\bar{p}_c|_{eq} = 0$. This implies that $p_c|_{eq} = \bar{p}_c|_{eq} + \pi_c|_{eq} = \pi_c|_{eq}$. Therefore the capillary pressure at equilibrium is interpreted as the difference in wetting potential and we arrive at an expression that is similar to that found in [46].

To avoid possible confusion we will continue to use the symbols $p_c|_{eq}$ in place of $\pi_c|_{eq}$ even though they are understood to be the same.

We finally arrive at an expression relating the classical liquid-phase pressure that appears in Darcy's law, $p^l|_{n.eq}$, and the capillary pressure, $p_c|_{eq}$:

$$-p^l|_{n.eq} = p_c|_{eq} + \left(\pi_c|_{n.eq} - \pi_c|_{eq} \right) - p^g|_{n.eq} - \tau \dot{\epsilon}^l. \quad (5.59)$$

If the deviation in the wetting potential from equilibrium is assumed to be small relative to the pressure and the dynamic effects we can approximate the liquid pressure as

$$-p^l|_{n.eq} \approx p_c|_{eq} - p^g|_{n.eq} - \tau \dot{\epsilon}^l, \quad (5.60)$$

where it is possible that $p^g \approx 0$ as well (in fact, this is a common assumption). To see why the deviation in wetting potential might be small, consider that in equation (5.58) if $p_c|_{n.eq} \approx p_c|_{eq}$ then the saturation dynamics is driven by the deviation in wetting potential. The deviation in wetting potential measures how much the shape of the curved liquid-gas interface is away from equilibrium. In slow flows it is unlikely that this deviation is significant.

As mentioned in Section 5.1.1, the (equilibrium) capillary pressure can be related to the effective saturation through the van Genuchten $p_c - S$ relationship. This relationship depends on several fitting parameters and is given as

$$p_c(S_e) = \left(\frac{1}{\alpha} \right) (S_e^{-1/m} - 1)^{1-m}, \quad (5.61)$$

where α has units of reciprocal pressure and m is the same fitting parameter as in the relative permeabilities (5.51a) [5, 61]. See Figure 5.4 for several examples of capillary pressure - saturation curves for various sets of parameters. Generally speaking, m increases (toward 1) as the soil becomes more densely packed.

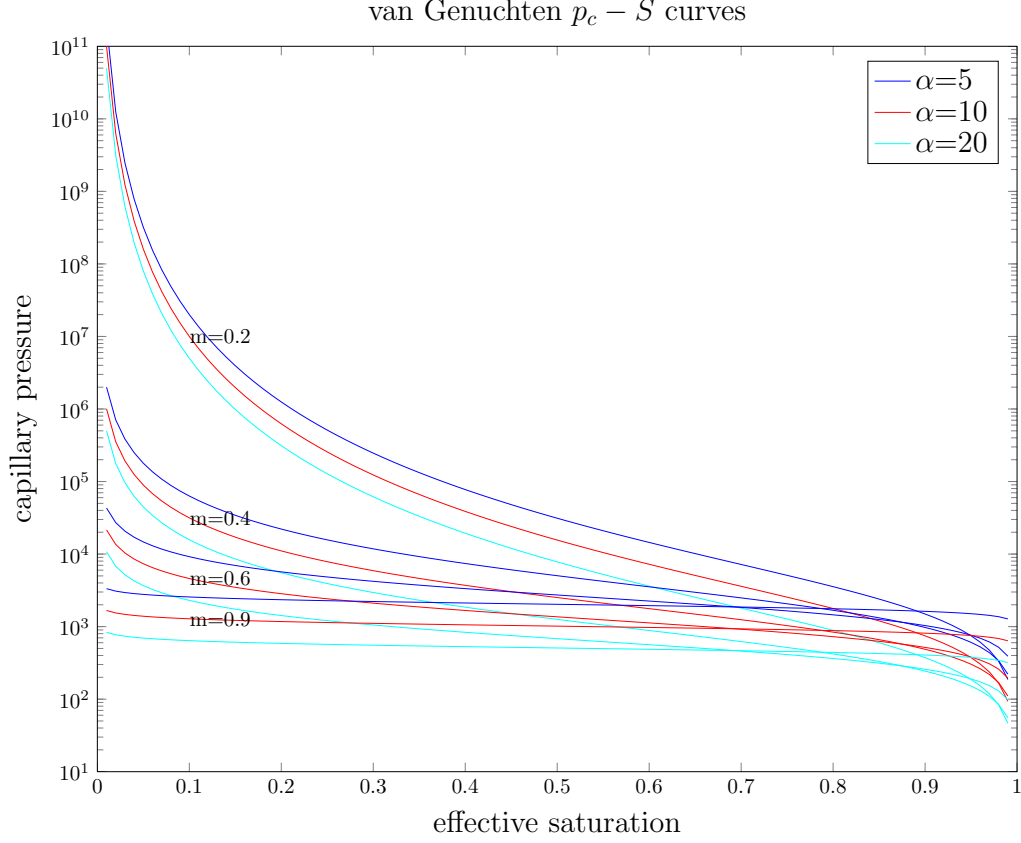


Figure 5.4: Examples of van Genuchten capillary pressure - saturation curves for various parameters.

Substituting the capillary pressure and van Genuchten relationships into Darcy's law, (5.46), the fluid flux becomes

$$\begin{aligned} \underline{\underline{\mathbf{R}}} \cdot (\varepsilon^l \mathbf{v}^{l,s}) = & \left(\frac{dp_c}{dS} - C_S^l \right) \nabla S - \tau \varepsilon \nabla \dot{S} + \rho^l \mathbf{g} \\ & - \nabla p^g - C_\varphi^l \nabla \varphi - C_T^l \nabla T + \nabla \underbrace{(\pi_c|_{n.eq} - \pi_c|_{eq})}_{\approx 0}. \end{aligned} \quad (5.62)$$

To understand the newly terms proposed here, we make the following three comments:

1. First consider the gas pressure and relative humidity terms. In the absence of gravity, if the saturation, temperature, and the change in capillary wetting potential are held fixed then (5.62) states that flow is driven by gradients in relative humidity and gas-phase pressure. The gas-phase pressure and the relative

humidity are proportional to each other where the constant of proportionality is a function of temperature and the species densities. With this in mind, these two terms together can be rewritten as a gradient in gas pressure. While a gradient in gas pressure can certainly cause flow, it is commonly assumed that p^g is approximately constant (known as Richards' assumption [61]) and therefore these terms are typically neglected. If these terms are not neglected then they are best written as a single gradient of relative humidity for easy coupling with the gas-phase diffusion equation

$$C_\varphi^l \nabla \varphi \leftarrow \nabla p^g + C_\varphi^l \nabla \varphi.$$

2. Next consider the gradient of temperature term. In the absence of gravity, if saturation and relative humidity are held fixed then (5.62) states that flow is driven by a gradient in temperature. Saito et al. [66] indicated that the thermally induced flow was negligible as compared to isothermal flow (also discussed in [75, 79]). This indicates that the ∇T term in (5.62) is likely quite small.
3. Finally we discuss the role of $C_S^l = 2\rho^l \frac{\partial \psi^l}{\partial S}$. This function (or constant) relates the changes in energy with respect to saturation. The term is already associated with the gradient in saturation as seen in equation (5.62). From the ∇S term in this equation we can see C_S^l as an *enhancement* of the capillary pressure - saturation relationship that directly models the affinity for the liquid phase to the other phases. It is entirely likely that this term is so closely linked with the capillary pressure that in experimental settings it is impossible to discern this effect from others.

The saturation equation can finally be written as

$$\varepsilon \frac{\partial S}{\partial t} - \nabla \cdot \left[\underline{\mathbf{K}}(S) \cdot \left(\left\{ -\frac{dp_c}{dS} + C_S^l \right\} \nabla S_e + \tau \varepsilon \nabla \dot{S}_e + C_T^l \nabla T + C_\varphi^l \nabla \varphi - \rho^l \mathbf{g} \right) \right]$$

$$= \frac{M}{\rho^l} (\rho^l - \rho^{g_v}) (\mu^l - \mu^{g_v}), \quad (5.63)$$

where we have assumed that $\pi_c|_{n.eq} - \pi_c|_{eq} \approx 0$ and, abusing notation slightly, the C_φ^l term has been redefined to incorporate changes in the gas pressure.

To account for the residual (minimum) saturation, the saturation is scaled to the *effective saturation* according to $S_e = (S - S_{min}) / (S_{max} - S_{min})$. Defining ε_S as the product of porosity and the difference in maximal and minimal saturation, $\varepsilon_S := \varepsilon(S_{max} - S_{min})$, and letting S notationally stand for S_e allows us to write the saturation equation as

$$\begin{aligned} \frac{\partial S}{\partial t} - \nabla \cdot \left[\varepsilon_S^{-1} \underline{\mathbf{K}}(S) \cdot \left(\left\{ -\frac{dp_c}{dS} + C_S^l \right\} \nabla S + \tau \varepsilon_S \nabla \dot{S} + C_T^l \nabla T + C_\varphi^l \nabla \varphi - \rho^l \mathbf{g} \right) \right] \\ = \frac{M^l}{\varepsilon_S \rho^l} (\rho^l - \rho^{g_v}) (\mu^l - \mu^{g_v}) \end{aligned} \quad (5.64)$$

At a quick glance, the sign of the ∇S term looks suspicious as it seems to indicate a backward heat equation. Observe that $p'_c(S) < 0$ for all values of S . Taking only the first line with $C_S^l = 0$ returns Richards' equations exactly. The $\nabla \dot{S}$ term (henceforth referred to as the *dynamic saturation term*) was originally proposed by Hassanizadeh et al. in several publications (examples include [46, 48]) and is gaining more widespread acceptance in the porous media community. Taking all of the terms on the first line (again with $C_S^l = 0$) along with the dynamic saturation term gives a closed pseudo-parabolic equation in saturation. The $C_S^l, C_T^l, C_\varphi^l$ terms along with the form of the right-hand side are all novel to this work. The temperature and relative humidity coupling terms can certainly be taken to be zero in certain physical instances, but generally the relative weight and functional forms of these terms is, as of yet, unknown.

We now turn our attention to the gas phase diffusion equation. Analysis and numerical solutions to the saturation equation will be considered in Chapter 7.

5.4.2 Gas Phase Diffusion Equation

In this subsection we make certain simplifications to the gas-phase diffusion equation so as to tie the chemical potential formulation to the more classical enhanced diffusion model. As a first step toward this simplification we consider the fact that the gas phase chemical potentials are related to each other through equation (4.85); the expression for the relative motion of diffusing species in a binary system:

$$\sum_{j=1}^N \left\{ \left(\frac{\rho^{\alpha_j}}{R^{g_j} T} \right) \underline{\underline{D}}^\alpha \cdot [\nabla \mu^{\alpha_j} - \mathbf{g}] \right\} = \mathbf{0}.$$

With this, the gradient of chemical potential of the inert air in (5.47b) can be rewritten as a function of the water vapor chemical potential

$$\rho^{g_a} \nabla \mu^{g_a} = - \left(\frac{R^{g_a} \rho^{g_v}}{R^{g_v}} \right) (\nabla \mu^{g_v} - \mathbf{g}) + \rho^{g_a} \mathbf{g}.$$

This means that the gas-phase mass balance equation can be rewritten as

$$\begin{aligned} & \frac{\partial}{\partial t} (\varepsilon \rho_{sat}^{g_v} \varphi (1 - S)) \\ & - \nabla \cdot \left\{ \rho^{g_v} \left[\underline{\underline{D}}^{g_v} + \rho^{g_v} \left(1 - \frac{R^{g_a}}{R^{g_v}} \right) \underline{\underline{K}}^g \right] \cdot [\nabla \mu^{g_v} - \mathbf{g}] \right\} \\ & - \nabla \cdot \left\{ \rho^g \rho^{g_v} \eta^g \underline{\underline{K}}^g \cdot \nabla T \right\} = -M (\rho^l - \rho^{g_v}) (\mu^l - \mu^{g_v}). \end{aligned} \quad (5.65)$$

Typically, one would choose a functional form of $\underline{\underline{D}}^{g_v}$ to match the enhancement model discussed in Section 5.1.2 and the functional form of $\underline{\underline{K}}^g$ from the van Genuchten model discussed in Section 5.4.1. In the present case we argue to use different functional forms of $\underline{\underline{D}}^{g_v}$ and $\underline{\underline{K}}^g$. This is done by considering the conversions between the pore-scale density and chemical potential to the relative humidity. For simplicity the tensorial notation is dropped and we assume that the diffusion and conductivity tensors are all scalar multiples of the identity matrix.

We begin with some logical considerations for the gas-phase diffusion coefficient. If the gas-phase volume fraction were to drop to zero then there would be no gas in the pore space (or there would be no pore space) and the diffusion coefficient should drop to zero. Similarly, if the gas-phase volume fraction were to increase to 1 (100%

gas with no solid or liquid), then the diffusion coefficient should return to the Fickian diffusion coefficient D^g . With these two limiting cases in mind we first propose that $D^{g_v} = C\varepsilon^g D^g$ where C is a scaling parameter.

As seen in Chapter 2, the diffusion coefficient is modified for Fick's law based on the dependent variable of interest. In equations (2.1) and (2.3) we see a scalar factor of $1/(R^{g_v}T)$ between the mass and chemical potential forms of Fick's law. Making the same modification here along with the factor of ε^g suggested above we get

$$\rho^{g_v} D^{g_v} \nabla \mu^{g_v} \rightarrow \rho^{g_v} \left(\frac{\varepsilon^g}{R^{g_v}T} \right) D^g \nabla \mu^{g_v} = \left(\frac{\varepsilon \rho_{sat} \varphi (1 - S)}{R^{g_v}T} \right) D^g \nabla \mu^{g_v} \quad (5.66)$$

where D^g is the same pore-scale diffusion coefficient as found in Chapter 2. One simple way to look at this conversion is that it scales out the units and magnitude of the chemical potential when converting to relative humidity. That is, $D^{g_v} \nabla \mu^{g_v}$ and $D^g/(R^{g_v}T) \nabla \varphi$ have the same units and magnitude. A further justification of this is found by recalling the pore-scale definition of the chemical potential:

$$\begin{aligned} \mu^{g_v} &= \mu_*^{g_v} + R^{g_v}T \ln \left(\frac{p^{g_v}}{p^g} \right) \\ &= \mu_*^{g_v} + R^{g_v}T \ln(\lambda \varphi), \end{aligned} \quad (5.67)$$

where $\lambda = p_{sat}^{g_v}/p^g$ and $p_{sat}^{g_v}$ is the partial pressure of the water vapor under saturated conditions. Taking the gradient of (5.67) and neglecting the temperature variation gives

$$\nabla \mu^{g_v} \approx \frac{R^{g_v}T}{\varphi} \nabla \varphi.$$

Hence we see the exact conversion used in Fick's law.

Next we turn our attention to the hydraulic conductivity term that arose from Darcy's law: $\rho^{g_v} K^g \nabla \mu^{g_v}$. Similar to that of Fick's law, we need to scale the conductivity to account for the fact that we're using the chemical potential as the dependent variable. Unlike the Fickian diffusion coefficient, this term already has the proper units since the units of $\rho^{g_v} \nabla \mu^{g_v}$ are the same as the gradient of pressure. Therefore

we seek a scaling that is unitless but scales the magnitude of the chemical potential down to that of pressure. That is, we need a constant, c , such that $c\rho^{g_v}K^g\nabla\mu^{g_v}$ and $K^g\nabla p^g$ have approximately the same magnitude.

Taking the gradient of both sides of the first line of equation (5.67) we arrive at

$$\begin{aligned}\nabla\mu^{g_v} &= \left(\frac{R^{g_v}T p^g}{p^{g_v}}\right) \nabla\left(\frac{p^{g_v}}{p^g}\right) \\ &= \left(\frac{R^{g_v}T p^g}{p^{g_v}}\right) \left(\left(\frac{1}{p^g}\right) \nabla p^{g_v} - \left(\frac{p^{g_v}}{(p^g)^2}\right) \nabla p^g\right) \\ &= \left(\frac{R^{g_v}T}{p^{g_v}}\right) \nabla p^{g_v} - \left(\frac{R^{g_v}T}{p^g}\right) \nabla p^g.\end{aligned}$$

The coefficient of the gradient of gas-phase pressure can be rewritten as

$$\frac{R^{g_v}T}{p^g} = \frac{\rho_{sat}R^{g_v}T}{\rho_{sat}p^g} = \frac{p_{sat}^{g_v}}{\rho_{sat}p^g} = \frac{\lambda}{\rho_{sat}}.$$

Since the chemical potential form already has a factor of $\rho^{g_v} = \rho_{sat}^{g_v}\varphi$ we scale K^g by λ to account for the difference in magnitude between the chemical potential and the pressure. Hence, the Darcy term in equation (5.65) is rewritten as

$$\rho^{g_v} \left(1 - \frac{R^{g_a}}{R^{g_v}}\right) K^g \nabla\mu^{g_v} \rightarrow \rho^{g_v} \left(1 - \frac{R^{g_a}}{R^{g_v}}\right) (\lambda K^g) \nabla\mu^{g_v}.$$

Keep in mind that this is a scaling of the hydraulic conductivity; just as the factor of $1/(R^{g_v}T)$ is a scaling of the diffusion coefficient in Fick's law.

One point of interest for this choice of scaling factor is that it is invisible when we consider a *pure* gas phase. That is, $\lambda = 1$ when no species are considered since the saturated partial pressure will simply be the bulk pressure. This indicates that we have not actually changed Darcy's law. Instead we have simply made a conversion to account for the use of a different dependent variable.

Next we focus on writing the gas-phase diffusion equation (5.65) in terms of relative humidity, saturation, and temperature. To do this we replace the chemical potential with relative humidity and temperature via equation (5.67). Taking the gradient of the chemical potential in equation (5.67) we get

$$\nabla\mu^{g_v} = \frac{R^{g_v}T}{\varphi} \nabla\varphi + \left(\frac{R^{g_v}T}{\lambda} \frac{d\lambda}{dT} + R^{g_v} \ln(\lambda\varphi)\right) \nabla T.$$

With the Fickian and Darcy terms written in terms of the relative humidity, along with the fact that the saturated vapor density is a function of temperature, the vapor diffusion equations can be written as

$$\begin{aligned} & \frac{\partial}{\partial t} (\varepsilon \rho_{sat} \varphi (1 - S)) \\ & - \nabla \cdot \left\{ \rho_{sat} \varphi \left[\frac{\varepsilon (1 - S)}{R^{g_v} T} D^g + \rho_{sat} \varphi \left(1 - \frac{R^{g_a}}{R^{g_v}} \right) (\lambda K^g) \right] \right. \\ & \quad \left. \cdot \left[\frac{R^{g_v} T}{\varphi} \nabla \varphi + \left(\frac{R^{g_v} T}{\lambda} \frac{d\lambda}{dT} + R^{g_v} \ln(\lambda \varphi) \right) \nabla T \right] \right\} \\ & - \nabla \cdot \{ \rho^g \rho_{sat} \varphi \eta^g (\lambda K^g) \nabla T \} = -M (\rho^l - \rho_{sat} \varphi) (\mu^l - \mu^{g_v}). \end{aligned}$$

Combining like terms, dividing by the porosity, replacing the hydraulic conductivity by the saturated and relative permeabilities, and simplifying gives

$$\begin{aligned} & \frac{\partial}{\partial t} (\rho_{sat} \varphi (1 - S)) \\ & - \nabla \cdot \left\{ \rho_{sat} \mathcal{D}(\varphi, S, T) \left[\nabla \varphi - \frac{\mathbf{g} \varphi}{R^{g_v} T} \right] \right\} - \nabla \cdot \{ \rho_{sat} N^g(\varphi, S, T) \nabla T \} \\ & = -\frac{M^l (\rho^l - \rho^{g_v})}{\varepsilon} (\mu^l - \mu^{g_v}), \end{aligned} \quad (5.68)$$

where the functions \mathcal{D} and N^g are

$$\mathcal{D}(\varphi, S, T) := (1 - S) D^g + \rho_{sat} \varphi R^{g_v} T \left(1 - \frac{R^{g_a}}{R^{g_v}} \right) \left(\frac{\lambda \kappa_s}{\varepsilon \mu_g} \right) \kappa_{rg}(S) \text{ and} \quad (5.69a)$$

$$N^g(\varphi, S, T) := \varphi \left[\mathcal{D}(\varphi, S, T) \left(\frac{1}{\lambda} \frac{d\lambda}{dT} + \frac{R^{g_v} \ln(\lambda \varphi)}{T} \right) + \rho^g \rho_{sat} \eta^g \left(\frac{\lambda \kappa_S}{\varepsilon \mu_g} \right) \kappa_{rg}(S) \right] \quad (5.69b)$$

The enhancement model suggested by de Vries, and subsequently used by several authors [24, 66, 75, 67, 79], is a multiplicative combination of the pure Fickian diffusion coefficient, D^g , the tortuosity, $\tau = \tau(\varepsilon^g)$, and an enhancement factor, η :

$$D = \tau \eta D^g. \quad (5.70)$$

In these works, the functional form of the enhancement factor is taken to be of the form suggested by Cass et al. [24]

$$\eta_{(a)} = \left(a + 3 \frac{\varepsilon^l}{\varepsilon} \right) - (a - 1) \exp \left\{ - \left[\left(1 + \frac{2.6}{\sqrt{f_c}} \right) \frac{\varepsilon^l}{\varepsilon} \right]^3 \right\}. \quad (5.71)$$

Here, f_c is the mass fraction of clay in the soil. In the absence of clay the enhancement factor is taken as

$$\eta_{(a)} = a + 3 \frac{\varepsilon^l}{\varepsilon^s} \quad (5.72)$$

(for an example where $f_c \neq 0$ see Saito et al. [66]). The tortuosity is taken to be a function of the volumetric gas content,

$$\tau = (2/3)\varepsilon^g. \quad (5.73)$$

Using equations (5.72) and (5.73) in the multiplicative expansion of the diffusion coefficient, (5.70) gives a diffusion coefficient of

$$D = \left(a + 3 \frac{\varepsilon^l}{\varepsilon} \right) \left(\frac{2}{3} \varepsilon^g \right) D^g. \quad (5.74)$$

The tortuosity and the porosity communicate to the diffusion coefficient the type of geometry under consideration. The present model (equation (5.68)) communicates this information via the porosity, the relative permeability, and the saturated permeability. The diffusion model using equation (5.74) relies on a fitting parameter, while the present model avoids this trouble. In the author's opinion, this highlights the main advantage to using the chemical potential as a modeling tool.

Comparing the enhancement model of Cass et al. (using the material parameters from the experiment by Smits et al. [75]) to the present model, we see, in Figure 5.5, that the relative humidity level curves of the present model underestimate the enhanced model for many values of the fitting parameter, a . That being said, these curves do suggest an enhancement over regular Fickian diffusion and, depending on the parameters of interest, give *similar* levels of enhancement as the model used in [75]. We simply state here that the present model offers a modified view of the enhancement model. There are several parameters that play roles in this model, but the advantage to the present approach is that all of the parameters are readily measured for a given

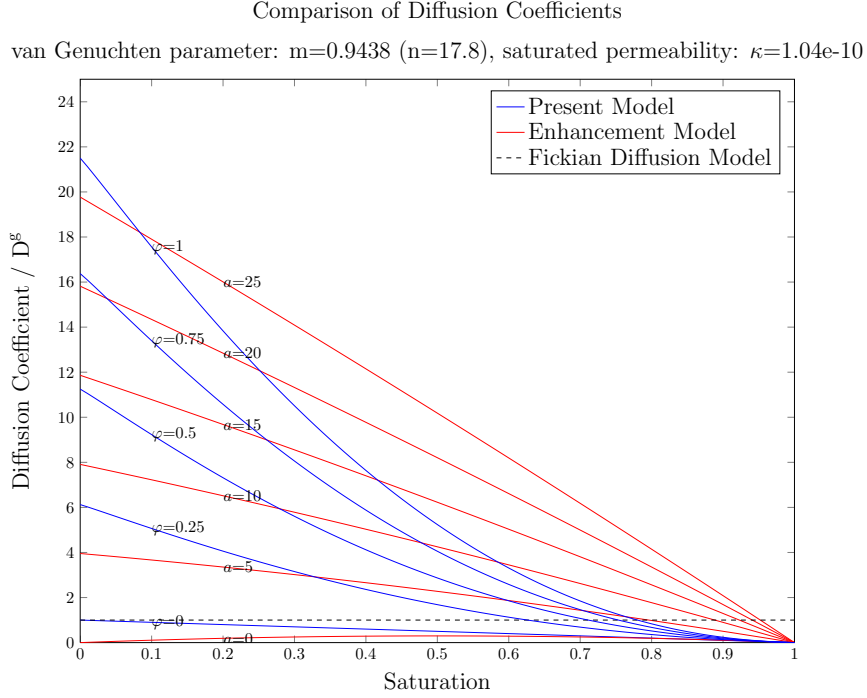


Figure 5.5: Comparison of different diffusion models at constant temperature ($T = 295.15K$). The value for the saturated permeability was chosen to match that of [75] ($\kappa_S = 1.04 \times 10^{-10}m^2$), where they found a fitting parameter $a = 18.2$. The “Present Model” refers to equation (5.68) (with $\nabla T = \mathbf{0}$ and no mass transfer) and the “Enhancement Model” refers to equation (5.3) along with (5.70), (5.72), and (5.73) for the diffusion coefficient, enhancement factor, and tortuosity respectively.

medium (at least in laboratory experiments). There is no *fitting* parameter, so the type of material should dictate the level of enhancement.

Another way to look at the present model is to consider that in most classical situations the gas-phase pressure is considered constant. The effect of this assumption is that the Darcy terms in the gas-phase mass balance equation are neglected. This assumption is valid in many cases, but in the present case the Darcy term is broken into component parts (air and water vapor) via the chemical potentials. The chemical potential formulation draws influence from the Darcy-type movement, along with the Fickian diffusion, of the individual constituents to define the general diffusion coefficient.

It is emphasized here that the traditional (de Vries-type) view of diffusion in porous media is not taken here. Shokri [72] suggested that the mechanism of enhanced diffusion is driven by the coupling of Darcy and Fickian diffusion. The novelty here is that the advection and diffusion are modeled in terms of the same dependent variable; the chemical potential. This suggests that the enhanced diffusion problem can be modeled by coupling Darcy-type flow along with Fickian diffusion in the gas phase. The relationship between the enhancement model and the present model will be discussed when we consider numerical solutions in Chapter 7.

5.4.3 Total Energy Equation

Continuing with the equation-by-equation derivation of the total heat and moisture transport model, we now turn our attention to the total energy equation. This picks up from equation (5.38) and we apply the simplifying assumptions presented in the beginning of Section 5.4.

If we assume that the vapor and air densities are functions of relative humidity and temperature only, the total energy equation (5.38) can be written as

$$\begin{aligned}
0 = & \rho c_p \dot{T} - \nabla \cdot (\underline{\underline{\mathbf{K}}} \cdot \nabla T) + \rho h + L \hat{e}_g \\
& + \varepsilon \left[p_c + 2\tau\varepsilon \dot{S} + T \frac{\partial}{\partial T} (\pi^g - \pi^l) \right] \dot{S} \\
& + \varepsilon(1 - S) \left[\sum_{j=v,a} \left[\left(\mu^{g_j} - T \frac{\partial \mu^{g_j}}{\partial T} \right) \frac{\partial \rho^{g_j}}{\partial T} \right] - (\Gamma^g + T\eta^g) \frac{\partial \rho^g}{\partial T} \right] \dot{T} \\
& + \varepsilon(1 - S) \left[\sum_{j=v,a} \left[\left(\mu^{g_j} - T \frac{\partial \mu^{g_j}}{\partial T} \right) \frac{\partial \rho^{g_j}}{\partial \varphi} \right] - (\Gamma^g + T\eta^g) \frac{\partial \rho^g}{\partial \varphi} \right] \dot{\varphi} \\
& + \left[\left(\rho^l c_p^l + e^l \frac{d\rho^l}{dT} \right) \nabla T + \frac{T}{S} \frac{\partial p^l}{\partial T} \nabla S \right] \cdot (\varepsilon^l \mathbf{v}^{l,s}) \\
& + \left[\left(\rho^g c_p^g - \Gamma^g \frac{\partial \rho^g}{\partial T} + \sum_{j=v,a} \left[\mu^{g_j} \frac{\partial \rho^{g_j}}{\partial T} \right] + T \frac{\partial}{\partial T} \left(\sum_{j=v,a} \left[\mu^{g_j} \frac{\partial \rho^{g_j}}{\partial T} \right] - \psi^g \frac{\partial \rho^g}{\partial T} \right) \right) \nabla T \right. \\
& + \left. \left(-\Gamma^g \frac{\partial \rho^g}{\partial \varphi} + \sum_{j=v,a} \left[\mu^{g_j} \frac{\partial \rho^{g_j}}{\partial \varphi} \right] + T \frac{\partial}{\partial T} \left(\sum_{j=v,a} \left[\mu^{g_j} \frac{\partial \rho^{g_j}}{\partial \varphi} \right] - \psi^g \frac{\partial \rho^g}{\partial \varphi} \right) \right) \nabla \varphi \right. \\
& \left. - \frac{T}{(1 - S)} \frac{\partial p^g}{\partial T} \nabla S \right] \cdot (\varepsilon^g \mathbf{v}^{g,s}). \tag{5.75}
\end{aligned}$$

Recall that $\rho = \rho(\varphi, S, T)$, $p_c = p_c(S_e)$, $\mu^{gj} = \mu^{gj}(\varphi, T)$, $\rho^{gj} = \rho^{gj}(\varphi, T)$, $\Gamma^g = \Gamma^g(\varphi, T)$, $\eta^g = \eta^g(T)$, $\rho^l = \rho^l(T)$. Also recall that $\varepsilon^\alpha \mathbf{v}^{\alpha,s}$ represents the Darcy flux for the α phase:

$$\varepsilon^l \mathbf{v}^{l,s} = -K^l \left[\{-p'_c(S_e) + C_S^l\} \nabla S_e + \tau \varepsilon \nabla \dot{S}_e + C_T^l \nabla T + C_\varphi^l \nabla \varphi - \rho^l \mathbf{g} \right] \quad (5.76a)$$

$$\varepsilon^g \mathbf{v}^{g,s} = -K^g \left[\lambda \rho^{g_v} \left(1 - \frac{R^{g_a}}{R^{g_v}} \right) \left(\frac{\partial \mu^{g_v}}{\partial T} \nabla T + \frac{\partial \mu^{g_v}}{\partial \varphi} \nabla \varphi \right) + \rho^g \eta^g \nabla T - \rho^g \mathbf{g} \right]. \quad (5.76b)$$

It is clear that there are several physical processes and couplings that occur for energy balance to be achieved. Equation (5.77) below shows the classical 1958 model of de Vries [31] (which is similar to that of Bear [5] and is also presented in [14] for the saturated case).

$$\begin{aligned} & \rho c_p \frac{\partial T}{\partial t} - \varepsilon (\rho^l W^l - \rho^g W^g) \frac{\partial S}{\partial t} \\ & = \nabla \cdot (\underline{\underline{\mathbf{K}}} \nabla T) - L \dot{e}_g^l - \left(\sum_{\alpha=l,g} \left(\frac{c_p^\alpha \rho^\alpha}{\varepsilon^\alpha} \right) (\varepsilon^\alpha \mathbf{v}^{\alpha,s}) \right) \nabla T. \end{aligned} \quad (5.77)$$

In this form of the energy equation, W^α is a *differential heat of wetting* [14], and the other variables are written in the present notation for convenience. At first observation, the \dot{T} , \dot{S} , $\underline{\underline{\mathbf{K}}}$, \dot{e}_g^l , and ∇T terms in equation (5.75) are similar to terms found in the de Vries model. That is, we capture the standard effects of specific heat along with differential heat of wetting, thermal conductivity, mass transfer, and convective heating. Implicit in the \dot{S} term in (5.75) is that we relate the partial derivative of the difference in wetting potentials, $T \partial(\pi^g - \pi^l) / \partial T$, as a differential heat of wetting. The present model also captures the effects of changing relative humidity, nonlinear effects such as $\nabla S \cdot \nabla S$ and $\nabla \varphi \cdot \nabla \varphi$, and cross effects such as $\nabla S \cdot \nabla \varphi$. It remains to determine which (if any) of these effects are negligible as compared to the others. To make this determination we perform a dimensional analysis in the next subsection. Let us first focus on the thermal conductivity term, $\nabla \cdot (\underline{\underline{\mathbf{K}}} \cdot \nabla T)$.

The functional form of the thermal conductivity, $\underline{\underline{\mathbf{K}}}$, can be approximated in several ways. A first approximation is to take the thermal conductivity as a weighted sum of the conductivities of the individual phases

$$\underline{\underline{\mathbf{K}}} = \sum_{\alpha} \varepsilon^{\alpha} \underline{\underline{\mathbf{K}}}_T^{\alpha}. \quad (5.78)$$

Comparing to results in [77], we note that this seems to overestimate the measured thermal conductivity as well as fail to capture the experimentally measured curvature of the thermal conductivity - saturation relationship. Since $\underline{\underline{\mathbf{K}}}$ is a linearization constant that arose from the entropy inequality, it can depend on any variable which is nonzero at equilibrium. In particular, $\underline{\underline{\mathbf{K}}}$ is a function of saturation. Smits et al. [77] use a combination of the Côté-Konrad and Johansen models to estimate the thermal conductivity in the scalar case:

$$K(S) = K_e(S) (K_{sat} - K_{dry}) + K_{dry}, \quad (5.79)$$

where K_{sat} is the conductivity of the saturated medium, K_{dry} is the conductivity of the dry medium, and $K_e(S)$ is a “normalized thermal conductivity known as the Kersten number.” Côté and Konrad proposed a functional form of K_e as

$$K_e(S) = \frac{\kappa S}{1 + (\kappa - 1)S}. \quad (5.80)$$

The parameter, κ , is a fitting parameter that is presumed to be different for each type of soil. In [77], κ was estimated for several types of sands and several types of soil packs. Figure 5.6 shows a thermal conductivity curve for (5.79) with tightly packed 30/40 sand that has a porosity of 0.334. For comparison, equation (5.78) is shown in red for the same experiment.

We make some comments here giving some possible reasons for the discrepancy between the weighted sum model (equation (5.78)) and the model that more closely matches what is experimentally observed (equation (5.79)). First, the thermal conductivity of air is neglected as compared to the thermal conductivity of water or

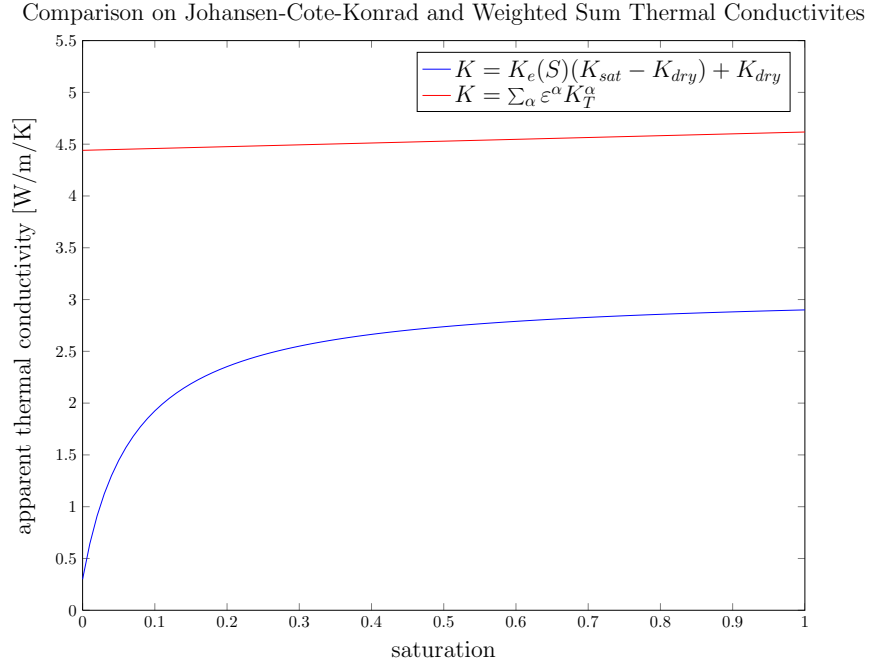


Figure 5.6: Johansen thermal conductivity model with Côté-Konrad $K_e - S$ relationship (with $\kappa = 15$) plotted in blue, and the weighted sum of the thermal conductivities of the individual phases plotted in red.

solid. Also, the thermal conductivity of liquid is much smaller than that of the solid, $K^l < K^s$. Furthermore, the geometry of the packed solid plays a crucial role. Observe that if we idealize the soil grains as individual spheres then there are relatively few contact points between the individual grains of the solid phase. This idealization can be used as a partial explanation for the left-hand tail seen in the Côté-Konrad model depicted in Figure 5.6. If there are few contact points between the individual grains then it is much harder for heat to transfer in the absence of a liquid phase connecting them. Thus, equation (5.79) tells us that all pertinent information is obtained by knowing what the thermal conductivity of the dry and saturated porous media is as well as an interpolation function for effective saturation. This captures more of the microscale geometry than just the volume fractions. The effects of these two proposed thermal conductivity functions on the behavior of the heat transport model will be explored when we consider numerical solutions in Section 7.4.2.

5.4.3.1 Dimensional Analysis

To determine which, if any, terms can be neglected from the energy transport equation we perform a dimensional analysis. Begin by noting that $\underline{\mathbf{K}}/(\rho c_p)$ has units of area per time. This suggests a natural choice of time scale for the thermal problem of

$$t = \left(\frac{\rho c_p x_c^2}{K} \right) t',$$

where t' is dimensionless time. Dividing by ρc_p (measured at a reference state), introducing x_c as a characteristic length (e.g. the height of a column experiment), and multiplying by $t_c = (\rho c_p x_c^2)/K$ gives the dimensionless form of the energy equation (the statement of which is suppressed for the sake of brevity).

Recall that the volumetric heat capacity, ρc_p , is linearly related to the specific heats of the individual phases

$$\rho c_p = \sum_{\alpha} (\varepsilon^{\alpha} \rho^{\alpha} c_p^{\alpha}) = \varepsilon S \rho^l c_p^l + \varepsilon(1 - S) \rho^g c_p^g + (1 - \varepsilon) \rho^s c_p^s.$$

Taking $S = 1$ as a reference state (or equivalently, $S = 0$) gives a characteristic value of ρc_p . Using values from Appendix E we see that $\rho c_p \sim \mathcal{O}(10^6)$. Hence, several of the quantities in (5.75) can be neglected:

$$\left(\frac{\varepsilon}{\rho c_p} \right) \left[\sum_{j=v,a} \left[\left(\mu^{gj} - T \frac{\partial \mu^{gj}}{\partial T} \right) \frac{\partial \rho^{gj}}{\partial T} \right] - (\Gamma^g + T \eta^g) \frac{\partial \rho^g}{\partial T} \right] \sim \mathcal{O}(10^{-4}) \quad (5.81a)$$

$$\left(\frac{\varepsilon}{\rho c_p} \right) \left[\sum_{j=v,a} \left[\left(\mu^{gj} - T \frac{\partial \mu^{gj}}{\partial T} \right) \frac{\partial \rho^{gj}}{\partial \varphi} \right] - (\Gamma^g + T \eta^g) \frac{\partial \rho^g}{\partial \varphi} \right] \sim \mathcal{O}(10^{-4}) \quad (5.81b)$$

$$\begin{aligned} & \left(\frac{t_c}{x_c^2 \rho c_p} \right) \left[-\Gamma^g \frac{\partial \rho^g}{\partial T} + \sum_{j=v,a} \left[\mu^{gj} \frac{\partial \rho^{gj}}{\partial T} \right] + T \frac{\partial}{\partial T} \left(\sum_{j=v,a} \left[\mu^{gj} \frac{\partial \rho^{gj}}{\partial T} \right] - \psi^g \frac{\partial \rho^g}{\partial T} \right) \right] \\ & \sim \mathcal{O}(10^{-2}) \end{aligned} \quad (5.81c)$$

$$\begin{aligned} & \left(\frac{t_c}{x_c^2 \rho c_p} \right) \left[-\Gamma^g \frac{\partial \rho^g}{\partial \varphi} + \sum_{j=v,a} \left[\mu^{gj} \frac{\partial \rho^{gj}}{\partial \varphi} \right] + T \frac{\partial}{\partial T} \left(\sum_{j=v,a} \left[\mu^{gj} \frac{\partial \rho^{gj}}{\partial \varphi} \right] - \psi^g \frac{\partial \rho^g}{\partial \varphi} \right) \right] \\ & \sim \mathcal{O}(10^{-2}) \end{aligned} \quad (5.81d)$$

$$\left(\frac{t_c}{x_c^2 \rho c_p} \right) e^l \frac{\partial \rho^l}{\partial T} \sim \mathcal{O}(10^{-1}) \quad (5.81e)$$

In order to make these approximations it is assumed that Gibbs potentials are given by the Gibbs-Duhem relationship, (4.61), and that the Helmholtz potential and internal energy are approximately the same order of magnitude as the Gibbs potential.

With these considerations we can rewrite the present version of the energy equation as

$$\begin{aligned}
0 = & \rho c_p \frac{\partial T}{\partial t} - \nabla \cdot (\underline{\underline{\mathbf{K}}} \cdot \nabla T) + \rho h + L \hat{e}_g^l + \varepsilon \left[p_c + 2\tau \varepsilon \dot{S} + T \frac{\partial}{\partial T} (\pi^g - \pi^l) \right] \frac{\partial S}{\partial t} \\
& + \left[\rho^l c_p^l \nabla T + \frac{T}{S} \frac{\partial p^l}{\partial T} \nabla S \right] \cdot (\varepsilon^l \mathbf{v}^{l,s}) \\
& + \left[\rho^g c_p^g \nabla T - \frac{T}{(1-S)} \frac{\partial p^g}{\partial T} \nabla S \right] \cdot (\varepsilon^g \mathbf{v}^{g,s}). \tag{5.82}
\end{aligned}$$

Unfortunately this analysis leads us to the conclusion that this new version of the heat transport equation is only *slightly* different than those proposed in past works [14, 31]. The major differences are the ∇S terms associated with the Darcy fluxes, the capillary pressure adjustment to the differential heat of wetting term, and the Darcy fluxes themselves. Recalling the forms of the Darcy fluxes from equations (5.76), the energy equation can be rewritten in a more compact notation as

$$\begin{aligned}
0 = & \rho c_p \frac{\partial T}{\partial t} - \nabla \cdot (\underline{\underline{\mathbf{K}}} \cdot \nabla T) + \rho h + L \hat{e}_g^l + \mathcal{W} \frac{\partial S}{\partial t} \\
& + (\chi_1 \nabla S + \chi_2 \nabla T + \chi_3 \nabla \varphi) \cdot \nabla T \\
& + (\chi_4 \nabla S + \chi_5 \nabla \varphi) \cdot \nabla \varphi + \chi_6 \nabla S \cdot \nabla S \tag{5.83}
\end{aligned}$$

where \mathcal{W} and each χ_j are implicitly defined via equations (5.82) and (5.76). It remains to determine the functional form(s) of the several constitutive variables in (5.83).

5.4.4 Constitutive Equations

Hidden within the coefficients of (5.83), (5.64), and (5.65) are a few final relationships necessary for closure. In particular, we need constitutive equations for

$$\tau = \frac{\partial p_c}{\partial \dot{\varepsilon}^l} \tag{5.84a}$$

$$\hat{e}_l^{g_v} = M (\rho^l - \rho^{g_v}) (\mu^l - \mu^{g_v}) \quad (5.84b)$$

$$\mathcal{W} = p_c(S) + 2\tau\varepsilon\dot{S} + T \frac{\partial}{\partial T} (\pi^g - \pi^l) = p_c(S) + 2\tau\varepsilon\dot{S} + W \quad (5.84c)$$

$$C_S^l = 2\rho^l \frac{\partial \psi^l}{\partial S} = \varepsilon (\pi^{l(v)} - \pi^{l(g)}) \quad (5.84d)$$

$$C_T^l = \rho^l \sum_{j=1}^N \left(\frac{\partial \psi^l}{\partial \rho^{g_j}} \frac{\partial \rho^{g_j}}{\partial T} \right) - \sum_{\alpha=g,s} \left(\frac{\varepsilon^\alpha \rho^\alpha}{\varepsilon^l} \frac{\partial \psi^\alpha}{\partial \rho^l} \frac{\partial \rho^l}{\partial T} \right) \quad (5.84e)$$

$$C_\varphi^l = \rho^l \sum_j \left(\frac{\partial \psi^l}{\partial \rho^{g_j}} \frac{\partial \rho^{g_j}}{\partial \varphi} \right). \quad (5.84f)$$

The simplest possible assumption would be that τ , C_S^l , C_T^l , C_φ^l , and W are constants. This would allow for the easiest sensitivity analysis but is likely contrary to physical reality. The following paragraphs discuss each of these terms and propose functional forms in terms of saturation, relative humidity, and temperature. The sensitivity of the numerical solution to several of these parameters is discussed in Chapter 7.

It is generally assumed that τ in equation (5.84a) is constant [46, 59], but according to the linearization process in HMT, τ can be a function of any variable that is not zero at equilibrium. In particular, it is possible that τ is a function of S ; but *which* function? In [17], the authors suggest several functional forms (constant, linear, quadratic, Gaussian, and error) and compare to experimental findings. Their findings suggest that "...an error function or Gaussian relationship for the damping coefficient τ provides reasonable agreement between data and simulations." Thus we consider the following forms:

$$\tau = \tau_{max} \quad (5.85a)$$

$$\tau = \frac{\tau_{max}}{2} \left(1 - \operatorname{erf} \left(\frac{S - \mu}{\sigma} \right) \right) \quad (5.85b)$$

$$\tau = \tau_{max} \exp \left(-\frac{(S - \mu)^2}{2\sigma^2} \right). \quad (5.85c)$$

Plots of equations (5.85) are shown in Figure 5.7 with typical mean and standard deviation parameters. To the author's knowledge, no other experiments have been conducted to make a better determination as to the functional form of τ . This

being said, since τ is a measure of the rate at which the pore-scale saturation profile rearranges in a dynamic situation, it is reasonable to assume that as $S \rightarrow 1$ the effect of this term should be minimized and as $S \rightarrow 0$ the effect should be maximized. Hence, in the author's opinion an error function is more sensible. It remains, of course, to determine the values of the maximum, mean and standard deviation parameters which are likely themselves functions of material properties.

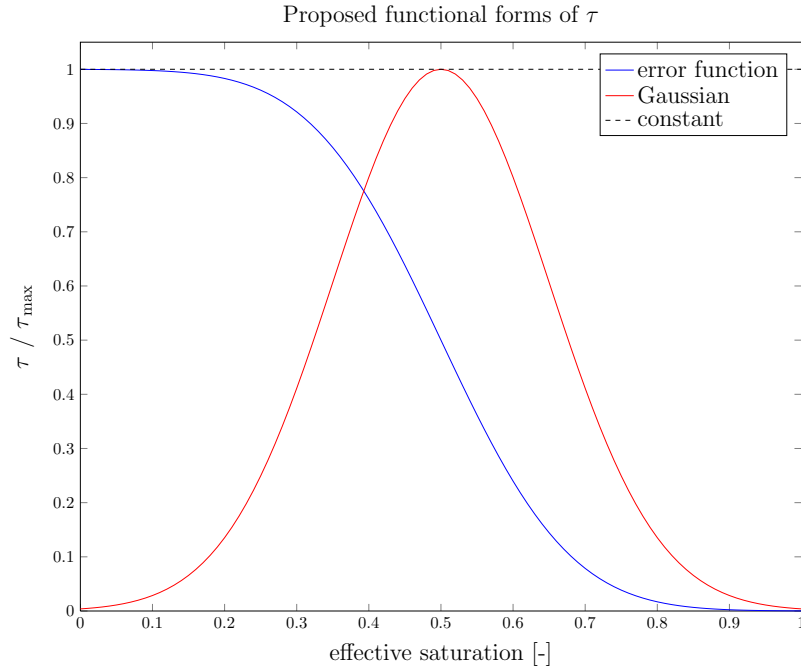


Figure 5.7: Three proposed functional forms of $\tau = \tau(S)$

The evaporation rate term, $\hat{e}_l^{g_v}$, given in equation (5.84b) is written as a function of the difference between the liquid and vapor chemical potentials. The chemical potential in the water vapor is a function of temperature and relative humidity [21],

$$\mu^{g_v} = \mu_*^{g_v} + R^{g_v} T \ln(\lambda\varphi).$$

The liquid-phase chemical potential, on the other hand, does not have such a natural description. At equilibrium, $\mu^l = \mu^{g_v}$. Away from equilibrium we only know that

$$\mu^l = \Gamma^l = \psi^l + \frac{p^l}{\rho^l},$$

and therefore is a function of every variable that ψ^l depends. In the most simplistic form we can assume that the liquid chemical potential is $\mu^l = \mu_*^l + (p^l - p_*^l)/\rho^l$. This assumption is taken from classical thermodynamics (see [21] for example). Furthermore, $\mu_*^l \approx \mu_*^{g_v}$ if we take the reference state to be equilibrium. Therefore,

$$\begin{aligned} \hat{e}_i^{g_v} &\approx \frac{M\varphi}{\rho^l} (\rho^l - \rho^{g_v}) \left(\frac{p^l - p_0^l}{\rho^l} - R^{g_v} T \ln(\lambda\varphi) \right) \\ &\approx \frac{M\varphi}{\rho^l} (\rho^l - \rho^{g_v}) \left(\frac{-p_c + \tau\varepsilon\dot{S} - p_0^l}{\rho^l} - R^{g_v} T \ln(\lambda\varphi) \right), \end{aligned} \quad (5.86)$$

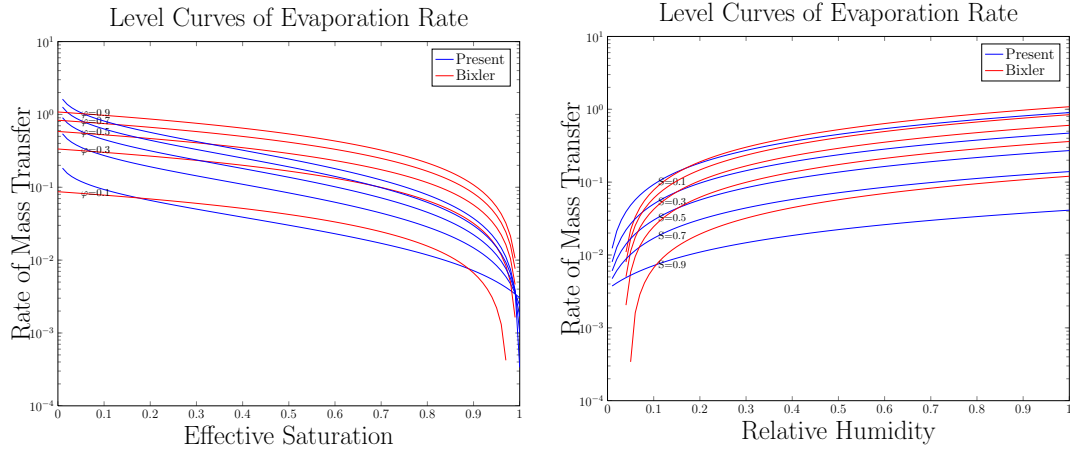
where M is a fitting parameter. The factor of relative humidity is included to achieve a better match with existing empirical models (discussed in the next paragraph).

There are several empirical rules for evaporation in porous media. One such rule, given by Bixler [19] and repeated in Smits et al. [75], is

$$\hat{e}_i^{g_v} = b(\varepsilon^l - \varepsilon_r^l) R^{g_v} T (\rho_{sat} - \rho^{g_v}), \quad (5.87)$$

where b is a fitting parameter and ε_r^l is the residual volumetric water content. Equations (5.86) and (5.87) are quite different, but under proper scaling they are *close* as seen in Figures 5.8. From these plots it is also clear that there is a large discrepancy between these model at very low saturations. These plots are generated at standard temperature with $\dot{S} = 0$. The dynamic saturation term will change the shape of these curves, but as the Bixler model, (5.87), is not dynamic we compare only with the steady state form of (5.86). Furthermore, the present model depends on the van Genuchten parameters for capillary pressure. In Figures 5.8 the parameters $m = 0.944$ and $\alpha = 5.7$ are used along with $b \approx 2.1 \times 10^{-5}$ to match the values used in [75].

The differential heat of wetting, W , in equation (5.84c) represents the heat gained or lost due to changes in saturation and adsorption. The present generalization suggests that the differential heat of wetting be supplemented by the capillary pressure and time rate of change of saturation. According to [63], the typical value of the



(a) Comparison of mass transfer rate vs. effective saturation shown with level curves in relative humidity. (b) Comparison of mass transfer rate vs. relative humidity shown with level curves in saturation.

Figure 5.8: Level curves of mass transfer rate functions.

differential heat of wetting is on the order to $10^3 J/kg$ depending on the type of soil. This value will be taken as constant throughout, but in reality value should be a function of saturation.

Finally, the values of C_S^l , C_T^l , and C_φ^l in equations (5.84d) - (5.84f) are new and hence there is no existing literature for which to make estimates or comparisons. For this reason we make the initial assumption that these terms are constant. This allows for relatively simple sensitivity analysis without introducing any unnecessary mathematical difficulties. As discussed in Section 5.4.1.1, the value of C_T^l is likely quite small since some research has been done to determine the affect of thermal gradients on Darcy flow [66].

5.5 Conclusion and Summary

In this chapter we have derived several new equations and terms for heat and moisture transport in unsaturated porous media. For the sake of readability, we summarize the results, assumptions, and equations derived here within Chapter 5.

The main assumptions are:

Assumption #1 The solid phase is rigid, incompressible, and inert.

Assumption #2 The liquid and gas phases are composed of N constituents. (this was later relaxed to let $N = 2$ in the gas phase and $N = 1$ in the liquid phase).

Assumption #3 No chemical reactions take place in any of these phase.

Assumption #4 Diffusion with the liquid phase is negligible compared to the advection of the liquid phase.

Assumption #5 The liquid phase is incompressible.

Assumption #6 The gas phase is an ideal binary gas mixture of water vapor and inert *air*.

Assumption #7 The gas-phase chemical potentials and densities are functions of relative humidity and temperature.

The secondary assumptions used up to this point are (in order of appearance):

- the medium of interest is granular so angular momentum conservation yields a symmetric stress tensor,
- the material is *simple* in the sense of Coleman and Noll [26],
- the phase interfaces are assumed to contain no mass, momentum, or energy,
- second-order effects in velocity are negligible (e.g. $\mathbf{v}^{\alpha_j, \alpha} \otimes \mathbf{v}^{\alpha_j, \alpha} \ll \mathbf{v}^\alpha$),
- the species in the solid phase do not diffuse,
- inertial terms in the momentum balance equation are negligible,
- the capillary pressure - saturation relationship is given by the van Genuchten function,
- the deviation in wetting potential is approximately zero ($(\pi_c|_{n.eq} - \pi_c|_{eq}) \approx 0$),

- the coefficient of the dynamic saturation term, τ , is constant,

Considering assumptions #1 - #7 along with all of the secondary assumptions, the final system of equations proposed to model heat and moisture transport in unsaturated porous media is:

$$\begin{aligned} \frac{\partial S}{\partial t} - \nabla \cdot \left[\varepsilon_S^{-1} K^l \left(\{p'_c + C_S^l\} \nabla S + \tau \varepsilon_S \nabla \dot{S} + C_T^l \nabla T + C_\varphi^l \nabla \varphi - \rho^l \mathbf{g} \right) \right] \\ = \frac{\hat{e}_l^{g^v}}{\rho^l} \end{aligned} \quad (5.88a)$$

$$\frac{\partial}{\partial t} (\rho_{sat} \varphi (1 - S)) - \nabla \cdot [\rho_{sat} (\mathcal{D} \nabla \varphi + N^g \nabla T)] = -\hat{e}_l^{g^v} \quad (5.88b)$$

$$\begin{aligned} 0 = \rho c_p \frac{\partial T}{\partial t} + \mathcal{W} \frac{\partial S}{\partial t} - \nabla \cdot (\underline{\underline{\mathbf{K}}} \cdot \nabla T) + \rho h + L \hat{e}_g^l \\ + (\chi_1 \nabla S + \chi_2 \nabla T + \chi_3 \nabla \varphi) \cdot \nabla T \\ + (\chi_4 \nabla S + \chi_5 \nabla \varphi) \cdot \nabla \varphi + \chi_6 \nabla S \cdot \nabla S, \end{aligned} \quad (5.88c)$$

where the relevant empirical, constitutive, and derived relations are

$$K^l(S) = \frac{\kappa_s}{\mu_l} \kappa_{rl} = \frac{\kappa_s}{\mu_l} \sqrt{S} \left(1 - [1 - S^{1/m}]^m \right)^2 \quad (5.89a)$$

$$K^g(S) = \frac{\kappa_s}{\mu_g} \kappa_{rg} = \frac{\kappa_s}{\mu_g} (1 - S)^{1/3} (1 - S^{1/m})^{2m} \quad (5.89b)$$

$$p_c(S) = \frac{1}{\alpha} (S^{-1/m} - 1)^{1-m} \quad (5.89c)$$

$$\tau = \frac{\partial p_c}{\partial \hat{\varepsilon}^l} \quad (\text{see equations (5.85)}) \quad (5.89d)$$

$$\hat{e}_l^{g^v} = M \varphi (\rho^l - \rho^{g^v}) \left(\frac{-p_c + \tau \varepsilon \dot{S} - p_0^l}{\rho^l} - R^{g^v} T \ln(\lambda \varphi) \right) \quad (5.89e)$$

$$\mathcal{D}(\varphi, S, T) := (1 - S) D^g + \rho_{sat} \varphi R^{g^v} T \left(1 - \frac{R^{g^a}}{R^{g^v}} \right) \left(\frac{\lambda \kappa_s}{\varepsilon \mu_g} \right) \kappa_{rg}(S) \quad (5.89f)$$

$$N^g(\varphi, S, T) = \varphi \left[\mathcal{D}(\varphi, S, T) \left(\frac{1}{\lambda} \frac{d\lambda}{dT} + \frac{R^{g^v} \ln(\lambda \varphi)}{T} \right) + \rho^g \rho_{sat} \eta^g \left(\frac{\lambda \kappa_S}{\varepsilon \mu_g} \right) \kappa_{rg}(S) \right] \quad (5.89g)$$

$$D^g(T) = 2.12 \times 10^{-5} \left(\frac{T}{273.15} \right)^2 \quad (5.89h)$$

$$\rho c_p = \sum_{\alpha} \varepsilon^{\alpha} \rho^{\alpha} c_p^{\alpha} \quad (5.89i)$$

$$\rho h = \sum_{\alpha} \rho^{\alpha} h^{\alpha} \quad (5.89j)$$

$$\mathcal{W} = p_c + 2\tau\varepsilon\dot{S} + W \quad (5.89k)$$

$$\underline{\underline{\mathbf{K}}} = \sum_{\alpha} \varepsilon^{\alpha} \underline{\underline{\mathbf{K}}}_{T}^{\alpha}, \quad \text{or} \quad K = \left(\frac{\kappa S (K_{sat} - K_{dry})}{1 + (\kappa - 1)S} \right) + K_{dry} \quad (5.89l)$$

$$\rho^l(T) = 3.79 \times 10^{-5}(T - 277.15)^3 - 7.37 \times 10^{-3}(T - 277.15)^2 + 10^3 \quad (5.89m)$$

$$\rho_{sat}(T) = \frac{1}{T} \exp \left(31.37 - 7.92 \times 10^{-3}T - \frac{6014.79}{T} \right) 10^{-3} \quad (5.89n)$$

$$\begin{aligned} \mu_l(T) = & (-2.56109 \times 10^{-6}(T - 273.15)^3 + 0.00057672(T - 273.15)^2 \\ & - 0.0469527(T - 273.15) + 1.75202) 10^{-3} \end{aligned} \quad (5.89o)$$

$$\mu_g(T) = \left(\frac{1.02312T^3}{10^9} - \frac{3.62788T^2}{10^6} + 0.00665915T + 0.11767 \right) 10^{-5} \quad (5.89p)$$

$$L(T) = 2.501 \times 10^6 - 2369.2(T - 273.15) \quad (5.89q)$$

$$\begin{aligned} \eta^g(T) = & 6.1771 \times 10^{-4}(T - 273.15)^4 - 7.3971 \times 10^{-2}(T - 273.15)^3 \\ & + 3.1324(T - 273.15)^2 - 34.4817(T - 273.15) + 191.208. \end{aligned} \quad (5.89r)$$

Equations (5.88) coupled with equations (5.89) give several adjustments to the classical models for saturation (Richards'), vapor diffusion (Phillip and de Vries), and heat transport (de Vries) presented in Section 5.1. In order for the present models to be accepted in the hydrology community we must show that the proposed terms are non-negligible and in some way put some of the empirical relations on a firmer theoretical footing. The proposed vapor diffusion equation (5.88b) is a prime example of this as there are no empirical fitting parameters within the diffusion coefficient (hence removing the need for an empirical *enhancement factor*).

In Chapter 6 we discuss the mathematical questions of existence and uniqueness of solutions to the individual equations. In Chapter 7 we discuss numerical simulations of the models.

6. Existence and Uniqueness Results

In this chapter we discuss the necessary regularity and assumptions for existence and uniqueness of solutions for the three equations. As the main thrust of this work is not to prove existence and uniqueness for general classes of systems of partial differential equations, we approach these problems by stating relevant existing theorems from the literature and satisfying the hypotheses of these theorems. The saturation and gas diffusion equations are both of parabolic type and can be treated similarly. The heat transport equation is an advection-reaction-diffusion equation that, in principle, should be parabolic in nature. The advection terms force a different approach to this equation. In Section 6.1, an existence and uniqueness result for the saturation equation with the third-order term (due to Mikelić [56]) is outlined. The theorems of Alt and Luckhaus [1, 2] are outlined in Section 6.2 and then used in Sections 6.2.1 and 6.2.2 to prove existence and uniqueness results for Richards' equation and the vapor diffusion equation respectively. Finally, an existence and uniqueness result for a special case of the heat transport equation is presented in Section 6.3.

6.1 Saturation Equation with $\tau \neq 0$

The saturation equation has been well studied since Richards' first introduced it in the 1930's. Recent modeling efforts, including those of Hassanizadeh et al., have introduced a new term into the classical Richards' equation and this has caused a resurgence in the analytical study of the saturation equation. The 2010 paper by Andro Mikelić [56] gives the necessary conditions for existence and uniqueness of a weak solution to the following equation:

$$\frac{\partial S}{\partial t} = \nabla \cdot \left\{ K(S) \left(-\frac{dp_c}{dS} \nabla S + \tau \nabla \left(\frac{\partial S}{\partial t} \right) + \mathbf{e}_3 \right) \right\} \text{ in } \Omega_T = \Omega \times (0, T) \quad (6.1a)$$

$$S = S_D \text{ on } \Gamma_D = \partial_D \Omega \times (0, T) \quad (6.1b)$$

$$K(S) \left(-\frac{dp_c}{dS} \nabla S + \tau \nabla \left(\frac{\partial S}{\partial t} \right) + \mathbf{e}_3 \right) \cdot \nu = R \text{ on } \Gamma_N = \partial_N \Omega \times (0, T) \quad (6.1c)$$

$$S(x, t = 0) = S_i(x) \text{ on } \Omega \quad (6.1d)$$

Here, e_3 is a unit vector pointing the z direction to account for gravitational effects, ν is an outward pointing normal, and the subscripts D and N represent Dirichlet and Neumann conditions respectively. Notice that (6.1) is a simplification of the present saturation equation as it contains no evaporation (source) term and no coupling with relative humidity or temperature.

Mikelić's theorem is stated here for completeness.

Theorem 6.1 (Mikelić 2010 [56], Theorems 3 & 4) *Consider the following hypotheses:*

H1: *there are constants $\beta > 0, S_K > 0$ and a nonnegative function $f \in C_0^\infty(\mathbb{R})$ such that K is given by*

$$K(z) = \frac{S_k z^\beta}{1 + S_K z^\beta f(z)}, \quad z \in [0, 1]$$

H2: *there exists $\lambda > 0, S_p > 0, M_p > 0$ and an arbitrary function $g \in C_0^\infty(\mathbb{R})$ such that $-p'_c$ is written as*

$$-p'_c(z) = \frac{S_p z^{-\lambda}}{1 + M_p z^\lambda g(z)}, \quad z \in [0, 1]$$

H3: *the product of the functions K and p'_c is bounded on $[0, 1]$.*

H4: *the initial Dirichlet data is smooth: $S_D \in C^1([0, T]; H^1(\Omega))$, and is bounded away from zero $0 < S_{D, \min} \leq S_D(x, t) \leq 1$ (or impose that $S_D \neq 0$ a.e.)*

H5: *$R = R_0 \zeta$; where $R_0 \in C^1(\bar{\Gamma}_N \times [0, T])$, $R_0 \geq 0$ and $\zeta \in C_0^\infty(\mathbb{R})$, $\zeta(z) \geq 0$ for $z > 0$, and $z\zeta(z) \geq 0$ for $z < 0$.*

H6: *Initial moisture content satisfies a "finite entropy" condition: $\int_\Omega (S_0(x))^{2-\beta} dx < +\infty$ where $\beta \geq \lambda > 2$*

Under these hypotheses there is a weak solution for (6.1) where $S \in H^1(\Omega_T)$ such that $0 \leq S(x, t)$ a.e. on Ω_T , $\nabla \partial_t S \in L^2(\Omega_T)$ and $S - S_D \in L^2(0, T; V)$ for $V = H^1(0, 1)$.

The proof of this theorem is beyond the scope of this work, but it indicates that under constant relative humidity and temperature conditions, where no mass transfer is expected, there exists a weak solution to the saturation equation. The sixth hypothesis restricts the shape of the initial condition. Simply put, the initial condition cannot drop to zero in such a way as to make $\int_{\Omega} S_0^{2-\beta} dx$ go to infinity. This avoids the natural degenerate nature of the problem. The regularity expected for the solution (H^1) is a nice result given that this is actually a third-order differential equation.

6.2 Alt and Luckhaus Existence and Uniqueness Theorems

We now turn our attention to demonstrating the necessary conditions for existence and uniqueness of Richards' equation (saturation with $\tau = 0$) and the vapor diffusion equation in the special cases where the other dependent variables are held fixed (possibly even constant). The two equations are treated together in this section since they both fall under the class of quasi-linear parabolic equations. As such, they can be analyzed using similar theory. For the purposes of demonstrating existence and uniqueness we apply general theorems by Alt and Luckhaus [1, 2] to these equations.

The following paragraphs are paraphrased from Alt and Luckhaus [2] and are presented here to introduce the reader to the notation used therein and for future reference.

Consider the general initial boundary value problem (IBVP) for a system of quasi-linear elliptic-parabolic differential equations

$$\partial_t b^j(\mathbf{u}) - \nabla \cdot a^j(b(\mathbf{u}), \nabla \mathbf{u}) = f^j(b(\mathbf{u})) \quad \text{in } (0, T) \times \Omega, j = 1 : m \quad (6.2a)$$

$$b(\mathbf{u}) = b^0 \quad \text{on } \{0\} \times \Omega \quad (6.2b)$$

$$\mathbf{u} = \mathbf{u}^D \quad \text{on } (0, T) \times \Gamma \quad (6.2c)$$

$$a^j(b(\mathbf{u}), \nabla \mathbf{u}) \cdot \nu = 0 \quad \text{on } (0, T) \times (\partial\Omega \setminus \Gamma), j = 1 : m \quad (6.2d)$$

In equations (6.2), $\mathbf{u} \in \mathbb{R}^m$, $b : \mathbb{R}^m \rightarrow \mathbb{R}^m$, and $a : \mathbb{R}^m \times \mathbb{R}^{m \times N} \rightarrow \mathbb{R}^m$ where N is the spatial dimension of the problem and m is the number of equations.

We call \mathbf{u} in the affine space $\mathbf{u}^D + L^r(0, T; V)$ a weak solution of (6.2) if the following two properties are fulfilled:

1. $b(\mathbf{u}) \in L^\infty(0, T; L^1(\Omega))$ and $\partial_t b(\mathbf{u}) \in L^{r^*}(0, T; V^*)$ with initial values b^0 , that is

$$\int_0^T \langle \partial_t b(\mathbf{u}), \zeta \rangle + \int_0^T \int_\Omega (b(\mathbf{u}) - b^0) \partial_t \zeta = 0$$

for every test function $\zeta \in L^r(0, T; V) \cap W^{1,1}(0, T; L^\infty(\Omega))$ with $\zeta(T) = 0$.

2. $a(b(\mathbf{u}), \nabla \mathbf{u}), f(b(\mathbf{u})) \in L^{r^*}((0, T) \times \Omega)$ and \mathbf{u} satisfies the differential equation, that is,

$$\int_0^T \langle \partial_t b(\mathbf{u}), \zeta \rangle + \int_0^T \int_\Omega a(b(\mathbf{u}), \nabla \mathbf{u}) \cdot \nabla \zeta = \int_0^T \int_\Omega f(b(\mathbf{u})) \zeta$$

for every $\zeta \in L^r(0, T; V)$.

Recall from Functional Analysis that V^* is the dual space of the vector space V , and $W^{k,p} = \{u \in L^p(\Omega) : D^\alpha u \in L^p(\Omega) \forall |\alpha| \leq k\}$ with the weak derivative $D^\alpha u$. The reader should also recall the common simplified notation $W^{k,2}(\Omega) = H^k(\Omega)$.

Consider the following hypotheses:

H1: $\Omega \subset \mathbb{R}^n$ is open, bounded, and connected with Lipschitz boundary, $\Gamma \subset \partial\Omega$ is measurable with $H^{n-1}(\Gamma) > 0$ and $0 < T < \infty$.

H2: b is a monotone vector field and a continuous gradient, that is, there is a convex C^1 function $\Phi : \mathbb{R}^m \rightarrow \mathbb{R}$ with $b = \nabla \Phi$. We can assume that $b(0) = 0$. The convexity of Φ then implies that we can define

$$B(\mathbf{z}) := b(\mathbf{z}) \cdot \mathbf{z} - \Phi(\mathbf{z}) + \Phi(0).$$

H3: $a(b(\mathbf{z}), \mathbf{p})$ is continuous in \mathbf{z} and \mathbf{p} and elliptic in the sense that

$$(a(b(\mathbf{z}), \mathbf{p}^{(1)}) - a(b(\mathbf{z}), \mathbf{p}^{(2)})) \cdot (\mathbf{p}^{(1)} - \mathbf{p}^{(2)}) \geq C |\mathbf{p}^{(1)} - \mathbf{p}^{(2)}|^r$$

with $1 < r < \infty$ and $f(b(\mathbf{z}))$ continuous in \mathbf{z} .

H4: The following growth condition is satisfied:

$$|a(b(\mathbf{z}), \mathbf{p})| + |f(b(\mathbf{z}))| \leq c(1 + B(\mathbf{z})^{(r-1)/r} + |\mathbf{p}|^{r-1}).$$

H5: We assume that u^D is in $L^r(0, T; W^{1,r}(\Omega))$ and in $L^\infty((0, T) \times \Omega)$ and we define

$$V := \{v \in W^{1,r}(\Omega) : v = 0 \text{ on } \Gamma\}$$

H6: Assume either that b^0 maps into the range of b and therefore there is a measurable function \mathbf{u}^0 with $b^0 = b(\mathbf{u}^0)$ or that

$$\partial_t u_D \in L^1(0, T; L^\infty(\Omega)).$$

The existence and uniqueness theorems of Alt and Luckhaus [2] are stated here for convenience and reference.

Theorem 6.2 (Alt and Luckhaus [2], Theorem 1.7) *Suppose the data satisfy H1 - H6, and assume that $\partial_t u^D \in L^1(0, T; L^\infty(\Omega))$. Then there is a weak solution to (6.2).*

Theorem 6.3 (Alt and Luckhaus [2], Theorem 2.4) *Suppose that the data satisfy H1 - H6 with $r = 2$ and*

$$a(t, x, b(\mathbf{z}), \mathbf{p}) = A(t, x)\mathbf{p} + e(b(\mathbf{z}))$$

where $A(t, x)$ is a symmetric matrix and measurable in t and x such that for $\alpha > 0$

$$A - \alpha I \quad \text{and} \quad A + \alpha \partial_t A$$

are positive definite. Moreover assume that

$$|e(b(\mathbf{z}_2)) - e(b(\mathbf{z}_1))|^2 + |f(b(\mathbf{z}_2)) - f(b(\mathbf{z}_1))|^2 \leq C(b(\mathbf{z}_2) - b(\mathbf{z}_1))(\mathbf{z}_2 - \mathbf{z}_1).$$

Then there is at most one weak solution.

6.2.1 Existence and Uniqueness for Richards' Equation

The existence and uniqueness of weak solutions to Richards equation is known, and a general tool for handling this problem is the Alt-Luckhaus theorem stated above. In this subsection we set up and state the theorems. We will show that the hypotheses of Theorems 6.2 and 6.3 are satisfied under restrictions on the Dirichlet boundary conditions and appropriate boundedness assumptions. The equation

$$\begin{aligned} \frac{\partial S}{\partial t} &= \frac{\partial}{\partial x} \left(\frac{\kappa_{rw}(S)}{\rho^l g} \frac{\partial p^l}{\partial x} - \kappa_{rw}(S) \right) \\ &= \frac{\partial}{\partial x} \left(\kappa_{rw}(S) \frac{\partial h}{\partial x} - \kappa_{rw}(S) \right) \end{aligned} \quad (6.3)$$

is Richards' equation in dimensionless time and one spatial dimension. In this formulation we take h as the hydraulic head: $h = p^l/(\rho^l g)$. Recall from previous discussions that the pressure (or head) is a function of saturation. This relationship is invertible so here we note that saturation can be written as a function of pressure (or head). As suggested in [2, 62], "saturation may be less regular than pressure, therefore we expect to achieve better [regularity] results by applying a Kirchhoff transform". A Kirchhoff transformation gives a smoothed relationship between head and a new unknown; a generalized pressure head

$$\mathcal{K} : \mathbb{R} \rightarrow \mathbb{R} \quad \text{as} \quad \mathcal{K}(h) = \int_{-\infty}^h \kappa_{rw}(S(q)) dq := u.$$

The pressure head is taken to be negative by convention (opposite sign of capillary pressure). The variable u now becomes the primary unknown of (6.3) since the spatial derivative can be written as

$$\frac{du}{dx} = \frac{d\mathcal{K}}{dh} \frac{dh}{dx} = \kappa_{rw} \frac{dh}{dx},$$

and if $b(u)$ is defined as $b(u) = S(\mathcal{K}^{-1}(u)) - 1$ then

$$\frac{\partial}{\partial t} (b(u)) = \frac{\partial}{\partial x} \left(\frac{\partial u}{\partial x} - \kappa_{rw}(b(u) + 1) \right). \quad (6.4)$$

Notice that the definition of b depends on the invertibility of \mathcal{K} . Also, since $\mathcal{K}^{-1}(u) = h$, b can be seen as a function of h : $b(h) = S(h) - 1$ (see Figure 6.1). Given the van Genuchten capillary pressure - saturation relationship, $S(h) = \left((\alpha h)^{1/(1-m)} + 1 \right)^{-m}$, and the van Genuchten relative permeability function, $\kappa_{rw}(S) = \sqrt{S} (1 - (1 - S^{1/m})^m)^2$, Figure 6.2 shows several plots of \mathcal{K} for various parameter values. There is a horizontal asymptote as $h \rightarrow -\infty$ and it is evident from the plot that \mathcal{K} is one-to-one and onto for all values of $h \in (-\infty, 0)$, but as h gets *large* in absolute value the inverse becomes unstable.

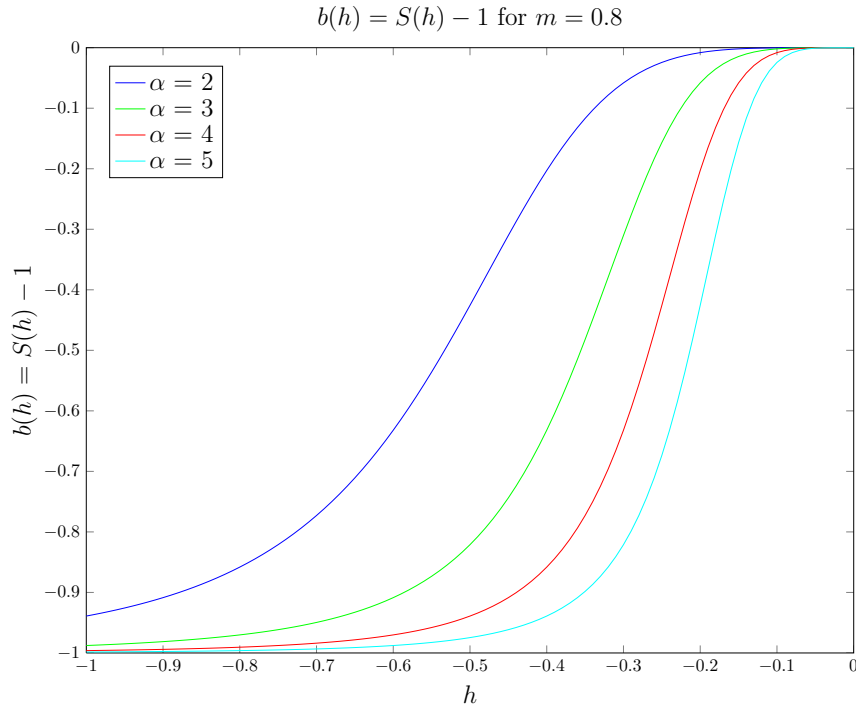


Figure 6.1: The function $b(h) = S(h) - 1$ for $m = 0.8$ and various values of α .

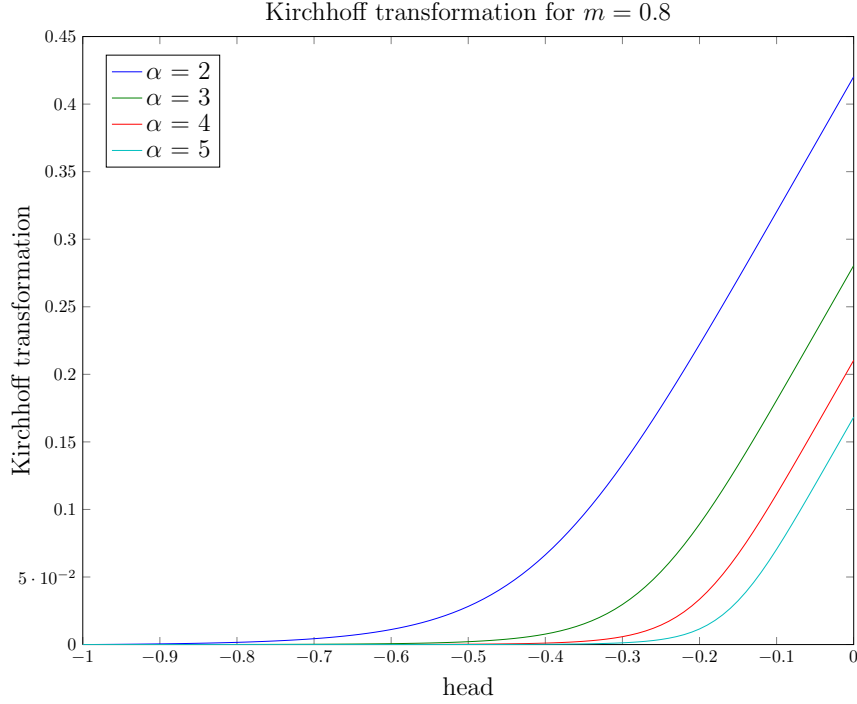


Figure 6.2: Kirchhoff transformation \mathcal{K} for $m = 0.8$ and various values of α .

Matching to equation (6.2a) we note that $j = 1$, define $a(b(u), \nabla u)$ as

$$a\left(b(u), \frac{\partial u}{\partial x}\right) = \frac{\partial u}{\partial x} + \kappa_{rw}(b(u) + 1),$$

and notice that $f = 0$. Given constant head Dirichlet boundary conditions, we finally rewrite Richards' equation as

$$\frac{\partial}{\partial t}(b(u)) = \frac{\partial}{\partial x}\left(\frac{\partial u}{\partial x} - \kappa_{rw}(b(u))\right) \quad \text{in } (0, T) \times \Omega \quad (6.5a)$$

$$u = u_D \quad \text{on } (0, T) \times \{0, 1\} \quad (6.5b)$$

$$u = u_0 \quad \text{on } 0 \times \Omega \quad (6.5c)$$

With this form of Richards' equation we propose the following existence and uniqueness result.

Theorem 6.4 *Suppose that the following conditions hold for the generalized head, u , in equation (6.5).*

1. $\Omega = (0, 1)$ and $t \in (0, T) \subset (0, \infty)$

2. $u_D \in L^\infty((0, T) \times \Omega)$

3. $\partial_t u_D \in L^1(0, T; L^\infty(\Omega))$

Then there exists a unique weak ($u \in u_D + L^2(0, T; H_0^1(\Omega))$) solution to (6.5).

The proof of Theorem 6.4 has been discussed in several articles. In particular, the transformation of Richards equation to the form seen in equations (6.5) are discussed as a model problem for the Alt and Luckhaus theorems [2]. Furthermore, this proof is presented in [62] as part of their numerical formulation of Richards' equation. The fundamental reason for presenting this result here is that the value of τ in the new saturation equations is not yet well known in experimental studies. Presenting this case simply covers all of the possible bases.

In the cases where $\nabla\varphi$, ∇T , or mass transfer terms are non-zero, these terms become source terms that depend on x . This means that $f = f(x, b(u)) \neq 0$. According to section 1.10 in [2] "it makes no difference if a and f depend on x ." This is made more clear in their subsequent work [1] where the theorem is explicitly stated to allow for x and t dependence.

For comparison sake we observe the difference between the regularity required for Richards equation (Theorem 6.4) and for the extended saturation equation with the third-order term (Theorem 6.1). For the equation with the third-order term ($\nabla \cdot \nabla \dot{S}$), the weak solution is in H^1 while in the second-order equation the weak solution is in L^2 . This extra required regularity is expected.

6.2.2 Vapor Diffusion Equation

To prove existence for the gas diffusion problem we proceed using the theorem of Alt and Luckhaus as with the saturation equation. Recall that under constant temperature and fixed saturation conditions

$$(1 - S(x)) \frac{\partial \varphi}{\partial t} - \frac{\partial}{\partial x} \left(\mathcal{D}(\varphi, S(x)) \frac{\partial \varphi}{\partial x} \right) = 0 \quad (6.6)$$

where

$$\mathcal{D}(\varphi, S(x)) = (1 - S(x))D^g + \rho_{sat}\varphi R^{g_v}T \left(1 - \frac{R^{g_a}}{R^{g_v}}\right) \lambda K(S(x)). \quad (6.7)$$

Allowing S to be a function of x constitutes a departure from the exact form of the parabolic-elliptic system found in Alt and Luckhaus (see equations (6.2)) as this is now a non-autonomous differential equation. In [1] this proof was generalized to allow for $b = b(x, u)$ and for $a = a(x, u, \nabla u)$ (see section 11 of [1]). The only additional assumptions for the existence theorems are that $b : \Omega \times \mathbb{R} \rightarrow \mathbb{R}$ and $a : \Omega \times \mathbb{R} \times \mathbb{R}^N \rightarrow \mathbb{R}^N$ are measurable in the first argument and continuous in the others. With this addition to Theorem 6.2 we proceed with the existence theorem for the gas-phase equation.

Assume that the initial-boundary conditions are

$$\varphi(0, t) = \varphi_{D,0} \in (0, 1), \quad \forall t \in (0, T) \quad (6.8a)$$

$$\varphi(1, t) = \varphi_{D,1}(t) \in (0, 1), \quad \forall t \in (0, T) \quad (6.8b)$$

$$\varphi(x, 0) = \varphi_0(x), \quad x \in \Omega. \quad (6.8c)$$

Note here that the Dirichlet boundary condition on the *right-hand* side of Ω is time dependent and the one on the left is independent of time. The problem could also be restated where the right-hand boundary is of Neuman type. The conditions are chosen to better match the experimental data that will be considered in Section 7.4.

Theorem 6.5 (Existence of Weak Solution to Diffusion Equation) *Suppose that the following conditions hold for equations (6.6) - (6.8).*

1. $\Omega = (0, 1)$ and $t \in (0, T) \subset (0, \infty)$
2. $\varphi \in (0, 1 - \epsilon]$ for all $x \in \Omega$ and for all $t \in (0, T)$ where $0 < \epsilon \ll 1$
3. $S \in [\epsilon, 1 - \epsilon]$ and $S(x) \in C^1(\Omega)$ (independent of time) where $0 < \epsilon \ll 1$

4. $\varphi_{D,1} \in L^2(0, T; H^1(\Omega))$ and $L^\infty((0, T) \times \Omega)$

Then there exists a weak solution to (6.6) - (6.8) in the sense that $\varphi \in \varphi_D + L^2(0, T; H_0^1(\Omega))$.

Matching equation (6.6) to the form of Alt and Luckhaus (equation (6.2a)) we have

$$b(x, z) = (1 - S(x))z, \quad a(x, z, p) = \mathcal{D}(x, z)p, \quad f = 0, \quad m = 1. \quad (6.9)$$

In the conditions for Theorem 6.5 we use the parameter ϵ to define two different sets. This is a small abuse of notation since φ and S need not belong to exactly the same set. We are simply stating that both of these functions must be bounded away from 0 and 1.

Proof: We proceed by verifying hypotheses H1 - H6 of Theorem 6.2 noting the extension proposed in [1] to non-autonomous functions.

H1: In 1 spatial dimension it is clear that Ω is an open, bounded, and connected domain with Lipschitz boundary. $\Gamma = \{0, 1\}$, and $H^0(\Gamma) > 0$ and $0 < T < \infty$.

H2: In this case we note that $b(x, z) = (1 - S(x))z$. Clearly $b(x, 0) = 0$. Define $\Phi(x, z) = (1 - S(x))z^2/2$ and observe that $\partial\Phi/\partial z = (1 - S(x))z = b(x, z)$ and $\partial^2\Phi/\partial z^2 = 1 - S(x) > 0$ since $S(x) \in (0, 1)$. Since $S \in C^1(\Omega)$ (assumption #3 in the statement of the theorem) it is clear that b is measurable in the first component. Furthermore, b is a continuous gradient of a convex function in the second component. Define $B(x, z) = b(x, z)z - \Phi(x, z) + \Phi(x, 0) = (1 - S(x))z^2/2$.

H3: Since a is a linear function of p it is easy to see that

$$\begin{aligned} (a(x, z, p^{(1)}) - a(x, z, p^{(2)})) (p^{(1)} - p^{(2)}) &= \mathcal{D}(x, z) (p^{(1)} - p^{(2)})^2 \\ &\geq C_\epsilon (p^{(1)} - p^{(2)})^2 \end{aligned} \quad (6.10)$$

where $\mathcal{D}(x, z) \geq C_\epsilon$ for all x, z (this ϵ -dependence reflects the choice of the saturation function, $S(x)$). Given the functional form of \mathcal{D} it is obvious that a is continuous and bounded on $z \in (0, 1)$, $p \in \mathbb{R}$, and is measurable in x . Hence a satisfies the ellipticity condition. Simply stated, the ellipticity of the diffusion coefficient means that the operator in question is bounded away from zero and is therefore invertible.

H4: Let $z \in [\epsilon, 1 - \epsilon]$ and $p \in \mathbb{R}$. From the definition of a and f ,

$$\begin{aligned} |a(x, z, p)| + |f(z)| &= |a(x, z, p)| = |\mathcal{D}(x, z)p| \\ &\leq c_{\mathcal{D}, \epsilon}|p| \\ &\leq c_\epsilon \left(1 + \sqrt{B(z)} + |p|\right) \end{aligned} \quad (6.11)$$

for all z , where $c_{\mathcal{D}, \epsilon}$ is the upper bound on $\mathcal{D}(x, z)$ over z . Therefore a (and f) satisfy the growth condition.

H5: The left Dirichlet boundary condition is fixed in time, $\varphi(0, t) = \varphi_{D,0}$. It is assumed that $\varphi_{D,0} \in L^2(0, T; H^1(\Omega))$ and $L^\infty((0, T) \times \Omega)$. The right Dirichlet boundary condition is allowed to vary in time. Assumption #4 in the statement of this theorem guarantees that hypothesis H5 is satisfied for this boundary condition.

H6: Since $b(x, z) = (1 - S(x))z$ it is clear that b is surjective so long as $S(x) \neq 1$ and that $b^0 = \varphi_0/(1 - S(x))$. That is, there exists a function $\varphi_0/(1 - S(x))$ such that $b^0 = b(x, \varphi^0)$.

Given the final assumption in the statement of this theorem we have, in particular, $\varphi_D \in L^1(0, T; L^\infty(\Omega))$ since $L^1(\Omega) \subset L^2(\Omega) \subset L^\infty(\Omega)$ for sets Ω of finite measure [37]. Therefore, from Theorem 6.2 there exists a weak solution, φ , in the affine space $\varphi_D + L^2(0, T; V)$ where $V = \{v \in H^1(\Omega) : v = 0 \text{ on } \{0, 1\}\}$. ■

The uniqueness of the weak solution to (6.6) - (6.8), unfortunately, doesn't fit Theorem 6.3 because the diffusion operator cannot be decomposed in the manner required. This does not mean that the weak solution is not unique, it simply means that this is not the tool to prove uniqueness. This small problem is left for future research.

6.2.3 Limits of the Alt and Luckhaus Theorem

The theorem of Alt and Luckhaus does not apply to the heat transport equation since there are advection-type terms present in that equation that can not satisfy the assumed form of Theorem 6.2. The next logical direction is to see if this tool can be used to prove existence of the coupled saturation-humidity system at constant temperature. The forcing term on the right-hand side of each equation is now non-zero. The equations are

$$\frac{\partial S}{\partial t} - \frac{\partial}{\partial x} \left((-D(S) + C_S^l) \frac{\partial S}{\partial x} + C_\varphi^l \frac{\partial \varphi}{\partial x} - K(S) \rho^l g \right) = \hat{e}_l^{g_v}(\varphi, S) \quad (6.12a)$$

$$(1 - S) \frac{\partial \varphi}{\partial t} - \varphi \frac{\partial S}{\partial t} - \frac{\partial}{\partial x} \left(\mathcal{D}(\varphi, S) \frac{\partial \varphi}{\partial x} \right) = -\hat{e}_l^{g_v}(\varphi, S). \quad (6.12b)$$

If we were to define $b(z) : \mathbb{R}^2 \rightarrow \mathbb{R}^2$ as

$$b(z) = \begin{pmatrix} 1 & 0 \\ -z_2(1 - z_1) \end{pmatrix} \begin{pmatrix} z_1 \\ z_2 \end{pmatrix}$$

one can show that there does not exist a function $\Phi : \mathbb{R}^2 \rightarrow \mathbb{R}$ such that $b = \nabla \Phi$. For this reason we restate the equations with a consolidated form of the time derivatives in the second equation

$$\frac{\partial S}{\partial t} - \frac{\partial}{\partial x} \left((-D(S) + C_S^l) \frac{\partial S}{\partial x} + C_\varphi^l \frac{\partial \varphi}{\partial x} - K(S) \rho^l g \right) = \hat{e}_l^{g_v}(\varphi, S) \quad (6.13a)$$

$$\frac{\partial u}{\partial t} - \frac{\partial}{\partial x} \left(\mathcal{D}(\varphi, S) \frac{\partial \varphi}{\partial x} \right) = -\hat{e}_l^{g_v}(\varphi, S) \quad (6.13b)$$

$$u = (1 - S)\varphi \quad (6.13c)$$

Solving for the relative humidity in equation (c) and substituting into equations (a) and (b) gives

$$\frac{\partial S}{\partial t} - \frac{\partial}{\partial x} \left((-D(S) + C_s^l) \frac{\partial S}{\partial x} + C_\varphi \frac{\partial}{\partial x} \left(\frac{u}{1-S} \right) - K(S) \rho^l g \right) = \hat{e}_l^{g_v} \left(\frac{u}{1-S}, S \right) \quad (6.14a)$$

$$\frac{\partial u}{\partial t} - \frac{\partial}{\partial x} \left(\mathcal{D} \left(\frac{u}{1-S}, S \right) \frac{\partial}{\partial x} \left(\frac{u}{1-S} \right) \right) = -\hat{e}_l^{g_v} \left(\frac{u}{1-S}, S \right). \quad (6.14b)$$

It can be seen from this form that the coupling in the time derivatives has been moved to a stronger coupling with the diffusion terms. It can be shown that the associated $a(\cdot, \cdot)$ function is not elliptic in the sense required in Theorem 6.2. Therefore we have determined that the Alt and Luckhaus theorems don't apply to the coupled system in this form.

Equations (6.14) poses the system in a form of strong coupling known as a *triangular system*. A triangular parabolic system has two equations; one parabolic equation with a contribution to diffusion from both dependent variables and the other with a contribution to diffusion from only one variable [52]. Future research into the existence and uniqueness results will likely start here as the theory of triangular systems is fairly well developed and may provide a springboard to results for this problem.

6.3 Heat Transport Equation

In this section we consider the question of existence and uniqueness for the heat transport equation. This is done under the assumptions that the relative humidity and saturation profiles are fixed in space and time.

If the saturation and the relative humidity are considered fixed and constant then the thermal transport equation (5.88c) collapses to

$$\rho c_p \frac{\partial T}{\partial t} - \nabla \cdot (K \nabla T) + \rho h + \chi_2 \nabla T \cdot \nabla T = 0, \quad (6.15)$$

where χ_2 is given as

$$\chi_2 = \rho^l c_p^l C_T^l K(S) + \rho^g c_p^g N(S, T).$$

In the absence of heat sources and if χ_2 is neglected we arrive at the standard heat equation; the existence and uniqueness results of which are well known (see any standard text on PDEs). It is likely that $C_T^l \approx 0$ since, in Saito [66], the authors indicated that the thermal liquid flux is negligible as compared to isothermal liquid flux. The entropy term appearing in N , on the other hand, is likely non-negligible and therefore must be considered. In the case where S and φ are fixed but non-constant, the terms in equation (5.88c) associated with ∇S and $\nabla \varphi$ are combined as a source term which depends on x, t , and T . Therefore, we only need to consider thermal equations in the form of (6.15). If $h = 0$ and Dirichlet boundary conditions are considered then this is the exact form of the equation considered by Rincon et al. in [65]:

$$\frac{\partial u}{\partial t} - \nabla \cdot (a(u) \nabla u) + b(u) |\nabla u|^2 = 0 \quad \text{in } \Omega \times (0, T) \quad (6.16a)$$

$$u = 0 \quad \text{on } \partial\Omega \times (0, T) \quad (6.16b)$$

$$u(x, 0) = u_0(x) \quad \text{in } \Omega. \quad (6.16c)$$

where we have defined u such that $u \leftarrow T - T_{ref}$ with reference temperature T_{ref} . Taking $h = 0$ means that we must assume that both S and φ are constant in space and fixed in time. This is not entirely physical, but it is a step toward a general existence uniqueness theory for the present equations. In this problem, $a(u)$ is the diffusion coefficient, $a(u) = K(u)$, defined either by the weighted sum of the thermal conductivities (equation (5.78)) or by the Johansen thermal conductivity function (equation (5.79)). The b function is defined as χ_2 as above.

For the Rincon existence and uniqueness theorem we consider the following hypotheses:

H1: $a(u)$ and $b(u)$ belong to $C^1(\mathbb{R})$ and there are positive constants a_0, a_1 such that

$$a_0 \leq a(u) \leq a_1 \text{ and } b(u)u \geq 0.$$

H2: There is a positive constant $M > 0$ such that

$$\max_s \left\{ \left| \frac{da}{du}(s) \right|, \left| \frac{db}{du}(s) \right| \right\} \leq M.$$

H3: $u_0 \in H_0^1(\Omega) \cap H^2(\Omega)$ such that $\|\Delta u_0\|_{L^2(\Omega)} < \epsilon$ for some constant $\epsilon > 0$.

Theorem 6.6 (Rincon et al. [65], Theorem 2.1) *Under hypotheses H1 - H3 there exists a positive constant ϵ_0 such that if $0 < \epsilon < \epsilon_0$ then the problem (6.16) admits a unique solution satisfying*

i. $u \in L^2(0, T; H_0^2(\Omega) \cap H^2(\Omega))$ and $\partial_t u \in L^2(0, T; H_0^1(\Omega))$

ii. $\frac{\partial u}{\partial t} - \nabla \cdot (a(u)\nabla u) + b(u)|\nabla u|^2 = 0$ in $L^2(\Omega \times (0, T))$

iii. $u(0) = u_0$

Theorem 6.7 *There exists a unique solution to equation (6.15) under the following conditions:*

1. $u(0, t) = u(1, t)$

2. $h = 0$

3. $u(x, 0) = u_0 \in H_0^1(\Omega) \cap H^2(\Omega)$ and there exists $\epsilon > 0$ such that $\|\Delta u_0\|_{L^2(\Omega)} < \epsilon$

Here we are using $u = T - T_{ref}$ for a scaled temperature (so that capital T will represent a finite time as in Theorem 6.6).

Proof: We will proceed by verifying the hypotheses of Theorem 6.6

H1: From the derivation of the heat transport equation, $a(u)$ is a weighted sum of thermal conductivities from the individual phases. The particular form of the weighted sum comes from either equation (5.78) or (5.79), but in this scenario,

the saturation is presumed to be constant. Therefore, in this case $a(u)$ is constant and is trivially $C^1(\Omega)$. The functional form of b depends on the functional form of the entropy and the saturation. So long as the saturation is fixed away from zero then b is in $C^1(\Omega)$. Furthermore, $b(u)$ is positive so $b(u)u$ is also positive for all u .

H2: Since a is a constant, $da/du = 0$ for all u . The functional form of b , on the other hand, is not constant so this hypothesis simply states that χ_2 needs to have a bounded first derivative. Taking the entropy term from the Darcy flux as

$$\eta^g = c_p^g \ln \left(\frac{T}{T_{ref}} \right) + \eta_{ref},$$

(from the definition of the specific heat) and defining χ_2 accordingly we see that b will have a bounded first derivative so long as $u + T_{ref} = T$ remains bounded away from 0. This is, of course, always true since T is the absolute temperature.

H3: The third assumption of the theorem satisfies this hypothesis.

Therefore, there exists a unique solution to (6.15) with no sources and equal Dirichlet boundary conditions. ■

6.4 Conclusion

At this point we turn our attention to the analysis and comparisons of numerical solutions of the equations (both individually and coupled). The existence and uniqueness theory presented here is by no means complete. In particular, we are missing a uniqueness result for the vapor diffusion equation, the theorem used for the heat transport equation is very limiting with respect to boundary conditions and sources, and we have not mentioned results for any of the coupled systems. Many numerical solvers will iterate coupled systems across the equations, so an existence and uniqueness theory for each equation is essential to give hope that the numerical method converges to *the* solution. These results are left for future work as the ultimate crux

of this thesis is to justify the modeling technique against physical experimentation and classical models.

7. Numerical Analysis and Sensitivity Studies

In this chapter we build and analyze the solution(s) to the heat and moisture transport model summarized in equations (5.88a) - (5.88c) with constitutive equations summarized in equations (5.89a) - (5.89r). To simplify matters we henceforth assume a 1-dimensional geometry modeling a column experiment common to soil science. Figure 7.1 gives a cartoon drawing of a typical column experiment with a definition of the geometric variable x . The grains represent a packed porous medium. Flow, diffusion, and heat transport are assumed to travel solely in the x direction (up or down).

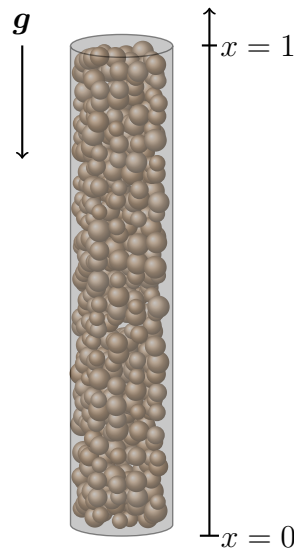


Figure 7.1: Cartoon of a 1-dimensional packed column experimental apparatus.

In this chapter we are interested in the behavior of equations (5.88) in several situations related to the apparatus depicted in Figure 7.1; some physical and some merely hypothetical.

1. In a **drainage experiment** the column is saturated with the wetting phase and then allowed to drain under the influence of gravity.

Possible simplifying assumptions include: constant relative humidity and temperature.

2. In an **imbibition experiment** the column starts partially saturated (or dry) and the wetting phase is introduced either at $x = 1$ or $x = 0$. If the wetting phase is introduced at $x = 1$ then the primary force driving the liquid flow will be gravity, and if it is introduced at $x = 0$ then the pressure head from the reservoir drives the flow.

Possible simplifying assumptions include: constant relative humidity and temperature.

3. In **evaporation studies**, a gradient in relative humidity is introduced between $x = 0$ and $x = 1$ and relative humidity is tracked throughout the column.

Possible simplifying assumptions include: constant temperature and/or fixed saturation profile.

4. In **Coupled saturation and evaporation experiments** the saturation and relative humidity are tracked throughout the column under boundary conditions that drive both.

Possible simplifying assumptions include: constant (or at least fixed) temperature.

5. In **fully coupled** systems we consider a heat source (typically located at $x = 1$) and boundary conditions that drive all three equations.

In Chapter 6 we discussed the questions of existence and uniqueness of solutions to equations (5.88). We now turn to numerical analysis. In Sections 7.1, 7.2, and 7.3 we discuss various numerical solutions associated with the situations outlined above. For example, in Section 7.1, we examine numerical solutions associated with drainage and imbibition experiments (types 1 and 2 above). In Section 7.4 we compare with a 1-dimensional column experiment outlined in Smits et al. [75]. No two- or three-dimensional experiments are performed in this work.

7.1 Saturation Equation

In this subsection we consider the saturation equation (5.88a) with fixed and constant relative humidity and temperature and no mass transfer. That is, we consider

$$\frac{\partial S}{\partial t} = \frac{\partial}{\partial x} \left(\varepsilon_S^{-1} K(S) \left([-p'_c(S) + C_S^l] \frac{\partial S}{\partial x} + \tau \varepsilon_S \frac{\partial^2 S}{\partial x \partial t} - \rho^l g \right) \right). \quad (7.1)$$

These assumptions are natural in an oil-water system or simply unsaturated systems where the relative humidity is considered fixed experimentally. We would like to determine qualitative behavior of solutions to this equation under certain boundary conditions, experimental setups, van Genuchten parameters, and values (or functional forms) of τ and C_S^l . As a first step toward this analysis let us consider dimensionless spatial and temporal scalings. Notice that the spatial dimension can already be viewed as dimensionless as seen in Figure 7.1. A characteristic time for this equation is $t_c = x_c/k_c = 1/k_c$ where $k_c = (\rho^l g \kappa_s)/\mu_l$ is the hydraulic conductivity. Multiplying by t_c and henceforth understanding t and x as dimensionless we get

$$\begin{aligned} \frac{\partial S}{\partial t} &= \frac{\partial}{\partial x} \left(t_c \varepsilon_S^{-1} K(S) [-p'_c(S) + C_S^l] \frac{\partial S}{\partial x} \right) \\ &\quad + \frac{\partial}{\partial x} \left(\tau K(S) \frac{\partial^2 S}{\partial x \partial t} \right) - \frac{\partial}{\partial x} (t_c K(S) \varepsilon_S^{-1} \rho^l g). \end{aligned} \quad (7.2)$$

In the case where $\tau = 0$, the qualitative behavior can be analyzed via the Péclet number; the ratio of the advective to diffusive coefficients

$$Pe = \frac{\rho^l g}{-p'_c(S) + C_S^l} = \frac{\rho^l g}{\left(\frac{\rho^l g (1-m)}{\alpha m} \right) S^{-(1+1/m)} (S^{-1/m} - 1)^{-m} + C_S^l}. \quad (7.3)$$

Since the diffusive coefficient depends on the dependent variable it is immediately clear that the Péclet number will change in time and space (in the study of linear PDEs the Péclet number is a fixed ratio that does not depend on the dependent variable). If $Pe < 1$ then the problem is *diffusion dominated* whereas if $Pe > 1$ then the problem is *advection dominated*. In a diffusion dominated problem we expect a smooth solution that spreads spatially in time, and in an advection dominated problem we expect more advection (transport) than smoothing. In quasilinear advection diffusion equations

(see a standard PDE text discussing the method of characteristics (e.g. [87, 34]), if the diffusion term is not significantly weighted then the advective term may yield shock-type solutions. For example, if the material parameters for a particular experiment are located in the top right of Figure 7.2 then the diffusive term is weighted very small as compared to the advection and a shock is more likely to develop. That being said, a shock-type solution is non-physical so it is not expected in these experiments. This gives an indication that if a shock does occur then the parameters must be non-physical or the numerical method is not accurately capturing the diffusion.

From the definition of the Péclet number it is clear that the action of C_S^l is to increase the damping of the diffusion term. Given the form of the Péclet number, it stands to reason that damping similar to that of C_S^l can be achieved by choosing different van Genuchten parameters. For this reason we presume for the remainder of this work that the effects of C_S^l are inseparably tied up with the effects of the $p_c - S$ relationship. Hence we can assume that $C_S^l \approx 0$. Recall that C_S^l is defined (see equation (5.45)) as

$$C_S^l = \pi^{l(v)} - \pi^{l(g)} = 2 \frac{\partial \psi^l}{\partial S}$$

and is interpreted as a wetting potential.

With the assumption that $C_S^l \approx 0$ (or is at least inseparable experimentally from $p'_c(S)$), the Péclet number becomes

$$Pe = \left(\frac{\alpha m}{1 - m} \right) S^{(1+1/m)} (S^{-1/m} - 1)^m.$$

The van Genuchten parameters, α and m , are independent in this form of the Péclet number. Furthermore, the van Genuchten capillary pressure - saturation function is only one of several choices for this relationship. Other common forms are the Brooks-Corey and Fayer-Simmons models; each of which will have their own associated Péclet number. Figure 7.2 shows the nature of the Péclet number as a function of these parameters as well as the saturation.

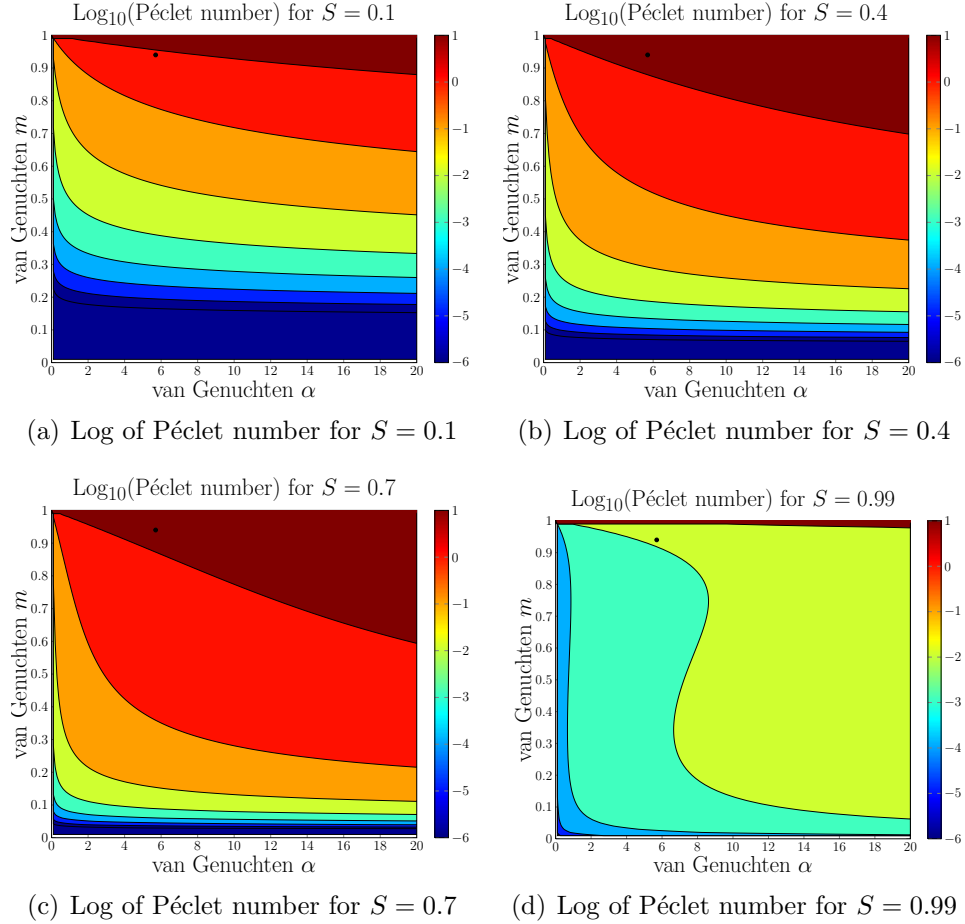


Figure 7.2: Log of Péclet numbers for various values of saturation. The point at $(\alpha = 5.7, m = 0.94)$ indicates the values used in Smits et al. [75]. Warmer colors are associated with higher Péclet number and therefore associated with an advective solution.

In Figure 7.2 it appears that the solutions to the saturation equation (with $\tau = 0$) become more diffusion dominated for smaller values of van Genuchten parameters. As $S \rightarrow 1$ the diffusion term gains more traction and hence dampens the advection. Of course, one cannot simply choose a set of van Genuchten parameters. Instead, the parameters are dictated by the material properties of the soil. In the study by Smits et al. [75], $\alpha = 5.7$ and $m \approx 0.94$ (indicated by the point in Figure 7.2). In this instance, we expect an advection dominated solution with very little diffusive damping. This poses a danger numerically as it is close to the regime where shock-type solutions

could arise.

The third-order term can be analyzed in a similar manner. To the author's knowledge there is no *name* for the ratio of the coefficients of the third-order term to the diffusive term

$$\begin{aligned}
 H &:= \frac{\tau \varepsilon_S}{-t_c p'_c(S)} = \frac{\tau \varepsilon_S \rho^l g \kappa_s}{-p'_c(S) \mu_l} \\
 &= \left(\frac{\tau \varepsilon_S \kappa_S}{\mu_l} \right) \left(\frac{\alpha m}{1 - m} \right) S^{(1+1/m)} (S^{-1/m} - 1)^m \\
 &= \left(\frac{\tau \varepsilon_S \kappa_S}{\mu_l} \right) Pe := H_0 Pe
 \end{aligned} \tag{7.4}$$

Thus the plots in Figure 7.2 are simply scaled versions of H . The question that remains is what effect the third-order term has on the solution. To answer this questions we examine a few solution plots. These solutions are found using `Mathematica`'s `NDSolve` function. This build-in command is a general differential equation solver handling ordinary and partial differential equations, systems of equations, vector equations, and stiff systems. For partial differential equations it uses a finite difference approach to discretize the spatial variable and a version of Gear's method for implicit stiff time stepping following a method-of-lines approach [86].

Figure 7.3 shows a drainage experiment for various values of $H_0 = (\tau \varepsilon_S \kappa_S) / \mu_l$. The initial condition is given in black. A Dirichlet boundary condition ($S = S_0$) is given at $x = 1$ and a homogeneous Neumann condition ($\partial S / \partial x|_{x=0} = 0$) is imposed at $x = 0$. Gravity points in the negative x direction, so that the liquid present in the column is expected to drain over time. Figure 7.3(a) shows that at earlier times a larger value of H_0 gives a steeper front with plausibly physical saturation profiles. Non-physical, non-monotonic, results are observed for $H_0 = 10^{-2}$ as seen near $x = 0.8$ in Figures 7.3(b) - 7.3(d). For values of H_0 smaller than 10^{-2} we continue to observe a sharper front as compared to solutions for $\tau = 0$ (shown in blue).

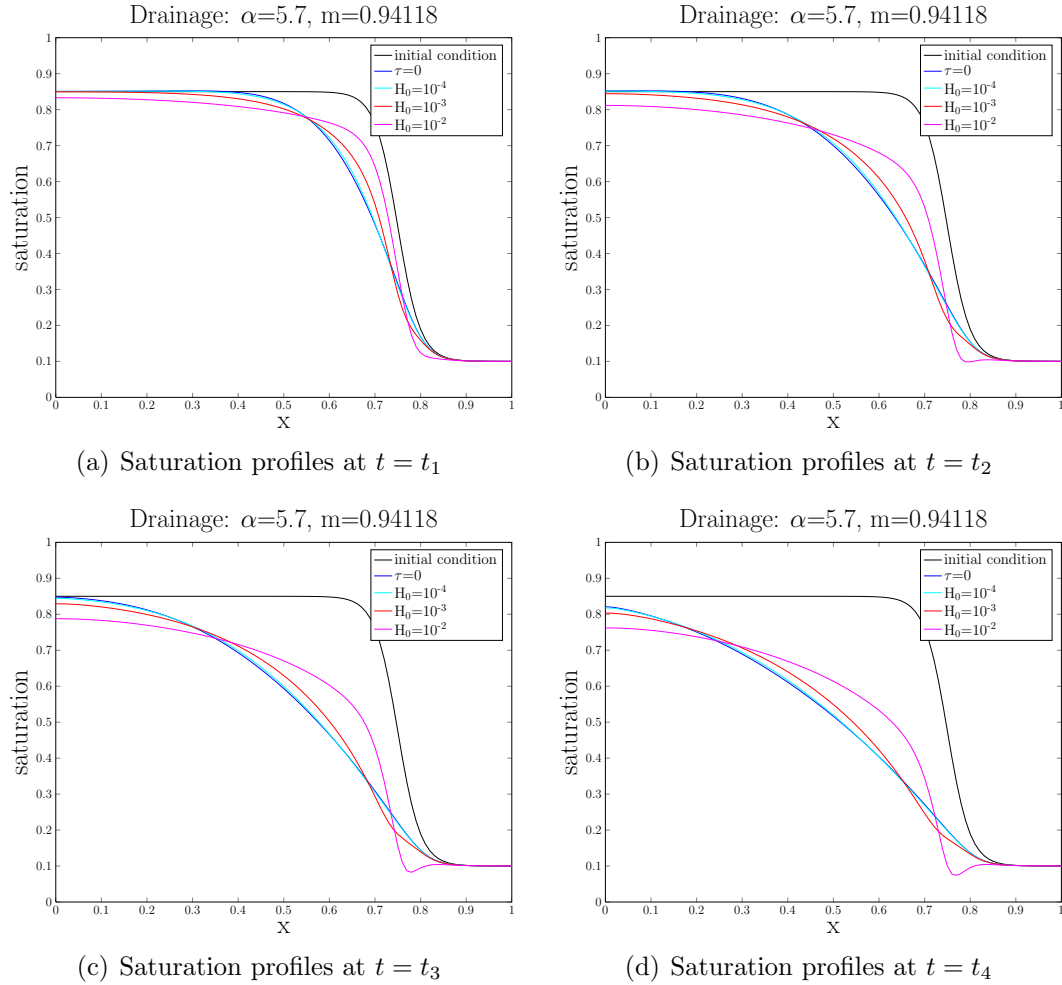


Figure 7.3: Saturation profiles at various times in a drainage experiment with $\alpha = 5.7$, $n = 17$.

To be sure that the non-physical results observed for $H_0 = 10^{-2}$ are not due to numerical noise we complete a numerical convergence test on this particular set of initial boundary conditions. A typical convergence test of a numerical method would compare against a known analytic solution, but in this case there is no known analytic solution. For this reason, we allow `Mathematica` to solve the problem using the default spatial and temporal tolerances and then compare solutions with fixed grids consisting of fewer mesh points to this solution. `Mathematica`'s differential equation solver uses a finite difference approach for spatial discretization. The defaults for this scheme are fourth-order central differences where spatial points are on a static grid and the

number of grid points is chosen automatically based on the initial condition. For the tests shown in Figure 7.3 there were 103 grid points selected automatically. To check this solution, we examine the relative $L^2(0, 1)$ error as a function of time,

$$E_{(N)}(t) = \frac{\|S_{(k)} - S_{(103)}\|_{L^2}}{\|S_{(103)}\|_{L^2}},$$

where N is the number of spatial points. In Figure 7.4 we measure $E_{(N)}(t)$ for N ranging from 20 spatial points to 100 spatial points. Notice that for any fixed *small* time the relative error decreases with increasing grid size; hence indicating numerical convergence at that fixed time. For dimensionless time greater than approximately 0.05, on the other hand, the error decreases at a slower rate and there is evidence that the numerical method may not be converging. In all cases the relative error grows in time until approximately 0.25. While the *bump* that appears in Figure 7.3 is certainly non-physical, Figure 7.4 seems to indicate that the numerical method is failing in this case and the results may not be trust-worthy for this set of parameters and initial boundary conditions.

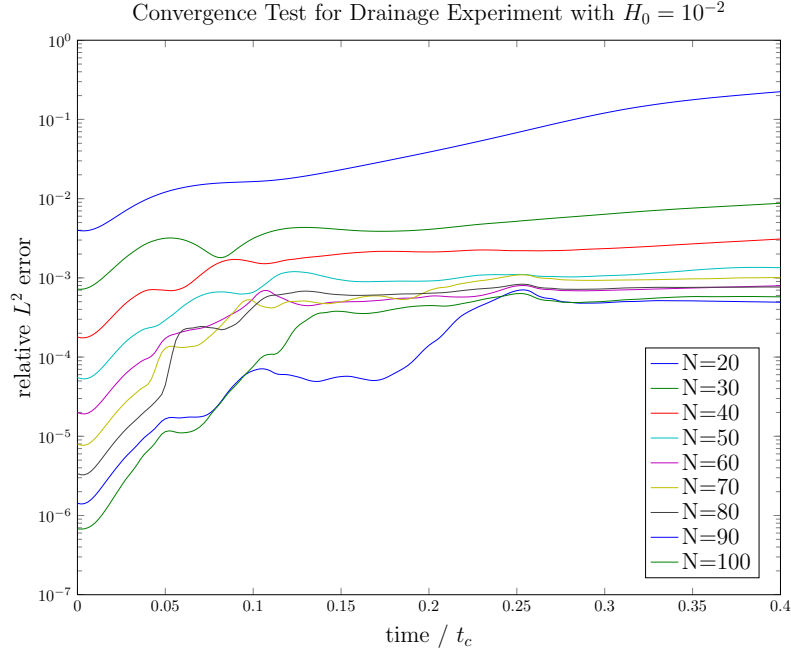


Figure 7.4: Convergence test for drainage experiment depicted in Figure 7.3. N is the number of spatial grid points. In Figure 7.3, $t_1 = 0.025t_c$, $t_2 = 0.050t_c$, $t_3 = 0.075t_c$, and $t_4 = 0.10t_c$

Figure 7.5 shows an imbibition experiment for various value of H_0 . As before, the initial condition is shown in black. For this experiment, Dirichlet boundary conditions are enforced at both $x = 0$ and $x = 1$. Gravity points in the negative x direction, and the boundary condition at $x = 1$ indicates that wetting fluid is being added over time. For $H_0 = 10^{-4}$ and $H_0 = 10^{-3}$ we see plausibly physical results and we see sharper wetting fronts as in the drainage experiment. For $H_0 \geq 10^{-2}$ we almost immediately see a non-physical non-monotonicity appear at the top edge of the wetting front. Similar behavior was observed by Peszynská and Yi [59] for their numerical scheme, and they stated

“... we cannot speculate whether the apparent nonmonotonicity of profiles ... relates to a numerical instability, or to a physical phenomenon.”

It is reasonable to ask whether this is associated with numerical noise, and Figure 7.6 shows a convergence test similar to that shown with the drainage experiment. From

Figure 7.6 it appears as if the numerical method is converging under mesh refinement for dimensionless time approximately less than 0.1. The non-monotonicity appears in the region where the method should be stable so we tentatively conclude that this effect is not a numerical artifact. Finally, we observe that for $H_0 = 10^{-1}$ the advection term has been overwhelmed by the diffusion and the third-order term and the numerical results are completely non-physical.

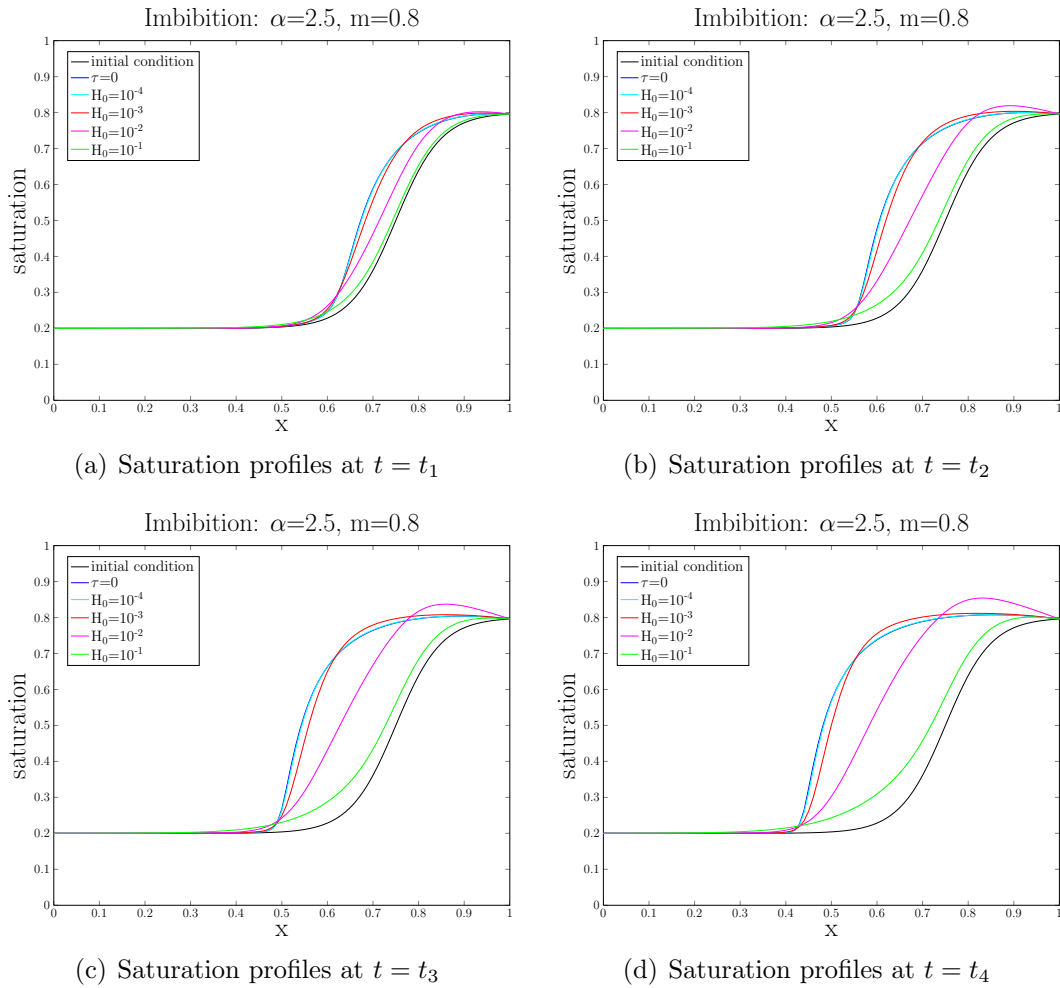


Figure 7.5: Saturation profiles in a imbibition experiment with $\alpha = 2.5, n = 5$.

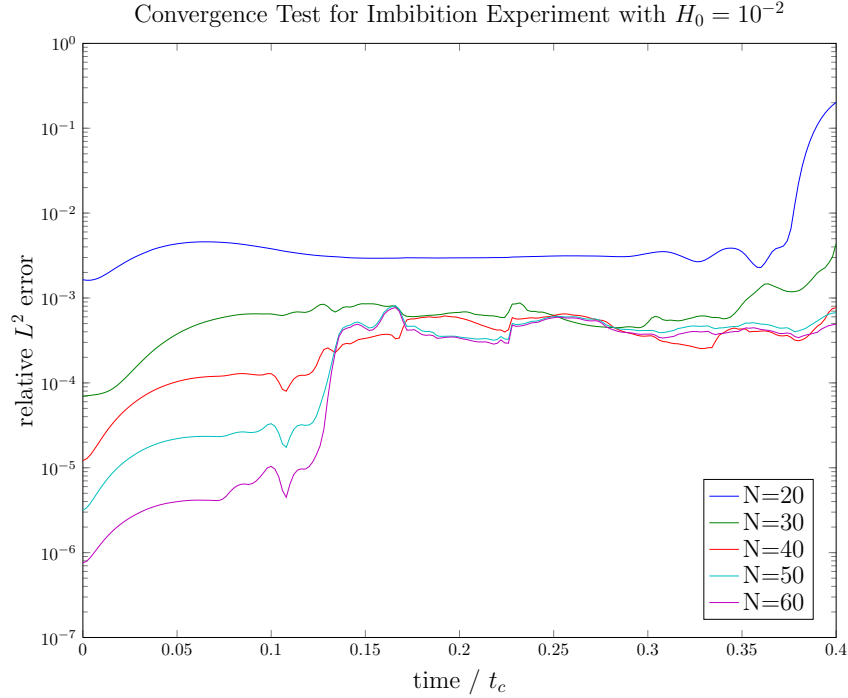


Figure 7.6: Convergence test for imbibition experiment depicted in Figure 7.5. In Figure 7.5, $t_1 = 0.025t_c$, $t_2 = 0.050t_c$, $t_3 = 0.075t_c$, and $t_4 = 0.10t_c$

Clearly there are infinitely many choices of initial boundary conditions, and the results presented herein inherently depend on the conditions chosen. Similar types of non-physical behavior can be observed for other families of van Genuchten parameters, but the associated plots are excluded here for brevity. An empirical conclusion is that for $H_0 = (\tau\varepsilon_S\kappa_S)/\mu_l$ greater than 10^{-3} possibly leads to non-physical behavior in the numerical solution.

To the author’s knowledge, an analysis of parameters of this type has not been completed in the literature. We have shown in this subsection that for reasonably small values of τ we predict sharper fronts than with the traditional Richards’ equation.

7.2 Vapor Diffusion Equation

Next let us consider the vapor diffusion equation under assumptions of fixed constant temperature and a fixed saturation profile. This particular study is a bit peculiar

since it is unlikely that a saturation profile will remain fixed during an evaporation (or condensation) study. Of course, we could consider $S \equiv 0$ everywhere and study only evaporation in dry porous media, but this is also not realistic as enhancement models depend partly on the presence of a liquid phase. In this section we compare the present model proposed in Section 5.4.2 to the classical enhancement model and to Fickian diffusion.

$$(1 - S) \frac{\partial \varphi}{\partial t} = \frac{\partial}{\partial x} \left(\mathcal{D}(\varphi, S) \frac{\partial \varphi}{\partial x} \right) \quad (\text{present model}) \quad (7.5)$$

$$(1 - S) \frac{\partial \varphi}{\partial t} = \frac{\partial}{\partial x} \left(\eta_{(a)}(S) \tau(S) D^g \frac{\partial \varphi}{\partial x} \right) \quad (\text{enhancement model}) \quad (7.6)$$

$$(1 - S) \frac{\partial \varphi}{\partial t} = D^g \frac{\partial^2 \varphi}{\partial x^2} \quad (\text{Fickian diffusion model}). \quad (7.7)$$

Recall that $\eta_{(a)}(S)$ is the empirical *enhancement factor* traditionally used, $\tau(S)$ is the tortuosity, and D^g is the constant Fickian vapor diffusion coefficient (see equations (5.71), (5.73), and obviously (7.7)). The reader should note that we are slightly abusing notation given that η previously stood for intensive entropy and τ is the label for the relaxation term in the saturation equation. This abuse of notation is contained to this section and should not cause confusion.

Qualitatively, the *shape* of the diffusion curve in the $x - \varphi$ plane for the present model is rather different than those of the enhancement and Fickian models. Figure 7.7 gives several snapshots of a sample diffusion experiment with enhancement parameter $a = 25$, van Genuchten parameter $m = 0.9$, and saturated permeability $\kappa_S = 1.04 \times 10^{-10} m^2$. Observe further that the steady state solutions are different for the two models. This is no surprise since the nonlinearities in the diffusion coefficient have different functional forms.

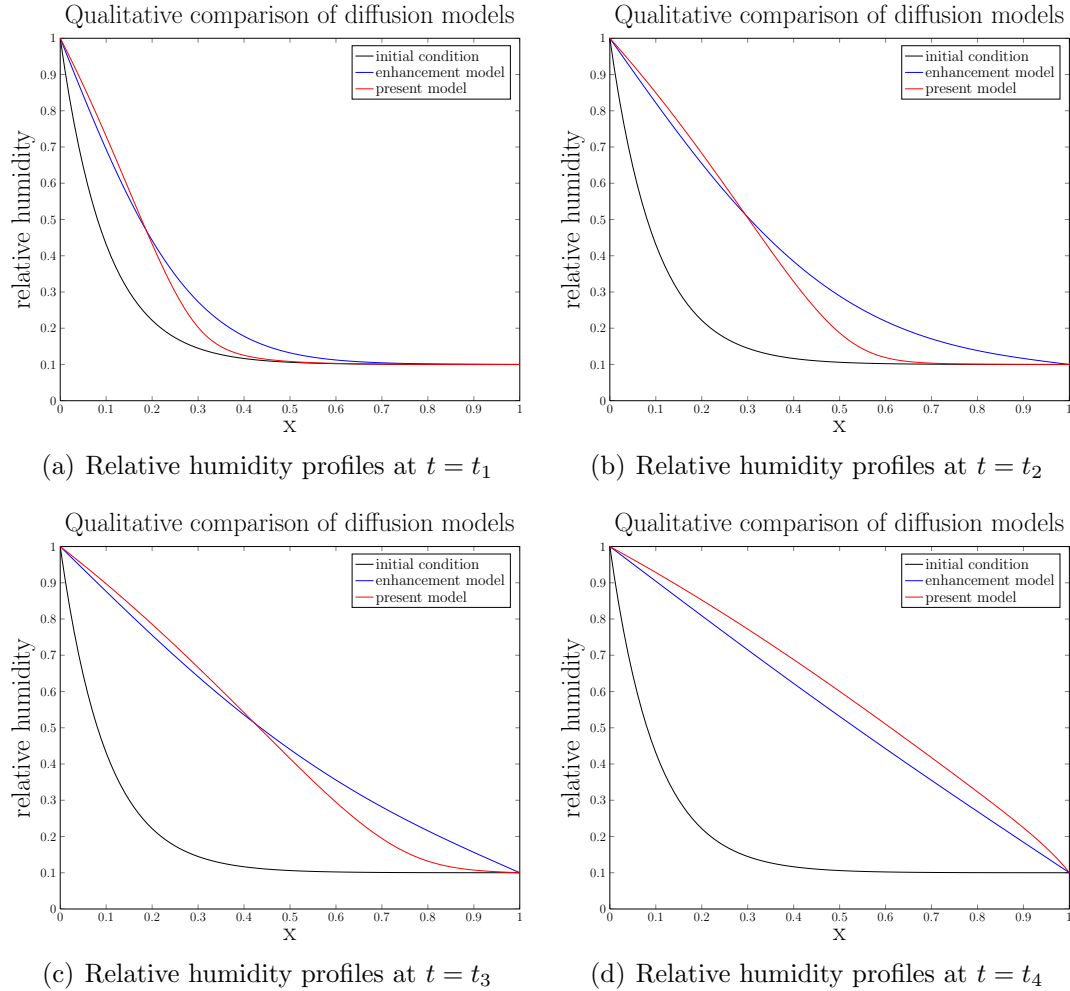


Figure 7.7: Sample diffusion experiment comparing the enhancement model to the present model. Here, $a = 25$, $m = 0.9$ ($n = 10$), and $\kappa = 10^{-10}$ with Dirichlet boundary conditions and an exponential initial profile.

In Figure 5.5 we saw that there is potentially a marked difference between the diffusion coefficient in the present model and the enhancement model. Figures 7.8 and 7.9 show a comparison of the diffusion coefficients for several values of the van Genuchten m parameter and two different saturated permeabilities. The functional dependence of the diffusion coefficient in the present model on the van Genuchten parameter can be readily seen between Figures 7.8(a) and 7.8(d) (similarly, 7.9(a) and 7.9(d)), and the functional dependence on the saturated permeability can be seen between the two sets of figures.

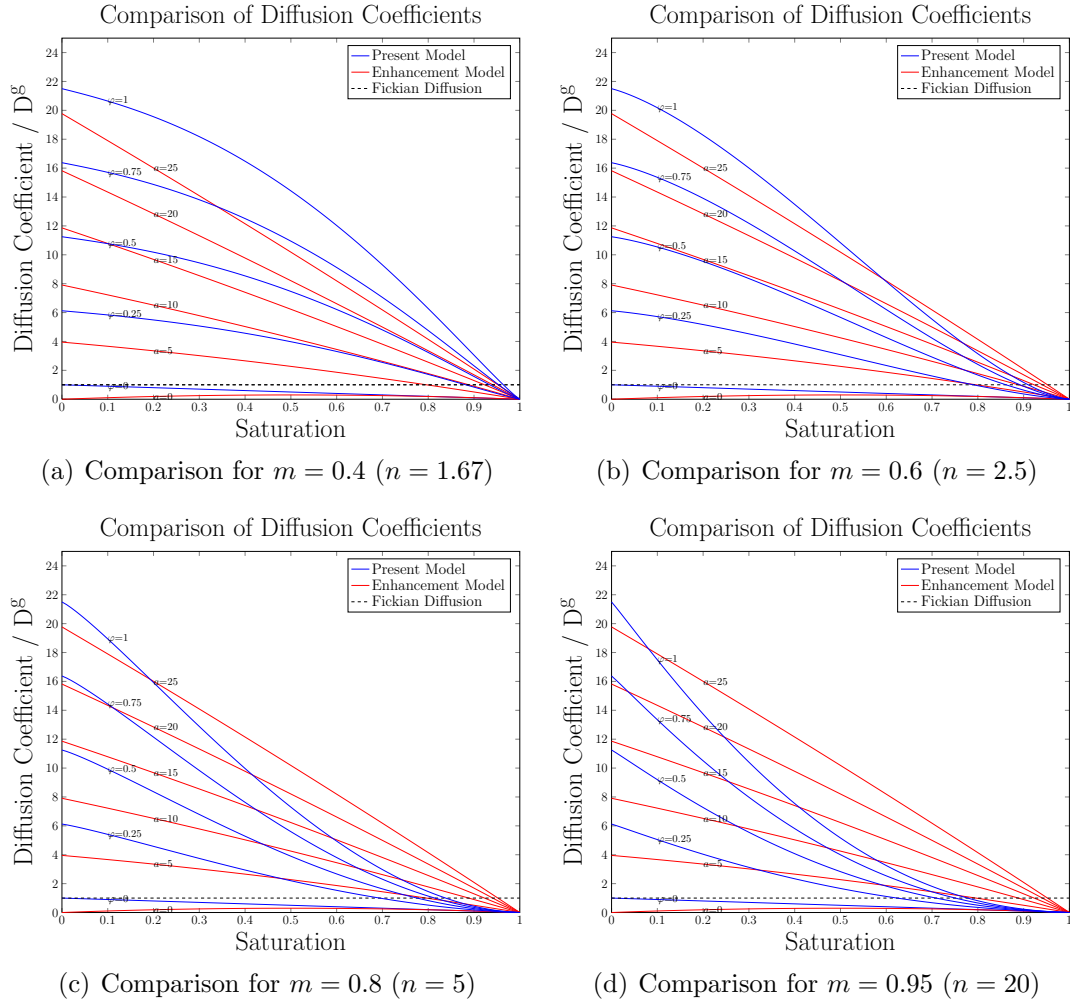


Figure 7.8: Comparison of diffusion coefficients for various van Genuchten parameters all taken with $\kappa_s = 1.04 \times 10^{-10}$ and $\varepsilon = 0.334$ to match the experiment in [75].

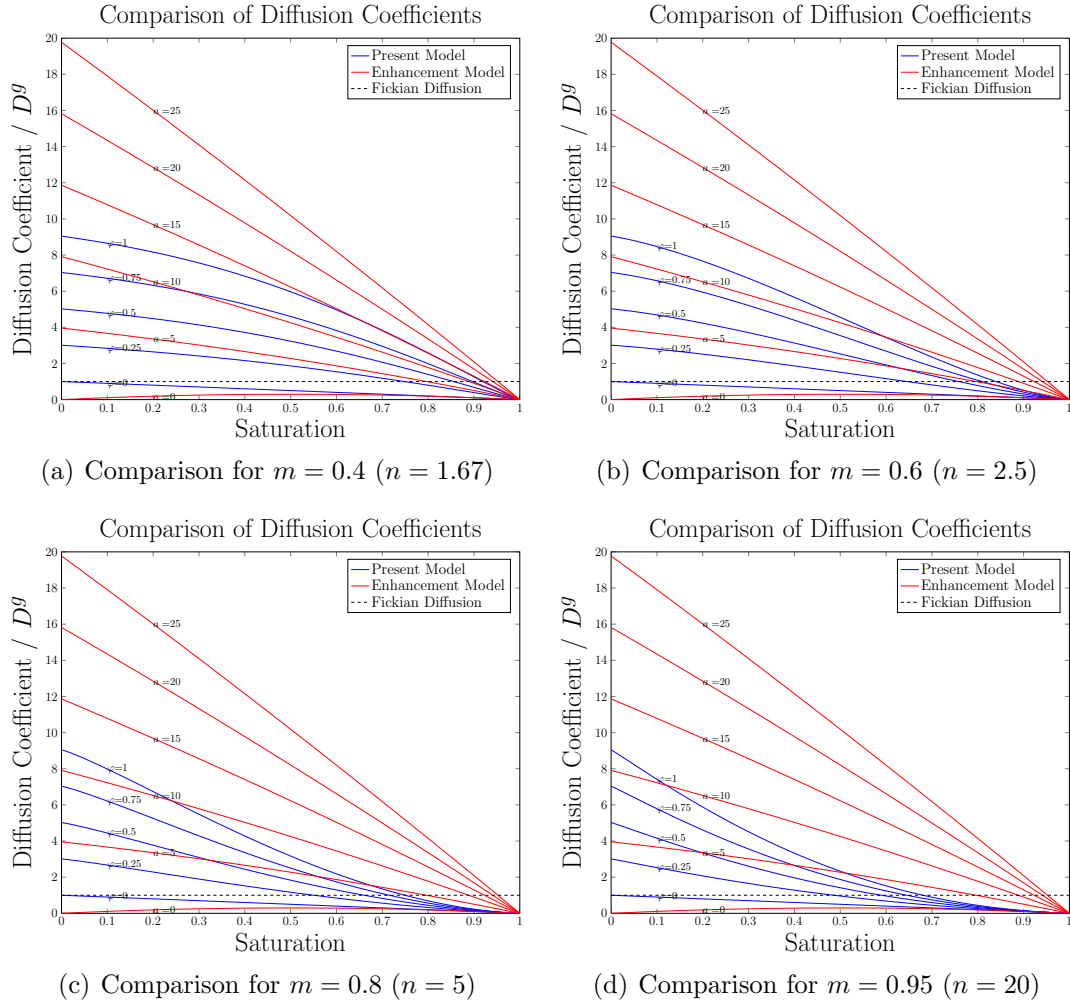


Figure 7.9: Comparison of diffusion coefficients for various van Genuchten parameters all taken with $\kappa_s = 4.0822 \times 10^{-11}$ and $\varepsilon = 0.385$ to match the experiment in [67].

In this thesis we propose that there is a relationship between the fitted a value and the material properties.

Proposition 7.1 *Given the van Genuchten m (or equivalently, n) parameter and the saturated permeability, κ_s , of the soil there is an a-priori estimate of the fitting parameter a .*

The immediate consequence of Proposition 7.1 is that if the fitting parameter can be predicted with the use of experimentation then it is, indeed, unnecessary.

To test Proposition 7.1 we use a simple heuristic approach to match the material coefficients, m and κ_S , to the calculated fitting parameter, a . This is done on the experiments by Smits et al. [75] and Sakai et al. [67]. In Smits et al., $\kappa_S = 1.04 \times 10^{-10}$ [m²] and $m = 0.944$ with a statistically tuned a -value of 18.2. In Sakai et al., $\kappa_S = 4.082 \times 10^{-11}$ [m²] and $m \approx 0.799$ with a -values of 5, 8, and 15 considered. Sakai et al. indicated the best agreement with $a = 8$ while simultaneously considering a modified van Genuchten (Fayer-Simmons) model for the soil water retention curve. We do not consider the Fayer-Simmons model here, but as the Fayer-Simmons model is designed to give better agreement of the capillary pressure - saturation relationship with very low saturations we don't believe this negates our approach.

The heuristic tests of Proposition 7.1 is as follows. The steady-state mass fluxes predicted by the proposed new model and the traditional enhanced diffusion model are

$$\rho_{sat} \mathcal{D}_{(m, \kappa_S)}(\varphi, S) \nabla \varphi \quad \text{and} \quad \rho_{sat} \eta_{(a)}(S) \tau(S) D^g \nabla \varphi.$$

Assuming that the mass fluxes are equal gives the equation

$$\mathcal{D}_{(m, \kappa_S)}(\varphi, S) \nabla \varphi = \eta_{(a)}(S) \tau(S) D^g \nabla \varphi.$$

Making the further assumption that the gradients in relative humidity are the same at steady state then the diffusion coefficients must be equal. If this mass flux is taken at a liquid-gas interface we can assume that $\varphi = 1$. Hence, the left-hand side of this equation is a function of S , m , and κ_s while the right-hand side is a function of S and a

$$\mathcal{D}_{(m, \kappa_S)}(1, S) = \eta_{(a)}(S) \tau(S) D^g.$$

At this point we could proceed by simply choosing a value for S and making comparisons or we could consider the integral over all of S to remove the dependence on the saturation. We choose the latter as it gives a cumulative effect of the diffusion coefficient over the entire range of saturations.

Therefore, for each m and κ_S and for fixed $\varphi = 1$, there is a value of a such that

$$\int_0^1 \mathcal{D}_{(m, \kappa_S)}(1, S) dS = \int_0^1 \eta_{(a)}(S) \tau(S) D^g dS. \quad (7.8)$$

The left-hand side is a function of material parameters and the right-hand side is a function of a . The right-hand side of equation (7.8) integrates easily to a linear function of a

$$\int_0^1 \eta_{(a)}(S) \tau(S) D^g dS = \frac{D^g}{3} \left(a + \frac{1}{1 - \varepsilon} \right).$$

The left-hand side of equation (7.8), on the other hand, isn't readily integrable due to the nonlinear nature of the van Genuchten relative permeability function. For this reason we seek an approximate solution to equation (7.8).

Figure 7.10 shows the left- and right-hand sides of equation (7.8). The intersections indicate the triple (m, κ_S, a) where the equation is true, and hence indicates where the two models have the same cumulative diffusive effect over $S \in [0, 1]$. For example, in Figure 7.10, if $m \approx 0.5$ and $\kappa_s \approx 10^{-10}$ then we predict a fitting parameter of $a \approx 30$.

In Figure 7.10, the blue and green curves are the right-hand sides of equation (7.8) for different saturated permeabilities. The blue curve is included to show the agreement with Smits et al. The green curve is included to show the agreement with Sakai et al. Observe that the experimental values are *close* to the values that make equation (7.8) true (the intersections indicated in the figure). This is to say that given m and κ_S , equation (7.8) could have been used as an a-priori estimate of the value of a in these two experiments. Table 7.1 gives a more concise summary of the results found in Figure 7.10.

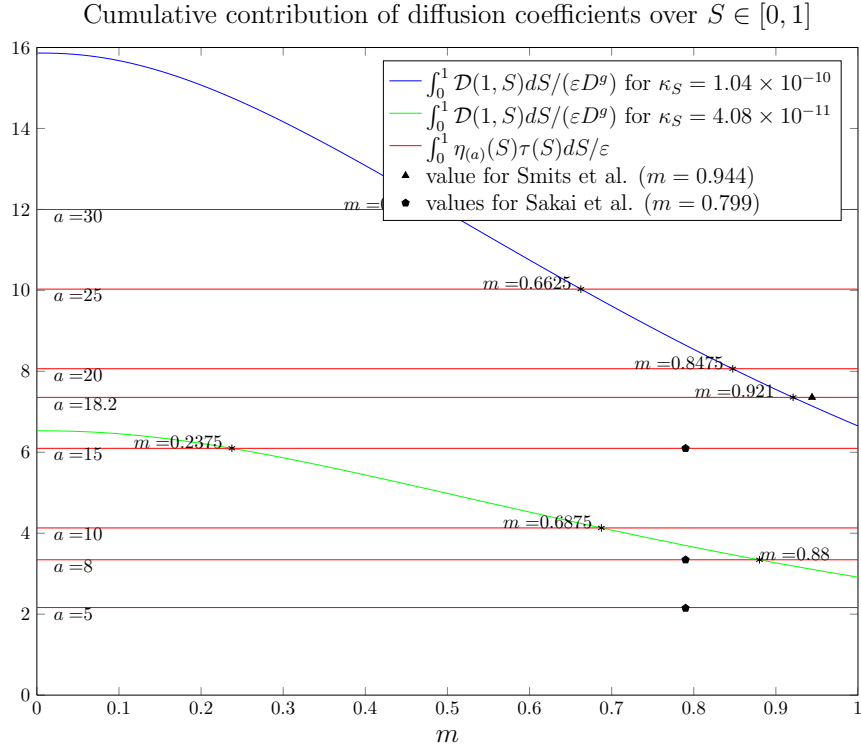


Figure 7.10: The blue and green curves show the left-hand side of equation (7.8) for different saturated permeabilities, and the red lines show level curves for right-hand side for various values of a . The blue and green curves can be used to predict the value of a before experimentation.

Table 7.1: Measured and predicted value of the fitting parameter a based on equation (7.8).

	a measured	a predicted from (7.8)
Smits et al.	18.2	≈ 18
Sakai et al.	8	≈ 9

Comparisons with the experiments of Smits et al. and Sakai et al. indicate that, while not perfect, the present model gives a diffusion equation that matches experimental findings reasonably well without the necessity of an a-posteriori fitting parameter.

7.3 Coupled Saturation and Vapor Diffusion

In this section we couple the saturation and vapor diffusion equations under reasonable boundary conditions. This is done while holding the temperature fixed.

The purpose of this short study is to determine the roles of the mass transfer, $\hat{e}_l^{g_v}$, the $C_\varphi^l \partial\varphi/\partial x$ term appearing in the saturation equation, and the time rate of change of saturation that appears in the vapor diffusion equation. The equations are restated here for reference.

$$\frac{\partial S}{\partial t} - \frac{\partial}{\partial x} \left(\varepsilon_S^{-1} K(S) \left(-p'_c(S) \frac{\partial S}{\partial x} + \tau \varepsilon_S \frac{\partial^2 S}{\partial x \partial t} + C_\varphi^l \frac{\partial \varphi}{\partial x} - \rho^l g \right) \right) = \frac{\hat{e}_l^{g_v}}{\varepsilon_S \rho^l} \quad (7.9a)$$

$$(1 - S) \frac{\partial \varphi}{\partial t} - \varphi \frac{\partial S}{\partial t} - \frac{\partial}{\partial x} \left(\varepsilon_S^{-1} \mathcal{D}(\varphi, S) \frac{\partial \varphi}{\partial x} \right) = \frac{-\hat{e}_l^{g_v}}{\varepsilon_S \rho_{sat}} \quad (7.9b)$$

where

$$\hat{e}_l^{g_v} = M\varphi (\rho^l - \rho_{sat}\varphi) \left(\frac{-p_c + \tau \varepsilon_S \dot{S} - p_0^l}{\rho^l} - R^{g_v} T \ln(\lambda\varphi) \right).$$

This is a system of advection-diffusion-reaction equations with a pseudo-parabolic damping term in saturation (for $\tau \neq 0$) and no advection term in the relative humidity equation. To judge the relative affect of C_φ^l compare the rate of movement of the water through the liquid phase with the rate of movement of water in the gas phase. As such, we consider the ratio of the coefficient of this term to the saturation diffusion

$$\frac{C_\varphi^l}{-p'_c} = \left(\frac{C_\varphi^l}{\rho^l g} \right) Pe = \left(\frac{C_\varphi^l \alpha m}{\rho^l g (1 - m)} \right) S^{1+1/m} (S^{-1/m} - 1)^m. \quad (7.10)$$

In the (unlikely) case that ratio (7.10) is approximately 1 then the diffusion in relative humidity has equal effect as the diffusion in saturation in controlling the transient nature of the saturation. This does not fit with our physical experience so we conjecture that the ratio is much smaller. Figures 7.11 show time snapshots of an imbibition experiment with simultaneous vapor diffusion and (temperature independent) evaporation. Both saturation and relative humidity are controlled with fixed Dirichlet boundary conditions and initial profiles consistent with imbibition into a low saturation column.

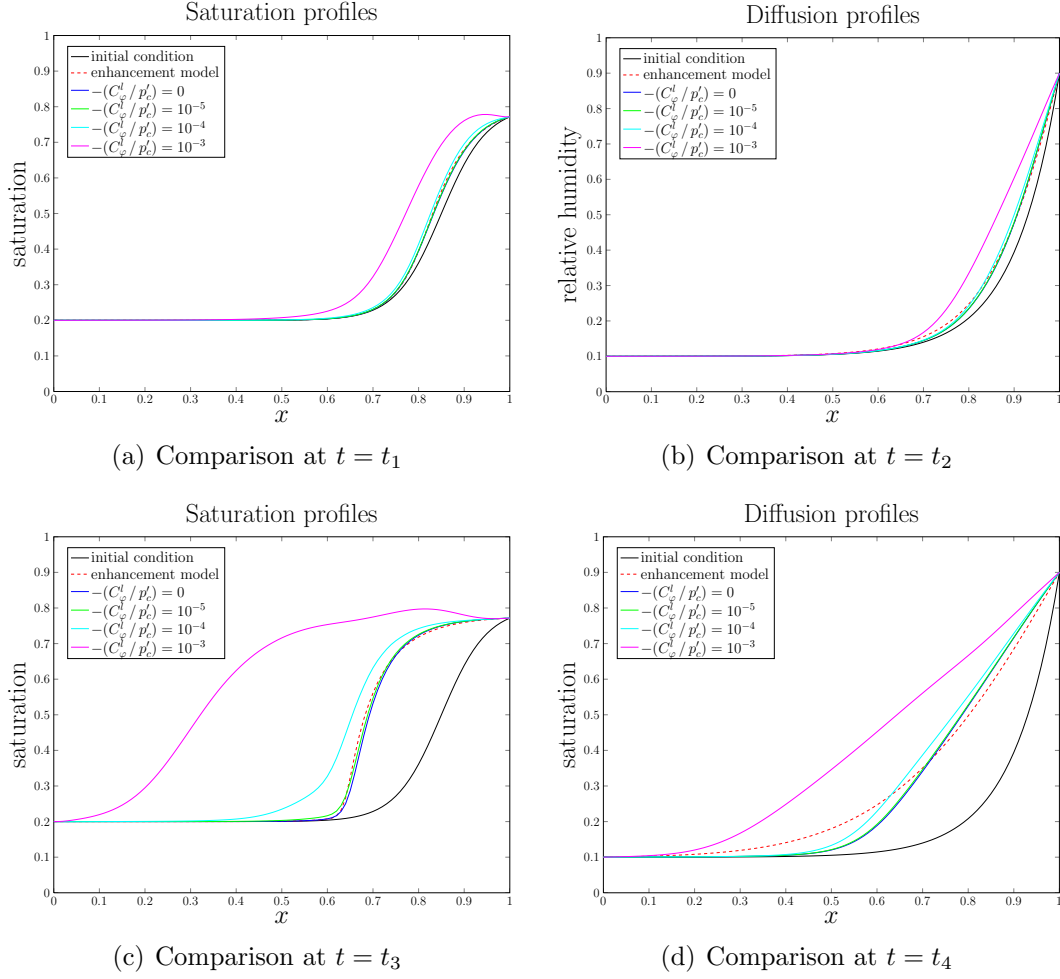


Figure 7.11: Comparison of coupled saturation-diffusion models for various weights of C_φ^l with parameters: $\kappa_s = 1.04 \times 10^{-10}$, $\varepsilon = 0.334$, $H_0 = 10^{-3}$, $\alpha = 4$, and $m = 0.667$.

From Figures 7.11, if ratio (7.10) is greater than or equal to 10^{-3} then non-physical results are observed for this particular set of initial boundary conditions. As there are infinitely many sets of initial boundary conditions we only present this one particular case as a proof of concept. In general we observe that this ratio must be kept below 10^{-3} . With a ratio this small we are simply saying that the enhancement in saturation seen due to increased levels of relative humidity have a small affect as compared to gradients in capillary pressure in the case of fixed temperature.

7.4 Coupled Heat and Moisture Transport System

In this final section we examine the fully coupled system of saturation, vapor diffusion, and heat transfer. The culminating goal of this section is to compare the numerical solution of the present model with the experimental results associated with [75]. Dr. Smits was generous enough to share the experimental results for this comparison. In Section 7.4.1, the physical apparatus is discussed as well as material parameters and initial boundary conditions. In Section 7.4.2 the full system is solved numerically and compared to the experimental data.

7.4.1 Experimental Setup, Material Parameters, and IBCs

The experiment of interest is to track temperature, relative humidity, and saturation in a column of packed sand. Soil moisture, relative humidity, and temperature sensors were placed throughout a 111cm column of packed sand. A heat source was turned on and off above the surface of the soil (to simulate natural temperature cycles). The goal of Smits et al. was to determine whether the equilibrium assumption between phases was valid in porous media evaporation studies. For the our purposes we use this data simply as a validation of the present modeling effort.

A schematic of the experimental apparatus used in Smits et al. [75] is shown in Figure 7.12 (recreated from Dr. Smits’ notes). Saturation and temperature sensors #1 - #10, are placed every 10cm from the bottom. Saturation and temperature sensor #11 is 1cm under the surface of the sand. Sensor #12 is 10cm above the surface. Sensor #13 is on the surface (“in good contact”). Temperature sensors #14 and #15 are placed within the insulation surrounding the apparatus (to measure the lateral heat loss (see the top view in Figure 7.12)). Relative humidity sensor #1 is 1cm under the surface, and sensor #2 is on the surface. The gray shaded area in Figure 7.12 represents the location of the soil pack. The initial water level is the surface of the soil pack. The spatial variable to be used numerically is $x \in [0, 1]$ where $x = 0$ represents the cool end of the apparatus and where $x = 1$ represents the surface of the soil 111cm above the cool end. The material properties used in this experiment

are shown in Table 7.2.

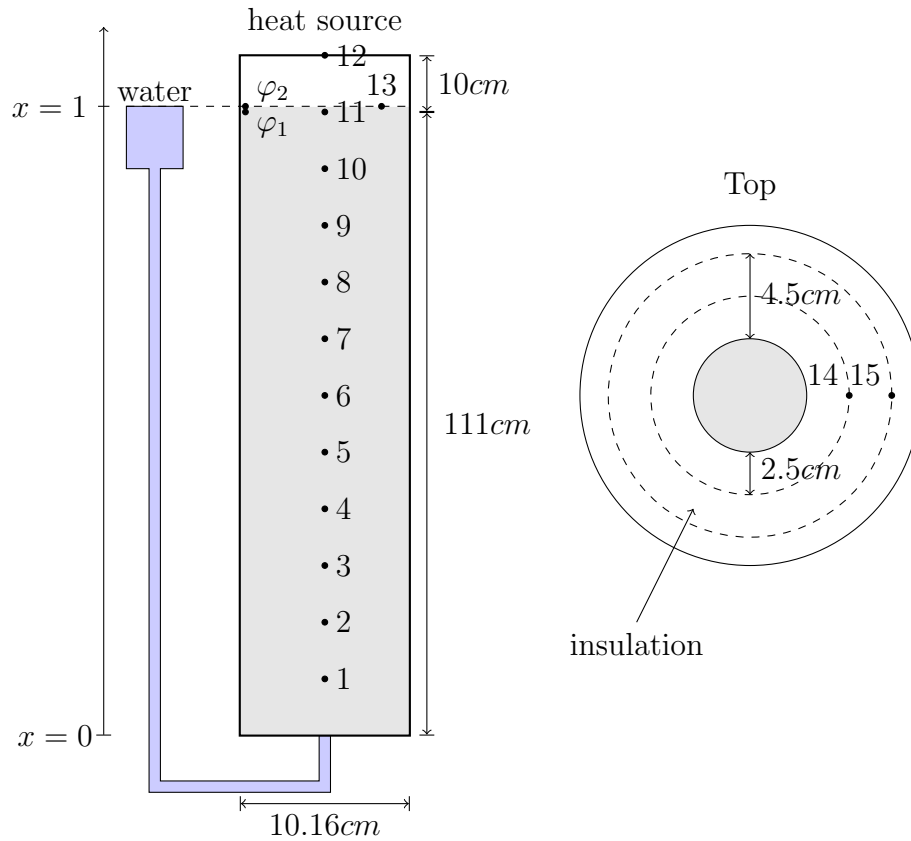


Figure 7.12: Schematic of the Smits et al. experimental apparatus. Saturation and temperature sensors numbered 1 - 11, temperature sensors 12 - 15, and relative humidity sensors 1 and 2 [75]. The geometric x coordinate is shown on the left. (Image recreated with permission from [75])

The experiment was run for 32 days, at which point there was a power outage and the experiment was stopped. In the midst of the experiment there were two sensors that failed: saturation sensor #3 (after the 1847th measurement ($t > 12.8$ days)), and relative humidity sensor #1 (after the 2155th measurement ($t > 14.9$ days)) (see Figure 7.13). The saturation sensors are accurate to within $\pm 2\%$ soil moisture content after soil calibration (performed by Smits et al.). The relative humidity sensor accuracy ranges between $\pm 2\%$ (for mid-range temperatures and humidities) and $\pm 12\%$ (for extreme temperatures and humidities). The temperature sensors are accurate to within 0.5°C for the temperature ranges of interest (www.decagon.com).

Table 7.2: Material parameters for experimental setup [75].

Parameter	Value	Units
Sand Number	30/40	[-]
Dry Bulk Density	1.77	[g cm ⁻³]
Porosity	0.318	[-]
Residual Water Content	0.028	[-]
Saturated Hydraulic Conductivity	0.104	[cm s ⁻¹]
van Genuchten α	5.7	[m ⁻¹]
van Genuchten n ($m = 1 - 1/n$)	17.8 (0.9438)	[-]

The initial and boundary conditions for the forthcoming numerical experiments can be taken from any point within the data set. The logical initial point for the numerical experiment is the beginning of the physical experiment. This particular point is of interest to the experimentalist as some of the interesting transient behavior occurs during this period. That being said, there is a significant amount of sensor noise in the initial phases of the experiment (see Figure 7.14(a)), and if a simple *proof of concept* is all that is needed for the purposes of this work, then a later time is preferred so as to avoid complications related to this noise.

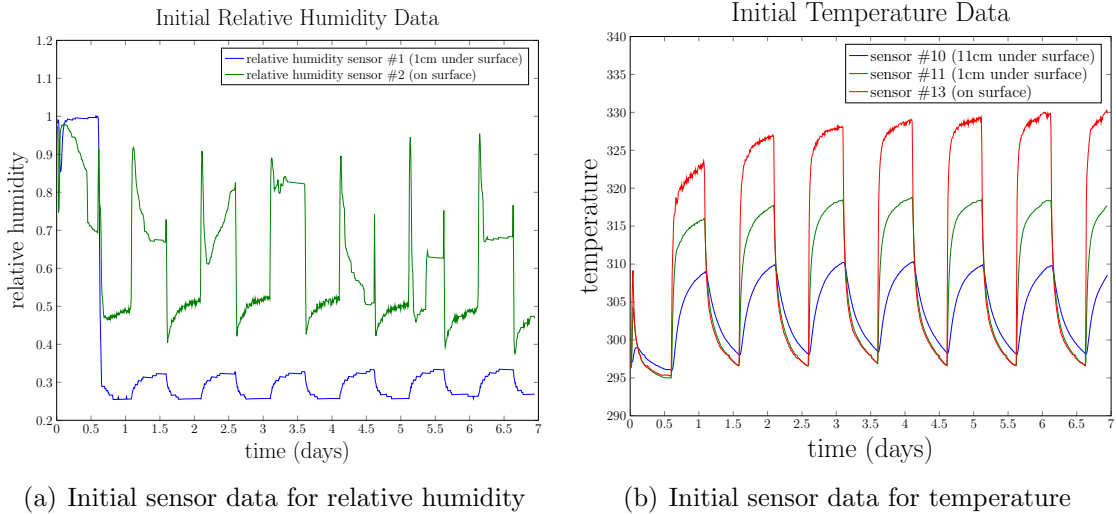


Figure 7.14: Relative humidity and temperature data showing measurement variations in the first few days of the experiment. (Image recreated with permission from [75])

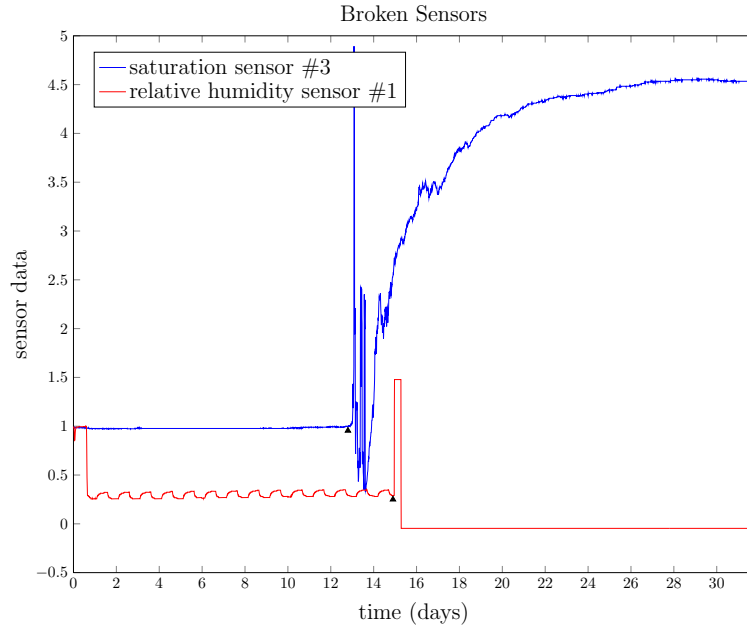


Figure 7.13: Broken sensor data. Saturation sensor #3 shown in blue and relative humidity sensor #1 shown in red. It is evident from these plots that these sensors are not working properly as they give non-physical readings. (Image recreated with permission from [75])

The section of data where we will initially focus is between time measurements 1800 (12.5 days) and 2150 (14.9 days). This section of data is chosen since, qualitatively, it shows the least amount of sensor noise in both relative humidity and temperature. Saturation sensor #3 is faulty in this time region, but the adjacent sensors indicate that there is little to no deviation from full saturation for these times. The relative humidity and temperature data for this time region are shown in Figure 7.15.

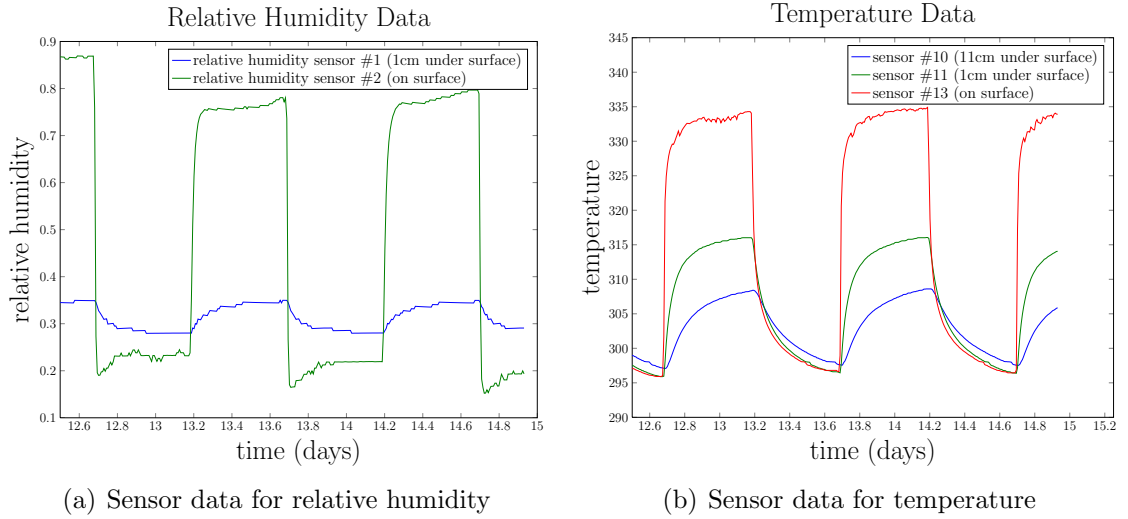


Figure 7.15: Relative humidity and temperature data at a window beginning roughly 12.5 days into the experiment. This window is chosen since the sensor noise is qualitatively minimal in this region. (Image recreated with permission from [75])

The peaks and valleys of the temperature and relative humidity data (associated with the on-off cycle of the heat lamp) have small variations that are likely due to sensor noise. To avoid modeling this noise directly we can approximate the data with either a simple sinusoidal function or a square wave approximation (found by applying the `sign` function to the sinusoidal approximation). The data suggests a square wave approximation, but the jumps in data may cause numerical difficulties as the derivatives at the points of discontinuity are technically delta functionals. A graphic of these approximations is shown in Figure 7.16.

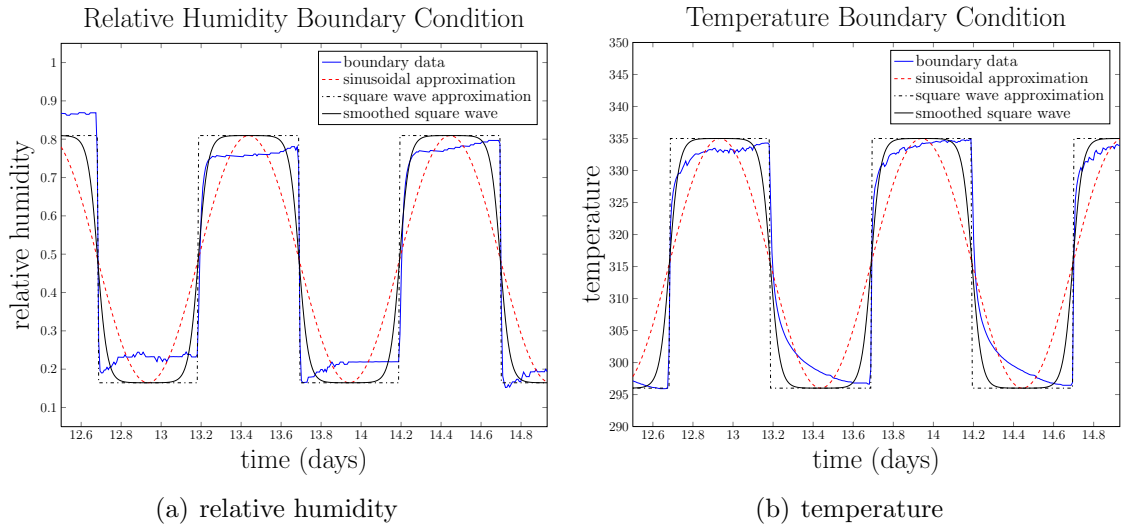


Figure 7.16: Approximations to relative humidity and temperature boundary conditions at the surface of the soil.

Any starting point can be taken within this window of time. We choose the 2000th time step as the initial condition (somewhat arbitrarily) and fit functions to the coarse spatial data for saturation, relative humidity, and temperature. For the relative humidity and saturation profiles we choose hyperbolic tangent functions since they exhibit the primary features observed in the data (see Figures 7.17(a) and 7.17(b) respectively). For the temperature initial condition we choose an exponential function (see Figure 7.17(c)).

To summarize, thus far we have boundary conditions for relative humidity and temperature at $x = 1$ and we have initial conditions for all of the variables. The boundary conditions at $x = 0$ are much simpler. For saturation and relative humidity we can take $S(x = 0, t) = 1$ and $\varphi(x = 0, t) = 1$ based on the fact that the saturation is fixed mechanically at 100% at the bottom end of the apparatus. For the temperature we can either take $T(x = 0, t) = T_0$ or $\partial T/\partial x(x = 0, t) = 0$. The Dirichlet condition simply states that the temperature is fixed, and the Neumann condition states that the bottom of the apparatus is insulated so that no heat is lost. Throughout the course of this experiment, the thermal effects are not appreciably translated to the

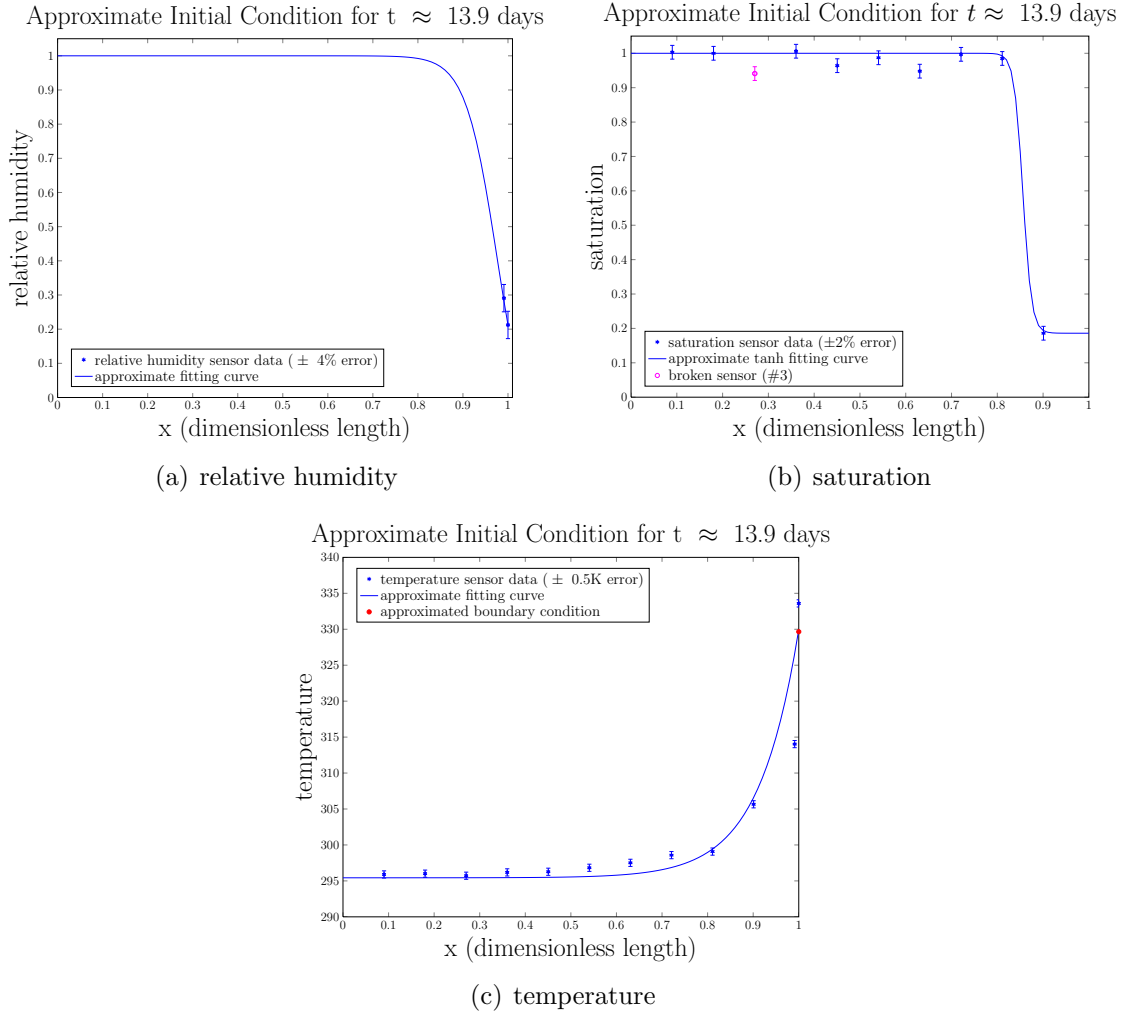


Figure 7.17: Approximate initial conditions at the 2000th data point ($t \approx 13.9$ days). Error bars indicate approximate sensor accuracy.

bottom of the apparatus so either boundary condition would be sufficient. Finally, the only boundary condition remaining is the saturation condition at the surface of the soil. A simple condition is to state that the flux of liquid is zero across this boundary. Mathematically, this translates to the Neumann condition $\partial S / \partial x(x = 1, t) = 0$.

A fine point needs to be stated regarding the relative humidity equation. The saturation initial condition states that much of the experimental apparatus is completely saturated with liquid water (below sensor #9 approximately). The issue is that there is no gas phase present when $S = 1$. Mathematically this translates to a Stefan-type

problem where the lower boundary for the gas phase is actually moving spatially as the liquid water evaporates. For the sake of illustration let us simply assume for a moment that the saturation equation is a hyperbolic linear advection equation where the front simply *advects* in time. Figure 7.18 illustrates how the gas-phase domain might evolve in time in this simplified example. Of course, the saturation equation is not such a simple equation but the essence of the moving domain is the same regardless.

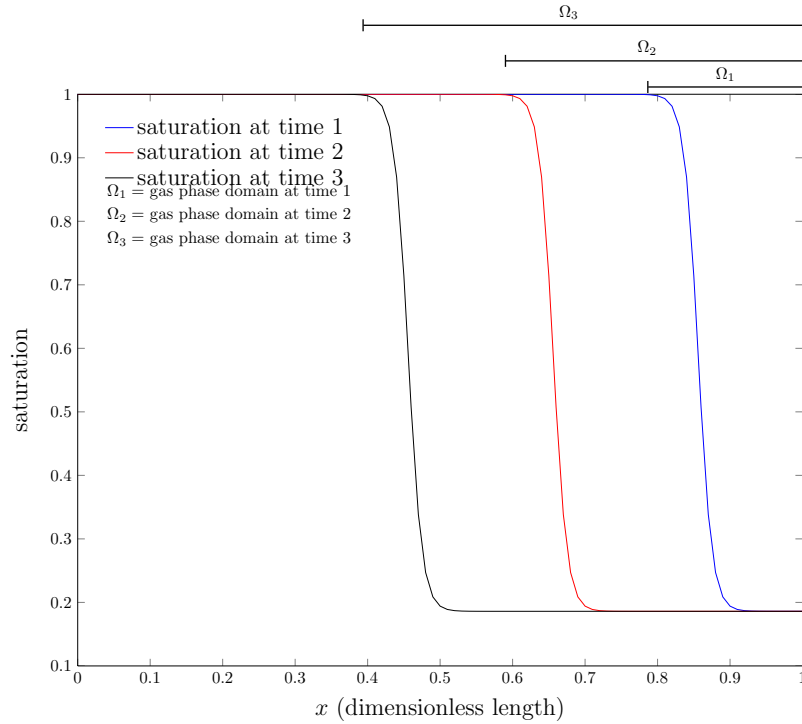


Figure 7.18: Illustration of how the gas-phase domain might evolve in time.

One way to model this Stefan problem is to assume that when $S = 1$ then $\varphi = 1$. Under this assumption we can define the gas-phase equation as a piecewise-defined differential equation:

$$\frac{\partial \varphi}{\partial t} = \begin{cases} 0, & S = 1 \\ \frac{-\varphi \frac{\partial}{\partial t} ((1 - S)\rho_{sat}) + \nabla \cdot (\rho_{sat} \mathcal{D} \nabla \varphi) + \hat{e}_l^{gv}}{(1 - S)\rho_{sat}}, & S \in (0, 1) \end{cases}. \quad (7.11)$$

This is a somewhat artificial setup, but it allows us to assume that a relative humidity exists for the entire domain even when a gas phase doesn't (strictly speaking) exist. Simply stated, equation (7.11) indicates that if the saturation is 100% then there is no change in relative humidity (even though technically there is no gas phase). Then if we take the initial condition as $\varphi(x, 0) = 1$ when $S = 1$ and the left-hand boundary condition as $\varphi(0, t) = 1$ we (artificially) create a relationship for the relative humidity that holds over the entire spatial domain. There are several concerns with this approach, not the least of which is that the existence and uniqueness theory discussed previously does not cover this sort of case. Moreover, numerically requiring that the transition point is exactly 1 is not reasonable and some artificial cutoff, $S_* < 1$, should be used to loosen this condition in numerical simulations.

A simpler way to model the relative humidity in this experiment is to prescribe an initial saturation that allows for *some* gas phase to exist throughout the experiment for all time. This is achieved by setting the initial saturation less than 1. From a numerical standpoint this makes the equations easier to solve as the boundaries are all stationary in time. On the other hand, this choice of initial condition does not match the experimental setup and is therefore less desirable for the purposes of model validation. The forthcoming numerical experiments are performed using a combination of these two approaches; if $S < S_* < 1$, then the relative humidity equation is *turned on* and diffusion is allowed to occur.

In the experiment, the relative humidity was only measured at the surface, at 1cm below the surface, and in the surrounding (ambient) conditions. Hence, we can only truly compare with this data in regions very close to the surface. The saturation and temperature sensors, on the other hand, are placed coarsely throughout and the model can be validated over the entire spatial domain.

7.4.2 Numerical Simulations

In this subsection we perform numerical simulations of the coupled system based on the initial and boundary conditions in Section 7.4.1. These numerical simulations are a first step toward validation of the newly proposed mathematical model. The main thrust of this work was not to create robust numerical solvers for coupled systems of PDEs. As such, we rely on the `NDSolve` package built into `Mathematica` as the primary numerical solver. The plotting and post processing are performed on a mix of `Mathematica` and `MATLAB`. The purpose of these numerical experiments is to provide a validation for the proposed equations. As such, we chose to directly model the Stefan problem with the relative humidity equation as shown in (7.11).

The `NDSolve` package is based on a method of lines approach to numerical time integration with a finite difference spatial discretization. In time we use a fourth-order Gear's scheme and in space we use a central differencing scheme. One disadvantage to using this type of spatial scheme in this problem is that the saturation and heat equations have advective components. It is well known [53, 54] that upwind schemes are typically better at capturing the physics of advective flow problems and the central differencing schemes will usually introduce artificial diffusion into the solution. In an evaporation-type experiment such as this one, the advective flow is expected to be less dominant than in drainage or imbibition experiments. Hence, the artificial diffusion introduced with a central difference scheme is expected to have little impact on the solution quality. To date, the use of non-central schemes and adaptive mesh refinement are not supported by `Mathematica`'s differential equation solving package.

The parameters that can be varied in this experiment are the coefficient of the dynamic saturation term, τ , the weight of the evaporation coefficient, M , and the weights of the $\nabla\varphi$ and ∇T terms in the saturation equation, C_φ^l and C_T^l . There are no parameters that can be varied in the relative humidity equation due to the newly proposed model for diffusion. This is in contrast to the standard enhancement model where the empirical fitting parameter for diffusion is used to match the experimental

data. The fact that we have three different fitting parameters in the saturation equation simply allows us to fine tune the *shape* of the saturation solution beyond what is predicted by the traditional Richards’ equation. Recall from Section 7.1 that larger values of the dynamic saturation term affects the sharpness of the moving front in the saturation equation.

In Section 5.4.4 it was demonstrated that for certain choices of M in the evaporation rule, the present evaporation model approximated that of Bixler [19]

$$\hat{e}_l^{g_v} = b (\varepsilon^l - \varepsilon_r^l) R^{g_v} T (\rho_{sat} - \rho^{g_v}).$$

In [75], the fitting parameter for Bixler’s model was $b = 2.1 \times 10^{-5}$. The corresponding fitted parameter in the present model is $M \approx 10^{-15}$ where $\hat{e}_l^{g_v}$ is given as

$$\hat{e}_l^{g_v} = M \varphi (\rho^l - \rho^{g_v}) (\mu^l - \mu^{g_v}).$$

This is only an order of magnitude approximation and fine tuning can be made to better fit the data.

Several experimental estimates of τ were presented in Table 2 of [46]. From this data, τ could possibly span several orders of magnitude: $10^4 < \tau < 10^8$. Unfortunately, the soil types were only listed as “sand” (or “dune sand”) and the relevant permeabilities and van Genuchten parameters were absent from this summary. These values at least give a *ballpark* estimate for experimentation with τ . The coefficients of $\nabla\varphi$ and ∇T in the saturation equation, on the other hand, are new to this study and appropriate values have yet to be determined. As such, we study different orders of magnitude for these values to estimate the effect of the terms to the overall numerical solution. The material parameters are all chosen to match those in Table 7.2.

The initial simulations will be run with sinusoidal boundary conditions as shown in Figures 7.16. This is to give a qualitative estimation of the behavior of the solutions without the trouble of the jump discontinuities associated with the square wave approximation or data interpolation. A smoothed square wave approximation (also

shown in Figures 7.16) is then used to give a *closer* match to the experimental data. The smoothing is achieved by taking piecewise defined hyperbolic tangent functions to approximate the steps. To measure the error between the data and the numerical solution we use a sum of the squares of the residual values measured at each sensor location:

$$e_u(t) = \frac{\sum_{\xi \in data} (u_{data}(\xi, t) - u_{num}(\xi, t))^2}{\sum_{\xi \in data} (u_{data}(\xi, t))^2}, \quad (7.12)$$

where u represents any of the three dependent variables of interest (S , φ , or T) and the subscript indicates where the value is taken from. Stating that “ $\xi \in data$ ” simply means that ξ spans the sensor locations relevant for the given u (i.e. $\xi \in \{110/111, 1\}$ for $u = \varphi$). Obviously $e_u(t)$ is a function of time so to get a single measure that describes the error we take the maximum of $e_u(t)$ over the length of an experimental day

$$E_u = \max_t (e_u(t)). \quad (7.13)$$

A single experimental day was chosen due to numerical difficulties and due to loss of relative humidity sensor information. Equation (7.13) gives a single numerical value measuring the fit of the numerical solution to the data. In the relative humidity this is a very simplistic exercise as there is only 1 data point to compare against; the sensor located 1cm below the surface of the soil. For the saturation and temperature, on the other hand, this gives a better quantitative measure.

Table 7.3 gives errors measured with equation (7.13) against the *classical* system of equations (Richards’, Enhanced Diffusion, and de Vries). Table 7.4 shows the error as measured with equation (7.13) for various values of τ , for different functional forms of the thermal conductivity (see Section 5.4.3), and for various values of C_φ^l and C_T^l . In order to make comparisons with τ , C_φ^l , and C_T^l we use the ratio of this coefficient as compared to the diffusive term in the saturation equation. This was done in Sections

Table 7.3: Relative errors measured using equation (7.13) for the classical mathematical model consisting of Richards’ equation for saturation, the enhanced diffusion model for vapor diffusion, and the de Vries model for heat transport. These are compared for the two thermal conductivity functions of interest (weighted sum (5.78) and Côté-Konrad (5.80)).

		Relative Errors		
Conductivity	Boundary Cond.	Saturation	Rel. Humidity	Temperature
Weighted Sum	Smoothed Square	0.00356	1.54048	0.000515
Côté-Konrad	Smoothed Square	0.00357	1.27818	0.000631

7.1 and 7.3, and the ratios of interest are repeated here for clarity:

$$\left(\frac{\tau \varepsilon_S}{-t_c p'_c(S)} \right) = \left(\frac{\tau \varepsilon_S \kappa_S}{\mu_l} \right) Pe(S) = H_0 Pe(S) \quad (7.14a)$$

$$- \left(\frac{C_\varphi^l}{p'_c(S)} \right) = \left(\frac{C_\varphi^l}{\rho^l g} \right) Pe(S) = R_0 Pe(S) \quad (7.14b)$$

$$- \left(\frac{C_T^l}{p'_c(S)} \right) = \left(\frac{C_T^l}{\rho^l g} \right) Pe(S) = \theta_0 Pe(S). \quad (7.14c)$$

Since each ratio is relative to the Péclet number (which is a function of S) we focus only on the ratios on the right-hand sides of equations (7.14). Due to the fact that this is a large parameter space, only some of the notable relative errors are presented. Mesh refinement was used in the comparisons in several instances to minimize numerical artifacts. Spatially, the meshes ranged between 100 and 1024 points. Only a uniform mesh was considered.

It is apparent in Table 7.4 that the best error approximations for saturation, relative humidity, and temperature are found with smaller values of H_0 (or equivalently, τ). This observation is particular to a drainage-type experiment. If the experiment were an imbibition-type then it is conjectured (based on the results in Section 7.1) that the value of τ would play a larger role. Also apparent in Table 7.4, we see that the values of C_φ^l and C_T^l play little role in the overall dynamics of the problem.

Keep in mind that the relative humidity errors are really just the difference between 1 single sensor and the numerical solution at that physical location. In the author’s opinion it is unreasonable to judge the effectiveness of the numerical solu-

Table 7.4: Relative errors measured using equation (7.13) for instances within the parameter space consisting of the thermal conductivity function (weighted sum (5.78) and Côté-Konrad (5.80)), C_φ^l, C_T^l , and τ . These are taken for a (smoothed) square wave approximation to the boundary conditions. (The starred rows indicate failure of the numerical method, and the errors from the classical model are repeated for clarity)

Parameters & Functions				Relative Errors		
Conductivity	R_0	θ_0	H_0	Saturation	Rel. Humidity	Temperature
Weighted Sum	Classical Model			0.00356	1.54048	0.000515
Weighted Sum	0	0	$10^{-2.5}$	0.011966	1.206005	0.000463
			$10^{-3.0}$	0.009020	1.201793	0.000463
			$10^{-3.5}$	0.006508	1.198274	0.000463
			$10^{-4.0}$	0.004904	1.199174	0.000463
			$10^{-4.5}$	0.004076	1.195180	0.000463
			$10^{-5.0}$	0.003712	1.196750	0.000463
			0	0.003536	1.199584	0.000463
Weighted Sum	10^{-5}	10^{-5}	10^{-5}	0.003712	1.196751	0.000463
	10^{-4}	10^{-4}	10^{-5}	0.003712	1.196756	0.000463
	10^{-3}	10^{-3}	10^{-5}	0.003710	1.196807	0.000463
	10^{-2}	10^{-2}	10^{-5}	0.003692	1.197041	0.000463
	10^{-1}	10^{-1}	10^{-5}	0.003509	1.202644	0.000462
*	1	1	10^{-5}	*	*	*
Côté-Konrad	Classical Model			0.00357	1.27818	0.000631
Côté-Konrad	0	0	$10^{-2.5}$	0.011964	0.946441	0.000516
			$10^{-3.0}$	0.009022	0.951573	0.000515
			$10^{-3.5}$	0.006513	0.950024	0.000515
			$10^{-4.0}$	0.004910	0.948023	0.000515
			$10^{-4.5}$	0.004084	0.944724	0.000516
			$10^{-5.0}$	0.003719	0.946599	0.000516
			0	0.003545	0.942403	0.000516
Côté-Konrad	10^{-5}	10^{-5}	10^{-5}	0.003719	0.948032	0.000516
	10^{-4}	10^{-4}	10^{-5}	0.003720	0.941801	0.000516
	10^{-3}	10^{-3}	10^{-5}	0.003717	0.945905	0.000515
	10^{-2}	10^{-2}	10^{-5}	0.003698	0.947884	0.000515
	10^{-1}	10^{-1}	10^{-5}	0.003510	0.966405	0.000513
*	1	1	10^{-5}	*	*	*

tion based solely on one point. One complication that arose within this solution is that the relative humidity exhibits small periods of non-physical behavior for certain parameters and boundary conditions. Mesh refinement removes some of this effect,

but even with further mesh refinement not all of the non-physical regions were removed. Possible sources of this problem are: (1) the fact that `Mathematica` uses cubic interpolation polynomials to deliver the solutions to numerical differential equations (cubic interpolation can overshoot sharp transitions in data), and (2) the Stefan nature of the problem causes numerical *stiffness* at the point of transition. Further studies are needed to determine the exact cause of this non-physical behavior.

Figures 7.19 show individual time steps of several solutions for various parameters with a sinusoidal approximation to the relative humidity and temperature boundary conditions. Figures 7.20 show the same plots with smoothed square wave boundary conditions. The square wave boundary conditions obviously give closer approximation to the boundary data, and at the same time the use of the square wave boundary conditions removes the non-physical behavior in this case. The plots associated with the sinusoidal approximation to the boundary conditions are presented here for comparison between very smooth and slightly sharper transitions in boundary data. A closeup of the regions of non-physical behavior is shown in Figures 7.21(a) and 7.21(b). Observe in these figures that the diffusion equation solved with smaller values of H_0 and larger diffusion (from the weighted sum equation) give the most plausible solutions. Figures 7.21(c) and 7.21(d) give an indication of the difference in the relative humidity equations given different thermal conductivity functions.

The comparisons of the temperature solutions are shown in Figures 7.22 and 7.23. There is very little difference between the models for various values of τ (or equivalently, H_0), so only the curves associated with $H_0 = 10^{-5}$ are shown. Observe that the thermal equation does a poor job capturing the extent of the diffusion near the top of the experimental apparatus, but it does well otherwise. Possible sources of this error come from: (1) the terms neglected in the simplification of the thermal model, (2) the initial condition, (3) the thermal conductivity functions (or parameters), and/or (4) the accuracy of the sensor information.

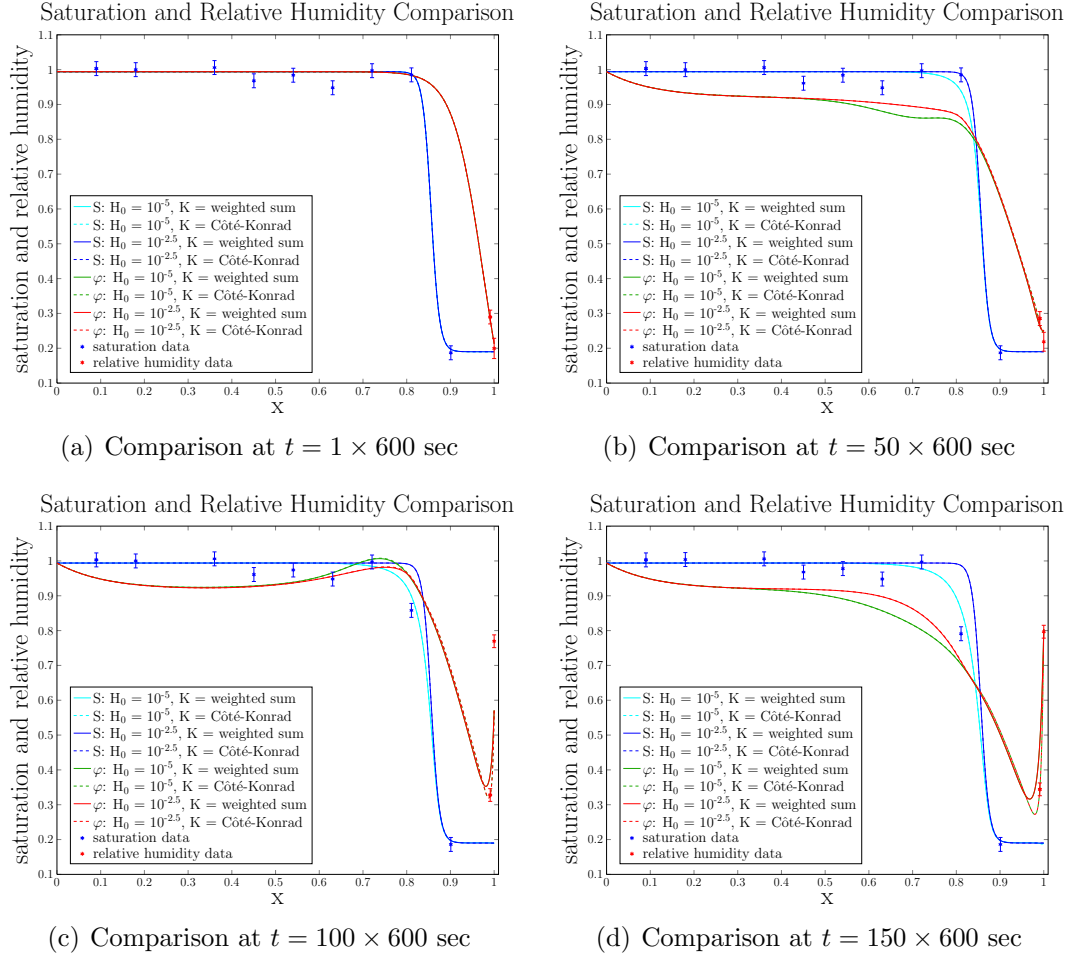


Figure 7.19: Comparison of relative humidity and saturation for the fully coupled saturation-diffusion-temperature model as compared to data from [75]. Boundary conditions are taken from a sinusoidal approximation of boundary data. Thermal conductivities are taken as either weighted sum (5.78) or Côté-Konrad (5.80).

Comparison of the error estimates between the two models (Table 7.3 compared to Table 7.4), we see that the present model gives slightly better approximations as measured with this metric. Table 7.5 gives the percent improvement of the present model over the classical model. These values are chosen from the tables presented herein, and as such this is a lower bound on the percent improvement. The fact that there was an improvement in error is less important, in the author's opinion, than the fact that the models predict nearly the same error while (1) removing the necessity for the enhanced diffusion parameter, and (2) putting the entire system of equations

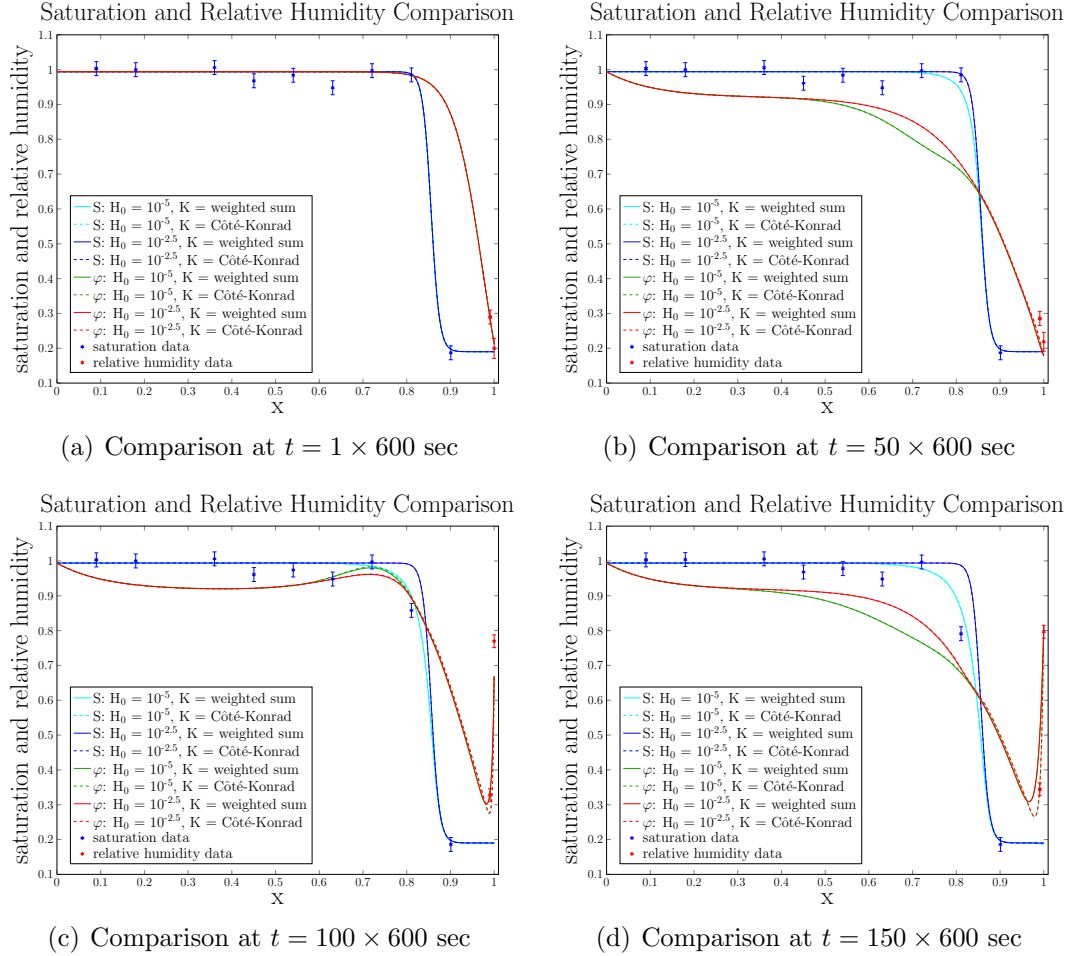


Figure 7.20: Comparison of relative humidity and saturation for the fully coupled saturation-diffusion-temperature model as compared to data from [75]. Boundary conditions are taken from a smoothed square wave approximation of boundary data. Thermal conductivities are taken as either weighted sum (5.78) or Côté-Konrad (5.80).

on a firm thermodynamic footing.

In this problem there are several parameters of interest, but the present study suggests that variations in these parameters play little role in the overall dynamics of the problem. This narrows us down to only 1 fitting parameter for this problem: the coefficient, M , in the rate of evaporation term. This was taken to best match with the fitted evaporation rate in [75] so it is expected that this value can be considered roughly constant. The classical model consisting of Richards' equation, Philip and de Vries diffusion equation (with enhancement fitting factors), and the de Vries heat

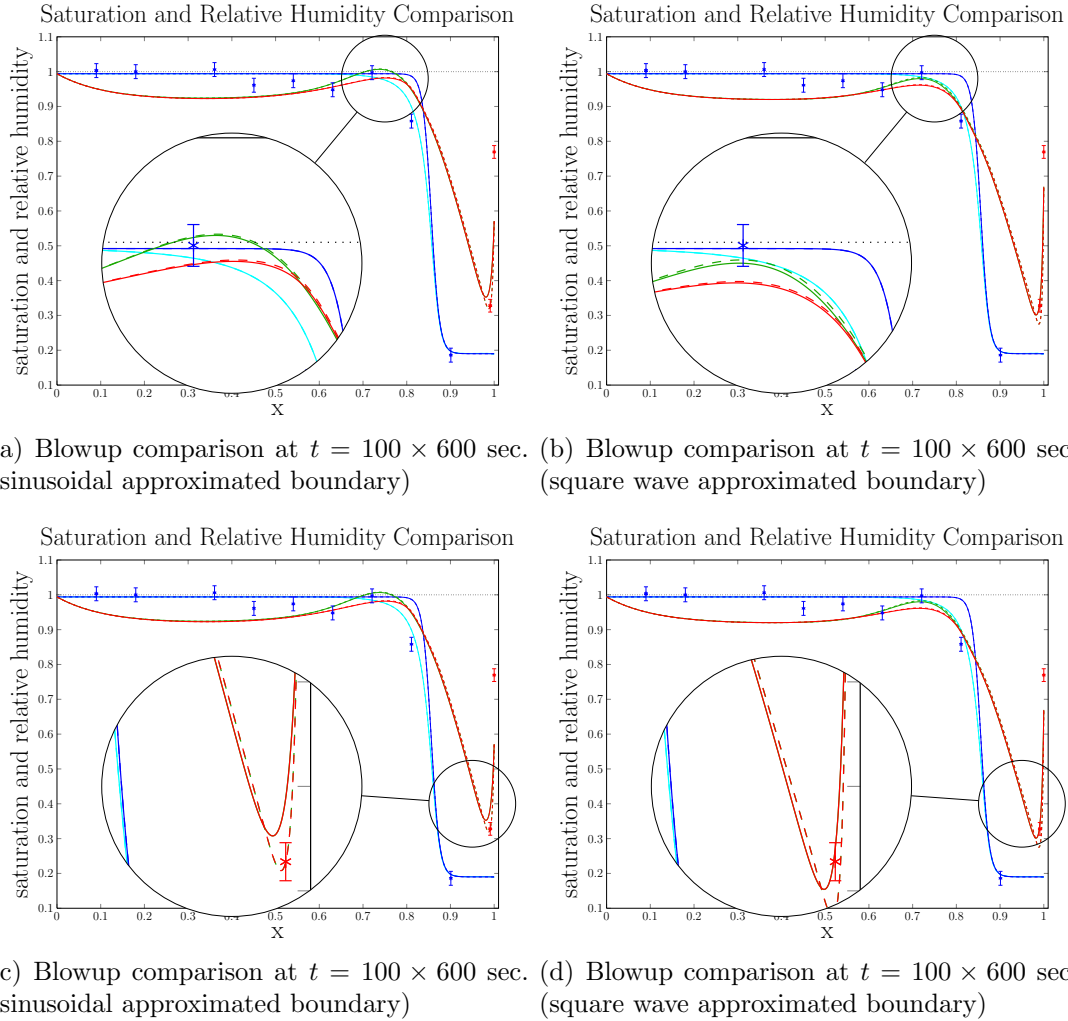


Figure 7.21: Blowup comparison of relative humidity and saturation for the fully coupled saturation-diffusion-temperature model as compared to data from [75]. The inset plots give a closer look at the behavior exhibited by these particular solutions.

transport equation contains at least two fitting parameters that are calculated using a least squares statistical approach.

7.5 Conclusion

In Sections 7.1 - 7.3, several numerical results were presented indicating the consistency of the present models with the classical mathematical models for saturation and relative humidity. Of particular importance is the analysis of the enhanced diffusion problem. The arguments presented in Section 7.2 indicate that modeling vapor

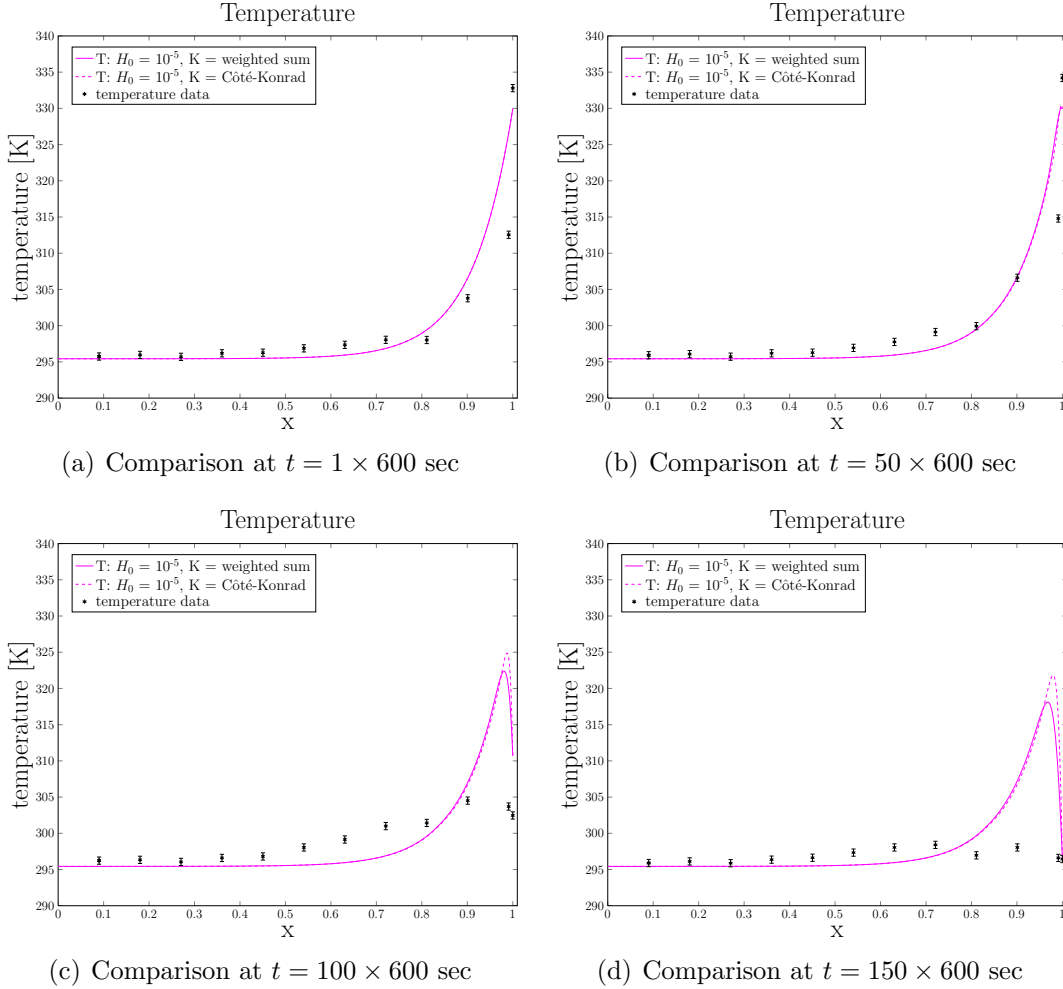


Figure 7.22: Comparison of temperature solutions for the fully coupled saturation-diffusion-temperature model as compared to data from [75]. Boundary conditions are taken from a sinusoidal approximation of boundary data.

diffusion in unsaturated media with the chemical potential can eliminate the necessity for a fitted enhancement factor. Also shown within this section is a sensitivity analysis of the τ parameter for the dynamic capillary pressure term as well as the coefficient of $\nabla\varphi$ that appears in the saturation equation.

In Section 7.4 it was shown that the fully coupled system matches quantitatively and qualitatively to experimental data for heat and moisture transport. There are several problems with the matching to this experimental data. First of all, the spatial data is very coarse so getting an exact fit for the initial conditions is difficult. Secondly,

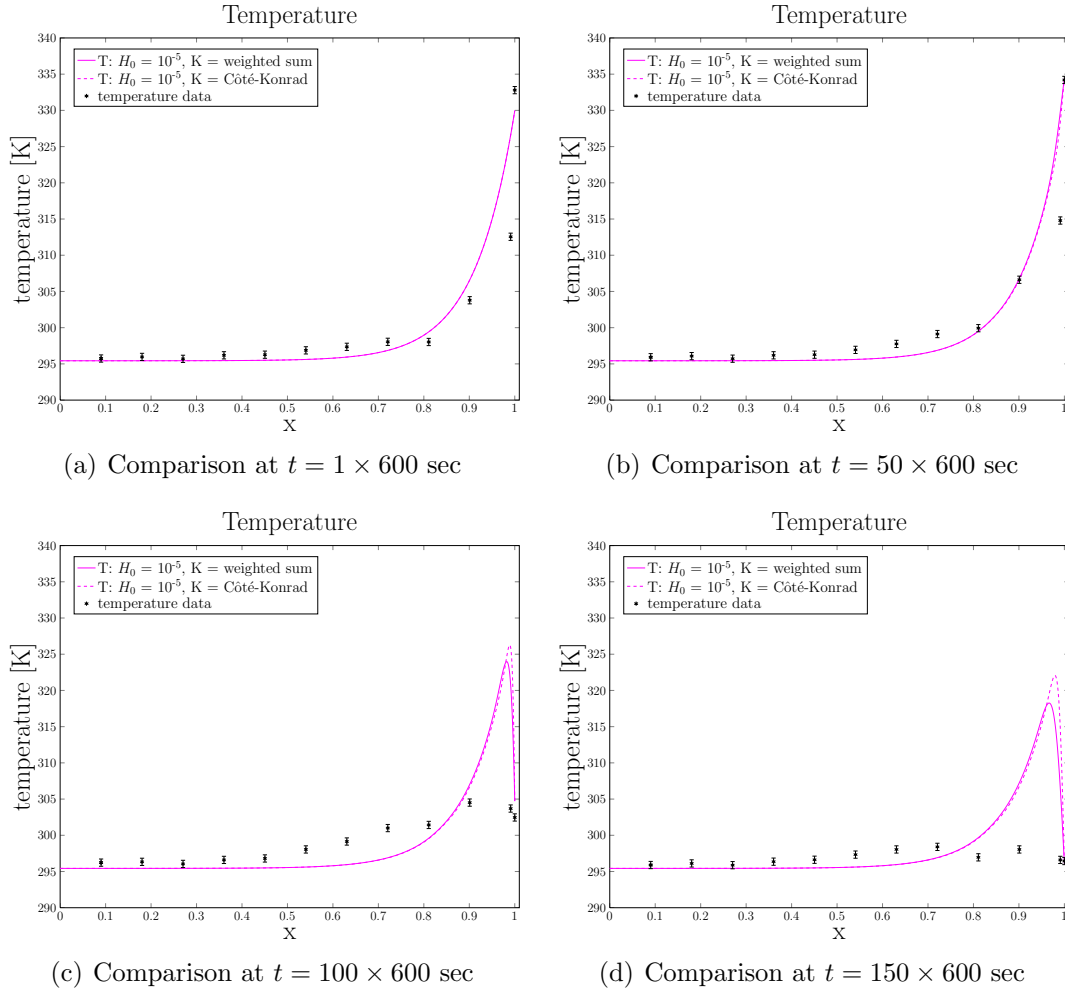


Figure 7.23: Comparison of temperature solutions for the fully coupled saturation-diffusion-temperature model as compared to data from [75]. Boundary conditions are taken from a smoothed square wave approximation of boundary data.

the data is noisy so getting a reasonable fit for the boundary conditions (especially in the initial experimental times), is difficult. Lastly, the Stefan nature of this problem causes numerical difficulties.

The numerical simulations presented herein indicate that the proposed models match both physical and experimental expectations for a heat and moisture transport model. The model is sensitive to the choice of thermal conductivity function and further investigation is needed to determine which function(s) are appropriate. The slight non-physical nature of the results for certain boundary conditions needs to be

Table 7.5: Percent improvement of the present model over the classical model using equation (7.13) as the error metric.

Boundary Cond.	% Improvement		
	Saturation	Rel. Humidity	Temperature
Sinusoidal	1.71%	22.85%	16.33%
Sq. Wave	1.71%	5.91%	26.78%

investigated. Further studies (both numerical and experimental) need to be performed and provide a baseline for future research endeavors. The coupling of these three processes, all of which were derived from a thermodynamic foundation, opens to the door to future research endeavors on coupled processes in unsaturated soils.

8. Conclusions and Future Work

Throughout this thesis it has been demonstrated that HMT and the macroscale chemical potential are powerful modeling tools that can be used to derive mathematical models for rather complex phenomena in porous media. Chapter-by-chapter, the results are as follows.

In Chapter 2, a short discussion of different Fickian diffusion coefficients was presented. While this work is not *new* in the sense of the creation of new theories or equations, it serves as an aid to understand the assumptions commonly used in diffusion-related research and experimentation. We showed that under certain assumptions that all of the pore-scale Fickian diffusion coefficients can be assumed constant. In Chapter 3, the focus turned back to porous media and the fundamental framework for volume averaging and Hybrid Mixture Theory were presented. This chapter serves as a reference for these topics and no new results were presented.

In Chapter 4 we derived and generalized the primary constitutive equations for unsaturated media. In particular, we generalized the forms of Darcy's and Fick's laws proposed by Bennethum [13], Weinstein [80], and others. The form of Fourier's law derived is similar to that of Bennethum [14], but contains terms particular to multiphase media. To the author's knowledge, the chemical potential form of Fourier's law is new to this work. The exact generalizations of Darcy's and Fick's laws presented here are novel to this work, but similar terms have been proposed in other works [13, 12, 80]. What is novel to this work is the extension of these terms to multiphase flow and the use of the macroscale chemical potential as a dependent variable to obtain additional insight.

In Chapter 5, a coupled system of equations for heat and moisture transport was derived. Of particular importance are the generalizations of Richards equation and the Philip and de Vries vapor diffusion equation. It was demonstrated that the enhanced diffusion model of Philip and de Vries can be re-framed in terms of the

macroscale chemical potential. This re-framing removes the necessity of the enhancement factor proposed by Philip and de Vries. The coupling of the vapor diffusion and saturation terms is achieved through the chemical potential. The relationship between relative humidity and chemical potential is well known in chemistry and thermodynamics, but to the author's knowledge it has not been previously used in the porous media literature. Also in Chapter 5, a generalization of the heat transport equation given by Bennethum [14] to multiphase media was derived via HMT. This new model collapses to Bennethum's model in the case of a saturated porous medium and also suggests corrections to the classical de Vries model proposed in 1958.

In Chapter 6, the questions of existence and uniqueness were studied for each individual equation (while holding the other dependent variables fixed). These results were known for the saturation equation, but the results presented for the vapor diffusion and thermal equation are unique to this work. This is, of course, because these equations are novel to this work. More work needs to be done on this front. In particular, the uniqueness result for vapor diffusion equation is absent. Also, the results for the thermal equation depend on strict boundary conditions which are not necessarily met physically. It is emphasized that the existence and uniqueness results presented herein are only preliminary.

The numerical results in Chapter 7 are performed for validation purposes. Whenever presenting new equations it is necessary to compare against existing models and, when possible, experimentally obtained data. To that end, in Sections 7.1, 7.2 and 7.3, numerical solutions to each equation were presented along with sensitivity analyses and comparisons to classical equations. In Section 7.4, numerical solutions to the coupled system were presented and compared to experimental data. It was shown that under certain parameter values the newly proposed model agrees with the experimental data.

There are many avenues for future research left uncompleted in this work. Relaxation of the assumptions outlined at the beginning of Chapter 5 (Sections 5.2 and 5.4) provide the initial avenues for further research.

1. It is well known that clay soils swell when wetted. Relaxing the rigidity assumption on the solid phase would allow for this phenomenon. Mathematically, though, this creates further complications in the liquid- and gas-phase mass conservation equations since the divergence of the solid-phase velocity will no longer be zero due to the remaining terms in the solid-phase mass balance equation:

$$\dot{\varepsilon}^s + \varepsilon^s \nabla \cdot \mathbf{v}^s = \sum_{\alpha \neq s} \hat{e}_\alpha^s.$$

The right-hand side of this equation may be zero in most cases (no dissolution or precipitation of solid particles), but a constitutive equation would be needed for ε^s or $\dot{\varepsilon}^s$. This has further complications in that saturation, $S = \varepsilon^l / (1 - \varepsilon^s)$, now varies with solid-phase volume fraction as well as liquid phase volume fraction.

The stress in the solid phase was discussed in Chapter 4 as a consequence of the entropy inequality. Upon further investigation this will give a generalization to the Terzhagi Stress Principle which states that the fluid phases can support some stress on the solid matrix. This principle will be necessary to express the stresses on the deforming solid.

2. Changing the soil parameters and studying the sensitivity to empirical and measured relationships can be another avenue of future research. In the present study the soil is assumed to be isotropic. For this reason it is possible to take the permeability as a scalar function. This is not necessarily a reasonable assumption in real physical problems, and one possible avenue of research is to relax this assumption and take a full tensor representation of the permeability. Clearly a 2- or 3-dimensional simulation would have to be considered in this

research.

Another adjustment to the soil properties is to the relative permeability and capillary pressure - saturation functions. The van Genuchten relationships were used for this work, but these are not the only functional forms available. The Fayer-Simmons model [35], for example, is an extension of the van Genuchten capillary pressure - saturation relationship that accounts for very small saturation content. A simple avenue for future research is to implement this model (and others like it) and the study to the sensitivity of the models to these small changes.

3. The present model can be extended to multiple fluid phases. In this model we have only considered one liquid phase and one gas phase. It is reasonable to assume that the gas phase is a binary ideal gas, but it is not always reasonable to assume that the only fluid present is a pure liquid.

One possible avenue for future research is to assume that the liquid phase has a dissolved contaminant. In that case it is not reasonable to assume that the density of the liquid is only a function of temperature. Furthermore, the diffusive term in the liquid phase equation may not be absent (depending on the type of contaminant).

Another possible case is where several liquid phases are present. In this case it would be necessary to include a mass conservation equation (and related Darcy-type constitutive law) for this other fluid phase. This is a common case when water, oil, and gas are present within the porous matrix. This type of system has seen recent media attention due to the practice of fracking (driving high pressure water and chemicals into porous rock to release oil and natural gas).

As mentioned previously in this chapter, an avenue for future research is to shift the focus from modeling to analysis. The existence and uniqueness results presented

in Chapter 7 are incomplete, and more research needs to be completed to give a full analytic description of the behavior of these equations. Of particular interest is the study of the fully coupled system. There are several papers discussing *strongly coupled system* of reaction diffusion equations (e.g. [3, 52]). These papers serve as a starting point to understanding the analysis for the coupled system.

A third avenue for future research is to focus on the numerical method for solving the coupled system. The numerical solutions presented in Chapter 7 were found using `Mathematica`'s `NDSolve` package. This is a general purpose finite difference solver designed to solve wide classes of ordinary and partial differential equations. Even so, there are problems with the methods used within that package. The foremost issue is the use of central differencing schemes. When solving advective (or hyperbolic-type) equations it is often advantageous to use upwind-type numerical schemes. This is not possible with the `NDSolve` package and causes some issues with the numerical solutions in advection-dominated simulations.

Future research for the numerical method can be approached in several ways:

1. The equations of interest in this work form a system of conservation laws, and as such a finite volume method is likely the best choice. Peszyńska and Yi [59] derived a cell centered finite difference method and a locally conservative Euler-Lagrange method based on the finite difference method for the saturation equation with the third-order dynamical capillary pressure term. These are both similar to finite volume methods, and the methods derived therein can possibly serve as a basis for extension to the coupled system. This paper is of particular interest as the bulk of the numerical difficulties in the saturation equation arise as a result of the weight of the third-order term.
2. There are other packages available to solve general classes of partial differential equations. `COMSOL` (Computational Multi Physics) is one such package that is common amongst engineering groups. This is a particularly non-mathematical

approach to future research, but COMSOL and other packages can be used to test many cases of parameters and terms suggested by the entropy inequality.

3. The numerical simulations used to compare to the experimental data were solved in one spatial dimension. While this assumption is approximately valid for the experiment of interest, these equations need to be compared against multi-dimensional data. One avenue of future research is to explore the numerical solution to the system and compare it to a two-dimensional experiment. One such experiment can be found in [76]. This experiment is of interest since many of the parameters are the same as those used in the column experiment.

Final Words

The initial purpose of this work was to explore the use of the chemical potential as a modeling tool in porous media. It was demonstrated that the chemical potential is a powerful modeling tool when the underlying physical processes are diffusive in nature. The down sides to using the chemical potential are that it is indirectly measured and not widely understood. Within this work the main advantage to using the chemical potential was to rewrite the gas-phase diffusion equation. This allowed for the removal of the enhancement factor from the classical diffusion equation.

In this work we derived three new equations that, when coupled, form a set of governing equations for heat and moisture transport in porous media that explains previously unexplained phenomena. The ideas and questions proposed within this chapter set up a research agenda for future years of scholarly work.

APPENDIX A. Microscale Nomenclature

This appendix contains nomenclature for Part I: Pore-Scale modeling. While there is some overlap in notation between the two parts, this appendix allows the notation in Chapter 2 to stand alone. The equation references indicate the approximate first instance of the symbol (these are hyperlinked in the digital version for ease of use). The supporting text for these equations usually gives context and more detail.

Superscripts, Subscripts, and Other Notations

$(\cdot)^{\alpha_j}$: j^{th} component of α -phase

$(\cdot)^\alpha$: α -phase

$(\cdot)^{a,b}$: difference of two quantities, $(\cdot)^{a,b} = (\cdot)^a - (\cdot)^b$

a: (bold symbol) vector quantity

$(\cdot)_*$: a reference quantity or a quantity evaluated at a reference state

Latin Symbols

c^{g_j} : molar concentration of the j^{th} constituent in the gas phase [mol/length³]

(2.2)

C^{α_j} : Mass fraction of j^{th} component $C^{\alpha_j} = \rho^{\alpha_j} / \rho^\alpha$ [-] (2.1)

D : diffusion coefficient [length²/time] (2.1) - (2.4)

D_γ : diffusion coefficient associated with the γ -form of Fick's law [length²/time]

(2.1) - (2.4)

\mathbf{J}^{g_j} : flux of species j in the gas phase [mass/(length²-time)] (2.1) - (2.4)

$m^{\alpha j}$: molar mass of the j^{th} constituent in phase α [mass/mol] (2.7)

$p^{\alpha j}$: partial pressure of species j in phase α [force/length²] (2.10)

p^α : pressure of α phase [force/length²] (2.10)

R : universal gas constant [energy/(mass-temperature)] (2.4)

R^{gj} : specific gas constant for species j in the gas phase [energy/(mass-temperature)] (2.3)

T : absolute temperature (2.3)

t : time (2.15)

$\mathbf{v}^{\alpha j}$: velocity of species j in phase α [length/time] (2.1)

\mathbf{v}^α : velocity of phase α [length/time] (2.1)

x^{gj} : molar concentration of j^{th} constituent in the gas mixture [-] (2.2)

Greek Symbols

μ^{gv} : chemical potential of water vapor in gas phase [energy/mass] (2.3) - (2.4)

μ_*^{gv} : chemical potential of water vapor at standard temperature and pressure [energy/mass] (2.7)

$\rho^{\alpha j}$: mass density of species j in phase α [mass/length³] (2.1)

ρ^α : mass density of phase α [mass/length³] (2.1)

ρ_{sat} : mass density of water vapor under saturated conditions [mass/length³]
(paragraph before (2.9))

APPENDIX B. Macroscale Appendix

B.1 Nomenclature

This appendix contains nomenclature for Part II: Macroscale modeling. While there is some overlap in notation between the two parts, this appendix allows Part II to stand alone. This appendix also clarifies any notational discrepancies between the pore-scale and macroscale models. The equation references indicate the approximate first instance of the symbol (these are hyperlinked in the digital version for ease of use). The supporting text for these equations usually gives context and more detail.

Superscripts, Subscripts, and Other Notations

$(\cdot)^{\alpha_j}$: j^{th} component of α -phase on macroscale

$(\cdot)^\alpha$: α -phase on macroscale

$(\hat{\cdot})$: denotes exchange from other interface, phase, or component

$(\cdot)^{a,b}$: difference of two quantities, $(\cdot)^{a,b} = (\cdot)^a - (\cdot)^b$

$(\cdot)^j$: pore scale property of component j

\mathbf{a} : (bold symbol) vector quantity

\mathbf{A} : second order tensor (matrix)

$(\cdot)_0$ or $(\cdot)_*$: reference state

Latin Symbols

a : fitting parameter for enhanced diffusion model [-] (5.71)

b^{α_j}, b^α : External entropy source [energy / (mass-time-temperature)] (3.37)

C^{α_j} : Mass fraction of j^{th} component [-] (3.23)

C_u^l : Coefficients of ∇u terms in generalized Darcy's law ($u = S, T, \varphi$) (5.44)

$\underline{\underline{C}}^s$: Right Cauchy-Green tensor of the solid phase = $(\underline{\underline{F}}^s)^T \cdot \underline{\underline{F}}^s$ [-] (4.4)

$\overline{\underline{\underline{C}}}^s$: Modified right Cauchy-Green tensor = $(\overline{\underline{\underline{F}}}^s)^T \cdot \overline{\underline{\underline{F}}}^s$ [-] (4.4)

$\underline{\underline{D}}^\alpha$: diffusivity tensor [length²/time] (4.81)

\mathcal{D} : generalized diffusivity function [length²/time] (5.69a)

$\underline{\underline{d}}^\alpha$: Rate of deformation tensor = $(\nabla \mathbf{v}^\alpha)_{sym}$ [1/time] (3.40)

e^{α_j}, e^α : energy density [energy/mass] (3.34)

$\hat{e}_\beta^{\alpha_j}$: rate of mass transfer from phase β to component j in phase α per unit mass density [1/time] (3.21)

\hat{e}_β^α : rate of mass transfer from phase β to phase α per unit mass density [1/time] (3.24)

$\underline{\underline{F}}^s$: Deformation gradient of the solid phase [-] (4.5)

$\overline{\underline{\underline{F}}}^s$: Modified deformation gradient of the solid phase [-] (4.5)

$\mathbf{g}, \mathbf{g}^{\alpha_j}, \mathbf{g}^\alpha$: gravity [length/time²] (3.14)

h^{α_j}, h^α : external supply of energy [energy / (mass-time)] (3.34)

$\hat{\mathbf{i}}^{\alpha_j}$: rate of momentum gain due to interaction with other species within the same phase per unit mass density [force/mass] (3.28)

J^s : Jacobian of the solid phase [-] (4.3)

$\underline{\underline{K}}^\alpha$: hydraulic conductivity tensor for α phase [length/time] (4.36)

$\underline{\underline{\mathbf{K}}}$: thermal conductivity tensor [energy/(mass-time-temperature)] (4.39)

m : van Genuchten parameter ($m = 1 - 1/n$) [-] (5.51a)

n : van Genuchten *pore-size distribution* parameter ($n = 1/(1 - m)$) [-] (5.51a)

p^α : classical pressure in the α phase [force/length²] (4.29)

$p^{\alpha(\beta)}$: cross coupling classical pressure [force/length²] (4.41)

$p_c = p^g - p^\ell$: capillary pressure [force/length²] (5.53)

\bar{p}^α : thermodynamic pressure [force/length²] (4.50)

$\bar{p}^{\alpha(\beta)}$: cross coupling thermodynamic pressure [force/length²] (4.47)

\mathbf{q}^α : heat flux for α phase [energy/(length²-time)] (3.35)

\mathbf{q} : total heat flux [energy/(length²-time)] (4.87f)

\mathbf{q}^α : Darcy flux for α phase [length/time] (4.67)

\hat{Q}^{α_j} : rate of energy gain due to interaction with other species within the same phase per unit mass density not due to mass or momentum transfer [energy/(mass-time)] (3.34)

$\hat{Q}_\alpha^{\beta_j}$: energy transfer from phase α to constituent j in phase β per unit mass density not due to mass or momentum transfer [energy/(mass-time)] (3.34)

\mathbf{r} : microscale spatial variable [length] (3.2)

\hat{r}^{α_j} : rate of mass gain due to interaction with other species within the same phase per unit mass density [1/time] (3.21)

R : gas constant [energy/(mol-temperature)] (5.48)

R^{gj} : specific gas constant for j^{th} constituent in gas phase [energy/(mass - temperature)] (4.82)

$\underline{\underline{R}}^\alpha$: resistivity tensor [time/length] (4.36)

$S = \varepsilon^l/(\varepsilon)$: liquid saturation [-] (5.2)

t : time

T : absolute temperature (3.39)

$\underline{\underline{t}}^{\alpha j}$: partial stress tensor for the j^{th} constituent in the α phase [force/length²] (3.28)

$\underline{\underline{t}}^\alpha$: total stress tensor for α phase [force/length²] (3.29)

$\hat{\underline{\underline{T}}}_\beta^{\alpha j}$: rate of momentum transfer through mechanical interactions from phase β to the j^{th} constituent of phase α [force/length³] (3.28)

$\hat{\underline{\underline{T}}}_\beta^\alpha$: rate of momentum transfer through mechanical interactions from phase β to phase α [force/length³] (3.29)

\mathbf{v}^α : velocity of the α phase relative to a fixed coordinate system [length/time] (3.24)

$\mathbf{v}^{\alpha j, \alpha} = \mathbf{v}^{\alpha j} - \mathbf{v}^\alpha$: diffusive velocity [length/time] (3.40)

$\mathbf{v}^{\alpha, s} = \mathbf{v}^\alpha - \mathbf{v}^s$: velocity relative to solid phase velocity [length/time] (3.40)

$\mathbf{w}_{\alpha\beta j}$: velocity of constituent j at interface between phases α and β [length/time] (3.10)

Greek Symbols

α : phase

α : van Genuchten parameter [-] (5.61)

β : phase

$\delta(t)$: Dirac delta function [-]

$\delta A_{\alpha\beta}$: Portion of the $\alpha\beta$ - interface in REV (3.10)

ε^α : volumetric content of α phase per volume of REV [-] (3.15)

$\varepsilon = \varepsilon^\ell + \varepsilon^g$: porosity [-] (4.1)

η^α : specific entropy of α phase [energy / (mass - temperature)] (3.38)

$\hat{\eta}^{\alpha j}$: entropy gain due to interaction with other species within the same phase per unit mass density [energy/(mass-time-temperature)] (3.38)

η : enhancement factor for diffusion [-] (5.70)

Γ^α : macroscale Gibbs potential [energy/mass] (4.61)

γ^α : indicator function which is 1 if in phase α and zero otherwise (3.10)

κ : permeability [length²] (4.68)

$\hat{\Lambda}^\alpha$: rate of entropy production for α phase [entropy / time] (3.38)

$\lambda^{\alpha j}$: Lagrange multiplier for the continuity equation of phase α (4.12)

$\lambda^{\alpha N}$: Lagrange multiplier for the N^{th} term dependence relation of the components in phase α (4.12)

$\lambda = p^{g_v}/p^g$: ratio of partial pressure to bulk pressure in gas phase [-] (5.43)

μ_α : dynamic viscosity for phase α [force-time] (4.68)

$\mu^{\alpha j}$: macroscale chemical potential of j^{th} species in α phase [energy/mass] (4.56)

ν_α : kinematic viscosity for phase α (4.69)

$\hat{\Phi}_\beta^{\alpha j}$: Entropy transfer through mechanical interactions from phase β to phase α per unit mass [energy/(mass-time-temperature)] (3.38)

π^α : wetting potential of α phase [force/length²] (4.51)

$\pi^{\alpha(\beta)}$: cross coupling wetting potential [force / length²] (4.48)

φ : relative humidity [-] (5.40)

ψ^α : specific Helmholtz potential of the α phase [energy/mass] (3.39)

ρ^α : mass density of α phase (mass α per volume of α) [mass / length³] (3.22)

$\rho^{\alpha j}$: mass density of j^{th} constituent in α phase (mass α_j per volume α) [mass / length³] (3.22)

ρ_{sat} : saturated vapor density [force / length²] (5.41)

τ : tortuosity [-] (5.70)

τ : scaling coefficient for dynamic saturation term [-] (4.53)

B.2 Upscaled Definitions

Definitions of bulk phase, species, and averaged variables resulting from upscaling. Recall that an overbar indicates a mass averaged quantity and angular brackets indicate a volume averaged quantity.

$$\langle(\cdot)\rangle^\alpha = \frac{1}{|\delta V_\alpha|} \int_{\delta V} (\cdot) \gamma_\alpha dv \quad \text{and} \quad \overline{(\cdot)}^\alpha = \frac{1}{\langle\rho\rangle^\alpha |\delta V_\alpha|} \int_{\delta V_\alpha} (\cdot) \gamma_\alpha dv$$

$$b^{\alpha j} = \overline{b^j}^\alpha \tag{B.1}$$

$$b^\alpha = \sum_{j=1}^N C^{\alpha j} b^{\alpha j} \tag{B.2}$$

$$C^{\alpha_j} = \frac{\rho^{\alpha_j}}{\rho^\alpha} \quad (\text{B.3})$$

$$e^{\alpha_j} = \overline{e^j}^\alpha + \frac{1}{2} \overline{\mathbf{v}^j \cdot \mathbf{v}^j}^\alpha - \frac{1}{2} \mathbf{v}^{\alpha_j} \cdot \mathbf{v}^{\alpha_j}, \quad (\text{B.4})$$

$$e^\alpha = \sum_{j=1}^N C^{\alpha_j} \left(e^{\alpha_j} + \frac{1}{2} \mathbf{v}^{\alpha_j, \alpha} \cdot \mathbf{v}^{\alpha_j, \alpha} \right) \quad (\text{B.5})$$

$$\hat{e}_\beta^{\alpha_j} = \frac{\varepsilon^\alpha}{|\delta V_\alpha|} \int_{A_{\alpha\beta}} \rho^j (\mathbf{w}_{\alpha\beta_j} - \mathbf{v}^j) \cdot \mathbf{n}^\alpha da \quad (\text{B.6})$$

$$\hat{e}_\beta^\alpha = \sum_{j=1}^N \hat{e}_\beta^{\alpha_j} \quad (\text{B.7})$$

$$\mathbf{g}^{\alpha_j} = \overline{\mathbf{g}^j}^\alpha \quad (\text{B.8})$$

$$\mathbf{g}^\alpha = \sum_{j=1}^N C^{\alpha_j} \mathbf{g}^{\alpha_j} \quad (\text{B.9})$$

$$h^{\alpha_j} = \overline{h^j}^\alpha + \overline{\mathbf{g}^j \cdot \mathbf{v}^j}^\alpha - \mathbf{g}^{\alpha_j} \cdot \mathbf{v}^{\alpha_j}, \quad (\text{B.10})$$

$$h^\alpha = \sum_{j=1}^N C^{\alpha_j} (h^{\alpha_j} + \mathbf{g}^{\alpha_j} \cdot \mathbf{v}^{\alpha_j, \alpha}) \quad (\text{B.11})$$

$$\hat{\mathbf{i}}^{\alpha_j} = \varepsilon^\alpha \rho^{\alpha_j} \left(\overline{\hat{\mathbf{i}}^j}^\alpha + \overline{\hat{r}^j \mathbf{v}^j}^\alpha - \mathbf{v}^{\alpha_j} \overline{\hat{r}^j}^\alpha \right) \quad (\text{B.12})$$

$$\mathbf{q}^{\alpha_j} = \langle \mathbf{q}^j \rangle^\alpha + \langle \underline{\mathbf{t}}^j \cdot \mathbf{v}^j \rangle^\alpha - \underline{\mathbf{t}}^{\alpha_j} \cdot \mathbf{v}^{\alpha_j} + \rho^{\alpha_j} \mathbf{v}^{\alpha_j} \left(e^{\alpha_j} + \frac{1}{2} \mathbf{v}^{\alpha_j} \cdot \mathbf{v}^{\alpha_j} \right) - \overline{\rho^{\alpha_j} \mathbf{v}^j \left(e^j + \frac{1}{2} \mathbf{v}^j \cdot \mathbf{v}^j \right)}^\alpha, \quad (\text{B.13})$$

$$\mathbf{q}^\alpha = \sum_{j=1}^N \left[\mathbf{q}^{\alpha_j} + \underline{\mathbf{t}}^{\alpha_j} \cdot \mathbf{v}^{\alpha_j, \alpha} - \rho^{\alpha_j} \left(e^{\alpha_j} + \frac{1}{2} \mathbf{v}^{\alpha_j, \alpha} \cdot \mathbf{v}^{\alpha_j, \alpha} \right) \mathbf{v}^{\alpha_j, \alpha} \right] \quad (\text{B.14})$$

$$\hat{Q}^{\alpha_j} = \varepsilon^\alpha \rho^{\alpha_j} \left[\overline{\hat{Q}^j}^\alpha + \overline{\hat{\mathbf{i}}^j \cdot \mathbf{v}^j}^\alpha - \left(\overline{\hat{\mathbf{i}}^j}^\alpha + \overline{\hat{r}^j \mathbf{v}^j}^\alpha - \mathbf{v}^{\alpha_j} \overline{\hat{r}^j}^\alpha \right) \cdot \mathbf{v}^{\alpha_j} + \overline{\hat{r}^j \left(e^j + \frac{1}{2} \mathbf{v}^j \cdot \mathbf{v}^j \right)}^\alpha - \overline{\hat{r}^j}^\alpha \left(\overline{e^j}^\alpha + \frac{1}{2} \overline{\mathbf{v}^j \cdot \mathbf{v}^j}^\alpha \right) \right], \quad (\text{B.15})$$

$$\hat{Q}_\beta^{\alpha_j} = \frac{\varepsilon^\alpha}{|\delta V_\alpha|} \left\{ \int_{A_{\alpha\beta}} \left[\mathbf{q}^j + \underline{\mathbf{t}}^j \cdot \mathbf{v}^j + \rho^j \left(e^j + \frac{1}{2} \mathbf{v}^j \cdot \mathbf{v}^j \right) (\mathbf{w}_{\alpha\beta_j} - \mathbf{v}^j) \right] \cdot \mathbf{n}^\alpha da - \left(e^{\alpha_j} - \frac{1}{2} \mathbf{v}^{\alpha_j} \cdot \mathbf{v}^{\alpha_j} \right) \int_{A_{\alpha\beta}} \rho^j (\mathbf{w}_{\alpha\beta_j} - \mathbf{v}^j) \cdot \mathbf{n}^\alpha da - \mathbf{v}^{\alpha_j} \int_{A_{\alpha\beta}} \left[\underline{\mathbf{t}}^j + \rho^j \mathbf{v}^j (\mathbf{w}_{\alpha\beta_j} - \mathbf{v}^j) \right] \cdot \mathbf{n}^\alpha da \right\} \quad (\text{B.16})$$

$$\hat{Q}_\beta^\alpha = \sum_{j=1}^N \left[\hat{Q}_\beta^{\alpha_j} + \hat{\mathbf{T}}_\beta^{\alpha_j} \cdot \mathbf{v}^{\alpha_j, \alpha} + \hat{e}_\beta^{\alpha_j} \left(e^{\alpha_j} + \frac{1}{2} \mathbf{v}^{\alpha_j, \alpha} \cdot \mathbf{v}^{\alpha_j, \alpha} \right) \right] \quad (\text{B.17})$$

$$\hat{r}^{\alpha_j} = \varepsilon^\alpha \rho^{\alpha_j} \overline{\hat{r}^j}^\alpha \quad (\text{B.18})$$

$$\underline{\underline{\mathbf{t}}}^{\alpha_j} = \langle \underline{\underline{\mathbf{t}}}^j \rangle^\alpha + \rho^{\alpha_j} \mathbf{v}^{\alpha_j} \otimes \mathbf{v}^{\alpha_j} - \rho^{\alpha_j} \overline{\mathbf{v}^j} \otimes \overline{\mathbf{v}^j}^\alpha \quad (\text{B.19})$$

$$\underline{\underline{\mathbf{t}}}^\alpha = \sum_{j=1}^N \left(\underline{\underline{\mathbf{t}}}^{\alpha_j} - \rho^{\alpha_j} \mathbf{v}^{\alpha_j, \alpha} \otimes \mathbf{v}^{\alpha_j, \alpha} \right) \quad (\text{B.20})$$

$$\hat{\mathbf{T}}_\beta^{\alpha_j} = \frac{\varepsilon^\alpha}{|\delta V_\alpha|} \left[\int_{A_{\alpha\beta}} \left[\underline{\underline{\mathbf{t}}}^j + \rho^j \mathbf{v}^j (\mathbf{w}_{\alpha\beta_j} - \mathbf{v}^j) \right] \cdot \mathbf{n}^\alpha da \right. \\ \left. - \mathbf{v}^{\alpha_j} \int_{A_{\alpha\beta}} \rho^j (\mathbf{w}_{\alpha\beta_j} - \mathbf{v}^j) \cdot \mathbf{n}^\alpha da \right] \quad (\text{B.21})$$

$$\hat{\mathbf{T}}_\beta^\alpha = \sum_{j=1}^N \left(\hat{\mathbf{T}}_\beta^{\alpha_j} + \hat{e}_\beta^{\alpha_j} \mathbf{v}^{\alpha_j, \alpha} \right) \quad (\text{B.22})$$

$$\mathbf{v}^{\alpha_j} = \overline{\mathbf{v}^j}^\alpha \quad (\text{B.23})$$

$$\mathbf{v}^\alpha = C^{\alpha_j} \mathbf{v}^{\alpha_j} \quad (\text{B.24})$$

$$\eta^{\alpha_j} = \overline{\eta^j}^\alpha \quad (\text{B.25})$$

$$\eta^\alpha = \sum_{j=1}^N C^{\alpha_j} \eta^{\alpha_j} \quad (\text{B.26})$$

$$\hat{\eta}^{\alpha_j} = \varepsilon^\alpha \rho^{\alpha_j} \left(\overline{\hat{\eta}^j}^\alpha + \overline{\hat{r}^j} \eta^{\alpha_j} - \overline{\hat{r}^j}^\alpha \eta^{\alpha_j} \right) \quad (\text{B.27})$$

$$\hat{\Lambda}^{\alpha_j} = \overline{\hat{\Lambda}^j}^\alpha \quad (\text{B.28})$$

$$\hat{\Lambda}^\alpha = \sum_{j=1}^N \hat{\Lambda}^{\alpha_j} \quad (\text{B.29})$$

$$\psi^{\alpha_j} = \overline{\psi^j}^\alpha \quad (\text{B.30})$$

$$\psi^\alpha = \sum_{j=1}^N C^{\alpha_j} \psi^{\alpha_j} \quad (\text{B.31})$$

$$\rho^{\alpha_j} = \overline{\rho^j}^\alpha \quad (\text{B.32})$$

$$\rho^\alpha = \sum_{j=1}^N \rho^{\alpha_j} \quad (\text{B.33})$$

B.3 Identities Needed to Obtain Inequality 3.40

$$\begin{aligned}
\sum_{j=1}^N \left(\frac{\varepsilon^\alpha \rho^{\alpha_j}}{T} \frac{D^{\alpha_j} \psi^{\alpha_j}}{Dt} \right) &= \frac{\varepsilon^\alpha \rho^\alpha}{T} \frac{D^{\alpha_j} \psi^\alpha}{Dt} + \frac{\psi^\alpha}{T} \hat{e}_\beta^\alpha \\
&+ \sum_{j=1}^N \left\{ \frac{1}{T} \mathbf{v}^{\alpha_j, \alpha} \cdot \nabla (\varepsilon^\alpha \rho^{\alpha_j} \psi^{\alpha_j}) - \frac{\psi^{\alpha_j}}{T} \hat{e}_\beta^{\alpha_j} \right. \\
&\quad \left. - \frac{\psi^{\alpha_j}}{T} \hat{r}^{\alpha_j} - \frac{\varepsilon^\alpha \rho^{\alpha_j}}{T} \psi^{\alpha_j} \nabla \cdot \mathbf{v}^{\alpha_j, \alpha} \right\} \tag{B.34}
\end{aligned}$$

$$\sum_{j=1}^N \left(\frac{\varepsilon^\alpha \rho^{\alpha_j}}{T} \eta^{\alpha_j} \frac{D^{\alpha_j} T}{Dt} \right) = \frac{\varepsilon^\alpha \rho^\alpha}{T} \frac{D^{\alpha_j} T}{Dt} + \sum_{j=1}^N \frac{\varepsilon^\alpha \rho^{\alpha_j}}{T} \eta^{\alpha_j} \mathbf{v}^{\alpha_j, \alpha} \cdot \nabla T \tag{B.35}$$

$$\sum_{j=1}^N \left(\frac{\varepsilon^\alpha}{T} \mathbf{t}^{\alpha_j} : \nabla \mathbf{v}^{\alpha_j} \right) = \sum_{j=1}^N \left\{ \frac{\varepsilon^\alpha}{T} \mathbf{t}^{\alpha_j} : \nabla \mathbf{v}^{\alpha_j, \alpha} + \frac{\varepsilon^\alpha}{T} \mathbf{t}^{\alpha_j} : \nabla \mathbf{v}^{\alpha_j} \right\} \tag{B.36}$$

$$\sum_{j=1}^N \sum_{\beta \neq \alpha} \hat{\Psi}_\beta^{\alpha_j} = - \sum_{j=1}^N \sum_{\beta \neq \alpha} \hat{e}_\beta^{\alpha_j} \eta^{\alpha_j} \tag{B.37}$$

$$\sum_{j=1}^N \hat{Q}^{\alpha_j} = - \sum_{\beta \neq \alpha} \left[\hat{\mathbf{i}}^{\alpha_j} \cdot \mathbf{v}^{\alpha_j, \alpha} + \hat{r}^{\alpha_j} \left(\psi^{\alpha_j} + T \eta^{\alpha_j} \frac{1}{2} (\mathbf{v}^{\alpha_j, \alpha})^2 \right) \right] \tag{B.38}$$

$$\begin{aligned}
\sum_{j=1}^N \sum_{\beta \neq \alpha} \hat{Q}_\beta^{\alpha_j} &= - \sum_{\alpha} \sum_{\beta \neq \alpha} \left\{ \hat{\mathbf{T}}_\beta^\alpha \cdot \mathbf{v}^{\alpha, s} + \frac{1}{2} \hat{e}_\beta^\alpha (\mathbf{v}^{\alpha, s})^2 \right. \\
&\quad \left. + \sum_{j=1}^N \left[\hat{\mathbf{T}}_\beta^{\alpha_j} \cdot \mathbf{v}^{\alpha_j, \alpha} + \frac{1}{2} \hat{e}_\beta^{\alpha_j} (\mathbf{v}^{\alpha_j, \alpha})^2 \right] \right\} \\
&+ \sum_{\beta \neq \alpha} \sum_{j=1}^N \left\{ \hat{e}_\beta^{\alpha_j} (\psi^{\alpha_j} + T \eta^{\alpha_j}) \right\} \tag{B.39}
\end{aligned}$$

APPENDIX C. Exploitation of the Entropy Inequality – An Abstract Perspective

This short appendix is meant to give a brief and abstract description of how the exploitation of the entropy inequality works. By “abstract” we mean that we will not assign any physical meaning to the variables. Instead we will simply state how the variables relate to each other and how they relate to the full set of chosen independent variables. The secondary purpose of this appendix is to make clear a few assumptions related to constitutive equations that are necessary in order for the exploitation of the entropy inequality to be successful. We conclude with an inequality that dictates how the linearization of the constitutive relations must behave in order not to violate the second law of thermodynamics. This is similar to the 1968 Nobel Prize winning analysis by Onsager, who showed the *reciprocal relations* that must hold at equilibrium for irreversible processes.

Let S be the set of all independent variables for the Helmholtz potential. This set defines the physical system of interest. Define the following sets:

- $\{x_j\} :=$ the set of all variables that are neither constitutive nor independent. Examples typically include \dot{T} , ∇T , $\nabla \rho^{l_j}$, \dots .
- $\{y_k\} :=$ the set of all constitutive variables which are zero at equilibrium. Examples typically include $\hat{\varepsilon}^\alpha$, $\hat{\varepsilon}_\alpha^{\beta_j}$, and \hat{r}^{α_j} .
- $\{\tilde{y}_\kappa\} :=$ the set of all constitutive variables which are not zero at equilibrium. Examples typically include $\hat{\mathbf{T}}_\beta^{\alpha_j}$, and $\hat{\mathbf{i}}^{\alpha_j}$.
- $\{z_l\} :=$ the set of all variables that are zero at equilibrium. Examples typically include ∇T , $\mathbf{v}^{\alpha,s}$, $\mathbf{v}^{\alpha_j,\alpha}$, and $\underline{\underline{\mathbf{d}}}^\alpha$.

Since each z_l is an independent variable it is clear that $\{z_l\} \subset S$. Furthermore we observe that $\{x_j\} \cap S = \emptyset$. The constitutive variables, on the other hand, are known to be functions of variables in S and as such the statement that $(\{y_k\} \cup \{\tilde{y}_\kappa\}) \cap S = \emptyset$ is easily misinterpreted. It is a true statement that $(\{y_k\} \cup \{\tilde{y}_\kappa\}) \cap S = \emptyset$, and it is correct not to choose constitutive variables as independent variables. The confusion is in the fact that $y_k = y_k(S)$ for all k (and for all κ).

The rate of entropy generation, $\hat{\Lambda}$, can be written as a linear combination of the variables from $\{x_j\}$, $\{y_k\}$, and $\{z_l\}$, where the coefficients are functions of variables from S . That is,

$$0 \leq \sum_{\alpha} \hat{\Lambda}^{\alpha} = \hat{\Lambda} = \sum_j (x_j X_j) + \sum_k (y_k Y_k) + \sum_l (z_l Z_l) \geq 0 \quad (\text{C.1})$$

where

$$X_j = X_j(S, \tilde{Y}_\kappa(S)), \quad Y_k = Y_k(S, \tilde{Y}_\kappa(S)), \quad \text{and} \quad Z_l = Z_l(S, \tilde{Y}_\kappa(S)). \quad (\text{C.2})$$

This is not the only way to algebraically rearrange $\hat{\Lambda}$, but this is what is commonly done during the exploitation process.

We now use inequality (C.1) to derive equations that hold for all time, at equilibrium, and near equilibrium.

C.1 Results that Hold For All Time

We have *no control* over the variables x_j since they are neither constitutive nor independent. This means that they could be positive or negative, large or small. In order for the second law of thermodynamics to hold for all time, the coefficients X_j must therefore be zero for all time. This implies that

$$\hat{\Lambda} = \sum_k (y_k Y_k) + \sum_l (z_l Z_l) \geq 0. \quad (\text{C.3})$$

C.2 Equilibrium Results

The definition of equilibrium is *the state at which all of the variables $\{y_k\}$ are zero*. This definition is based on physical intuition and will vary depending on the system of interest. From thermodynamics, the rate of entropy generation must be minimized at equilibrium. This implies that the gradient of the entropy generation function must be the zero vector (as understood with S as the independent variables for the gradient).

$$0 = \left. \frac{\partial \hat{\Lambda}}{\partial s_i} \right|_{eq} \text{ for all } i. \quad (\text{C.4})$$

Taking this partial derivative of the right-hand side of (C.3) we see that

$$0 = \left. \frac{\partial \hat{\Lambda}}{\partial s_i} \right|_{eq} = \left[\sum_k \left(y_k \frac{\partial Y_k}{\partial s_i} \right) + \sum_k \left(Y_k \frac{\partial y_k}{\partial s_i} \right) + \sum_l \left(z_l \frac{\partial Z_l}{\partial s_i} \right) + \sum_l \left(Z_l \frac{\partial z_l}{\partial s_i} \right) \right]_{eq}. \quad (\text{C.5})$$

Since $z_l|_{eq} = 0 = y_k|_{eq}$ for all l, k and $\frac{\partial z_l}{\partial s_i} = \delta_{il}$ (since $z_l \in S \forall l$) we get

$$0 = \left. \frac{\partial \hat{\Lambda}}{\partial s_i} \right|_{eq} = \left[\sum_k \left(Y_k \frac{\partial y_k}{\partial s_i} \right) + Z_i \delta_{il} \right]_{eq}. \quad (\text{C.6})$$

At this point we make an assumption that greatly affects the constitutive variables.

Assumption: At equilibrium we must have

$$\left. \frac{\partial y_k}{\partial z_l} \right|_{eq} = 0 \text{ for all } l, k \quad (\text{C.7})$$

Under this assumption it is clear that $Z_l = 0$ at equilibrium for all l . Notice that this says nothing about when $s_i \notin \{z_l\}$. From this argument, each equation $Z_l = 0$ gives a constraint on some of the variables in S . The assumption made can be viewed as a further restriction on the constitutive variables, but it is not clear whether this assumption is physical.

C.3 Near Equilibrium Results

For the near equilibrium results we consider two types of variables: variables that are zero at equilibrium and constitutive variables. In each case we linearize about the equilibrium state. A typical linearization result for variables which are zero at equilibrium is

$$\begin{aligned} Z_l|_{n.eq} &= \underbrace{(Z_l)|_{eq}}_{=0} + \sum_m \frac{\partial Z_l}{\partial z_m} \Big|_{eq} z_m + \sum_n \frac{\partial Z_l}{\partial y_n} \Big|_{eq} y_n + \dots \\ &= \sum_m \frac{\partial Z_l}{\partial z_m} \Big|_{eq} z_m + \sum_n \frac{\partial Z_l}{\partial y_n} \Big|_{eq} y_n + \dots \end{aligned} \quad (C.8)$$

The value of $(Z_l)|_{eq}$ is zero by the above arguments, and the partial derivatives are now functions of all of the other variables which are not zero at equilibrium:

$$C_{lm} := \frac{\partial Z_l}{\partial z_m} \Big|_{eq} = \frac{\partial Z_l}{\partial z_m} \Big|_{eq} (\xi_1, \xi_2, \dots), \quad (C.9)$$

$$D_{ln} := \frac{\partial Z_l}{\partial y_n} \Big|_{eq} = \frac{\partial Z_l}{\partial y_n} \Big|_{eq} (\xi_1, \xi_2, \dots) \quad (C.10)$$

for $\xi_n \in S \setminus \{z_l\}$. Written more simply

$$Z_l|_{n.eq} = C_{lm} z_m + D_{ln} y_n \quad (C.11)$$

where the summations are implicit over repeated indices.

For the constitutive variables we do a similar linearization, but note that the equilibrium state is not necessarily zero. Therefore,

$$Y_k|_{n.eq} = (Y_k)|_{eq} + \sum_p \frac{\partial Y_k}{\partial y_p} \Big|_{eq} y_p + \sum_q \frac{\partial Y_k}{\partial z_q} \Big|_{eq} z_q + \dots \quad (C.12)$$

Making similar definitions as before,

$$E_{kp} := \frac{\partial Y_k}{\partial y_p} \Big|_{eq} \quad (C.13)$$

$$F_{kq} := \frac{\partial Y_k}{\partial z_q} \Big|_{eq}, \quad (C.14)$$

the linearization result for the constitutive equations is

$$Y_k|_{n.eq} = Y_k|_{eq} + E_{kp} y_p + F_{kq} z_q \quad (C.15)$$

where the summations are implicit over repeated indices.

The trouble here is that we must have some information about the equilibrium state of the constitutive variable. The presumption that this is zero may be non-physical. An example of this is the capillary pressure relationship derived in multi-phase unsaturated media.

$$p_c = (p_c)|_{eq} + \tau \varepsilon^l, \quad (\text{C.16})$$

where p_c is the capillary pressure, $\tau = \partial p_c / \partial \varepsilon^l$, and the equilibrium capillary pressure is given as a function of saturation $p_c|_{eq} = p_c(S)$ via the van Genuchten approximation. This equilibrium constitutive equation is known not to be zero. In other systems the issue may be more subtle, but in any case one needs to have some information (whether from experiments or from other theory) to define the equilibrium state of the constitutive variable.

C.4 Linearization and Entropy

Consider again equation (C.3), but now substitute the linearized results into Y_k and Z_l

$$\begin{aligned} 0 \leq \hat{\Lambda} &= (y_k Y_k) + (z_l Z_l) \\ &= y_k (Y_k|_{eq} + E_{kp} y_p + F_{kq} z_q) + z_l (C_{lm} z_m + D_{ln} y_n) \\ &= y_k Y_k|_{eq} + y_k E_{kp} y_p + y_k F_{kq} z_q + z_l C_{lm} z_m + z_l D_{ln} y_n \end{aligned} \quad (\text{C.17})$$

(summations are again taken over repeated indices). Recognizing the quadratic terms as matrix products and rewriting in block matrix form gives

$$0 \leq y_k Y_k|_{eq} + \begin{pmatrix} \mathbf{y} \\ \mathbf{z} \end{pmatrix}^T \begin{pmatrix} \underline{\underline{\mathbf{E}}} & \underline{\underline{\mathbf{F}}} \\ \underline{\underline{\mathbf{D}}} & \underline{\underline{\mathbf{C}}} \end{pmatrix} \begin{pmatrix} \mathbf{y} \\ \mathbf{z} \end{pmatrix} = y_k Y_k|_{eq} + \boldsymbol{\zeta}^T \underline{\underline{\mathbf{A}}} \boldsymbol{\zeta} \quad (\text{C.18})$$

Notice that in the absence of constitutive variables (C.18) simplifies to

$$0 \leq \mathbf{z}^T \underline{\underline{\mathbf{C}}} \mathbf{z}. \quad (\text{C.19})$$

Simply stated this means that $\underline{\underline{\mathbf{C}}}$ must be positive semidefinite in order for the second law of thermodynamics to hold. This is Onsager’s Nobel Prize winning result. Recall that $Z_l|_{n.eq} = C_{lm}z_m$. If we take, for example, $z_m = \nabla T$ and observe that $Z_l|_{n.eq}$ is minus the heat flux near equilibrium (the coefficient in the entropy inequality associated with ∇T is minus the heat flux), then the $l - m$ entry in $\underline{\underline{\mathbf{C}}}$ is the heat flux tensor. Onsager’s result dictates the positivity of the heat flux tensor and the linearized result give Fourier’s law: $-\mathbf{q} = \underline{\underline{\mathbf{K}}}\nabla T$. In other words, there is no accident that many physical “laws” take the same form as Fourier’s law; they are a result of the non-negativity of $\underline{\underline{\mathbf{C}}}$ and the entropy inequality. This is a simple example, but it should help to elucidate the problem that arises when constitutive equations are introduced.

Returning to equation (C.18) we see that it is not immediately obvious that $\underline{\underline{\mathbf{A}}}$ needs to be positive semidefinite. In fact, the only way that we can guarantee that $\underline{\underline{\mathbf{A}}}$ has this property is if $y_k Y_k|_{eq} \leq 0$. That is, there must be a physical restriction on $y_k Y_k|_{eq}$ that, when violated, one perceives nonphysical results.

To give a physical example of this we return to the capillary pressure example. In this case we have $y_k = \varepsilon^l$ and $Y_k|_{eq} = p_c(S)$ where we are ignoring all other constitutive equations (or we are taking $Y_r|_{eq} = 0$ for all $r \neq k$). The restriction derived herein states that $p_c(S)\varepsilon^l \leq 0$ for all time. The time derivative can clearly take either sign, but what this seems to be indicating is that in drainage (when $\dot{\varepsilon}^l < 0$) the equilibrium capillary pressure must be positive, and in imbibition (when $\dot{\varepsilon}^l > 0$) the equilibrium capillary pressure must be negative. This is a bit contradictory since “drainage” and “imbibition” are non-equilibrium phenomena, and as such it is not possible to measure the *equilibrium* capillary pressure at these states. This leaves us with a conundrum: Is there a fundamental misinterpretation of the capillary pressure in this example, or is there is a deep-seated flaw in the exploitation of the entropy inequality.

APPENDIX D. Summary of Entropy Inequality Results

The following is a concise collection of the results derived from the entropy inequality. This appendix is to be used for reference when building the macroscale models.

D.1 Results that Hold For All Time

- Helmholtz potential and entropy are conjugate variables (equation (4.14))

$$\frac{\partial \psi^\alpha}{\partial T} = -\eta^\alpha. \quad (\text{D.1})$$

- Lagrange multiplier for fluid phase (equation (4.15))

$$\lambda^{\beta_j} = \sum_{\alpha} \frac{\varepsilon^\alpha \rho^\alpha}{\varepsilon^\beta} \frac{\partial \psi^\alpha}{\partial \rho^{\beta_j}}. \quad (\text{D.2})$$

- Lagrange multiplier for the dependence of the diffusive velocities on the N^{th} species (equation (4.16))

$$\underline{\underline{\lambda}}^{\alpha_N} = -\frac{1}{\rho^\alpha} \sum_{j=1}^N [\underline{\underline{\mathbf{t}}}^{\alpha_j} + (\rho^{\alpha_j} \lambda^{\alpha_j}) \underline{\underline{\mathbf{I}}}] + \psi^\alpha \underline{\underline{\mathbf{I}}}. \quad (\text{D.3})$$

- Solid phase pressure (equation (4.19))

$$p^s = -\frac{1}{3} \text{tr}(\underline{\underline{\mathbf{t}}}^s) = -\frac{J^s}{\varepsilon^s} \sum_{\alpha} \left(\varepsilon^\alpha \rho^\alpha \frac{\partial \psi^\alpha}{\partial J^s} \right). \quad (\text{D.4})$$

- Solid phase stress (equation (4.23))

$$\underline{\underline{\mathbf{t}}}^s = -p^s \underline{\underline{\mathbf{I}}} + \underline{\underline{\mathbf{t}}}^s_e + \frac{\varepsilon^l}{\varepsilon^s} \underline{\underline{\mathbf{t}}}^l_h + \frac{\varepsilon^g}{\varepsilon^s} \underline{\underline{\mathbf{t}}}^g_h \quad (\text{D.5})$$

where

$$\underline{\underline{\mathbf{t}}}^s_e = 2 \left(\rho^s \underline{\underline{\mathbf{F}}}^s \cdot \frac{\partial \psi^s}{\partial \underline{\underline{\mathbf{C}}}^s} \cdot (\underline{\underline{\mathbf{F}}}^s)^T - \frac{1}{3} \rho^s \frac{\partial \psi^s}{\partial \underline{\underline{\mathbf{C}}}^s} : \underline{\underline{\mathbf{C}}}^s \underline{\underline{\mathbf{I}}} \right), \quad (\text{D.6a})$$

$$\underline{\underline{t}}_h^l = 2 \left(\rho^l \underline{\underline{F}}^s \cdot \frac{\partial \psi^l}{\partial \underline{\underline{C}}^s} \cdot (\underline{\underline{F}}^s)^T - \frac{1}{3} \rho^l \frac{\partial \psi^l}{\partial \underline{\underline{C}}^s} : \underline{\underline{C}}^s \underline{\underline{I}} \right), \quad (\text{D.6b})$$

$$\underline{\underline{t}}_h^g = 2 \left(\rho^g \underline{\underline{F}}^s \cdot \frac{\partial \psi^g}{\partial \underline{\underline{C}}^s} \cdot (\underline{\underline{F}}^s)^T - \frac{1}{3} \rho^g \frac{\partial \psi^g}{\partial \underline{\underline{C}}^s} : \underline{\underline{C}}^s \underline{\underline{I}} \right). \quad (\text{D.6c})$$

D.2 Equilibrium Results

- Fluid pressures (equations (4.29), (4.41), (4.42), and (4.47) - (4.52))

$$p^\beta = -\frac{1}{3} \text{tr}(\underline{\underline{t}}^\beta) = \sum_{j=1}^N \sum_{\alpha} \left(\frac{\varepsilon^\alpha \rho^\alpha \rho^{\beta j}}{\varepsilon^\beta} \frac{\partial \psi^\alpha}{\partial \rho^{\beta j}} \right) \quad (\text{D.7})$$

$$p^{\alpha(\beta)} = \sum_{j=1}^N \left(\frac{\varepsilon^\alpha \rho^\alpha \rho^{\beta j}}{\varepsilon^\beta} \frac{\partial \psi^\alpha}{\partial \rho^{\beta j}} \Big|_{\varepsilon^\alpha, \rho^{\alpha k}, \varepsilon^\beta, \rho^{\beta m}} \right) \quad (\text{D.8})$$

$$p^\beta = \sum_{\alpha} p^{\alpha(\beta)} \quad (\text{D.9})$$

$$\bar{p}^{\alpha(\beta)} := -\varepsilon^\alpha \rho^\alpha \frac{\partial \psi^\alpha}{\partial \varepsilon^\beta} \Big|_{\varepsilon^\alpha, \varepsilon^\alpha \rho^{\alpha k}, \varepsilon^\beta \rho^{\beta k}} \quad (\text{D.10})$$

$$\pi^{\alpha(\beta)} := \varepsilon^\alpha \rho^\alpha \frac{\partial \psi^\alpha}{\partial \varepsilon^\beta} \Big|_{\varepsilon^\alpha, \rho^{\alpha k}, \rho^{\beta k}} \quad (\text{D.11})$$

$$p^{\alpha(\beta)} = \bar{p}^{\alpha(\beta)} + \pi^{\alpha(\beta)} \quad (\text{D.12})$$

$$\bar{p}^\beta := \sum_{\alpha} \bar{p}^{\alpha(\beta)} \quad (\text{D.13})$$

$$\pi^\beta := \sum_{\alpha} \pi^{\alpha(\beta)} \quad (\text{D.14})$$

$$p^\beta = \bar{p}^\beta + \pi^\beta. \quad (\text{D.15})$$

- Momemntum transfer between phases (equation (4.31))

$$\begin{aligned} -(\hat{\mathbf{T}}_s^\beta + \hat{\mathbf{T}}_\gamma^\beta) &= \left(\varepsilon^\beta \rho^\beta \frac{\partial \psi^\beta}{\partial \varepsilon^\beta} - p^\beta \right) \nabla \varepsilon^\beta + \varepsilon^\beta \rho^\beta \frac{\partial \psi^\beta}{\partial \varepsilon^\gamma} \nabla \varepsilon^\gamma \\ &+ \varepsilon^\beta \rho^\beta \sum_{j=1}^{N-1} \frac{\partial \psi^\beta}{\partial C^{s_j}} \nabla C^{s_j} + \varepsilon^\beta \rho^\beta \frac{\partial \psi^\beta}{\partial \varepsilon^l} \nabla \varepsilon^l + \varepsilon^\beta \rho^\beta \frac{\partial \psi^\beta}{\partial \varepsilon^\gamma} \\ &- \sum_{j=1}^N \left[\left(\varepsilon^\gamma \rho^\gamma \frac{\partial \psi^\gamma}{\partial \rho^{\beta j}} + \varepsilon^s \rho^s \frac{\partial \psi^s}{\partial \rho^{\beta j}} \right) \nabla \rho^{\beta j} \right] + \varepsilon^\beta \rho^\beta \sum_{j=1}^N \frac{\partial \psi^\beta}{\partial \rho^{\gamma j}} \nabla \rho^{\gamma j} \end{aligned}$$

$$+ \varepsilon^\beta \rho^\beta \frac{\partial \psi^\beta}{\partial J^s} \nabla J^s + \varepsilon^\beta \rho^\beta \frac{\partial \psi^\beta}{\partial \underline{\underline{C}}^s} : \nabla (\underline{\underline{C}}^s), \quad (\text{D.16})$$

- Momentum transfer between constituents (equation (4.34))

$$\sum_{\beta \neq \alpha} \hat{\mathbf{T}}_\beta^{\alpha_j} + \hat{\mathbf{i}}^{\alpha_j} = -\nabla (\varepsilon^\alpha \rho^{\alpha_j} \psi^{\alpha_j}) + \lambda^{\alpha_j} \nabla (\varepsilon^\alpha \rho^{\alpha_j}) + \psi^{\alpha_j} \nabla (\varepsilon^\alpha \rho^{\alpha_j}). \quad (\text{D.17})$$

- Partial heat flux (equation (4.35))

$$\sum_{\alpha} \varepsilon^\alpha \mathbf{q}^\alpha = \mathbf{0} \quad (\text{D.18})$$

- Chemical potential definition (equations (4.56) and (4.57))

$$\mu^{\beta_j} = \left. \frac{\partial \psi_T}{\partial (\varepsilon^\beta \rho^{\beta_j})} \right|_{\varepsilon^\alpha, \varepsilon^\beta, \rho^{\alpha_k}, \rho^{\beta_m}} = \sum_{\alpha} \left. \frac{\partial (\varepsilon^\alpha \rho^{\alpha_j} \psi^\alpha)}{\partial (\varepsilon^\beta \rho^{\beta_j})} \right|_{\varepsilon^\alpha, \varepsilon^\beta, \rho^{\alpha_k}, \rho^{\beta_m}} \quad (\text{D.19})$$

$$= \psi^\beta + \lambda^{\beta_j} \quad (\text{D.20})$$

- Mass transfer (equation (4.60))

$$\mu^{l_j} \Big|_{eq} = \mu^{g_j} \Big|_{eq} \quad (\text{D.21})$$

D.3 Near Equilibrium Results

- Momentum transfer between phases (equation (4.36))

$$\left(\sum_{\alpha \neq \beta} \hat{\mathbf{T}}_\alpha^\beta \right)_{near} = \left(\sum_{\alpha \neq \beta} \hat{\mathbf{T}}_\alpha^\beta \right)_{eq} - (\varepsilon^\beta)^2 \underline{\underline{\mathbf{R}}}^\beta \cdot \mathbf{v}^{\beta,s}. \quad (\text{D.22})$$

- Momentum transfer between constituents (equation (4.38))

$$\left(\sum_{\beta \neq \alpha} \hat{\mathbf{T}}_\beta^{\alpha_j} + \hat{\mathbf{i}}^{\alpha_j} \right)_{near} = \left(\sum_{\beta \neq \alpha} \hat{\mathbf{T}}_\beta^{\alpha_j} + \hat{\mathbf{i}}^{\alpha_j} \right)_{eq} - \varepsilon^\alpha \rho^{\alpha_j} \underline{\underline{\mathbf{R}}}^{\alpha_j} \cdot \mathbf{v}^{\alpha_j, \alpha}. \quad (\text{D.23})$$

- Partial heat flux (equation (4.39))

$$\left(\sum_{\alpha} \varepsilon^\alpha \mathbf{q}^\alpha \right) = -\underline{\underline{\mathbf{K}}} \cdot \nabla T \quad (\text{D.24})$$

D.4 Constitutive Equations

- Darcy's law

– Pressure formulation (equation (4.66))

$$\begin{aligned}
& \varepsilon^\beta \underline{\underline{\mathbf{R}}}^\beta \cdot (\varepsilon^\beta \mathbf{v}^{\beta,s}) \\
&= -\varepsilon^\beta \nabla p^\beta - \pi^{\beta(\beta)} \nabla \varepsilon^\beta - \pi^{\beta(\gamma)} \nabla \varepsilon^\gamma + \varepsilon^\beta \rho^\beta \mathbf{g} \\
&+ \sum_{j=1}^N \left[\left(\varepsilon^\gamma \rho^\gamma \frac{\partial \psi^\gamma}{\partial \rho^{\beta j}} + \varepsilon^s \rho^s \frac{\partial \psi^s}{\partial \rho^{\beta j}} \right) \nabla \rho^{\beta j} \right] - \varepsilon^\beta \rho^\beta \sum_{j=1}^N \frac{\partial \psi^\beta}{\partial \rho^{\gamma j}} \nabla \rho^{\gamma j} \\
&- \varepsilon^\beta \rho^\beta \frac{\partial \psi^\beta}{\partial J^s} \nabla J^s - \varepsilon^\beta \rho^\beta \frac{\partial \psi^\beta}{\partial \underline{\underline{\mathbf{C}}}^s} : \nabla (\underline{\underline{\mathbf{C}}}^s) + \nabla \cdot \left(\underline{\underline{\mathbf{v}}}^\beta : \underline{\underline{\mathbf{d}}}^\beta \right). \quad (\text{D.25})
\end{aligned}$$

– Chemical potential formulation (equation (4.76))

$$\begin{aligned}
& \underline{\underline{\mathbf{R}}} \cdot (\varepsilon^\beta \mathbf{v}^{\beta,s}) \\
&= - \sum_{j=1}^N (\rho^{\beta j} \nabla \mu^{\beta j}) - \rho^\beta \eta^\beta \nabla T + \rho^\beta \mathbf{g} + \frac{1}{\varepsilon^\beta} \nabla \cdot \left(\underline{\underline{\mathbf{v}}}^\beta : \underline{\underline{\mathbf{d}}}^\beta \right) \quad (\text{D.26})
\end{aligned}$$

- Fick's law (equation (4.80))

$$\varepsilon^\alpha \rho^{\alpha j} \underline{\underline{\mathbf{R}}}^{\alpha j} \cdot \mathbf{v}^{\alpha j, \alpha} = -\rho^{\alpha j} \nabla \mu^{\alpha j} + \rho^{\alpha j} \mathbf{g}. \quad (\text{D.27})$$

- Total heat flux (equation (4.92))

$$\mathbf{q} = -\underline{\underline{\mathbf{K}}} \cdot \nabla T - \sum_{\alpha=l,g} \left[\left(\sum_{j=1}^N (\rho^{\alpha j} \mu^{\alpha j}) + \rho^\alpha T \eta^\alpha \right) \mathbf{v}^{\alpha,s} \right]. \quad (\text{D.28})$$

APPENDIX E. Dimensional Quantities

This appendix contains typical values for the quantities found in the macroscale heat and moisture transport model. Note that since many of the tables are large so some are turned sideways and some are bumped to different pages by default.

Table E.1: Dimensional quantities

Symbol	Quantity	Dimensions	reference value	
			liquid (water)	gas (air)
ε^α	volume fraction	—	—	—
ρ^α	density	ML^{-3}	$1000 \frac{kg}{m^3}$	$1 \frac{kg}{m^3}$
ρ^{g_v}	vapor density	ML^{-3}	—	$2 \times 10^{-2} \frac{kg}{m^3}$
ρ^{g_a}	dry air density	ML^{-3}	—	$1.2 \frac{kg}{m^3}$
T	temperature	K	$298.15K$	$298.15K$
R^{g_a}	gas constant (air)	$L^2t^{-2}K^{-1}$	—	$286.9 \frac{J}{kg \cdot K}$
R^{g_v}	gas constant (vapor)	$L^2t^{-2}K^{-1}$	—	$461.5 \frac{J}{kg \cdot K}$
$\underline{\underline{D}}^\alpha$	diffusion coefficient	L^2t^{-1}	$2 \times 10^{-9} \frac{m^2}{s}$	$2.5 \times 10^{-5} \frac{m^2}{s}$
μ^{g_v}	chem. potential (vapor)	L^2t^{-2}	—	$-1.27 \times 10^7 \frac{J}{kg}$
μ^{g_a}	chem. potential (air)	L^2t^{-2}	—	$1.47 \times 10^7 \frac{J}{kg}$
\mathbf{g}	gravity	Lt^{-2}	$9.81 \frac{m}{s^2}$	$9.81 \frac{m}{s^2}$
κ	permeability	L^2	(see Tab. E.2)	(see Tab. E.2)
μ_α	dynamic viscosity	$ML^{-1}t^{-1}$	$10^{-3} Pa \cdot s$	$10^{-5} Pa \cdot s$
η^α	specific entropy	$L^2t^{-2}K^{-1}$	$3886 \frac{J}{kg \cdot K}$	$6519 \frac{J}{kg \cdot K}$
M	evaporation coefficient	tL^{-2}		

Table E.2: Typical values of hydraulic conductivity (K) for water and air, and associated values for permeability (κ). Note that $K = \kappa \rho g / \mu$ where $\rho^g = 1 \text{ kg/m}^3$, $\rho^l = 1000 \text{ kg/m}^3$, $\mu_l = 10^{-3} \text{ Pa} \cdot \text{s}$, and $\mu_g = 10^{-5} \text{ Pa} \cdot \text{s}$. Modified from Bear pg. 136 [5]

K [m/s] (water)	10^0	10^{-1}	10^{-2}	10^{-3}	10^{-4}	10^{-5}	10^{-6}	10^{-7}	10^{-8}	10^{-9}	10^{-10}	10^{-11}	10^{-12}		
K [m/s] (air)	10^{-1}	10^{-2}	10^{-3}	10^{-4}	10^{-5}	10^{-6}	10^{-7}	10^{-8}	10^{-9}	10^{-10}	10^{-11}	10^{-12}	10^{-13}		
κ [m^2]	10^{-7}	10^{-8}	10^{-9}	10^{-10}	10^{-11}	10^{-12}	10^{-13}	10^{-14}	10^{-15}	10^{-16}	10^{-17}	10^{-18}	10^{-19}		
Permeability	pervious			semipervious			impervious								
Aquifer	good			poor			none								
Sand and Gravel	clean gravel	good			clean sand			fine sand							
Clay and Organic	-	-			peat			stratified clay			unweathered clay				
Rocks	-			oil rocks			sandstone			limestone			granite		
K [cm/s] (water)	10^2	10^1	10^0	10^{-1}	10^{-2}	10^{-3}	10^{-4}	10^{-5}	10^{-6}	10^{-7}	10^{-8}	10^{-9}	10^{-10}		
K [cm/s] (air)	10^1	10^0	10^{-1}	10^{-2}	10^{-3}	10^{-4}	10^{-5}	10^{-6}	10^{-7}	10^{-8}	10^{-9}	10^{-10}	10^{-11}		
κ [cm^2]	10^{-3}	10^{-4}	10^{-5}	10^{-6}	10^{-7}	10^{-8}	10^{-9}	10^{-10}	10^{-11}	10^{-12}	10^{-13}	10^{-14}	10^{-15}		

REFERENCES

- [1] Hans Wilhelm Alt. An Abstract Existence Theorem for Parabolic Systems. *Communications on Pure and Applied Analysis*, 11(09):2079–2123, 2012.
- [2] Hans Wilhelm Alt and Stephan Luckhaus. Quasilinear Elliptic-Parabolic Differential Equations. *Mathematische Zeitschrift*, 183:311–341, August 1983.
- [3] H Amann. Dynamic theory of quasilinear parabolic equations. II. Reaction-diffusion systems. *Differential Integral Equations*, 3(1):13–75, 1990.
- [4] Peter William Atkins and Julio De Paula. *Atkins' Physical chemistry*. Oxford University Press, 2010.
- [5] Jacob Bear. *Dynamics of fluids in porous media*. Courier Dover Publications, 1988.
- [6] M Benkhalifa and G Arnaud. The viscous air flow pattern in the Stefan diffusion tube. *Transport in porous media*, pages 15–36, 1995.
- [7] Lynn Bennethum. *Multiscale Hybrid Mixture Theory for swelling systems with interfaces*. PhD thesis, Purdue University, 1994.
- [8] Lynn Schreyer Bennethum. Modified Darcy's law, Terzaghi's effective stress principle and Fick's law for swelling clay soils. *Computers and Geotechnics*, 20(3-4):245–266, 1997.
- [9] Lynn Schreyer Bennethum. Theory of flow and deformation of swelling porous materials at the macroscale. *Computers and Geotechnics*, 34(4):267–278, July 2007.
- [10] Lynn Schreyer Bennethum. *Notes for Introduction to Continuum Mechanics*. 2011.
- [11] Lynn Schreyer Bennethum and John H. Cushman. Clarifying Mixture Theory and the Macroscale Chemical Potential for Porous Media. *International Journal of Engineering Science*, 34(14):1611–1621, 1996.
- [12] Lynn Schreyer Bennethum and John H Cushman. Multiscale, Hybrid Mixture Theory for Swelling Systems - II: Constitutive Theory. *International Journal of Engineering Science*, 34(2):147–169, 1996.
- [13] Lynn Schreyer Bennethum and John H Cushman. Multiscale, hybrid mixture theory for swelling systems - I: balance laws. *International Journal of Engineering Science*, 34(2):125–145, 1996.

- [14] Lynn Schreyer Bennethum and John H. Cushman. Coupled Solvent and Heat Transport of a Mixture of Swelling Porous Particles and Fluids : Single Time-Scale Problem. *Sciences-New York*, pages 211–244, 1999.
- [15] Lynn Schreyer Bennethum, Marcio A. Murad, and John H. Cushman. Macroscale Thermodynamics and the Chemical Potential for Swelling Porous Media. *Transport in Porous Media*, 39(2):187–225, 2000.
- [16] Lynn Schreyer Bennethum and Tessa F. Weinstein. Three Pressures in Porous Media. *Transport in Porous Media*, 54:1–34, 2004.
- [17] C.W.J. Berentsen, S. M. Hassanizadeh, A Bezuijen, and O Oung. Modeling of Two-Phase Flow in Porous Media Including Non-Equilibrium Capillary Pressure Effects. In *Computational Methods in Water Resources XVI*, 2006.
- [18] Robert Byron Bird, Warren E. Stewart, and Edwin N. Lightfoot. *Transport Phenomena 2ed.* J. Wiley, 2007.
- [19] N.E. Bixler. NORIA – A finite element computer program for analyzing water, vapor, air, and energy transport in porous media, Rep SAND84-2057, UC-70. Technical report, Sandia Natl. Lab., Albuquerque, N.M., 1985.
- [20] S. Bottero, S. Majid Hassanizadeh, and P. J. Kleingeld. From Local Measurements to an Upscaled Capillary Pressure Saturation Curve. *Transport in Porous Media*, 88(2):271–291, March 2011.
- [21] Herbert B. Callen. *Thermodynamics and an introduction to thermostatistics.* Wiley, 1985.
- [22] B Camassel, N Sghaier, M Prat, and S Bennisrallah. Evaporation in a capillary tube of square cross-section: application to ion transport. *Chemical Engineering Science*, 60(3):815–826, February 2005.
- [23] Gaylon S. Campbell. *Soil physics with BASIC: transport models for soil-plant systems.* Elsevier, 1985.
- [24] A Cass, GS Campbell, and TL Jones. Enhancement of Thermal Water Vapor Diffusion In Soil. *Soil Science Society of America*, 48(1):25–32, 1984.
- [25] Michael a Celia and Jan M Nordbotten. Practical modeling approaches for geological storage of carbon dioxide. *Ground Water*, 47(5):627–38, 2009.
- [26] Bernard D. Coleman and Walter Noll. The thermodynamics of elastic materials with heat conduction and viscosity. *Archive for Rational Mechanics and Analysis*, 13(1):167–178, December 1963.
- [27] John Crank. *The Mathematics of Diffusion.* Clarendon Press, 1979.
- [28] J.H. Cushman. Multiphase transport based on compact distributions. *Acta Applicandae Mathematicae*, 3(3):239–254, 1985.

- [29] John H. Cushman, Bill X. Hu, and Lynn Schreyer Bennethum. A primer on upscaling tools for porous media. *Advances in Water Resources*, 25(8-12):1043–1067, August 2002.
- [30] H. Darcy. *Les fontaines publiques de la ville de Dijon*. Dalmont, 1856.
- [31] D. A. DeVries. Simultaneous Transfer of Heat and Moisture in Porous Media. *Transactions, American Geophysical Union*, 39(5):909–916, 1958.
- [32] Luc Dormieux, Djimedo Kondo, and Frans-Josef Ulm. *Microporomechanics*. John Wiley & Sons, 2006.
- [33] A. Cemal Eringen. Note On Darcys Law. *Journal of Applied Physics*, 94(2):1282, 2003.
- [34] Lawrence C. Evans. *Partial differential equations*. AMS Bookstore, 2010.
- [35] MJ Fayer and C.S. Simmons. Modified soil water retention functions for all matric suctions. *Water Resources Research*, 31(5):1233–1238, 1995.
- [36] A Fick. Ueber Diffusion. *Annalen der Physik*, 2006.
- [37] Gerald B. Folland. *Real Analysis – Modern Techniques and Their Applications*. John Wiley & Sons, 2 edition, 1999.
- [38] W G Gray and P C Y Lee. On the Theorems for Local Volume Averaging of Multiphase Systems. *International Journal of Multiphase Flow*, 3:333–340, 1977.
- [39] W. G. Gray and C. T. Miller. Consistent thermodynamic formulations for multiscale hydrologic systems: Fluid pressures. *Water Resources Research*, 43(9):W09408, September 2007.
- [40] William G. Gray and S. Majid Hassanizadeh. Macroscale continuum mechanics for multiphase porous-media flow includeing phases, interfaces, common lines, and common points. *Advances in Water Resources*, 21:261–281, 1998.
- [41] William G. Gray and Bernhard A Schrefler. Analysis of the solid phase stress tensor in multiphase porous media. *International Journal for Numerical and Analytical Methods in Geomechanics*, (July 2006):541–581, 2007.
- [42] M Hassanizadeh and W G Gray. General conservation equations for multi-phase systems: 1. Averaging procedure. *Advances in Water Resources*, 2:131–144, 1979.
- [43] S. Majid Hassanizadeh. Derivation of basic equations of mass transport in porous media, Part 1. Macroscopic balance laws. *Advances in Water Resources*, 9(4):196–206, December 1986.

- [44] S. Majid Hassanizadeh. Derivation of basic equations of mass transport in porous media, Part 2. Generalized Darcy's and Fick's laws. *Advances in Water Resources*, 9(4):207–222, December 1986.
- [45] S. Majid Hassanizadeh and A. Y. Beliaev. A Theoretical Model of Hysteresis and Dynamic Effects in the Capillary Relation for Two-phase Flow in Porous Media. *Transport in Porous Media*, (1):487–510, 2001.
- [46] S. Majid Hassanizadeh, M.A. Celia, and H.K. Dahle. Dynamic effect in the capillary pressure-saturation relationship and its impacts on unsaturated flow. *Vadose Zone Journal*, 1(1):38, 2002.
- [47] V. Joekar-Niasar, S. M. Hassanizadeh, and a. Leijnse. Insights into the Relationships Among Capillary Pressure, Saturation, Interfacial Area and Relative Permeability Using Pore-Network Modeling. *Transport in Porous Media*, 74(2):201–219, December 2007.
- [48] V. Joekar-Niasar, S. Majid Hassanizadeh, and H. K. Dahle. Non-equilibrium effects in capillarity and interfacial area in two-phase flow: dynamic pore-network modelling. *Journal of Fluid Mechanics*, 655:38–71, July 2010.
- [49] Vahid Joekar-Niasar and S. Majid Hassanizadeh. Uniqueness of Specific Interfacial Area-Capillary Pressure-Saturation Relationship Under Non-Equilibrium Conditions in Two-Phase Porous Media Flow. *Transport in Porous Media*, 94(2):465–486, February 2012.
- [50] Piet J. a. M. Kerkhof. New light on some old problems: Revisiting the Stefan tube, Graham's law, and the Bosanquet equation. *Industrial & Engineering Chemistry Research*, 5885(1879):915–922, 1997.
- [51] Natalie Kleinfelter, Moongyu Park, and John H Cushman. Mixture theory and unsaturated flow in swelling soils. *Transport in Porous Media*, 68(1):69–89, 2007.
- [52] Dung Le and TT Nguyen. Global Existence for a Class of Triangular Parabolic Systems on Domains of Arbitrary Dimension. *Proceedings of the American Mathematical Society*, 133(7):1985–1992, 2005.
- [53] Randall J. LeVeque. *Numerical methods for conservation laws*. Birkhäuser, 1992.
- [54] Randall J. LeVeque. *Finite difference methods for ordinary and partial differential equations ...* Society for Industrial and Applied Mathematics, 2007.
- [55] Donald Allan McQuarrie and John Douglas Simon. *Physical chemistry: a molecular approach*. University Science Books, 1997.
- [56] Andro Mikelić. A global existence result for the equations describing unsaturated flow in porous media with dynamic capillary pressure. *Journal of Differential Equations*, 248(6):1561–1577, March 2010.

- [57] J. M. Nordbotten, M. a. Celia, H. K. Dahle, and S. M. Hassanizadeh. On the definition of macroscale pressure for multiphase flow in porous media. *Water Resources Research*, 44(6):1–8, June 2008.
- [58] John Tinsley Oden and Leszek Demkowicz. *Applied functional analysis*. CRC Press, 2009.
- [59] M Peszynska and SY Yi. Numerical methods for unsaturated flow with dynamic capillary pressure in heterogeneous porous media. *Int. J. Numer. Anal. Model*, 5:126–149, 2008.
- [60] J. R. Philip and D. A. DeVries. Moisture Movement in Porous Materials under Temperature Gradients. *Transactions, American Geophysical Union*, 38(2):222–232, 1957.
- [61] George F. Pinder and Michael A. Celia. *Subsurface Hydrology*. John Wiley & Sons, 2006.
- [62] I.S. Pop, F. Radu, and P. Knabner. Mixed finite elements for the Richards equation: linearization procedure. *Journal of Computational and Applied Mathematics*, 168(1-2):365–373, July 2004.
- [63] Lyle Prunty. Spatial distribution of heat of wetting in porous media. *ASAE Annual International Meeting/CIGR XVth World*, 2002.
- [64] L.A. Richards. Capillary Conduction of Liquids Through Porous Mediums. *Journal of Applied Physics*, 1:318–331, 1931.
- [65] M.A. Rincon, J. Límaco, and I. Shih Liu. Existence and Uniqueness of Solutions of a Nonlinear Heat Equation. *TEMA - Tendências em Matemática Aplicada e Computacional*, 6(2):1–11, August 2005.
- [66] Hirotaka Saito, Jiri Šimnek, and Binayak P. Mohanty. Numerical Analysis of Coupled Water, Vapor, and Heat Transport in the Vadose Zone. *Vadose Zone Journal*, 5(2):784, 2006.
- [67] Masaru Sakai, Nobuo Toride, and Jií Šimnek. Water and Vapor Movement with Condensation and Evaporation in a Sandy Column. *Soil Science Society of America Journal*, 73(3):707, 2009.
- [68] Lynn Schreyer-Bennethum. Macroscopic Flow Potentials in Swelling Porous Media. *Transport in Porous Media*, 94(1):47–68, April 2012.
- [69] Ebrahim Shahraeeni and Dani Or. Pore-scale analysis of evaporation and condensation dynamics in porous media. *Langmuir : the ACS journal of surfaces and colloids*, 26(17):13924–36, September 2010.
- [70] Ebrahim Shahraeeni and Dani Or. Pore scale mechanisms for enhanced vapor transport through partially-saturated porous media. *Water Resources Research*, 2012.

- [71] Ebrahim Shahraeeni and Dani Or. Pore scale mechanisms for enhanced vapor transport through partially saturated porous media. *Water Resources Research*, pages 1–35, 2012.
- [72] N. Shokri, P. Lehmann, and D. Or. Critical evaluation of enhancement factors for vapor transport through unsaturated porous media. *Water Resources Research*, 45(10):1–9, October 2009.
- [73] T.S. Silverman. *A pore-scale experiment to evaluate enhanced vapor diffusion in porous media*. PhD thesis, New Mexico Institute of Mining and Technology, 1999.
- [74] John C Slattery. Flow of viscoelastic fluids through porous media. *AIChE Journal*, 13(6):1066–1071, 1967.
- [75] Kathleen M. Smits, Abdullah Cihan, Toshihiro Sakaki, and Tissa H. Illangasekare. Evaporation from soils under thermal boundary conditions: Experimental and modeling investigation to compare equilibrium- and nonequilibrium-based approaches. *Water Resources Research*, 47(5):1–14, May 2011.
- [76] Kathleen M. Smits, Viet V. Ngo, Abdullah Cihan, Toshihiro Sakaki, and Tissa H. Illangasekare. An evaluation of models of bare soil evaporation formulated with different land surface boundary conditions and assumptions. *Water Resources Research*, 48(12):W12526, December 2012.
- [77] Kathleen M. Smits, Toshihiro Sakaki, Anuchit Limsuwat, and Tissa H. Illangasekare. Thermal Conductivity of Sands under Varying Moisture and Porosity in Drainage Wetting Cycles. *Vadose Zone Journal*, 9(1):172, 2010.
- [78] M. Th. van Genuchten. A Closed-form Equation for Predicting the Hydraulic Conductivity of Unsaturated Soils. *Soil Science of America*, 44:892–989, 1980.
- [79] SW Webb. Review of Enhanced Vapor Diffusion in Porous Media. *Sandia National Laboratories, Albuquerque, New*, 1998.
- [80] Tessa F. Weinstein. *Three-Phase Hybrid Mixture Theory for Swelling Drug Delivery Systems*. PhD thesis, University of Colorado Denver, 2005.
- [81] Stephen Whitaker. Diffusion and dispersion in porous media. *AIChE Journal*, 13(3):420–427, 1967.
- [82] Stephen. Whitaker. Advances in theory of fluid motion in porous media. *Industrial & Engineering Chemistry*, 61(12):14–28, 1969.
- [83] Stephen Whitaker. Coupled Transport in Multiphase Systems: A Theory of Drying. *Advances in Heat Transfer*, 31:1–104, 1991.
- [84] Stephen Whitaker. Role of the species momentum equation in the analysis of the Stefan diffusion tube. *Industrial & Engineering Chemistry Research*, pages 978–983, 1991.

- [85] Keith J. Wojciechowski. *Analysis and Numerical Solution of Nonlinear Volterra Partial Integrodifferential Equations Modeling Swelling Porous Materials*. PhD thesis, University of Colorado Denver, 2011.
- [86] Wolfram. Mathematica 9 Documentation – NDSolve reference.wolfram.com/mathematica/ref/NDSolve.html, 2012.
- [87] E. C. Zachmanoglou and Dale W. Thoe. *Introduction to partial differential equations with applications*. Courier Dover Publications, 1986.